Nonlinear Acoustics Instabilities In Combustion Chambers

Thesis by
Elias A. Awad

In Partial Fulfillment
of the Requirements for the Degree of
Doctor of Philosophy

Division of Engineering and Applied Sciences

California Institute of Technology
Pasadena, California

1983
(Submitted May 16, 1983)

To the memory of my father

ACKNOWLEDGEMENTS

I would like to thank Professor Fred E. C. Culick for sponsoring me as a graduate student, for proposing the subject of the thesis, and for guidance and helpful discussions during the preparation of this work. His help is gratefully acknowledged. Special thanks are due to Professor Toshi Kubota for his useful suggestions. I am thankful to Professor Thomas Caughey, Professor Donald Cohen, and Professor Frank Marble for remarks they gave during discussions and for being on the Examining Committee. I thank Professor Christopher Brennen for personal suggestions at the beginning of this work and for being on the Examining Committee.

I would like to thank my colleagues at GALCIT, Jet Propulsion Center, and Thomas Laboratory for their friendship and their fruitful discussions. I thank Chris Catherasoo for his thesis macro.

I appreciate deeply the technical support of Cecilia Lin and Betty Wood for the preparation of this manuscript. I heartily thank Dorothy Eckerman for her personal, technical, and administrative help.

Financial support for my graduate carreer at Caltech has generously been provided by the California Institute of Technology as a teaching assistantship, by the Air Force Office of Scientific Research, Grant No. AFOSR-80-0265, and the Naval Weapons Center, Contract N 60530-82-C-0137. Their support is gratefully acknowledged.

My warmest thanks are addressed to my wife Patricia for her encouragement, understanding, and patience during the preparation of this work.

Finally, my most profound thanks are addressed to my family for their immense moral and financial support during the years of my education. This thesis is lovingly dedicated to them.

ABSTRACT

In this report, we show, following a second order expansion in the pressure amplitude, analytical expressions for the amplitude, and the conditions for existence and stability of limit cycles for pressure oscillations in combustion chambers. Two techniques are used. The first technique is an asymptotic-perturbation technique where the asymptotic oscillatory behavior is sought by expanding the asymptotic solution in a measure of the amplitude of the wave, mainly the amplitude of the fundamental. The second technique is a perturbation-averaging technique where an approximate solution is sought by applying a perturbation method followed by an expansion of the solution in the normal modes of the acoustic field in the chamber. It is shown, to third order in the amplitude of the wave, that both techniques yield the same results regarding the amplitude and the conditions for existence and stability of the limit cycle. However, while the first technique can be extended to higher orders in the pressure amplitude, the second technique suffers serious difficulties. The advantage of the second technique is in its ability to handle easily a large number of modes.

A stable limit cycle seems to be unique. The conditions for existence and stability are found to be dependent only on the linear parameters. The nonlinear parameter affects only the wave amplitude. In very special cases, the initial conditions can change the stability of the limit cycle. The imaginary parts of the linear responses, to pressure oscillations, of the different processes in the chamber play an important role in the stability of the limit cycle. They also affect the direction of flow of energy among modes. In the absence of the imaginary parts, in order for an infinitesimal perturbation in the flow to reach a

finite amplitude, the lowest mode must be unstable while the highest must be stable; thus energy flows from the lowest mode to the highest one. The same case exists when the imaginary parts are non-zero, but in addition, the contrary situation is possible. There are conditions under which an infinitesimal perturbation may reach a finite amplitude if the lowest mode is stable while the highest is unstable. Thus energy can flow "backward" from the highest mode to the lowest one. It is also shown that the imaginary parts *increase* the final wave amplitude.

Second, the triggering of pressure oscillations in solid propellant rockets is discussed. In order to explain the triggering of the oscillations to a non-trivial stable limit cycle, the treatment of two modes and the inclusion in the combustion response of *either* a *second* order nonlinear velocity coupling *or* a *third* order nonlinear pressure coupling seem to be sufficient. Moreover, some mechanisms which are likely to be responsible for triggering are identified.

TABLE OF CONTENTS

LIST OF FIGURES

LIST OF SYMBOLS

A	Arbitrary quantity
A_i	Coefficient of $\cos\omega_i t$
B_i	Coefficient of $\sin\omega_i t$
a_{10}	Amplitude of the first mode of the limit cycle
a_{20}	Amplitude of the second mode of the limit cycle
A_{i0}	Limit value of A_i
B_{i0}	Limit value of B_i
c.c.	Complex conjugate
c_i	Coefficients introduced in Chapter 7
C_i	Coefficients introduced in Chapter 7
d_i	Coefficients introduced in Chapter 7
D_{11}, E_{11}	Coefficients introduced in Chapter 7
d_0	Diameter of the chamber
e_i	Coefficients introduced in Chapter 7
f	Function introduced in Chapter 4
f_i	Coefficients introduced in Chapter 6
F_1, F_2	Coefficients introduced in Chapter 6
F_n	Function representing nonhomogenuous and nonlinear terms
f_i	Coefficients introduced in Chapter 6
G, G_1, G_2	Coefficients introduced in Chapter 6
h_2	Coefficient introduced in Chapter 6
i	$\sqrt{-1}$
K	Complex frequency
k	Wavenumber
$\dot{m}$	Mass burning rate

m'	Perturbation of mass burning rate
p	Pressure
p'	Perturbation of pressure
$p_{lm,n}$	Coefficient of $\varepsilon^l \mu^m e^{ni\bar{K}t}$ in the expansion of p
r_0	Steady state mass burning rate
r	Burning rate
T	Temperature
T'	Perturbation of Temperature
t	Time
u	Velocity
u'	Perturbation of velocity
$u_{lm,n}$	Coefficient of $\varepsilon^l \mu^m e^{ni\bar{K}t}$ in the expansion of u
V_i	Coefficients in Appendix 7B
W_i	Coefficients in Appendix 7B
x	Axial coordinate
y	Function defined in Chapter 3
α_i	Growth rate of the i th mode
α	Growth rate
β	The nonlinear coefficient
β_1, β_2	Arbitrary coefficients
δ_i	Parameters defined in Chapter 6
∇^2	Laplacian
$\nabla \cdot$	Divergence
ε	Perturbation parameter, also a measure of the amplitude
κ	Thermal diffusivity

μ	Mach number of the mean flow
μ_p	Linear combustion response to pressure oscillations
ν	Frequency shift of the limit cycle.
ρ	Density
ρ'	Density perturbation
$\rho_{lm.n}$	Coefficient of $\varepsilon^l \mu^m e^{niKt}$ in the expansion of ρ
σ	Small parameter
ω	Real frequency
$( )^*$	Complex conjugate
$(\tilde{a})$	Nondimensional quantity

Chapter 1

INTRODUCTION

Oscillation of pressure in combustion chambers is a common, usually unwanted feature of most types of high-capacity combustion systems. The highly concentrated energy release by chemical reactions is responsive to flow disturbances, and the resulting combustion disturbances can, under certain conditions, amplify the original flow fluctuations. In combustion systems designed for steady state operation, such oscillations can be harmful to an extent ranging from a mild noise through causing vibration of doors and loose parts, up to the extreme when they cause a high-pressure combustion chamber to explode or a low-pressure one to implode. The major reason for studying combustion instability is to understand the mechanisms responsible for such unsteadiness, to know what control variables can be altered to reduce the harmful effects without excessively increase the capital cost of the combustion system or lowering the combustion efficiency.

Three types of combustion instabilities have been shown experimentally and theoretically to occur. The first type is the combustion roaring where a "white" noise, with a whole spectrum of frequencies, takes place. The second type is the Helmholtz resonator oscillation which corresponds to the bulk oscillation of the gas in the chamber; its frequency range is usually 10 to 100 Hz. But the most troublesome instability, especially in high-energy combustors, involves oscillation of the flow near one of the natural acoustic frequencies of the chamber. The frequencies range from a few hundred Hertz to a few thousand. The reason for the importance of this kind of oscillations is the fact that the combustion processes tend to respond most sensitively in this range of frequencies.

Depending on the amplitude of the oscillations, two regimes of behavior may be distinguished: linear behavior for which the disturbances are infintesimal; and nonlinear behavior for which the oscillations are so strong that nonlinear effects become important. The linear or nonlinear behavior of oscillatory combustion depends fundamentally on the combustion processes. It is indeed the effects of the oscillations on these processes and, hence, on the combustion rate itself, that supplies to the system an amount of energy sufficient to balance the energy absorbed by dissipative processes, thereby sustaining the oscillations.

A quantitative understanding of the responsible combustion processes and of the damping processes is essential to explain correctly the instability phenomenon and to provide for improved control. Because of the complexity of the over-all combustion system, stability analysis lacks rigor of representation of the physical problems, but such analysis provides the necessary link between basic knowledge and combustion behavior. Theoretical studies of combustion instabilities usually require the solution of *nonlinear* partial differential equations governing the physical processes in the combustor. To solve these equations one usually treats first the linearized version of these equations and then attempts to solve the full equations.

The linear acoustic instabilities correspond to small fluctuations in the flow. The investigations in the area of linear instabilities are well advanced. However, the obvious shortcoming of the linear theories is their inability to predict observed behavior when the instability is in the nonlinear regime. Two important problems usually arise:

(a) What is the asymptotic oscillatory condition produced in the chamber in the case of linear instability? Clearly the oscillation cannot grow indefinitely but is actually limited by nonlinear effects.

(b) Is it possible, in the case of linear stability, that fluctuations above a certain amplitude may become amplified?. The corresponding phenomenon is called nonlinear instability, or triggering.

Both problems are clearly nonlinear. This work is devoted to answering these two questions. Since we are dealing with nonlinear behavior, it is clear that a nonlinear analysis should be used. To solve the nonlinear equations one has two choices: solve the equations numerically; or use an approximate analysis.

The major advantages of using an approximate analysis are first, the very low cost of computing the asymptotic oscillatory condition, especially for three-dimensional problems; and second, an approximate analysis will yield direct insight into the quantitative and qualitative influences of the different processes in the chamber. The major disadvantage is that, by definition, the method is approximate and therefore cannot represent accurately the various contributing processes. On the other hand, numerical analysis, while yielding in general a more accurate representation, costs much more and cannot explain easily either quantitatively or qualitatively the role of each process in the chamber in establishing the limit cycle. From the point of view of physical understanding of the nonlinear instabilities in combustion chambers, an analytical solution will yield a deeper insight than the numerical solution. The results of this work will show the point.

Generally, to solve partial differential equations governing physical processes, we use a perturbation method taking advantage of a small parameter. If the nonlinearity of the differential equation is not strong, the differential equation can be separated into linear and nonlinear parts. The nonlinear part is multiplied by a small parameter ε and a series approximation method is used to find the solution. This perturbation method was first introduced by Poincare[1]. It has received much attention[2,3,4,5] for the solution of nonlinear problems with

weak nonlinearity. The solution is sought in the following form

$$y(x,t) = y_0(x) + \varepsilon\, y_1(x, t) + \varepsilon^2\, y_2(x, t) + \varepsilon^3\, y_3(x, t) + \text{etc} \qquad (1.1)$$

where y_0 is the steady state solution, y_1 is the first order approximation (linear problem), y_2 and y_3 are respectively the second and third order approximation (nonlinear problem).

To find the *asymptotic* oscillatory behavior, two techniques in particular are commonly used. The first technique is to expand the asymptotic solution (limit of $y(x,t)$ when $t \to \infty$) in powers of a measure of the amplitude of the asymptotic solution, while *specifying* the asymptotic behavior in time, harmonic for example. For asymptotic harmonic motion, the small parameter, or the perturbation parameter, can be chosen to be, for example, the amplitude of the fundamental. Then we equate the coefficients of like power in the amplitude. A form of this technique is used in Chapters 3 to 6. This technique will be referred to as the "asymptotic-perturbation technique."

Recently, this technique has been applied to the problems of pressure oscillations in combustion chambers by, among others, Maslen and Moore[6] and Zinn[7]. However, the expansion which will be presented in this report is different from those reported in references 6 and 7 in many aspects shown in Chapter 3. The major difference is the capability of our expansion to yield simple *analytical* results regarding the amplitude and the conditions for stability of the asymptotic solution.

The second technique involves substituting in the differential equation the series (1.1) and retain terms to the desired order (y_2 for second order, etc). The solution functions y_2, y_3, etc. are then expanded in terms of the spatial normal functions of the linearized equation, the first order problem. Spacial

averaging, using Green's theorem (Chapter 3, Section 3.6), is then applied to the differential equation. The partial differential equation is then reduced to an infinite system of second order ordinary differential equations for the time-dependent parts. The asymptotic behavior is found by taking the limit of the time-dependent parts of the solution when $t \to \infty$. This technique will be referred to as the "perturbation-averaging technique."

Among others, Zinn and Powell[8] and Lores and Zinn[9] have used this technique to study the unsteady motion in liquid propellant rocket motors. They solved numerically a truncated part of the infinite set of second order ordinary nonlinear diffential equations for the time-dependent parts. Keller and Kogelman[10] used the same technique of expansion in the normal modes to study a nonlinear partial differential equation, the Klein-Gordon[11] with a nonlinear term of the sort appearing in the the Van der Pol equations. To solve the set of second order ordinary nonlinear differential equations they used their two-time[12] method. However, they, among others[13,14], noticed that the the two-time method is completely equivalent to the method of averaging. For low order approximations, it is often easier to apply the method of averaging. It was Culick[15] who first applied the method of averaging to study the nonlinear behavior of acoustic waves in combustion chambers.

The method of averaging was developed originally by Krylov and Bogoliubov[16] and by Bogoliubov and Mitropolskii[17] for the purpose of providing approximate solutions to ordinary differential equations with small nonlinearity. More recently, this method has been applied to nonlinear partial differential equations in several contexts. Benney[18] and McGoldrick[19] used it to treat the problem of water waves interaction. Montgomery and Tidman[20] used the same technique to treat the problem of plasma waves, and Montgomery[21] to solve the nonlinear Klein-Gordon equation[11]. The same technique has been used by many

investigators[22,23,24] to solve the equations of nonlinear waves in solids. The analysis in Chapters 6 and 7 are based on this technique.

The most distinctive point between the " perturbation-averaging " technique and the " asymptotic-perturbation " technique, as will be shown in Chapter 2, is the treatment of high order approximations. In both techniques (perturbation-averaging and asymptotic-perturbation), our objective is to find the limiting amplitude of pressure oscillations in combustion chambers by solving the conservation equations of the flow field.

The limiting of the growth of pressure oscillations in combustion chambers has long been the object of investigation, but the best available data have been obtained with systems using solid propellants. Experimental results[25] with T-Burners, a cylindrical chamber with center vent and with one or both ends terminated with end-burning propellant grains, show the general behavior most clearly : the pressure oscillation grows initially in time but, after few cycles, it levels off toward a limiting value. Figure 1.1 is an idealized envelope of the pressure history. From this figure, it is clear that the process is nonlinear. The final oscillatory condition is said to reach a limit cycle.

In general, a limit cycle corresponds to a periodic solution to nonlinear autonomous, i.e. no time-dependent coeffcients, systems. A limit cycle is independent of the initial conditions but it may depend on their range.

One classical example of the existence of limit cycles is the Van der Pol's oscillator[26], when the damping is amplitude-dependent. Following this analogy, Culick[27] introduced a theoretical interpretation of the limiting amplitude, of pressure oscillations in combustion chambers, by introducing a model of one nonlinear oscillator for which the nonlinear terms represent the wall losses and particle attenuation. But a detailed examination of the structure of the

LIMITING AMPLITUDE

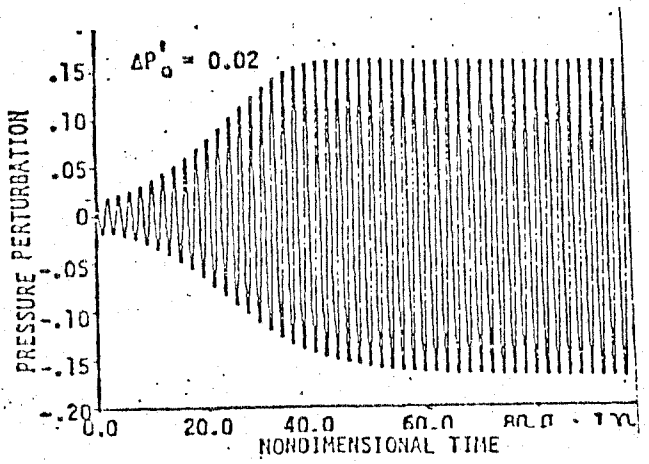

Figure 1.1 Sketch of the limiting amplitude phenomenon.

waveform of a limit cycle, found experimantally[25], confirmed that the process is more complicated. The waveform shows a distortion of the fundamental acoustic mode and involves generation of higher harmonics by different nonlinear processes, mainly the nonlinear gasdynamics of the flow. This is essentially the phenomenon responsible for the formation of shock waves in fluid flow.

To explain the effect of the nonlinear gasdynamics on the formation of limit cycle, Culick[15] presented an approximate analysis for the contribution of this kind of nonlinearity. By expanding the pressure field in the normal acoustic modes of the chamber, he showed that the nonlinear behavior could be represented by the equations for a system of nonlinear oscillators. Using reference 15 as a basis, Jensen and Beckstead[28] examined the influence of the energy transfer among modes on the formation of limit cycles . They found that indeed the gasdynamics nonlinearity played a major role in establishing the limit cycle. As a means of checking the approximate analysis, Culick and Levine[29] integrated numerically the conservation equations in rocket chambers, using the method of characteristics. They found that for small pressure disturbances the approximate analysis yielded satisfactory results.

Interest in dealing with the limiting amplitude in combustion chambers lies not only in interpreting some experimental data but in understanding the general behavior of pressure oscillations in combustion chambers. In fact, the results which will be elaborated in this report are of general application and can be applied easily to any sort of combustion chambers (ramjet engines, solid and liquid propellant rocket, furnaces, etc.) . Here, we will apply the results to solid propellant rocket motors because of the availability of data.

None of the references cited above provides satisfactory answers to the following questions: when does a limit cycle exist? what are the effects of the linear parameters on the existence, stability, and amplitude of the limit cycles? and

what are the effects of the nonlinear parameters?

The aim of this work is to answer these questions by giving explicit analytical results, while limiting the discussion to a finite number of modes.

In Chapter 2 we define the physical problem, the motivations of this work, and the objectives. In Section 2.2, we show some experimental results and numerical solutions, reported by other investigators. This constitutes the physical ground of the analysis in this work. Section 2.3 deals with the interpretations of these experimental results and numumerical solutions. This helps to define the scope of the analysis to be carried out. In Section 2.4, we define the physical problem in mathematical terms where we emphasize the structure of the initial and boundary conditions. Section 2.5 deals with the analysis of linear stability of pressure oscillations in a one-dimensional model for a cylindrical solid propellant rocket motor. This helps define the physical and geometrical properties of the chamber in mathematical terms. Finally, we state in Section 2.6 the precise purpose of this work.

In Chapter 3, we establish the groundwork for the expansion in the amplitude of the wave starting from simple examples. Section 3.2 deals with the expansion of the frequency in the amplitude of the oscillator in order to find the limiting amplitude, or limit cycle, for the solution of the well-known Van der Pol's equation.

In Section 3.3 we present a method of expansion in two parameters. The purpose is to show how the method can be expanded in many parameters.

Having verified in Section 3.2 the usefulness of the expansion, in Sections 3.4 and 3.5 we deal with the extension of the analysis to the solution of a nonlinear hyperbolic equation. The point is to demonstrate how the limiting amplitude may be found.

Chapter 3 ends with a discussion of the basis for an expansion of the solution of the nonlinear conservation equations in combustion chambers. The expansion presented in Chapter 3 will be extended in Chapters 4 and 5 to find the limiting amplitude for pressure oscillations in combustion chambers.

In Chapter 4 we apply the expansion developed in Chapter 3 to the conservation equations in combustion chambers. We start by developing the conservation equations in dimensionless form followed by analysis of the linear problem, to determine the linear growth rates for different harmonics. The results of the linear analysis are then applied to a one-dimensional problem. After that, the nonlinear problem is treated. It is convenient to distinguish two classes of problems: the class of purely longitudinal modes for which the frequencies are integral multiples of the fundamental; and all other possibilities. For the second class, only a single mode is taken into account. The point is to show that the " asymptotic-perturbation " technique can be extended easily to third order in the pressure amplitude. The results are applied to a one-dimensional problem. The first class will be the subject of Chapter 5.

In Section 4.6, we apply the perturbation-averaging technique, discussed in Chapter 3, to the conservation equations in combustion chambers. The analysis is carried only to second order in the pressure amplitude. Only the results for longitudinal modes are discussed in detail.

In Chapter 5 we discuss the class of pure longitudinal modes. We will be show, by applying the " asymptotic-perturbation " technique presented in Chapter 3, how the limit cycle can be obtained. The conditions for existence of the limit cycles will be determined. The results will again be applied to a one-dimensional problem.

The crucial point of whether such limit cycles physically exist, i.e. are stable, is treated in Section 5.7.

For simplicity, the analysis in Section 5.7 will be restricted to the treatment of longitudinal modes, partly because that is the case treated in Section 5.5 and partly to simplify the calculations. However, the analysis can easily be applied to three-dimensional problems once the limit cycles are found.

In section 5.7.2, the conservation equations are linearized around the limit cycles which are found using the asymptotic-perturbation technique. A system of two *linear* partial differential equations is obtained. Application of Green's theorem yields a ***parametric*** linear system of ordinary differential equations for the time-dependent parts. The method of averaging will then yield a linear system with *constant* coefficients. When the expansion of the pressure in the acoustic modes is limited to two modes and to second order in the pressure amplitude, explicit analytical results for the conditions for stability of the limit cycles are obtained. The particular case when the imaginary parts of the linear responses of the different processes in the chamber vanish is carried to completion.

Section 5.7.3 deals with the results for the stability of the limit cycles. One major conclusion is that, when two modes are accounted for, the stabilty depends only on the linear parameters. The nonlinearity affects only the amplitude. It is found that, in order for an infinitesimal disturbance in the flow to reach a finite amplitude, the first mode should be unstable and the second mode should be stable and should decay at least twice as fast as the first mode.

In Chapter 6, we will deal with the determination of the limit cycle using the technique of expansion in the normal modes of the chamber, following the method reported in reference 15 and using the results obtained in Chapter 4,

Section 4.6. In this chapter, we will use the analysis presented by Culick[15] for the solution of the nonlinear waves in combustion chambers. The objective is to support our results obtained in Chapters 4 and 5 by using a different approach to determine the limiting amplitude. In this chapter, we use the peturbation-averaging technique to find the amplitude and the conditions for existence and stability of the limit cycle. Broadly, the analysis breaks into two parts. First, for a chosen type of limit cycle (there are two), the conditions for existence and the amplitudes are found. Then a perturbation procedure is used to examine the stability of the limit cycle.

In Section 6.1, we treat the case when the fundamental frequency of the limit cycle is equal to the fundamental frequency of the chamber. Section 6.1.1 deals with two modes only. The objectives are to calculate the amplitude and to determine the conditions for existence and stability of the limit cycle. The purpose is to explain the influence of the linear and nonlinear parameters on the formation of limit cycle. Levine and Baum[30] reported some numerical results showing that the limit cycle seems to be independent of the initial conditions. We will show analytically in Section 6.1.1 how, in special cases, the initial conditions can change the stability of the limit cycle. The influence of the imaginary parts of the linear responses on the final amplitude is demonstrated. The objective is to see how these imaginary parts alter the amplitude and the conditions for stability of the limit cycle. The reason for studying this effect is the suspicion that the phase relationships between the pressure oscillations and the different processes in the chamber play a major role in the stability of the limit cycle. In section 6.1.2, we deal with three modes. The purpose here is to confirm the basic conclusions found in the treatment of two modes and to show how the analysis can be extended to any number of modes.

In Section 6.2, we treat the case when the fundamental frequency of the limit cycle is slightly different from the fundamental acoustic frequency of the chamber. The objective is to extend the results to a wider range of linear coefficients, thus making the application of the results to practical problems more accurate. Two modes are fully treated. In order to confirm the results, the case of three modes is treated only numerically.

Section 6.3 is a comparison between the analytical results on one hand and the numerical and experimental results, reported by other investigators, on the other hand. The main purpose of this part is to show how the analytical results can be applied to real problems, in order to understand the physical mechanisms behind the limiting amplitude phenomenon. Because of the availabilty of data on solid propellant rocket motors, these results will be applied solely to this kind of systems. But the validity and the scope of application are much wider and the results can be applied to any sort of chamber.

Chapter 7 is devoted to the treatment of the problem of nonlinear instability, or triggering. The system is linearly stable but nonlinearly unstable. Figure 1.2 shows an idealized sketch of pressure history illustrating this phenomenon. It is seen from this figure that for a small initial disturbance the oscillation decays in time but for a large initial disturbance the oscillation will be amplified and eventually levels off toward a non-trivial limit cycle. Our aim in Chapter 7 is to establish a framework for further research on this phenomenon. In this chapter, an analytical formulation, using a third order expansion in the pressure amplitude and treating two modes, for the triggering of pressure oscillations in solid propellant rockets is presented. In this section, we will show major mechanisms responsible for triggering and how they affect this phenomenon. The reason for studying this problem is the realization that triggering, or nonlinear instability, is a general phenomenon and is not related to a particular

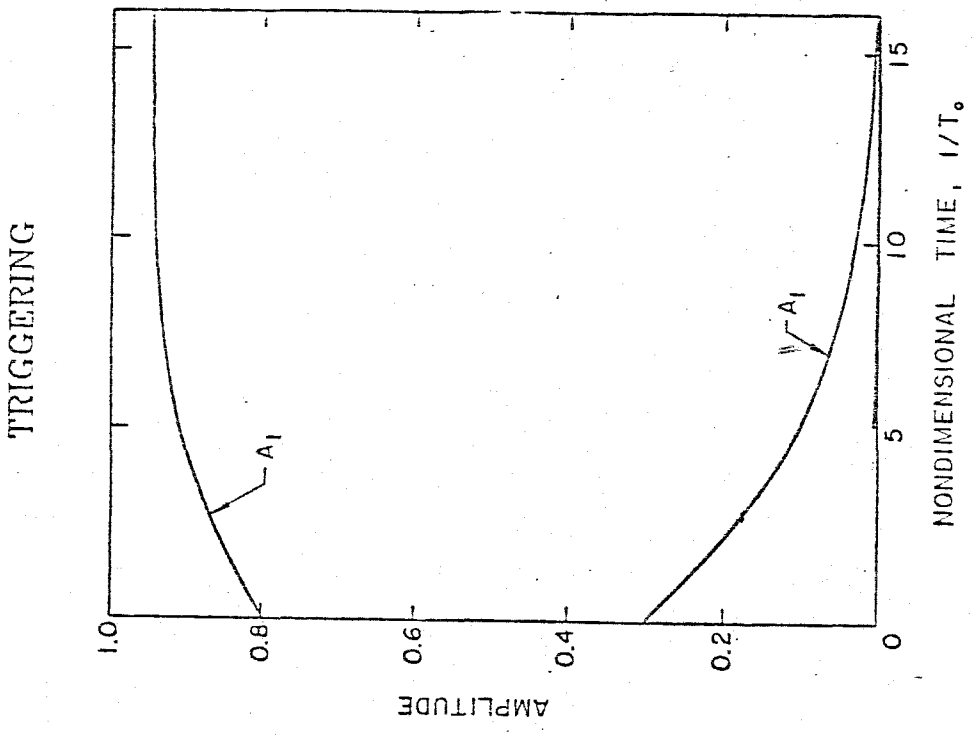

Figure 1.2 Sketch of the triggering phenomenon.

chamber geometry or to a specific propellant. This is, to our knowledge, the first global analytical representation of triggering.

In Chapter 8, we compare the applications of the perturbation-averaging technique and asymptotic-perturbation technique to the solution of the third order acoustics in the nonlinear conservation equations in combustion chambers. The purpose of this chapter is to examine the role of each technique in describing triggering.

The final results are summarized in Chapter 9. Future extensions of the analysis are discussed.

The most tangible contributions of this work are first the establishment of analytical results for the amplitudes and conditions for existence and stability of limit cycles for pressure oscillations in combustion chambers (this is an answer to question (a) above), and second the elaboration of a successful groundwork to predict triggering (answer to question (b) above). The practical applications are very wide and the results can be used directly to interpret experimental data.

REFERENCES 1

1. Poincare, H. *"Les Methodes Nouvelles de la Mecanique Celeste,"* Vol. 1, Gautiers-Villars, Paris, 1892.

2. Cunningham, W. J. " *Nonlinear Analysis* ," McGraw-Hill, New York, 1958.

3. Ku, Y. H. " *Analysis and Control of Nonlinear Systems,*" Ronald Press, New York, 1958.

4. Malkin, I. G. " *Theory of Stability of Motion,*" U.S. AEC translation 3352, Washington D.C., 1958.

5. Minorsky, N. " *Nonlinear Oscillations,*" D. Van Nostrand Co., Princeton N.J., 1962.

6. Maslen, S. H. and Moore, F. K. " On Strong Transverse Wave Without Shock in a Circular Cylinder," IJour. Aeronautical Sciences, Vol. 23, No. 6, pp. 583, 1956.

7. Zinn, B. T. " A Theoritical Study of Nonlinear Combustion Instability in Liquid-Propellant Rocket Engines," *AIAA Journal*, Vol. 6, No. 10, 1966.

8. Zinn, B. T. and Powell, E. A. " Application of the Galerkin Method in the Solution of Combustion-Instability Problems," *Propulsion Re-Entry Physics*, Pergamon Press, Oxford, 1970.

9. Lores, M. E. and Zinn, B. T. "Nonlinear Instability in Rocket Motors," *AIAA paper* 73-217, 1973.

10. Keller, J. B. and Kogelman, S. " Asymptotic Solutions of Initial Value Problems for Nonlinear Partial Differential Equations," *SIAM J. Appl. Math.*, Vol. 18, pp. 748-758, 1970.

11. Witham, G. B. " *Linear and Nonlinear Waves,*" Wiley, New York, 1974.

12. Cole, J. D. and Kevorkian, J. " Uniformely Valid Approximations for Certain Nonlinear Differential Equations," *Proc. Int. Symp. on Nonlinear Diff. Eqs. and Nonlinear Mechanics*, pp. 113-120, Academic Press, 1963.

13. Morrison, J. A. " Comparison of the Modified Method of Averaging and the Two Variable Expansion Procedure," *SIAM* Review, Vol. 8, pp. 66-85, 1966.

14. Lardner, R. W. " Asymptotic Solutions of Nonlinear Wave Equations Using the Method of Averaging and Two-Timing," *Quarterly of Applied Math*, July 1977, pp. 225-238.

15. Culick, F. E. C. " Nonlinear Behavior of Acoustic Waves in Combustion Chambers," *Acta Astronautica*, Vol. 3 , No. 9, Sept. 1976.

16. Krylov, N. N. and Bogoliubov, N. N. " *Introduction to Nonlinear Mechanics* ," University of Princeton Press, 1947.

17. Bogoliubov, N. N., and Mitropolsky, Y. A. " *Asymptotic Methods in the*

Theory of Nonlinear Oscillations," Hindustan Publications, New Delhi, 1961. See also " *Asymptotic Methods in the Theory of Nonlinear Oscillations*, " Gordon and Breach Pub., 1961.

18. Benney, D. J. " Nonlinear Gravity-wave Interactions," *J. Fluid Mech., Vol.* 14, pp. 577-584, 1962.

19. McGoldrick, L. F. " Resonant Interactions Among Capillary-Gravity Waves," *J. Fluid Mech.*, Vol. 21,pp. 305-331, 1965.

20. Montgomery, D. and Tidman, D. A. " Secular and Non-Secular Behaviour of the Cold Plasma Equations," *Physics Fluids*, Vol 7, pp. 242-249, 1964.

21. Montgomery, D. " Generalized Perturbation Expansion for the Klein-Gordon Equation with Small Nonlinearity," *J. Math. and Phys.*, Vol. 5, pp. 1788-1795, 1964.

22. Mitropolskii, Y. A. and Moseenkov " *Lectures on the Application of Asymptotic Methods to the Solutions of Partial Differential Equations*," Academy of Sciences of Ukraine SSR, Kiev, 1968.

23. Bojadziev, G. N. and Lardner, R. W. " Monofrequent Oscillations in Mechanical Systems Governed by second order hyperbolic equations with small nonlinearities," *Internation Journal of Nonlinear Mechanics*, Vol. 8, pp. 289-309, 1973.

24. Bojadziev, G. N. and Lardner, R. W. "Second-Order Hyperbolic Equations with Small Nonlinearities in the Case of Internal Resonance," *International Journal of Nonlinear Mechanics*, Vol. 9, pp. 397-407 (1974).

25. " *T-Burner Manual*," edited by Culick, F. E. C., CPIA pub. 191, Nov. 1969.

26. Stoker, J. J. " *Nonlinear Vibration in Mechanical and Electrical Systems* ," Interscience Publishers Inc., New York, 1950, pp. 119-128.

27. Culick, F. E. C. " Nonlinear Growth and Limiting Amplitude of Acoustic Oscillations in Combustion Chambers," *Combustion Science and Technology*, 1971, Vol. 3, pp. 1-16.

28. Jensen, R. C. and Beckstead, M. W. " Nonlinear Mechanisms of Solid Propellant Instabilities," *AIAA* paper 73-1297, November 1973.

29. Culick, F. E. C. and Levine, J. N." Comparison of Approximate and Numerical Analysis of Nonlinear Combustion Instabilities," *AIAA* paper 74-201, January 1974.

30. Levine, J. N. and Baum, J. D." A Numerical Study of Nonlinear Instabilities in Solid Rockets Motors," *AIAA* paper 81-1524, July 1981.

Chapter 2

DESCRIPTION OF THE PROBLEM

2.1. Introduction

In this chapter, we define the general problem to be solved in this report. Broadly, the problem breaks into two parts. First, we discuss the limiting amplitude phenomenon in combustion systems. This phenomenon will be discussed in details in Section 2.2.1 where some experimental results and some numerical solutions, reported by other investigators, will be shown in detail. The importance and the generality of this phenomenon will be pointed out. Second, the triggering phenomenon of pressure oscillations in combustions devices will be discussed in detail in Section 2.2.1 where we show some experimental results and numerical solutions. The need for interpreting these phenomena by relating them to some physical mechanisms is at the origin of this work. Following a discussion of the experimental results and the numerical solutions, we give in Section 2.3 some possible interpretations of these phenomena. This will constitute the ground for the analysis carried out in this report. In Section 2.4, we formulate the general problem to be solved and we define the basic characteristics of the physical problem.

2.2. Observed results and numerical solutions

In this section, we will show some experimental results and some numerical solutions regarding the limiting amplitude and triggering phenomena in combustion chambers. The interpretation of these phenomenon motivates the analysis to be followed in this work. In Section 2.2.1, we show some experimental results and numerical solutions showing the existence of the limiting amplitude phenomenon, while in Section 2.2.2 deals with the existence of the triggering

phenomenon. This section constitutes the physical basis for the analysis in this report.

2.2.1. *Limiting amplitude for a linearly unstable system .*

In the firings of T-burners, laboratory devices used to determine the propellant response to pressure oscillations and shown in Figure 2.1, the pressure oscillations show a peculiar result. The pressure grows initially in time, indicating the system is linearly unstable, leveling off after few cycles to a non-trivial limit cycle. Figure 2.2 shows one the test results reported in reference 1. Figure 2.3 shows the variation in time of the pressure and frequency from the test shown in Figure 2.2. In Figure 2.4, we show, from reference 1, some other test results for different propellants.

The phenomenon also occurs in liquid-propellant rockets. Figure 2.5 shows one of the test results reported in reference 2.

Clearly, the phenomenon is nonlinear, otherwise the pressure would grow indefinitely. We see that the limiting amplitude phenomenon is of general nature, since it may occur in any combustion device. To interpret this phenomenon, Culick and Levine[3] and Levine and Baum[4] integrated numerically the conservation equations in solid propellant rockets and they found that the nonlinear gasdynamics may well be a major cause for limiting the pressure amplitude. Figure 2.6 is one of the numerical results reported in reference 4. Moreover, in reference 4, the authors integrated the conservation equations for different initial conditions. They found that the limiting amplitude is always the same. Figure 2.7 shows two of their numerical results for different initial conditions. This suggests that the limiting amplitude phenomenon may well be independent of the initial disturbances.

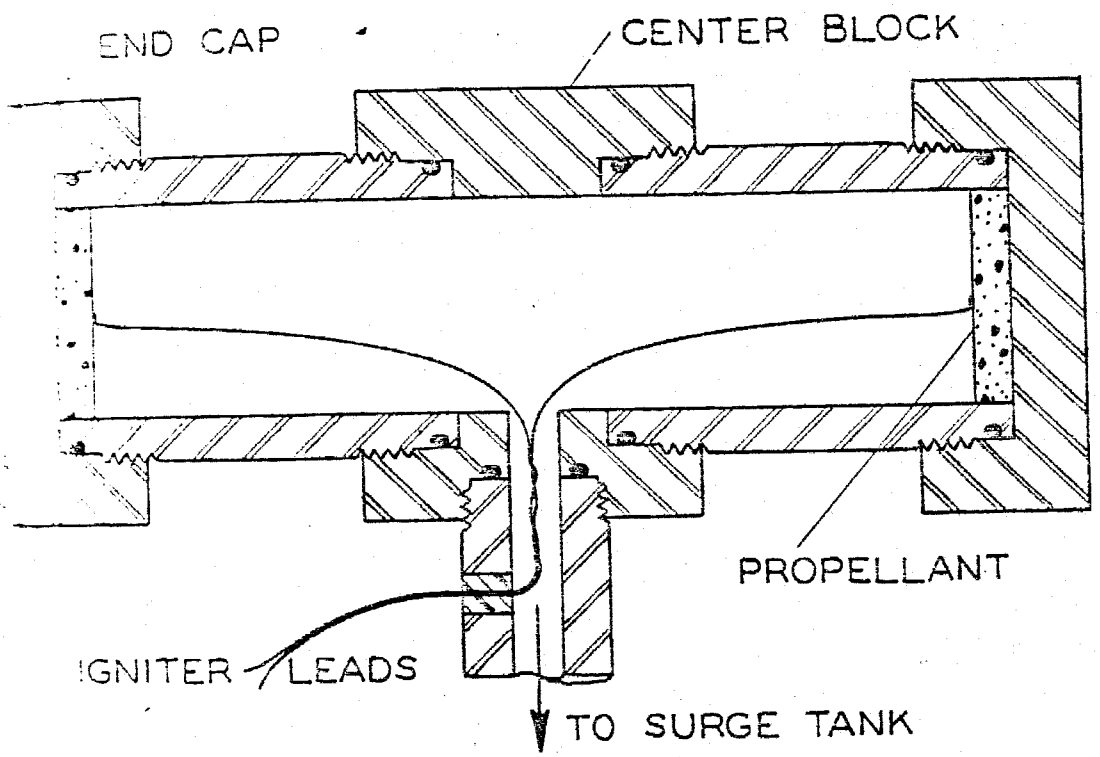

Figure 2.1 Sketch of a T-burner.

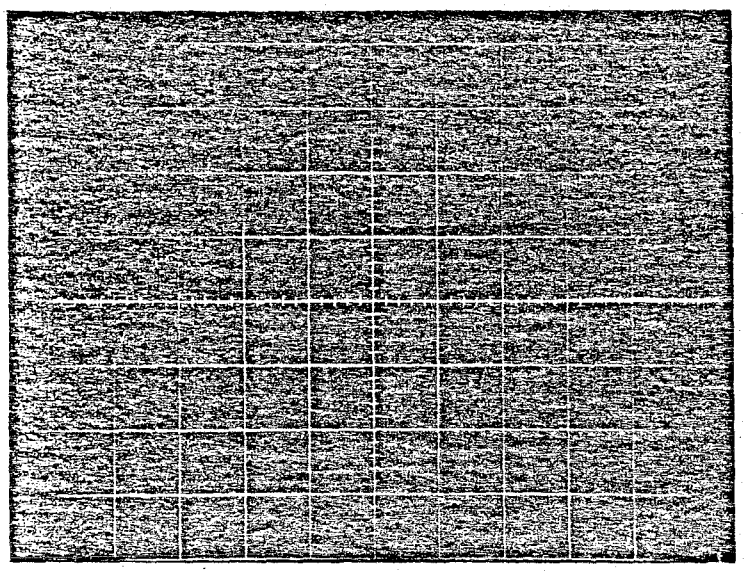

vertical	5 psi/cm
horizontal	0. 25 sec/cm

Figure 2.2 Oscilloscope trace of a typical good T-burner test. Reference 2.1.

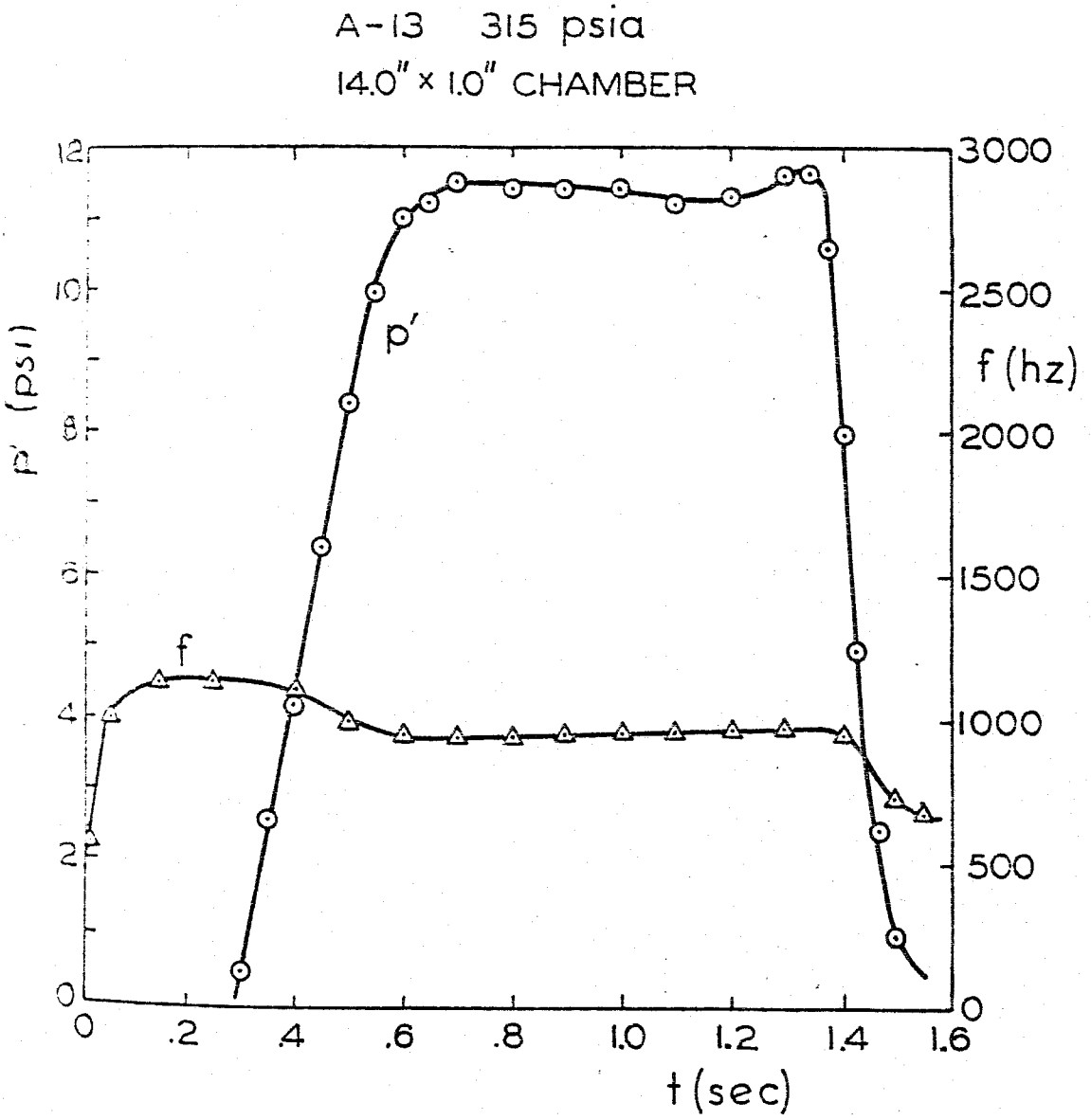

Figure 2.3 Frequency and amplitude versus time for the test shown in Figure 2.3

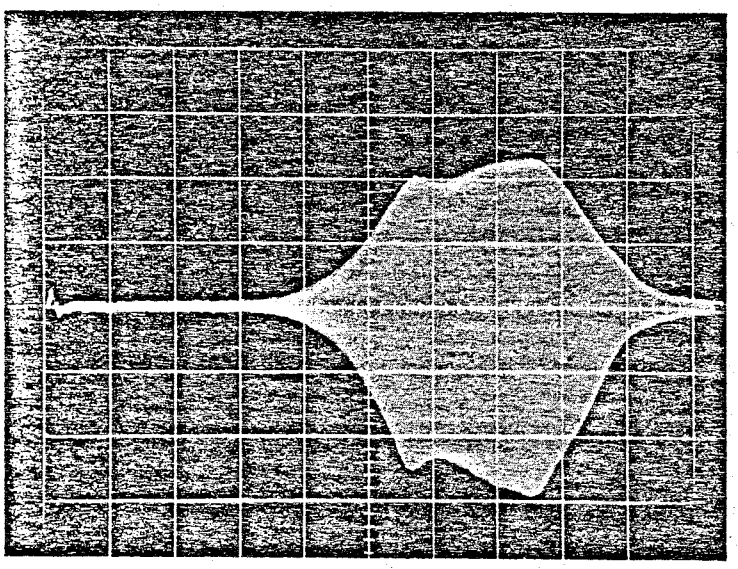

Run 1 (T-17)

vertical: 20 psi/cm

horizontal: 0.125 sec/cm

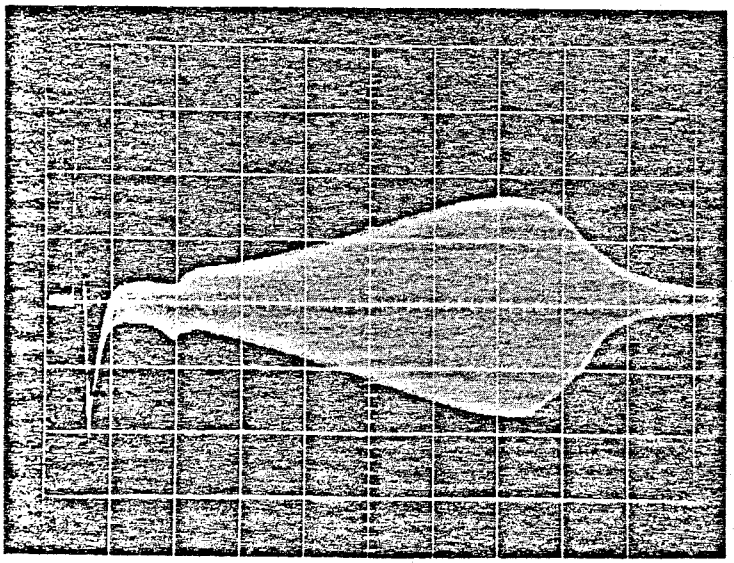

Run 2 (A-13)

vertical: 10 psi/cm

horizontal: 0.125 sec/cm

Figure 2.4 Oscilloscopes traces for firings of two different propellants. Reference 2.1.

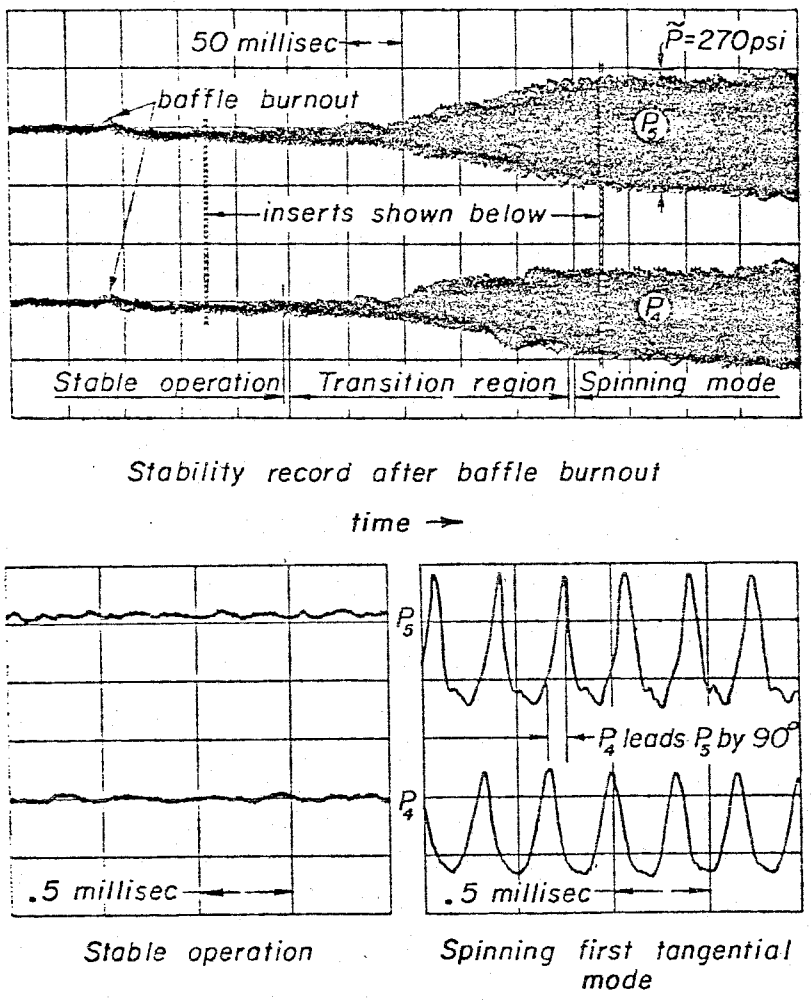

Figure 2.5 Limit cycle in the case of a liquid-propellant rocket. Reference 2.2

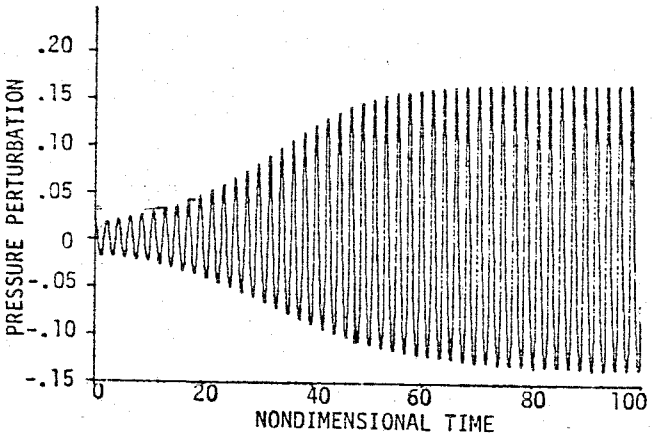

Figure 2.6 Numerical solution from reference 2.4.

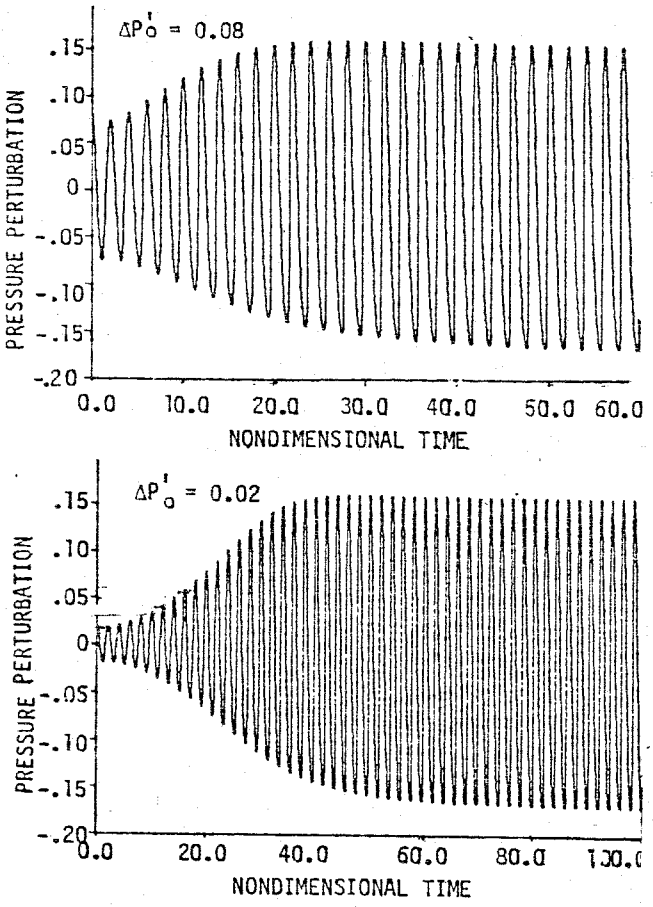

Figure 2.7 The limit cycle for two different initial conditions. Reference 2.4.

However, many important questions still do not have satisfactory answers. First, when does the limit cycle exist ? Second, what is the amplitude of this limit cycle ? Third, when is the limit cycle stable ? All the above references do not give satisfactory answers to these questions. Our main concern in Chapters 4 to 6 is to answer these questions. The results would be applicable to any combustion system.

2.2.2. *Triggering of pressure oscillations in combustion chambers* .

In the firings[5] of solid rocket motors at Aerojet Corporation, the rocket motor is pulsed into instability. Figure 2.8 is a schematic of the rocket motor used in reference 5. In Figure 2.9, we show the pressure waveform and its spectrum for a given test reported in reference 5. When the initial pulse is strong enough, the wave grows in time leveling off to a non-trivial limit cycle. A similar phenomenon was encountered experimentally by Brownlee[6]. Figure 2.10 shows one the test results in reference 6 where the pressure grows to a non-trivial limit cycle if the initial pulse is strong enough.

The same phenomenon is encountered in liquid-propellant rockets. Figure 2.11 shows one of the test results reported in reference 2. We see from this figure that for a strong pulse the wave grows in time leveling off to a non-trivial limit cycle.

On the numerical level, Kooker and Zinn[7] integrated numerically the conservation equations in a one-dimensional solid propellant rocket. Figure 2.12 is one of their results. They found that a nonlinear combustion response of the propellant to pressure oscillations may well be a major cause for triggering. More simply, Levine and Baum[4] integrated numerically the conservation equations in a cylindrical solid propellant rocket with a given nonlinear response of the propellant. They found that a nonlinear combustion response is capable of predicting triggering. Figure 2.13 is one of their numerical results. In both references 4 and

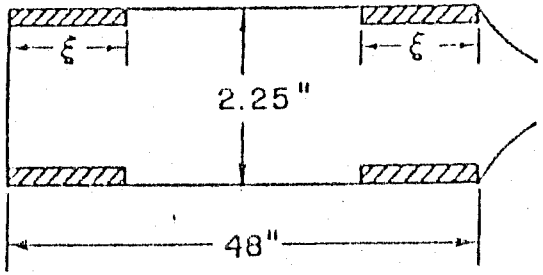

$\xi = 10"$	$a_1 = -0.75\ s^{-1}$	$n = 0.43$
$P_0 = 1500\ psi$	$a_2 = -50.0\ s^{-1}$	$\gamma = 1.23$
$G_1 = 240$	$G_2 = -2400\ s^{-1}$	$K = 2.7.10^{-7}\ m^2 s^{-1}$
$N = 400\ Hz$	$\tau = 2.10^{-4} s$	$\rho s = 1.7.10^3\ Kg\ m^{-3}$
$T_r = \frac{1}{N}$	$\omega = 2\pi N$	$a = 0.01\ ms^{-1}$

Figure 2.8 The experimental apparatus in reference 2.5.

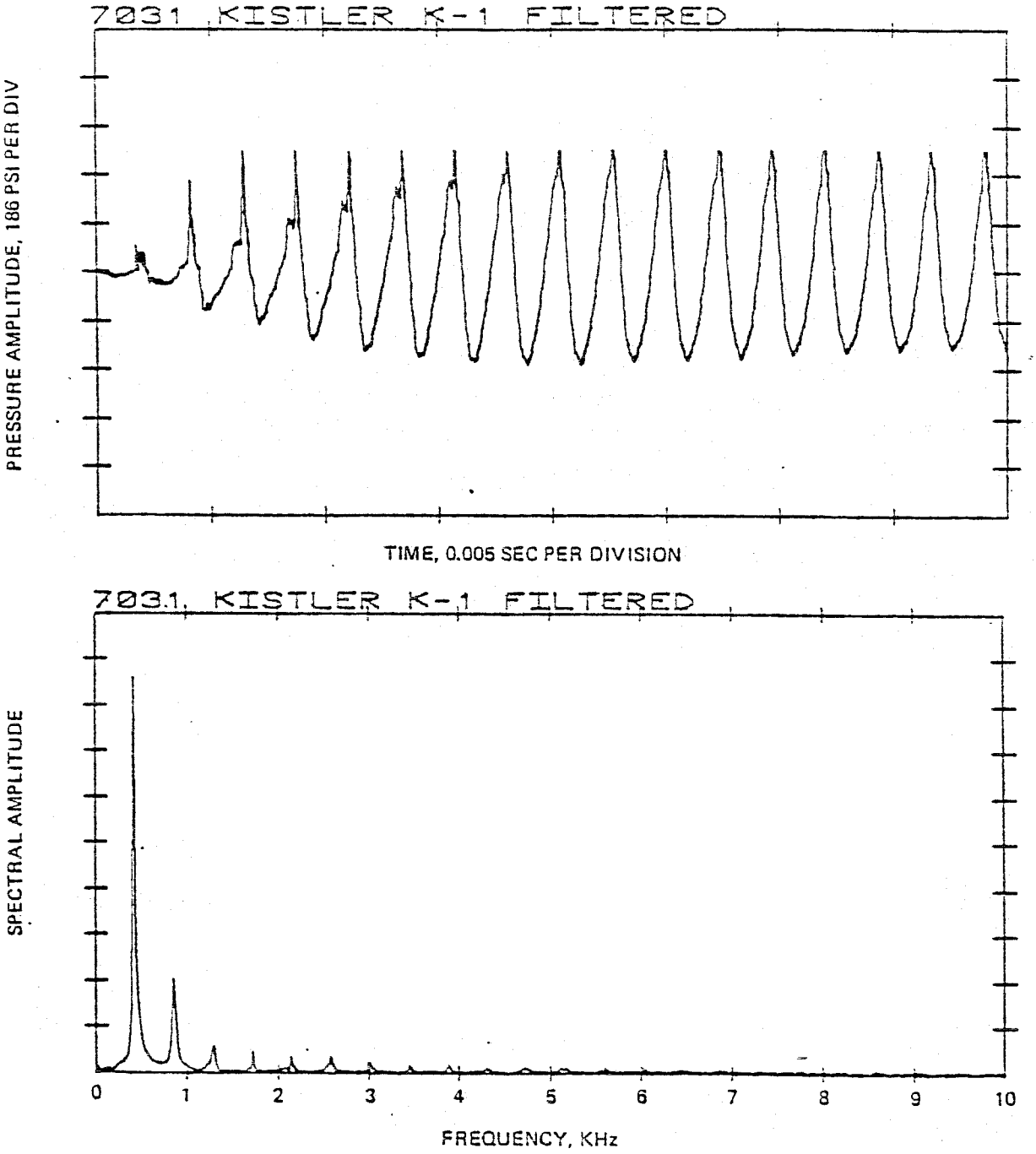

Figure 2.9 High pressure pulse waveform and spectrum. Reference 2.5.

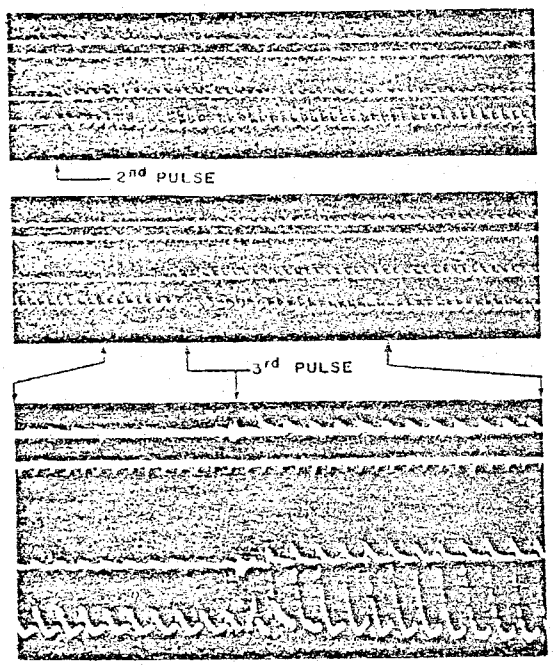

Figure 2.10 Nonlinear amplification of flow disturbances in an 1 X 2 X 20 in. solid propellant rocket. Reference 2.6.

Pulse orientation tests using like-on-like injection, alcohol oxygen 1.4$\bar{r}$ design, 9"diameter chamber with 7"injection, 150 psia and 1000 lb thrust

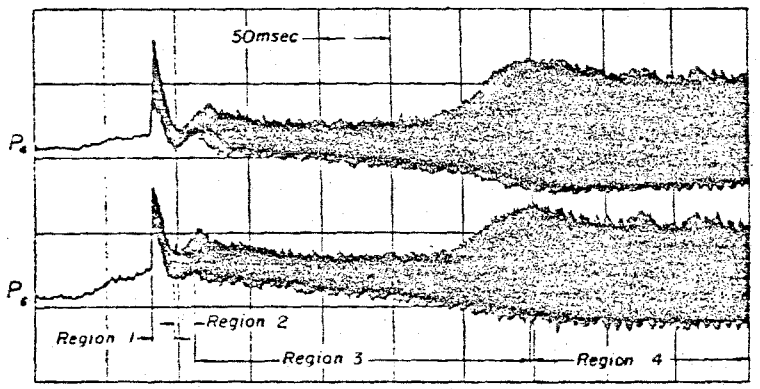

Figure 2.11 Nonlinear amplification of flow disturbances in a liquid- propellant rocket. Reference 2.2.

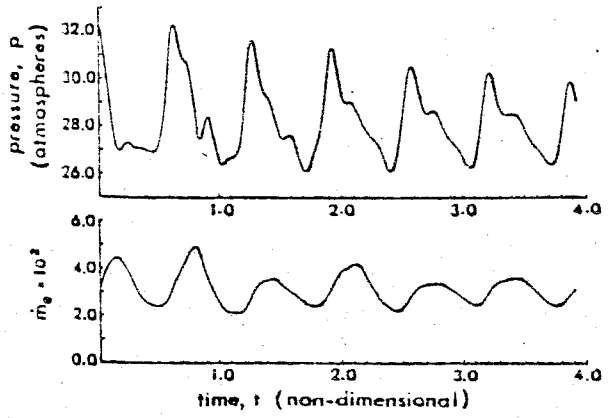

Figure 2.12a Time-history and propellant mass flow rate at the head end of the combustion chamber as the result of a 20% amplitude disturbance. Reference 2.7.

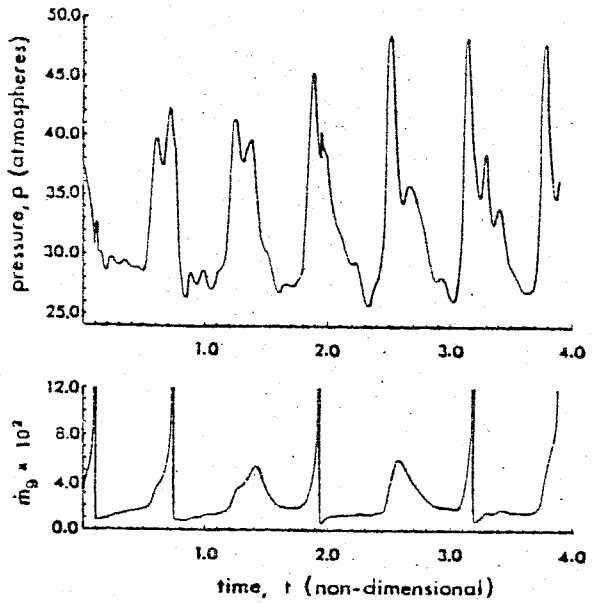

Figure 2.12b Time-history and propellant mass flow rate at the head end of the combustion chamber as the result of a 40% amplitude disturbance. Reference 2.7.

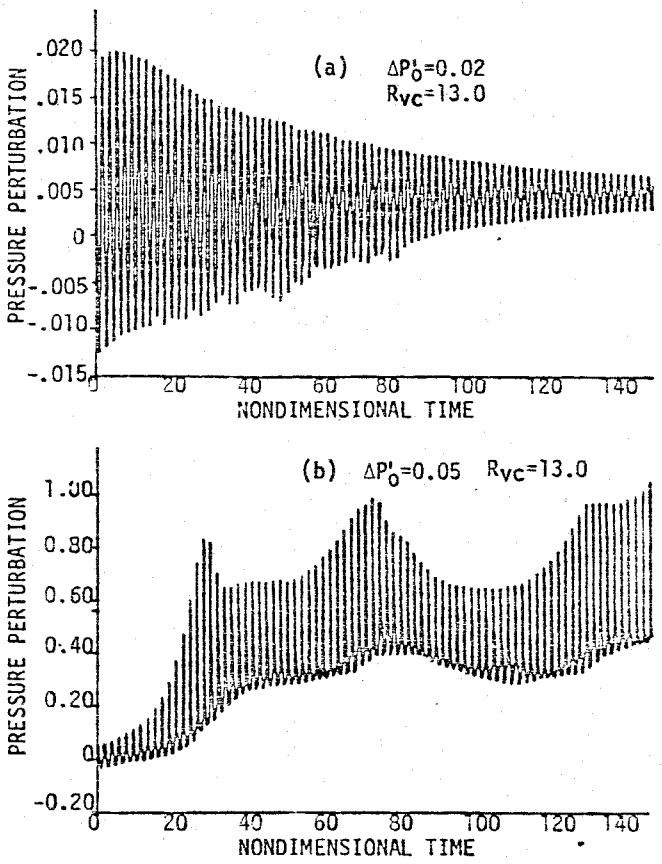

Figure 2.13 Time evolution of pressure oscillations at head end of the motor, using a nonlinear combustion response. Reference 2.4.

7, the limit cycle, or triggering limit, was found to be independent of the pulse amplitude, as long as this amplitude is above a theshold value. This is an important information in the sense that the triggering limit may not a continuous function of the initial conditions.

2.3. Possible interpretations of the observed results and the numerical solutions

First, we give some interpretations to the limiting amplitude phenomenon in a linearly unstable system. Second, we draw some causes for the triggering phenomenon in a linearly stable system. The conclusions we draw will constitute the basis for all the analysis in this report. In fact, the analysis in this work is aimed mainly at examining the validity of these conclusions.

From the experimental results and the numerical solutions regarding the limiting amplitude phenomenon, we saw in the last section that the nonlinear gasdynamics may well be a major cause for limiting the amplitude. This is essentially the same mechanism responsible for the formation of shock waves in gasdynamics. The growth of the wave generates higher harmonics. However, the shock wave does not occur because of the damping of the higher harmonics by the different processes in the chamber, mainly the response of the fuel to pressure oscillations. In fact, if the fuel response is frequency-dependent then the combustion of the fuel may drive the lower harmonics while damping the higher ones. The limiting amplitude corresponds to the situation where the damping mechanisms exactly balance the driving mechanisms.

Chapters 4 to 6 deals with the examination and the extension of these hypothesis. The results will be verified by comparing them to some experimental results and numerical solutions.

To interpret the triggering phenomenon of pressure oscillations in combustion chambers, we saw in the last section that a nonlinear combustion response

coupled with the nonlinear gasdynamics may well be a major cause for triggering. For a small initial disturbance, the response of the fuel may be always damping regardless of the harmonic content of the disturbance. Therefore, there is no physical mechanism which can provide energy to the wave. Consequently, the wave decays in time. However, for a large initial disturbance, the fuel response may become driving for some harmonics. The wave grows in time. However, because of the nonlinear gasdynamics, higher harmonics will be generated and, subsequently, damped by the different combustion processes. The triggering limit occurs when the damping mechanisms exactly balance the driving ones.

In Chapter 7 we examine and extend these hypothesis. The results will compared with some experimental results and numerical solutions to check the validity of these hypothesis.

To start the analysis, the problem should be defined in mathematical and physical terms. The conclusions of the analysis may, therefore, be direcltly related to some physical characteristics of the chamber. This is the object of the next section.

2.4. Formulation of the problem

In this section, we start with the conservation equations in combustion chambers and we determine the adequate boundary conditions. These equations will be discussed in details for the linear problem of a one-dimensional cylindrical solid propellant rocket. The objective of this discussion is to relate the mathematical terms to the geometrical and physical characteristics of the chamber. Therefore, the analytical results which will elaborated in this work

may directly be interpreted in some physical terms.

2.4.1. *Conservation equations in dimensionless form .*

In the derivation of the conservation equations, we make the following assumptions

1) No mass addition within the volume.

2) No heat transfer within the volume.

3) No viscous stresses within the volume.

4) The effects of the combustion are assumed to occur at the boundaries of the chamber.

5) The entropy waves are neglected.

These assumptions can be removed at the expense of much labor in carrying out the analysis but the essential idea remains the same, namely the influence of the gasdynamics nonlinearity and the effect of the dispersion, or frequency-dependence, of the boundary conditions. Therefore, in order to gain understanding of the nonlinearity phenomenon most simply, we maintain these assumptions.

Following the above assumptions, the conservation equations can be written in the following form

$$\frac{\partial \rho}{\partial t} + \nabla .(\rho \underline{u}) = 0 \qquad (2.1)$$

$$\rho(\frac{\partial \underline{u}}{\partial t} + \underline{u}.\nabla \underline{u}) + \nabla p = \underline{F} \qquad (2.2)$$

$$p\,\rho^{-\gamma} = \text{constant.} \tag{2.3}$$

where p, u, ρ, and γ are respectively the pressure, velocity, density, and heat ratio. $\underline{F}$ represents the interaction between the gas and the particles in the flow field. In most of the analysis we will assume $\underline{F} = 0$. The inclusion of $\underline{F}$ would require additional conservation equations for the particles. Essentially, we are examining the influence of the nonlinear gasdynamics and the boundary conditions. Elimination of ρ between (2.1) and (2.3) yields

$$\frac{\partial p}{\partial t} + \gamma\, p \nabla \cdot \underline{u} + \underline{u} \cdot \nabla\, p = 0 \tag{2.4}$$

Define the dimensionless quantities

$$\tilde{p} = \frac{p}{p_f}, \quad \tilde{\rho} = \frac{\rho}{\rho_f}, \quad \underline{\tilde{u}} = \frac{\underline{u}}{a_f}, \quad \tilde{x} = \frac{x}{L}, \quad \tilde{t} = t\,\frac{a_0}{L}$$

where p_f, ρ_f, a_0 and L are respectively the pressure, density, sound velocity of the mean flow and the characteristic length. By substituting the above quantities in (2.2)-(2.4), one gets

$$\frac{\partial \tilde{p}}{\partial \tilde{t}} + \gamma\, \tilde{p} \nabla \cdot \underline{\tilde{u}} + \underline{\tilde{u}} \cdot \nabla\, \tilde{p} = 0 \tag{2.5}$$

$$\tilde{\rho}\left(\frac{\partial \underline{\tilde{u}}}{\partial \tilde{t}} + \underline{\tilde{u}} \cdot \nabla\, \underline{\tilde{u}} \right) + \frac{\nabla\, \tilde{p}}{\gamma} = 0 \tag{2.6}$$

$$\tilde{p}\,\tilde{\rho}^{-\gamma} = 1 \tag{2.7}$$

Eqs. (2.5)-(2.7) will be the basis for the analysis. We will omit the sign ~ hereafter.

2.4.2. *Boundary conditions* .

To fix ideas, we will focus on the boundary conditions in solid propellant rockets, mainly because these conditions will be used later in the analysis, Chapters 4 to 7, to compare with some experimental results and numerical solutions. We have mainly two kinds of boundary conditions, one condition at the burning surface relating the burning rate to pressure oscillations and one condition at the nozzle entrance relating pressure and velocity fluctuations. In general, a boundary condition is derived from Eq. (2.6) as

$$\underline{n}.\frac{\nabla \tilde{p}}{\gamma} = -\underline{n}.\tilde{\rho}\left(\frac{\partial \tilde{\underline{u}}}{\partial t} + \tilde{\underline{u}}.\nabla\,\tilde{\underline{u}}\right)$$

at boundary, where $\underline{n}$ is the normal to the surface of the chamber. In all the analysis in this work, the boundary conditions are assumed to be linear, except in Chapter 7 where a nonlinear combustion response is assumed. The linear boundary condition at the nozzle entrance is given, for a quasi steady motion, by[8]

$$\frac{\underline{n}.\underline{u}'}{p'} = M_E\frac{\gamma-1}{2} \tag{2.8}$$

where M_E is the Mach number at the entrance of the nozzle, u' and p' are respectively the linear fluctuations of the velocity and pressure.

The boundary condition at the burning surface is defined[9] by an admittance function of the form

$$\frac{n.u'}{p'} = - M_b A_b \tag{2.9}$$

where M_b is the Mach number at burning surface and A_b is the admittance function. We have $M_b = \frac{u_f}{a_f}$, where u_f and a_f are respectively the gas velocity and sound speed at the burning surface. Usually, the expression for the mass burning rate is given, in dimensional quantities, by

$$\frac{m'}{m_f}\frac{p_f}{p'} = R_b(\omega) \tag{2.10}$$

where $m_f = \rho_f u_f$; ω is the real frequency of the oscillation; and R_b is the linear combustion response of the propellant. In dimensional quantities, the admittance function becomes

$$\frac{n.u'}{u_f}\frac{\gamma p_f}{p'} = - M_b A_b \tag{2.11}$$

Using the definition of A_b, assuming that the references quantities are those at the burning surface and that the processes are isentropic between the density and the pressure, we get from (2.10) and (2.11)

$$A_b = M_b(\gamma R_b - 1) \tag{2.12}$$

A common expression for R_b is the following relation[9] between fluctuations of the mass burning rate and pressure:

$$R_b = \frac{nAB}{\lambda + \frac{A}{\lambda} - (1 + A) + AB} \tag{2.13}$$

where A and B are related to the propellant combustion parameters. Usually A is in the range of 10 and B in the range of 1 for practical propellants; see reference 9 for more details. The coefficient λ here is a complex quantity and is the root of the following equation

$$\lambda(\lambda - 1) = i\Omega \tag{2.14}$$

where here $\Omega = \frac{\kappa\omega}{r_0^2}$ is the dimensionless frequency, with κ and r_0 respectively the thermal diffisuvity and the burning rate $r_0 = \frac{m_f}{\rho_f}$. With $\lambda = \lambda^{(r)} + i\lambda^{(i)}$, the roots of equation (2.14) become

$$\lambda^{(r)} = \frac{1}{2}\left[1 + \frac{1}{2^{\frac{1}{2}}}\left[(1 + 16\Omega^2)^{\frac{1}{2}} + 1\right]^{\frac{1}{2}}\right]^{\frac{1}{2}} \tag{2.15}$$

$$\lambda^{(i)} = \frac{1}{2\sqrt{2}}\left[(1 + 16\Omega^2)^{\frac{1}{2}} - 1\right]^{\frac{1}{2}} \tag{2.16}$$

Therefore, R_b is a complex quantity and frequency-dependent. It may be written as follows

$$R_b = R_b^{(r)}(\omega) + iR_b^{(i)}(\omega) \tag{2.17}$$

Expressions (2.8), (2.13), and (2.17) will be used in Section 2.5 to relate the mathematical results regarding the growth rates of the wave to some physical and geometrical characteristics of the chamber.

2.4.3. *Influence of the initial conditions* .

In general, the initial conditions should be given in order for the system of conservation equations (2.5)-(2.7) to be well defined. However, since both phenomena we examine are related only to *periodic* motions, one needs only to determine the periodic motion of Eqs. (2.5)-(2.7). These conditions can be simply written as follows

$$p(x,t + T_0) = p(x,t),\ u(x,t + T_0) = u(x,t),\ \text{etc.}$$

where T_0 is the period of the oscillations. The conclusion here is that the initial conditions need not be specified unless the method of solution involves the incorporation of the initial conditions. For example, if the method of solution describes the behavior of the wave from t = 0 then it is essential to include the influence of the initial conditions on the behavior of the wave, even though the asymptotic solution when $t \to \infty$ may well be independent of these conditions. We will see in the next chapter that one the two methods we use to solve the system of equations (2.5)-(2.7) has this feature, the second method treats directly the periodic solutions only.

2.5. One-dimensional linear problem for a solid propellant rocket

The purpose of this section to show how to relate the mathematical results of the linear analysis to the geometrical and physical characteristics of a given combustion chamber. In particular, we will express the growth rates of the pressure wave in terms of some physical characteristics of the chamber. In Chapters 4 to 7, the analytical results will be given in terms of these growth rates.

Therefore, the results of these chapters can be directly translated into some conditions on the geometrical and physical characterisics of the chamber.

2.5.1. *Conservation equations.*

Consider the solid propellant rocket shown in Figure (2.14). For a one-dimensional analysis with constant cross sectional area, the conservation equations can be written[10] in the following form

$$\frac{\partial \rho}{\partial t} + \frac{\partial(\rho u)}{\partial x} = \dot{m} \tag{2.18}$$

$$\frac{\partial}{\partial t}\rho u + \ + \frac{\partial}{\partial x}\rho u^2 + \frac{\partial p}{\partial x} = 0 \tag{2.19}$$

$$\frac{\partial}{\partial t}\rho(e + \frac{1}{2}u^2) + \frac{\partial}{\partial x}\rho u(e + \frac{1}{2}u^2) + \frac{\partial}{\partial x}pu = \dot{m}(e_0 + \frac{1}{2}u_0^2) \tag{2.20}$$

where ρ, u, p, and $\dot{m}$ are respectively the density, velocity internal energy, pressure and mass burning rate. The coefficients e_0 and u_0 correspond respectively to the internal energy and velocity of the gas leaving the burning surface. internal energy, pressure and mass burning rate. The equation of state is for a perfect gas

$$\frac{p}{\rho} = RT$$

where R is the gas constant. Equations (2.18) and (2.19) give

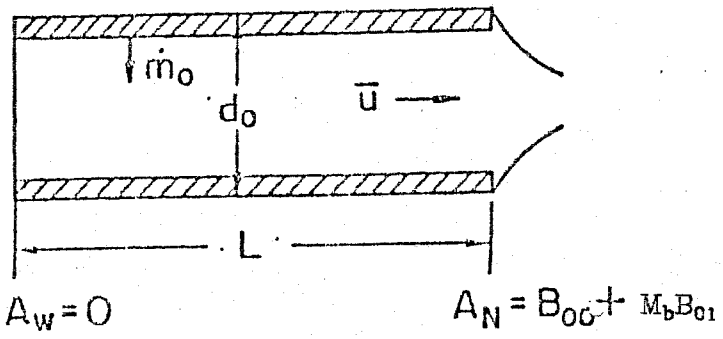

Figure 2.14 Schematic of a cylindrical rocket.

$$\frac{\partial \rho}{\partial t} + \frac{\partial(\rho u)}{\partial x} = \dot{m} \tag{2.26}$$

$$\rho \frac{\partial u}{\partial t} + \; + \rho u \frac{\partial u}{\partial x} + \frac{1}{\gamma} \frac{\partial p}{\partial x} = -u\dot{m} \tag{2.27}$$

$$\rho \frac{\partial T}{\partial t} + \rho u \frac{\partial T}{\partial x} - \frac{\gamma - 1}{\gamma} \frac{\partial p}{\partial t} - \frac{\gamma - 1}{\gamma} u \frac{\partial p}{\partial x} = -\dot{m}\left((T - 1) - \frac{1}{2}u^2 \right) \tag{2.28}$$

Equation (2.26)-(2.28) will be the basis to what follows in this chapter.

2.5.2. *The steady state* .

From Eqs. (2.26)-(2.28), the steady state equations becomes

$$\frac{d(\rho u)}{dx} = \dot{m} \tag{2.29}$$

$$\rho u \frac{du}{dx} + \frac{1}{\gamma} \frac{dp}{dx} = -u\dot{m} \tag{2.30}$$

$$\rho u \frac{dT}{dx} - \frac{\gamma - 1}{\gamma} u \frac{dp}{dx} = -\dot{m}\left((T - 1) - \frac{1}{2}u^2 \right) \tag{2.31}$$

$\dot{m}$ is generally a function of the pressure alone. In steady state, a common expression for $\dot{m}$ is $\dot{m} = ap^n$, where the exponent n indicates the sensitivity of the combustion to the pressure.

From the steady state gasdynamics, the pressure and density are constant to second order in the Mach number M_b at the burning surface. This means that $\dot{m}$ is constant to this order. Consequently, Eq. (2.29) gives

$$\rho\frac{\partial u}{\partial t} + \ + \rho u\frac{\partial u}{\partial x} + \frac{\partial p}{\partial x} = -u\dot{m} \tag{2.21}$$

On the other hand, Eqs. (2.18) and (2.20) yield

$$\rho\frac{\partial}{\partial t}(e + \frac{1}{2}u^2) + \rho u\frac{\partial}{\partial x}(e + \frac{1}{2}u^2) + \frac{\partial}{\partial x}pu = \dot{m}(e_0 - e + \frac{1}{2}u_0^2 - \frac{1}{2}u^2) = 0 \tag{2.22}$$

where we have have the approximation that gas leaving the burning surface has the same properties as the gas in the chamber, i.e. $e_0 = e$ and $u_0 = u$.

Multiplication of (2.19) by u and subtraction of the results from Eq. (2.22) gives

$$\rho\frac{\partial e}{\partial t} + \rho u\frac{\partial e}{\partial x} + p\frac{\partial u}{\partial x} = -\dot{m}(e - \frac{1}{2}u^2) \tag{2.23}$$

By introducing the enthalpy $h = e + \frac{p}{\rho}$ in (2.23) we get

$$\rho\frac{\partial h}{\partial t} + \rho u\frac{\partial h}{\partial x} - \frac{\partial p}{\partial t} - u\frac{\partial p}{\partial x} = -\dot{m}(h - \frac{1}{2}u^2) \tag{2.24}$$

If we now choose the enthalpy to be zero at the flame temperature and if the g as is perfect then the energy equation (2.24) becomes

$$\rho c_p\frac{\partial T}{\partial t} + \rho u c_p\frac{\partial T}{\partial x} - \frac{\partial p}{\partial t} - u\frac{\partial p}{\partial x} = -\dot{m}(c_p(T - T_f) - \frac{1}{2}u^2) \tag{2.25}$$

where T and c_p are respectively the gas temperature and the heat capacity at constant pressure. By using the dimensionless quantities introduced in Section 2.4.1, Eqs. (2.18), (2.21), and (2.25) become

$$u = \int_0^1 \dot{m} x$$

giving $u = bx$, where b is a constant determined by an overall mass balance of the chamber

$$M_b \pi d_0 = b\pi \frac{d_0^2}{4}$$

where d_0 is the constant diameter of the chamber. This equation gives

$$b = \frac{4}{d_0} M_b$$

which means that

$$u = \frac{4}{d_0} M_b x = M_b \bar{u}$$

with $\bar{u} = \frac{4}{d_0} x$.

2.5.3. *Linear stability analysis* .

In this section we will keep terms to order 0 (M_b); therefore the results in the last section are applicable, mainly that the pressure, density, and temperature are constant in the steady state. Expand[11] p, ρ, T, u, and $\dot{m}$ as follows

$$p = 1 + \varepsilon(p_{10} + M_b p_{11}) e^{ikt}$$

$$\rho = 1 + \varepsilon(\rho_{10} + M_b\rho_{11})eikt$$

$$T = 1 + \varepsilon(T_{10} + M_bT_{11})eikt$$

$$u = M_b\bar{u} + \varepsilon(u_{10} + M_bu_{11})eikt$$

$$\dot{m} = \bar{m} + m' = M_b + M_bR_b(\omega)\varepsilon(p_{10} + M_bp_{11})eikt$$

where use has been made in the last expression of the relationship $m' = R_b(\omega)\, p'$. The coefficient K is the linear complex frequency

$$K = \omega - i\alpha$$

with ω the real frequency and α the growth rate. Furthermore, we expand the complex frequency as follows

$$K = K_{00} + M_bK_{01} + \cdots$$

The objective of the following analysis is to determine K. By matching the coefficients of εe^{iKt} in the conservation equations, we get

$$iK_{00}\rho_{10} + \frac{du_{10}}{dx} = 0 \qquad (2.32)$$

$$iK_{00}u_{10} + \frac{1}{\gamma}\frac{dp_{10}}{dx} = 0 \qquad (2.33)$$

$$iK_{00}T_{10} - \frac{\gamma - 1}{\gamma} p_{10} = 0 \tag{2.34}$$

From the equation of state $\frac{p}{\rho} = RT$ we have

$$\frac{p'}{p} = \frac{\rho'}{\rho} - \frac{T'}{T} \tag{2.35}$$

Using (2.34) and (2.35) we get

$$\rho_{10} = \frac{p_{10}}{\gamma} \tag{2.36}$$

Substituting ρ_{10} in (2.32) and eliminating p_{10} between (2.32) and (2.33), yields

$$\frac{d^2u_{10}}{dx^2} + K_{00}u_{10} = 0. \tag{2.37}$$

In the following calculations we determine the boundary conditions satisfied by u_{10}. The boundary condition at the nozzle entrance is proportional, as we have seen in Section 2.4, to the Mach number M_e at the entrance of the nozzle. However, an overall mass balance over the whole length of the chamber gives

$$M_e \pi \frac{d_0^2}{4} = M_b d_0 L \tag{2.38}$$

which means $M_e = 4M_b \frac{L}{d_0}$. Consequently, the boundary condition at the nozzle is proportional to M_b for $\frac{L}{d_0}$ of order unity. In this case u_{10} satisfies

$$u_{10}(0) = u_{10}(1) = 0 \tag{2.39}$$

By solving Eq. (2.37) subject to conditions (2.39) we get

$$K_{00} = n\pi,\ n = 0,1,2,\cdots \tag{2.40}$$

and

$$u_{10} = A\sin K_{00}x$$

We now equate the coefficients of $\varepsilon M_b e^{iKt}$. The objective is to determine K_{01}. Equations (2.26)-(2.28) then give

$$iK_{00}\rho_{11} + \frac{du_{11}}{dx} = -\bar{u}\frac{d\rho_{10}}{dx} - \rho_{10}\frac{d\bar{u}}{dx} + R_p(\omega)p_{10} - iK_{01}\rho_{10} \tag{2.41}$$

$$iK_{00}u_{11} + \frac{1}{\gamma}\frac{dp_{11}}{dx} = -\bar{u}\frac{du_{10}}{dx} - u_{10}\frac{d\bar{u}}{dx} - u_{10} - iK_{01}u_{10} \tag{2.42}$$

$$iK_{00}T_{11} - \frac{\gamma - 1}{\gamma}p_{11} = -T_{10} \tag{2.43}$$

with, from the equation of state $\frac{p}{\rho} = RT$,

$$\rho_{10} = \frac{p_{10}}{\gamma},\ p_{11} = \rho_{11} + T_{11} \tag{2.44}$$

By using (2.44) and following the same procedure leading to (2.37), Eqs. (2.41)-

(2.43) yield the following equation for u_{11}

$$\frac{d^2u_{11}}{dx^2} + K_{00}u_{11} = [\ -2\frac{c}{\gamma} + R_p(\omega) - \frac{\gamma-1}{\gamma}] \tag{2.45}$$

$$-iK_{00}(c+1)u_{10} - \frac{c}{\gamma}\frac{d^2p_{10}}{dx^2} - iK_{00}cx\frac{du_{10}}{dx} - 2K_{01}K_{00}u_{10}$$

with $u_{10} = \sin K_{00}x$ and $p_{10} = -\gamma\cos K_{00}x$. The coefficient c is equal to $\frac{4}{d_0}$. The boundary conditions for u_{11} are, by using the nozzle boundary condition given in Section 2.4,

$$u_{11}(0) = 0,\ u_{11}(1) = \frac{\gamma-1}{2}\frac{M_e}{M_b}p_{10}(1)$$

which gives, using (2.38),

$$u_{11}(0) = 0,\ u_{11}(1) = 2\frac{\gamma-1}{d_0}p_{10}(1) \tag{2.45}$$

Following the same procedure leading to expression (2.40), we obtain the following expression for K_{01}

$$K_{01} = i\frac{\gamma}{2}[\ 2\frac{c}{\gamma} - R_p(\omega_{00}) - \frac{\gamma-1}{\gamma} + \frac{c+1}{\gamma} + 4\frac{\gamma-1}{d_0}] \tag{2.46}$$

where $c = \frac{4}{d_0}$. This means that the linear frequency shift is simply

$$\omega_{01} = -\frac{\gamma}{2} R_p^{(i)}(\omega_{00})$$

and the linear growth rate is

$$\alpha_{01} = \frac{\gamma}{2}\left[-2\frac{c}{\gamma} + R_p^{(r)}(\omega_{00}) + \frac{\gamma - 1}{\gamma} - \frac{c + 1}{\gamma} - 4\frac{\gamma - 1}{d_0}\right] \qquad (2.47)$$

For the second harmonic, we have the frequency shift

$$\omega_{01} = -\frac{\gamma}{2} R_p^{(i)}(2\omega_{00})$$

and the growth rate is

$$\alpha_{01} = \frac{\gamma}{2}\left[-2\frac{c}{\gamma} + R_p^{(r)}(2\omega_{00}) + \frac{\gamma - 1}{\gamma} - \frac{c + 1}{\gamma} - 4\frac{\gamma - 1}{d_0}\right] \qquad (2.48)$$

where we replace simply ω_{00} by $2\omega_{00}$.

Expressions (2.47) and (2.48) give the relationships between the growth rates for different harmonics of the wave and the physical and geometrical characteristics of the chamber. The interest of pursuing the calculations in this section will become evident when in the next chapters the amplitude and the conditions for existence and stability of the limit cycle will be given in terms of these growth rates.

After we have completed the formulation of the problem, we will state in the next section the objectives of this work.

2.6. Purpose of this work

We saw in Section 2.1 that the processes involved are clearly nonlinear. In Section 2.1.1 we saw that the gasdynamics nonlinearity may represent a major cause for leveling off the growth of the pressure wave in the combustion chamber. The effects of the nonlinear gasdynamics will be the object of Chapters 4 to 6. In these chapters, the linear problem is assumed to be well defined. In particular, the linear growth rates are assumed to be known quantities. The boundary conditions are assumed to be linear. We will discuss in details the influence of the nonlinear gasdynamics on the establisment of the limit cycle. The results will be given in terms of the linear and the nonlinear parameters of the problem, mainly the linear growth rates.

In Section 2.1.2 we saw that the nonlinear gasdynamics and a nonlinear combustion response may well be at the origin of the triggering phenomenon. Chapter 7 deals with this issue. Also, in that chapter, the linear problem is assumed to be well defined.

The methods to be used to solve approximately the nonlinear conservation equations will be discussed, through simple examples, in Chapter 3. The reader who is familiar with these methods may skip that chapter.

2.7. Concluding remarks

In this chapter, we presented the physical problem to be solved and we outlined the motivations and the objectives of this work. To achieve these objectives, a nonlinear analysis is necessary to carry out in order to interpret the phenomena involved. For solving analytically the conservation equations in combustion chamber, we can use only some approximate methods. The purpose of the next chapter is to introduce two known methods for expanding the conservation equations. We will apply these methods to some simple problems in order to show, in a simple way, the basic features of each method. The two

methods will be applied in Chapter 4 to the nonlinear conservation equations in combustion chambers.

REFERENCES 2

1. " *T-Burner Manual*," edited by Culick, F. E. C., CPIA pub. 191, Nov. 1969.

2. Crocco, L. " Theoretical Studies on Liquid-Propellant Rocket Instability ", *Tenth Symposium (International) on Combustion*, The Combustion Institute, 1965.

3. Culick, F. E. C. and Levine, J. N." Comparison of Approximate and Numerical Analysis of Nonlinear Combustion Instabilities," *AIAA* paper 74-201, January 1974.

4. Levine, J. N. and Baum, J. D." A numerical Study of Nonlinear Instabilities in Solid Rockets Motors," *AIAA* paper 81-1524, July 1981.

5. Micheli, P. L. et al " Experiments on Subscale Tactical Solid Propellant Rockets," Aerojet Corporation, Sacramento, CA, 1982. (To be published).

6. Brownlee, W. G. " Nonlinear Axial Combustion Instability in Solid Propellant Motors ", *AIAA* Journal, Vol. 2, NO. 2, 1964.

7. Kooker, D. E. and Zinn, B. T. " Triggering Axial Instabilities in Solid Rockets: Numerical Predictions," *AIAA* paper 73-1298.

8. Culick, F. E. C. " Acoustic Oscillations in Solid Propellant Rockets Chambers," *Acta Astronautica*, Vol. 12, NO. 2, 1966.

9. Culick, F. E. C. " A Review of Calculations for Unsteady Burning of a Solid Propellant ", *AIAA* Journal, Vol. 6, NO.12, 1968.

10 Levine, J. N. and Culick, F. E. C. " Numerical Analysis of Nonlinear Longitudinal Combustion Instability in Metalized Propellant Solid Rocket Motors ", *AFRPL*-TR-72-88, 1972.

11. Flandro, G. A. "Stability prediction for solid propellant rocket motors with high speed mean flow," AFRPL-TR 79-98, 1980.

Chapter 3

EXPANSION METHODS

3.1. Introduction

The approximate methods to solve nonlinear partial differential equations may be classified in three categories: the asymptotic, the weighted residual, and the iterative methods. In the asymptotic methods we look for a solution when a physical parameter, or variable, of the problem is very small. A typical asymptotic method is the perturbation method[1].

In the methods of weighted residual, we desire the approximate solution to be close to the exact one in a way that the difference, or residual, be minimized in some sense. A typical weighted residual method is Galerkin's method[2,3] which requires the weighted integrals of the residuals to vanish. A typical case of Galerkin's method is the expansion of the solution in the normal functions of the linearized problem.

The third category is the iterative methods[4,5] which attempt to solve the equations by repetitive calculations starting from the solution of a simplified form of the equations and then successively improve the approximation. In this work, we deal only with the first two categories.

We shall discuss possible approximate methods for finding the final oscillatory behavior, or the asymptotic solution in time, of a nonlinear partial differential equation. We deal here with two methods.

A particular case, derived from the method of weighted residuals, consists of expanding the solution in the normal functions, or modes, of the linear

problem. As a means of minimizing the residual, we use a spacial averaging technique based on the use of Green's theorem (see Chapter 4, Section 4.6). For hyperbolic equations, this averaging technique usually leads to a system of nonlinear ordinary differential equations of second order for the time-dependent parts. We further reduce this system by applying the time-averaging technique, which is a perturbation method, to find a system of first order nonlinear ordinary differential equations. The asymptotic solution is obtained by examining the solution of this system when $t \to \infty$.

One may also use a method derived from the perturbation method in which the solution is expanded in powers of a small parameter. Since our objective is to find the *asymptotic* solution with a given behavior in time, i.e. harmonic, we assume *a priori* the behavior in time. Essentially, the method reduces to finding the harmonic solutions for the partial differential equations. Therefore, the problem of secular terms, which correspond to the infinite growth of the approximate solution in time and usually encountered[6] in perturbation methods, is avoided here by specifying the behavior of the solution in time. Hereafter, this technique will be referred to as the "asymptotic-perturbation technique". In tne next section we will show that this technique is a particular case of Stokes' expansion. We will use interchangeably the name of asymptotic-perturbation technique or Stokes' expansion to designate the same method of solution. This corresponds to the first method introduced in Chapter 1.

Finally, we can use a mixed procedure. We start with a perturbation method in a small parameter but we keep terms of higher orders. The direct result is that the partial differential equation remains nonlinear. Now, we apply the method of averaging in space and then in time, described above. The advantage is that we reduce the nonlinearity to any desired order and avoid the secularity of the solution by use of the regular perturbation method. Hereafter, this

technique will be referred to as the " perturbation-averaging technique ". This is a particular case of Galerkin's method. We will use interchangeably the name of perturbation-averaging technique or Galerkin's method to designate the same method of solution. This corresponds to the second method introduced in Chapter 1.

The aim of this chapter is to show, using simple examples, how the asymptotic-perturbation and the perturbation-averaging techniques allow the determination of the asymptotic oscillatory behavior of nonlinear partial differential equations and what are the advantages of each.

Since our goal is to find the limiting amplitude, we present in Section 3.2 an example of a nonlinear oscillator which exhibits a limit cycle behavior. The equivalence of the asymptotic-perturbation and perturbation-averaging techniques in determining the limit cycle is shown. In Section 3.3 we present a two-parameter Stokes' expansion. The purpose of this section is to show how Stokes' expansion can be expanded in many small parameters. This point will used in Chapter 4 where the two small parameters will be the amplitude of the wave and the Mach number of the mean flow. The ultimate goal of Chapter 3 is to present a basis for an expansion of the solution of the nonlinear conservation equations in combustion chambers. These equations are usually hyperbolic. For this reason, we present in Sections 3.4 and 3.5 an example of a nonlinear hyperbolic equation, where both techniques are used to find the asymptotic solution.

3.2. Limit cycle for a nonlinear oscillator

In this section, we will review how the limiting amplitude of the motion of a nonlinear oscillator can be determined with an expansion in the asymptotic amplitude of the motion of the nonlinear oscillator. Let us consider the well-known Van der Pol's equation[6]

$$\ddot{y} + \sigma (y^2 - \sigma^2) \dot{y} + y = 0 \qquad (3.1)$$

where $\sigma << 1$. We would like to determine the limit cycle and its amplitude. First, we apply the asymptotic-perturbation technique; and second, we apply the method of averaging. The two methods will be shown to yield the same results.

3.2.1. *Asymptotic-perturbation technique or Stokes' expansion.*

In this section, we will review how the limiting amplitude of the motion of a nonlinear oscillator can be determined with an expansion in the asymptotic amplitude of the motion of the nonlinear oscillator.

We would like to determine the limit cycle for Eq. (3.1) and its amplitude. First, we apply the asymptotic-perturbation technique and second, in the next section we apply the method of averaging. The two methods will be shown to yield the same results.

Now we introduce the asymptotic-perturbation technique and we apply it to the same nonlinear problem given in (3.1). The solution is expanded in terms of the amplitude of the solution to the linear problem as a small parameter. However, using the expansion in the amplitude requires some choice of the expansion: what terms should be included and in which form. Here, we will use a form of an expansion invented by Stokes[7] in the last century. In 1847, Stokes, in the course of study of the velocity of propagation of oscillatory waves on an incompressible flow in an open channel, expanded the height y of the wave as follows

$$y = a \cos \omega x + f_2 a^2 \cos 2\omega x + \text{etc.} \qquad (3.2)$$

where a is the height of the wave to first approximation, x is the direction of propagation, ω is the frequency of the wave, and f_2, etc. are coefficients to be

determined from a recursive solution of the nonlinear equations governing the behavior of the wave by equating the coefficients of $a^m \cos n\omega x$. This is true only if we are looking for *periodic* solutions, since we can specify the final solution independently of the initial conditions. In fact, the periodicity conditions replace the initial conditions. In (3.2), only one mode is taken into account in the linear regime. The reader is invited to read the book by Kevorkian and Cole[8] and the paper by Millman and Keller[9] on this subject.

Here, we apply the same procedure to problem (3.1). The structure of the expansion is dictated by the form of the nonlinear terms. Assume, for example, that the solution to the linear problem is of the form $\frac{1}{2}\varepsilon e^{iKt} + \frac{1}{2}\varepsilon e^{-iKt}$, where ε is the amplitude of the solution; then the cubic nonlinearity generates third order terms in ε of the form $\varepsilon^3 e^{3iKt} + \varepsilon^3 e^{iKt}$ + etc. These terms interact with the linear terms, by means of the cubic nonlinearity, to produce seventh, eighth, and ninth order terms in ε, and so forth.

We start by first assuming that the asymptotic solution has the following form :

$$2\, y_{lim} = \varepsilon\, e^{iKt} + \varepsilon^2\, b_0 + \varepsilon^3\, b_3\, e^{iKt} + \ldots + c.c. \qquad (3.3)$$

where c.c. stands for complex conjugate. Only one mode is taken into account in the linear regime. This form is generated following the structure of the nonlinear term $y^2\dot{y}$ in (3.1). For example, the square of $\varepsilon\, e^{iKt}$ + c.c generates a second order in ε constant term represented by b_0; $y^2\dot{y}$ then will couple the second order term b_0 and the first order term $\varepsilon\, e^{iKt}$ to produce a third order term represented by b_3. The complex conjugate must be present, since the quantity y_{lim} is real. We now expand the frequency K as follows

$$K = K_0 + \varepsilon K_1 + \varepsilon^2 K_2 + \ldots$$

with K_1, K_2, in general, complex quantities and ε a measure of the amplitude of the asymptotic solution. Now expansion (3.3) gives

$$4y_{lim}^2 = \varepsilon^2 e^{2iKt} + 2\varepsilon^2 + 2\varepsilon^3 b_0 e^{iKt} + \ldots + c.c.$$

$$2\dot{y}_{lim} = iK\varepsilon e^{iKt} + iK\varepsilon^3 b_3 e^{iKt} + \ldots + c.c.$$

$$2\ddot{y}_{lim} = -K^2\varepsilon e^{iKt} - K^2\varepsilon^3 b_3 e^{iKt} + \ldots + c.c.$$

Multiplying the first two of these expresions, we have

$$8y_{lim}^2\dot{y}_{lim} = iK\varepsilon^3 e^{iKt} + iK\varepsilon^3 e^{3iKt} + \ldots + c.c..$$

After substitution of these expansions and that of K in (3.1), equating the coefficients of εe^{iKt} yields

$$-K_0^2 - i\sigma^3 K_0 + 1 = 0$$

For $\sigma << 1$, this equation gives

$$K_0 = -i\frac{\sigma^3}{2} \pm 1 \qquad (3.4)$$

For illustration, we keep the + sign term only. We collect now the coefficients of $\varepsilon^2 e^{iKt}$ to get

$$K_1(2K_0 + i\,\sigma) = 0$$

which means that $K_1 = 0$. Gathering terms proportional to $\varepsilon^3 e^{iKt}$, we have

$$2\,K_2\,K_0 - \frac{i}{8}\sigma\,K_0 + i\,\sigma^3\,K_2 = 0$$

with solution

$$K_2 = \frac{i}{8}\sigma\,\frac{K_0}{2\,K_0 + i\,\sigma^3}$$

For $\sigma << 1$, K_2 reduces, using (3.4), to

$$K_2 = \frac{\sigma^2}{16} + i\,\frac{\sigma}{8}. \qquad (3.5)$$

When the limiting amplitude is reached, the complex frequency K should be real, giving

$$\mathrm{Im}(\,K_0 + \varepsilon^2\,K_2 + \text{etc.}\,) = 0$$

where Im stands for imaginary part. Therefore, using (3.4) and (3.5),

$$\varepsilon = 2\sigma << 1. \qquad (3.6)$$

Eqs. (3.4) and (3.5) also yield

$$\omega = 1 + \frac{\sigma^4}{16}.$$

Consequently, from (2.18), the limit solution becomes

$$y_{lim} = \sigma(e^{it} + c.c.) + 0(\sigma^2)$$

$$= 2\,\sigma \cos t + 0(\sigma^3). \qquad (3.7)$$

This is a periodic solution. In the phase plane (y , $\dot{y}$), this is a circle. That is the origin of the name "limit cycle". In general, a limit cycle corresponds to a closed orbit in the phase plane (y , $\dot{y}$). Moreover, we see from (3.6) that $\varepsilon << 1$; therefore, the expansion is legitimate.

3.2.2. *Application of the method of averaging* . As a means of supporting the results of the expansion in the amplitude and in order to show its appropriateness in giving useful results, we will check the results in (3.7) by using the method of time-averaging, which is a step in the perturbation-averaging technique or Galerkin's method. Write the solution in the following form :

$$y = a \cos (t + \varphi (t)) = a \cos \psi.$$

This form assumes *a priori* that the initial conditions contain only the first harmonic and that the higher harmonics are negligible. This is an important feature of the Galerkin's method, where essentially all the harmonics should be present in the expansion. However, for $\sigma << 1$, we expect all the harmonics higher than the first to be negligible in comparison with the first harmonic.

It is a common practice to assume Minorsky's condition[10]

$$\dot{a}\,(t)\cos\psi - a\,\dot{\varphi}\sin\psi = 0. \tag{3.8}$$

which simply states that the velocity of the oscillator is

$$\dot{y} = -a\,(t)\sin\psi \tag{3.9}$$

as if the oscillator were linear. The acceleration then becomes, using Eqs. (3.1) and (3.9),

$$\ddot{y} = -a\sin\psi - a\,(1-\dot{\varphi})\cos\psi. \tag{3.10}$$

Now, we substitute Eq. (3.10) in (3.1) to get

$$a\,(t)\,\dot{\varphi}\cos\psi + \dot{a}\sin\psi = \sigma\, a^3\cos^2\psi\,\text{sinpsi}. \tag{3.11}$$

Eqs. (3.8) and (3.11) may then be solved for $\dot{a}$ and $\dot{\varphi}$, to give

$$\dot{a} = -\frac{\sigma}{2\pi}\int_0^{2\pi}(a^3\cos^2\psi\sin\psi - a\sigma^3\sin\psi)\sin\psi d\psi$$

$$\dot{\varphi} = \frac{\sigma}{2\pi}\int_0^{2\pi}(a^3\cos^2\psi\sin\psi - a\sigma^3\sin\psi)\cos\psi d\psi$$

These two expressions give

$$\dot{a} = -\frac{\sigma}{2} a \left(\frac{a^2}{4} - \sigma^2 \right). \tag{3.12}$$

$$\dot{\varphi} = 0 \tag{3.13}$$

which are correct to first[11] order in σ. When the limit cycle is approached, $\dot{a}$ vanishes and $\dot{\varphi}$ becomes a constant. Equations (3.12) and (3.13) then give the amplitude and frequency of the limit cycle :

$$a = 2\sigma + 0(\sigma)$$

$$\omega = 1 + 0(\sigma).$$

The limit cycle solution becomes

$$y_{lim} = 2\sigma \cos t + 0(\sigma).$$

Hence, Eq. (3.7) is recovered. The two methods yield the same result.

3.2.3. *Stability of the limit cycle .*

One notices, from (3.12), that the existence of the limit cycle is independent of the sign of σ . However, the stability of the limit cycle depends on this sign. In fact, from Eq. (3.12), the phase diagram (a, $\dot{a}$), Figure 3.1, shows that the limit cycle is stable if, and only if,

$$\sigma > 0. \tag{3.13}$$

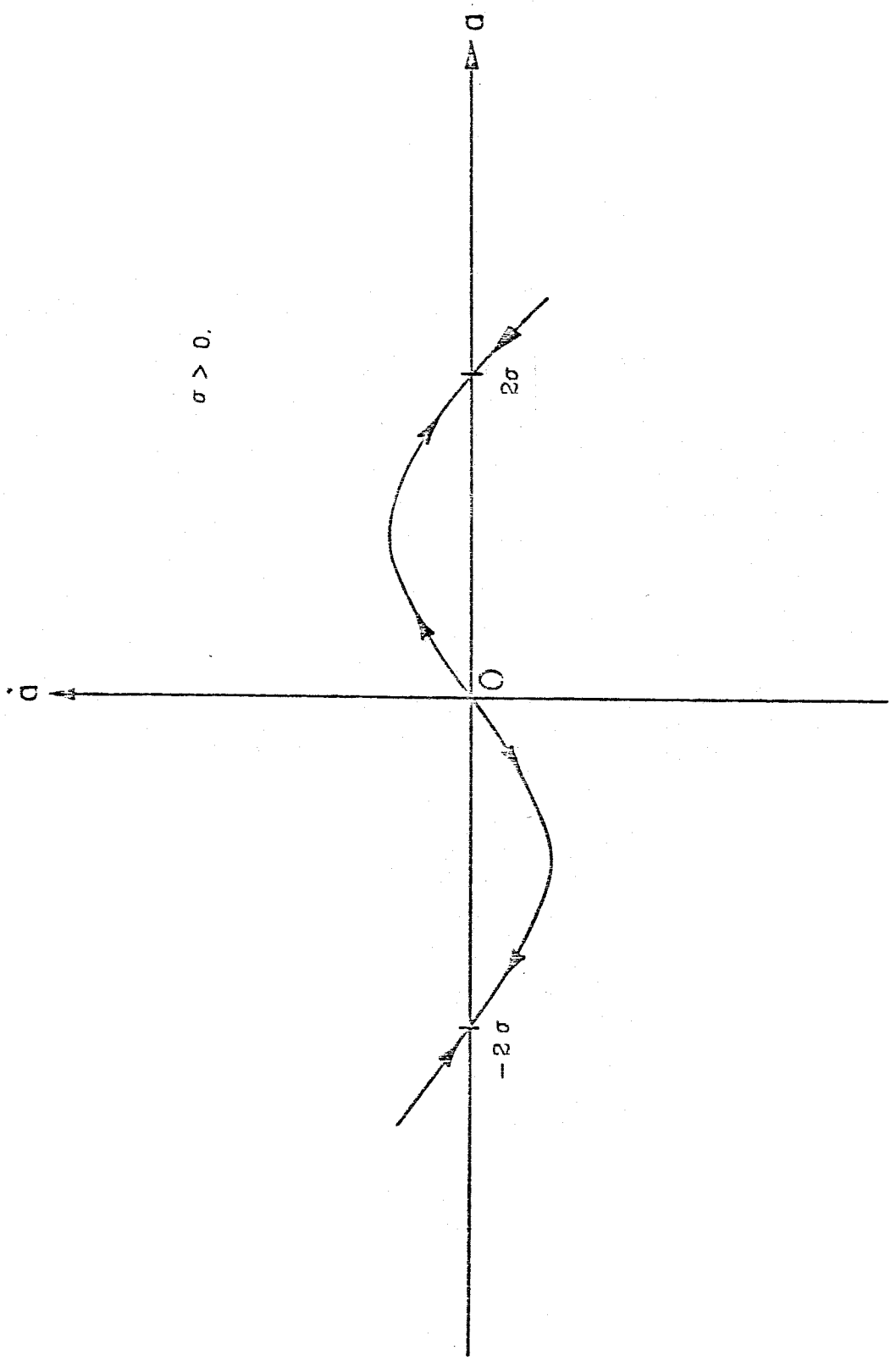

Figure 3.1 Phase diagram of (a,ȧ)

This result can also be found using the asymptotic-perturbation technique Write the solution y of (3.1) as follows

$$y = y_{lim} + y'$$

where y_{lim} is the limit cycle solution, y_{lim} = 2 sigma cost, and y' is a small perturbation around the limit cycle. Linearizing (3.1) near y_{lim} yields

$$\ddot{y}' + y' = -\sigma \left[(4\sigma^2\cos^2 t - \sigma^2)\, \dot{y}' - 4\sigma^2 \sin 2t\, y' \right] \tag{3.14}$$

This is a linear system. We can always expand y' as follows

$$y'(t) = a(t) \sin(\omega t + \varphi) \equiv A(t) \sin t + B(t) \cos t$$

where $A = a\cos\varphi$ and $B = a\sin\varphi$. Following the method of averaging (see Chapter 4, Section 4.6), A (t) and B (t) satisfy the following equations

$$\frac{dA}{dt} = \frac{1}{2\pi}\int_0^{2\pi} F_n \cos t\, dt \tag{3.15}$$

$$\frac{dB}{dt} = -\frac{1}{2\pi}\int_0^{2\pi} F_n \sin t\, dt. \tag{3.16}$$

where F_n is the right-hand side of (3.14). These equations reduce to

$$\frac{dA}{dt} = 0., \quad \frac{dB}{dt} = -\sigma B$$

giving

$$B = B_0 e^{-\sigma t}$$

Hence, the limit cycle is stable for

$$\sigma > 0.$$

This is the same result (3.13). This technique will be used in Chapter 5 to find the stability criteria for the limit cycles of pressure oscillations in combustion chambers.

3.3. Two-parameter expansion using Stokes method

In this section, we apply Stokes' expansion in two parameters, mainly the amplitude ε of the solution and another small parameter, for example σ given (3.1). We apply the technique to the same problem (3.1) treated in the last section. The only difference is that here we expand in two parameters. The interest of this section will be demonstrated in the next chapter where the small parameter σ corresponds to the average Mach number of the mean flow. The treatment of the interaction between the acoustic field and the mean flow field will be greatly facilatated if we can expand in two parameters.

For convenience, we write again Eq. (3.1)

$$\ddot{y} + \sigma (y^2 - \sigma^2) \dot{y} + y = 0 \qquad (3.1)$$

where $\sigma << 1$. Expand y as follows

$$2y_{lim} = \varepsilon(1 + \sigma y_{11} + \sigma^2 y_{12} + \sigma^3 y_{13} + ...)e^{iKt}$$

$$+ \varepsilon^3(y_{30} + \sigma y_{31} + \sigma^3 y_{32} + \sigma^3 y_{33} + \ldots)e^{iKt}$$

Moreover, the complex frequency K is expanded as follows

$$K = K_{00} + \sigma K_{01} + \cdots + \varepsilon(K_{10} + \sigma K_{11} + \cdots)$$

$$+\varepsilon^2(K_{20} + \sigma K_{21} + \cdots)$$

Formally speaking, it is always possible to expand in many parameters, regardless of their relative magnitudes. However, when we cut off the expansion the relative magnitudes of the different parameters should be taken into account. This point will be explained further at the end of this section when some results regarding the limit cycle are obtained.

We now determine the limit cycle of (3.1) using the two-parameter Stokes' expansion. By equating the coefficients of $\varepsilon\sigma^0 e^{iKt}$, we get

$$K_{00}^2 = 1 \tag{3.17}$$

We now collect terms proportional to $\varepsilon\sigma e^{iKt}$ and $\varepsilon\sigma^2 e^{iKt}$ to get

$$K_{01} = K_{02} = 0$$

By gathering terms proportional to $\varepsilon\sigma^3 e^{iKt}$, we obtain

$$- 2K_{03}K_{00} - K_{00}^2 y_{13} + y_{13} - iK_{00} = 0$$

giving, with the use of (3.17),

$$K_{03} = -\frac{i}{2} \tag{3.18}$$

On the other hand, equating the coefficients of $\varepsilon^3\sigma^0 e^{iKt}$ yields $K_{20} = 0$. We now collect the terms proportional to $\varepsilon^3\sigma e^{iKt}$ to obtain

$$-2K_{21}K_{00} - K_{00}^2 y_{31} + y_{31} + \frac{i}{4}K_{00} = 0$$

which gives, using (3.17),

$$K_{21} = \frac{i}{8} \tag{3.19}$$

$$\varepsilon^2\sigma\frac{i}{8} - \sigma^3\frac{i}{2} = 0$$

which means that

$$\varepsilon = 2\sigma \tag{3.20}$$

This is the same relation (3.6) found in the last section. The purpose of this example is to show that Stokes' expansion can be extended to many parameters. The only requirement is to when to cut off the expansion. For example, from (3.20), if we cut off the expansion in the linear part of y_{lim} to $\varepsilon\sigma^3$ then the terms in $\varepsilon^3\sigma$ should be the last terms to be included in the nonlinear expansion of y_{lim}, since ε and σ are of the same magnitude. But the relationship between ε and σ has no effect on the expansion itself. Similar situation will be encountered in Chapter 4, where σ will correspond to the Mach number of the mean flow and ε

to the amplitude of the periodic acoustic wave.

In the following calculations, we apply the two methods to some nonlinear hyperbolic equations and we will compare the results of the applications

3.4. Application of the two methods to some nonlinear hyperbolic equations

In this section, we apply Stokes' expansion and Galerkin's method to some nonlinear hyperbolic equations. Some conclusions will be drawn as to the features of each method.

3.4.1. *Application of Stokes expansion* . We now apply Stokes' method to the following nonlinear wave equation

$$\frac{\partial^2 p}{\partial t^2} - \frac{\partial^2 p}{\partial x^2} = \sigma \left((\mid p \mid^2 - 1) \frac{\partial p}{\partial t} + c\, p^2 \right) \tag{3.21}$$

where c is an arbitrary constant; The boundary and initial conditions are

$$\frac{\partial p}{\partial x}(0,t) = 0. \,, \quad \frac{\partial p}{\partial x}(\pi,t) = \frac{\pi}{2} a_b p\,(\pi,t) \tag{3.22}$$

$$p(x,t) = p_0\,(x, t + T_0)$$

where T_0 is the period of the solution; and a_b is a constant different from zero for reason shown in Eq. (3.28). We now use Stokes' expansion in the amplitude of the wave to find the limit cycle. Write the asymptotic solution p(x,t) and the complex frequency K in the following forms :

$$p\,(\,x,\,t\,) = \varepsilon\, e^{iKt}\; p_1\,(\,x\,) + \varepsilon^3\, e^{iKt}\; p_3\,(\,x\,) + ... + \text{c.c.} \tag{3.23}$$

The frequency K is expanded in ε

$$K = K_0 + \varepsilon K_1 + \varepsilon^2 K_2 + \ldots$$

Expansion (3.23) gives

$$| p |^2 = 2 \varepsilon^2 | p_1 (x) |^2 + \varepsilon^2 p_1^2 (x) e^{2 i K t}$$

$$+ \varepsilon^3 p_1^* (x) p_2 (x) e^{i K t} + \varepsilon^3 p_1 (x) p_2^{(0)} (x) e^{i K t} + \cdots + \text{c.c.}$$

$$\frac{\partial p}{\partial t} = i K \varepsilon e^{i K t} p_1 (x) + 2 i K \varepsilon^2 p_2 e^{2 i K t} + i K \varepsilon^3 p_3 (x) e^{i K t} + \cdots + \text{c.c.}$$

$$\frac{\partial^2 p}{\partial t^2} = - K^2 p_1 (x) \varepsilon e^{i K t} - 4 K^2 \varepsilon^2 p_2 (x) \varepsilon e^{2 i K t}$$

$$- K^2 \varepsilon^3 p_3 (x) \varepsilon e^{i K t} + \cdots + \text{c.c.}$$

$$p^2 = 2 \varepsilon^2 | p_1 (x) |^2 + \varepsilon^2 p_1^2 (x) e^{2 i K t} +$$

$$2 \varepsilon^3 p_1^* (x) p_2 (x) e^{i K t} + 2 \varepsilon^3 p_1 (x) p_2^{(0)} (x) e^{i K t} + \cdots + \text{c.c.}$$

Substitution of the above expressions in (3.21) gives an expansion in $\varepsilon^l e^{n i K t}$, with l,n=1, 2, etc. By equating the coefficients of $\varepsilon e^{i K t}$ in (3.21), we get

$$\frac{d^2 p_1}{dx^2} + (K_0^2 - i\,\sigma\,K_0)\,p_1(x) = 0$$

The solution to this equation is

$$p_1(x) = A\,e^{i k_1 x} + B\,e^{-i k_1 x} \tag{3.24}$$

where

$$k_1 = (K_0^2 - i\,\sigma\,K_0)^{\frac{1}{2}}. \tag{3.25}$$

The boundary conditions (3.22) have to be satisfied. This gives A = B and the following values for k_1 :

$$k_1 \tan k_1 = -\frac{1}{2}\pi a_b \tag{3.26}$$

For simplicity, we assume that a_b is pure real number, k_1 then becomes a real number and the first mode can be written as

$$\varepsilon\,p_1(x) = \frac{\varepsilon}{2} e^{i k_1 x} + \frac{\varepsilon}{2} e^{-i k_1 x}$$

with ε the amplitude of this mode.

Our objective is to find K_2 which will show, as we will see later in the analysis (Eq. (3.29)), the effects of the various terms in Eq. (3.21). To do so, $p_2^{(0)}$ and p_2 are required. By gathering terms proportional to $\varepsilon^2 e^{0iKt}$, we get

$$\frac{d^2 p_2^{(0)}}{dx^2} = -2\sigma c$$

after using conditions (3.22), the solution is

$$p_2^{(0)} = -c\sigma x^2 + \delta \tag{3.27}$$

where

$$\delta = -4\frac{c\sigma}{a_b} + c\sigma\pi^2 \tag{3.28}$$

We see that when a_b vanishes, δ, and therefore $p_2^{(0)}$, cannot be determined. A similar situation will be encountered in the next chapter when we treat the non-linear conservation equations in combustion chambers. Now equate the coefficients of $\varepsilon^2 e^{iKt}$, to find

$$K_1 [-2K_0 + i\sigma] p_1(x) = 0$$

which means $K_1 = 0$. Gathering terms proportional to $\varepsilon^2 e^{2iKt}$ yields

$$\frac{d^2 p_2}{dx^2} + (4K_0^2 - 2i\sigma K_0) p_2(x) = c\sigma p_1^2(x)$$

The solution satisfying conditions (3.22) is

$$p_2(x) = \gamma_0 + \gamma_2 (e^{2ik_1 x} + e^{-2ik_1 x}) + \frac{\gamma_3}{\gamma_4} (e^{ik_2 x} + e^{-ik_2 x})$$

where

$$k_2^2 = 4K_0^2 - 2i\sigma K_0$$

$$\gamma_0 = \frac{\sigma c}{2k_2^2}\,,\ \gamma_2 = \frac{\sigma c}{4(k_2^2 - 4k_1^2)}$$

$$\gamma_3 = -2ik_1\gamma_2\,(e^{2i\pi k_1} - e^{-2i\pi k_1}) + \frac{\pi}{2}[\gamma_0 + \gamma_2(e^{2i\pi k_1} + e^{-2i\pi k_1})]$$

$$\gamma_4 = ik_2(e^{i\pi k_2} - e^{-i\pi k_2}) - \frac{\pi}{2}a_b(e^{i\pi k_2} + e^{-i\pi k_2})$$

Finally, we equate the coefficients of $\varepsilon^3 e^{iKt}$ to find

$$\frac{d^2p_3}{dx^2} + (K_0^2 - i\,\sigma\,K_0)\,p_3\,(x) = -2\,K_2\,K_0\,p_1(x) - 2\,i\,\sigma\,K_0\,|p_1(x)|^2 p_1(x)$$

$$+ i\,\sigma\,K_2\,p_1(x) + 2\,\sigma\,c\,p_1^*(x)p_2(x) + 2\,\sigma\,c\,p_1 p_2^{(0)}(x)$$

We apply Green's theorem to this equation, which consists here of multiplying both sides of the equation by $p_1(x)$ and integrating from 0 to π, to find

$$K_2[i\sigma - 2K_0]\,E_1^2 = [p_1(x)f_3(x)]_0^\pi - [f_1(x)p_3(x)]_0^\pi - \int_0^\pi hp_1(x)dx \qquad (3.29)$$

where

$$E_1^2 = \int_0^{\pi} p_1^2(x)dx \, , \, f_j(x) = \frac{dp_j}{dx} \, , \, j = 1,3.$$

$$h = (3.30) - 2\,i\,\sigma\,K_0\,|p_1(x)|^2 p_1(x) + 2\,\sigma\,c\,p_1^*(x)p_2(x) + 2\,\sigma\,c\,p_1(x)p_2^{(0)}(x)$$

Expression (3.29) gives the complex shift of frequency K_2 . The effects of the various parameters in Eq. (3.21) are clear, especially the effect of the second order nonlinear term cp^2.

Expression (3.29) leads to the suspicion that the knowledge of $p_3(x)$ is necessary to determine K_2. However, it will be shown in Appendix 4A that only second, or lower, order terms are necessary. It should also be emphasized that K_0 corresponds to first order, in ε, problem; K_1 to second order; and K_2 to third order. This means that the determination of the eigenvalue to the *third* order problem, here K_2, necessitates only the previous determination of the *second*, or lower, order eigenfunctions.

One notices also that the boundary conditions (3.22) are *locally* satisfied by the expansion in the amplitude. This is not the case of the expansion in the normal mode $\eta(t)\cos x$ since $\cos x$ doesn't satisfy the second condition in (3.22). However, the global satisfaction over the whole volume is satisfied by means of Green's theorem. This is a general characteristic of the method of expansion in the normal modes.

3.4.2. *The method of perturbation-averaging: Application and disadvantages* . In this section, we apply the perturbation-averaging technique to a simple problem and we show how disadvantageous it is to use this technique to obtain high order approximations for the asymptotic solution. Consider the following nonlinear hyperbolic equation

$$\frac{\partial^2 p}{\partial t^2} - \frac{\partial^2 p}{\partial x^2} = p^2 \tag{3.31}$$

with same initial and boundary conditions given for problem (3.21). We expand p as follows

$$p = \varepsilon\, p_1 + \varepsilon^2 p_2 + \varepsilon^3\, p_3 + \text{etc.}$$

where ε is a measure of the amplitude of the solution to the linear problem. We would like to determine the third order correction p_3. First, we start with the linear problem

$$\frac{\partial^2 p_1}{\partial t^2} - \frac{\partial^2 p_1}{\partial x^2} = 0. \tag{3.32}$$

The following expansion of p_1 satisfies (3.32) and (3.22)

$$\varepsilon\, p_1 = \eta_0\,(t) + \eta_1\,(t)\cos x + \eta_2\,(t)\cos 2x + \text{etc.} \tag{3.33}$$

where, in the linear problem,

$$\ddot{\eta}_1 + \eta_1 = a_b\, \eta_1$$

$$\ddot{\eta}_2 + 4\eta_1 = a_b\, \eta_2$$

Now we treat the second order problem. The quantity p_2 satisfies the following equation

$$\frac{\partial^2 p_2}{\partial t^2} - \frac{\partial^2 p_2}{\partial x^2} = p_1^2. \tag{3.34}$$

Add (3.32) and (3.34) to get

$$\frac{\partial^2 p'}{\partial t^2} - \frac{\partial^2 p'}{\partial x^2} = \varepsilon^2 p_1^2. \tag{3.35}$$

where $p' = \varepsilon p_1 + \varepsilon^2 p_2$. Expand p' and p_1 in the *same* normal modes of the linear problem

$$\varepsilon p_1 = \eta_0 (t) + \eta_1 (t) \cos x + \eta_2 (t) \cos 2x + \text{etc.} \tag{3.36}$$

$$p' = \eta_0 (t) + \eta_1 (t) \cos x + \eta_2 (t) \cos 2x + \text{etc.}$$

Substitute these expansions in (3.35) and apply Green's theorem, to find an infinite set of nonlinear oscillators, one oscillator for each mode,

$$\ddot{\eta}_0 = \frac{1}{2}\eta_1^2 + \frac{1}{2}\eta_2^2$$

$$\ddot{\eta}_1 + \eta_1 = a_b \eta_1 + \eta_1\eta_2$$

$$\ddot{\eta}_2 + 4\eta_1 = a_b \eta_2 + \frac{1}{2}\eta_1^2$$

This is the same method reported by Culick[12]. As we see from the last two equations, the zeroth mode $\eta_0(t)$ does not influence the first and the second

modes. This is not the case for the asymptotic-perturbation technique where the zeroth mode $p_2^{(0)}$ is present, Eq. (3.30) in the correction K_2 of the complex frequency K of the first mode. To include these effects in the analysis here, one may extend the analysis to third order by determining p_3 The quantity p_3 satisfies

$$\frac{\partial^2 p_3}{\partial t^2} - \frac{\partial^2 p_3}{\partial x^2} = 2\, p_1 p_2. \tag{3.37}$$

Adding this equation to (3.34) and (3.32) gives

$$\frac{\partial^2 p'}{\partial t^2} - \frac{\partial^2 p'}{\partial x^2} = \varepsilon^2\, p_1^2 + 2\varepsilon^3\, p_1 p_2. \tag{3.38}$$

where now $p' = \varepsilon\, p_1 + \varepsilon^2\, p_2 + \varepsilon^3\, p_3$. As usual, we expand p_1 as follows

$$\varepsilon\, p_1 = \eta_0\,(t) + \eta_1\,(t) \cos x + \eta_2\,(t) \cos 2x + \text{etc.} \tag{3.39}$$

However, the expansion of p_2 should now satisfy (3.34). Currently, there is, up to our knowledge, no formal and consistent way to handle (3.37) by expansion in the normal modes of the linear problem. This is a major reason why we use the asymptotic-perturbation technique to handle high orders. Extension of the perturbation-averaging technique to third order is part of our future research.

The choice of example (3.31) to show the simplicity of the application of the method of expansion in the asymptotic amplitude is intended as an illustration of what will happen when we deal with more complicated problems. The conservation equations of the flow field in combustion chambers present a kind of

second order nonlinearity similar to the one shown in Eq. (3.30). For example, the convection term $u.\nabla u$ is a form of second order nonlinearity. Remarkably, Stokes[9] found that a third order approximation in ε, the asymptotic amplitude, was necessary to show the dependence of the velocity of propagation of the wave in an open channel on the amplitude of the wave. For this purpose he used an expansion similar to the expansion in Section 3.4. It is clear that when higher order approximations are needed a perturbation in the amplitude is useful to apply.

3.5. Concluding remarks

The major result of this chapter is that the asymptotic-perturbation technique, presented in Section 3.4 can indeed predict the limiting amplitude of the solution of a nonlinear hyperbolic equation and can be carried out to higher orders in a systematic manner. This chapter has provided us, through simple examples, with adequate tools to handle more complicated problems and showed us a comparison between the two techniques of expansion: asymptotic-perturbation and perturbation-averaging. Regarding the *asymptotic* solution, the two expansions gave the *same* results. This conclusion will be confirmed in Chapter 6 where we treat the conservation equations in combustion chambers using an expansion in the normal modes. However, carrying out the expansion to higher order approximations showed the shortcomings of the expansion in the normal modes and, in general, the perturbation-averaging technique to predict, in a simple way, the asymptotic solution of the nonlinear equation.

These results will be extended in the next chapter to the analysis of the nonlinear conservation equations in combustion chambers.

REFERENCES 3

1. Poincare, H. "*Les Methodes Nouvelles de la Mecanique Celeste*," Vol. 1, Gautiers-Villars, Paris, 1892.

2. Galerkin, B. G. " *Vestn. Inzhenerov i tekhnikov* ," pp. 879, 1915.

3. Kantrovitch, L. V. and Krylov, V. I. " *Approximate Methods to Higher Analysis*," Wiley Interscience, N.Y., 1958.

4. Bellman, R. E. and Kalaba, R. E. " *Nonlinear Partial Differential Equations: Methods of Solutions*," Academic Press, N.Y., 1967.

5. Morse, P. M. and Feshbach, H. " *Methods of Theoretical Physics*," Vol. 2, McGraw Hill, N.Y., 1953.

6. Stoker, J. J. " *Nonlinear Vibration in Mechanical and Electrical Systems* ," Interscience Publishers Inc., New York, 1950, pp. 119-128.

7. Stokes, G. G. " On the Theory of Oscillatory Waves," *Transactions of the Cambridge Philosophical Society*, Vol. 8, p. 441. See also Stokes, G. G. " *Mathematical and Physical papers* ", Cambridge University Press, 1880, Vol 1, p. 197.

8. Kevorkian, J. and Cole, J. D. "*Perturbation Methods in Applied Mathematics*," Spriger-Verlag, New York, 1981.

9. Millman, M. H. and Keller, J. B. " Perturbation Theory of Nonlinear Boundary-Value Problems," *Journal of Mathematical Physics*, Vol. 10, NO. 2, February 1969.

10. Minorsky, N. " *Nonlinear Oscillations*," D. Van Nostrand Co., Princeton N.J., 1962.

11. Bogoliubov, N. N., and Mitropolsky, Y. A. " *Asymptotic Methods in the Theory of Nonlinear Oscillations*," Hindustan Publications, New Delhi, 1961. See also " *Asymptotic Methods in the Theory of Nonlinear Oscillations*, " Gordon and Breach Pub., 1961.

12. Culick, F. E. C. "Some Recent Results for Nonlinear Waves Motion in Solid Propellant Rockets," *AIAA* paper 79-1208, 1979.

Chapter 4

EXPANSION OF THE CONSERVATION EQUATIONS

4.1. Introduction

The purpose of this chapter is to apply the technique of expansion in the asymptotic amplitude to the conservation equations in combustion chambers. The analysis will be shown to be of general application. However, our attention will be directed to the acoustic oscillations of the pressure in a cylindrical chamber. There are three kinds of oscillations: the tangential, or azimutal; the radial; and the longitudinal, or axial, oscillations. The linear, unperturbed acoustic pressure may be written[1] in the following form:

$$p' = \cos k_l x \cos m\theta \, J_m(k_{lm} r) \, e^{i\omega t}.$$

In this expression, $\cos k_l x$ corresponds to the longitudinal modes with k_l the wave number and x the axial location; $\cos m\theta$ corresponds to the tangential modes with m an integer representing the tangential mode order and θ the angle in polar coordinates; and $J_m(k_{lm} r)$ corresponds to the radial modes with J_m the standard Bessel function of order m and $k_{ml} = (\frac{\omega}{a_0})^2 - k_l^2$.

In combustion chambers, the combustion products generate a mean flow. The effects of this flow on the acoustic field are important[2]. The waveform is distorted and the frequency is shifted. The acoustic modes are said to be perturbed by the mean flow. Therefore, the inclusion in the analysis of the mean flow effects is essential to accurately predict the behavior of the pressure oscillations in the chamber. This is the motive to include in the expansion of the

asymptotic solution a second small parameter, the average Mach number, μ, of the flow field. It will be shown in this chapter how the inclusion of this second parameter will permit the determination of the perturbed modes.

The linear analysis is performed using a double expansion to first order in the wave amplitude (linearized problem) and to any order in the average Mach number. The perturbed modes and the frequency shift will be determined. In particular, the frequency becomes a complex quantity. The imaginary part of this quantity is called the linear growth rate because it determines the wave growth, or decay, in time. The results of the linear analysis are applied to a one-dimensional case.

The finite amplitude effects, or nonlinear effects, need a more elaborate treatment. The generation of different harmonics by the nonlinear motion of the wave as well as the dependence of the frequency on the amplitude of the wave have to be included in the analysis,, as we have seen in the last chapter. Therefore, the nonlinear analysis will be performed using a double expansion to *any* order in the wave amplitude and in the average Mach number.

In the nonlinear analysis, it is convenient to distinguish two cases: first, the case for which the modes are pure longitudinal and whose frequencies are integer multiples of the fundamental; and second, all other possibilities. For the second case, we present in Section 4.4.1 a double expansion in the wave amplitude and in the average Mach number. The objective in this section is to support the conclusion of Chapter 3, Section 3.3, regarding the capability of the expansion to handle higher-than-second orders of approximation. A third order expansion of the conservation equations is carried out and the dependence of the frequency on the amplitude of the wave is determined. The results are applied to a one-dimensional problem.

In section 4.7, we apply the perturbation averaging technique to the conservation equations in combustion chambers. The analysis is carried to second order in the pressure amplitude. Only the results for longitudinal modes are discussed in detail.

4.2. Conservation equations in dimensionless form

In the derivation of the conservation equations, we make the following assumptions

1) No mass addition within the volume.

2) No heat transfer within the volume.

3) No viscous stresses within the volume.

4) The effects of the combustion are assumed to occur at the boundaries of the chamber.

5) The entropy waves are neglected.

These assumptions can be removed at the expense of much labor in elaborating the expansion but the essential idea remains the same, namely the influence of the gasdynamics nonlinearity and the effect of the dispersion, or frequency-dependence, of the boundary conditions. Therefore, in order to gain understanding of the nonlinearity phenomenon most simply, we maintain these assumptions.

Following the above assumptions, the conservation equations can be written in the following form

$$\frac{\partial \rho}{\partial t} + \nabla .(\rho \underline{u}) = 0 \qquad (4.1)$$

$$\rho\left(\frac{\partial \underline{u}}{\partial t} + \underline{u}.\nabla\,\underline{u}\right) + \nabla\, p = 0 \tag{4.2}$$

$$p\,\rho^{-\gamma} = \text{constant.} \tag{4.3}$$

where p, u, ρ, and γ are respectively the pressure, velocity, density, and heat ratio. Elimination of ρ between (4.1) and (4.3) yields

$$\frac{\partial p}{\partial t} + \gamma\, p \nabla .\underline{u} + \underline{u}.\nabla\, p = 0 \tag{4.4}$$

Define the dimensionless quantities

$$\tilde{p} = \frac{p}{p_0},\quad \tilde{\rho} = \frac{\rho}{\rho_0},\quad \underline{\tilde{u}} = \frac{\underline{u}}{a_0},\quad \tilde{x} = \frac{x}{L},\quad \tilde{t} = t\,\frac{a_0}{L}$$

where p_0 , ρ_0 , a_0 and L are respectively the pressure, density, sound velocity of the mean flow and the characteristic length. By substituting the above quantities in (4.2)-(4.4), one gets

$$\frac{\partial \tilde{p}}{\partial \tilde{t}} + \gamma\, \tilde{p} \nabla .\underline{\tilde{u}} + \underline{\tilde{u}}.\nabla\, \tilde{p} = 0 \tag{4.5}$$

$$\tilde{\rho}\left(\frac{\partial \underline{\tilde{u}}}{\partial \tilde{t}} + \underline{\tilde{u}}.\nabla\,\underline{\tilde{u}}\right) + \frac{\nabla\, \tilde{p}}{\gamma} = 0 \tag{4.6}$$

$$\tilde{p}\,\tilde{\rho}^{-\gamma} = 1 \tag{4.7}$$

Eqs. (4.5)-(4.7) will be the basis for the expansion. We will omit the sign ~

hereafter. The linear problem will now be treated by linearizing these equations, to determine the linear growth rates for sinusoidal motions.

4.3. The Linear Problem

In the linear problem, we expand the quantities p, ρ, and u to first order in the wave amplitude (by definition of the linearized problem) and to any order in the average Mach number. A particular acoustical mode is considered.

4.3.1. *Introduction* .

An ample discussion can be found in the work of Culick[2] and Flandro[3]. Here, we will point out the main features and some additional results. In what follows, we will expand the pressure, density, and velocity in the two small parameters ε and μ:

$$p = 1 + \mu^2 p_{02} + \cdots + \varepsilon(p_{10} + \mu p_{11} + \cdots)e^{iKt} = p_0 + \varepsilon p' \tag{4.8}$$

$$\rho = 1 + \mu^2 \rho_{02} + \cdots + \varepsilon(\rho_{10} + \mu \rho_{11} + \cdots)e^{iKt} = \rho_0 + \varepsilon \rho' \tag{4.9}$$

$$u = \mu\bar{u} + \varepsilon(u_{10} + \mu u_{11} + \cdots)e^{iKt} = u_0 + \varepsilon u' \tag{4.10}$$

The average Mach number of the flow is caracterized by μ; ε is a measure of the amplitude of the acoustic wave, for example the amplitude of the first harmonic; p_{11} , etc., represent the distortion of the acoustic wave by the mean flow; and K is the dimensionless complex frequency of the acoustic wave. The real part of K is the dimensionless frequency of the acoustic mode and the imaginary part is the dimensionless linear growth rate of the wave. The purpose of the following calculations is to determine this growth rate for a given configuration of the chamber.

In general, the dimensionless complex frequency K is a function of both the amplitude of the wave and the average Mach number of the flow. But, for linear problems, K depends only on the average Mach number. Hence, K may be expanded as follows

$$K = K_{00} + \mu K_{01} + \mu^2 K_{02} + \cdots \tag{4.11}$$

where, in K_{ij}, i is the power in the expansion in the wave amplitude, and j is the power in the expansion in Mach number.

4.3.2. *Analysis and results* . The point in this section is to determine K_{01}, K_{02}, etc. We do so by matching the coefficients of $\varepsilon^l \mu^m e^{iKt}$, to obtain the following systems of ordinary differential equations

For (l,m) = (1,0), we get the linear acoustic equations

$$iK_{00}p_{10} + \gamma \nabla . u_{10} = 0 \tag{4.12}$$

$$iK_{00}u_{10} + \frac{\nabla p_{10}}{\gamma} = 0 \tag{4.13}$$

with the boundary condition

$$f_{10} = \underline{n}.\nabla p_{10}$$

From these two equations, we get

$$\nabla^2 p_{10} + K_{00}^2 p_{10} = 0. \tag{4.14}$$

Many textbooks treat this problem (see for example reference 1). The expression for the pressure given at the beginning of this chapter is that for the case of a constant cross-section, cylindrical chamber with $f_{10} = 0$.

For (l,m) = (1,1), we get the equations for the distortion of the acoustic wave by the mean flow :

$$iK_{00}p_{11} + \gamma \nabla \cdot u_{11} = -iK_{01}p_{10} - \gamma p_{10}\nabla \cdot \bar{u} - \bar{u} \cdot \nabla\ p_{10} \qquad (4.15)$$

$$iK_{00}u_{11} + \frac{\nabla\ p_{11}}{\gamma} = -iK_{01}u_{10} - \bar{u}.\nabla\ u_{10} - u_{10}.\nabla\ \bar{u} \qquad (4.16)$$

To determine K_{01} we proceed as follows. Take the divergence of Eq. (4.16) and use Eqs. (4.12) and (4.15) to find

$$\nabla^2 p_{11} + K_{00}^2 p_{11} = -2K_{01}K_{00}p_{10} + h_{11} \qquad (4.17)$$

where

$$h_{11} = -\frac{i}{K_{00}}\left(\nabla \cdot (\bar{u} \cdot \nabla u_{10} + u_{10} \cdot \nabla \bar{u}) \right) + i K_{00}\, \bar{u} \cdot \nabla p_{10} + \gamma\, i K_{00}\, p_{10} \nabla \cdot \bar{u}$$

Multiply (4.17) by p_{10} and Eq. (4.14) by p_{11}, subtract the results, integrate over the volume, and apply Green's theorem, giving

$$\int_v (p_{10}\nabla^2 p_{11} - p_{11}\nabla^2 p_{10})dv = \int_s p_{10}f_{11}\, ds - \int_s p_{11}f_{10} ds$$

where v is the volume; s is the surface; and $f_{lm} = \underline{n}.\nabla\, p_{lm}$. This relation can be soved to give the following expresion for K_{01}

$$2K_{01}K_{00}\,E_{10}^2 = -\int_s p_{10}f_{11}\,ds + \int_s p_{11}f_{10}\,ds + \int_v p_{10}h_{11}\,dv \qquad (4.18)$$

where

$$E_{10}^2 = \int_v p_{10}^2 dv$$

The same technique will be used throughout this chapter and chapter 4 to find the coefficients in the expansion of the frequency in the average Mach number, and, in Section 4.4 and Chapter 4, in the wave amplitude.

One may conclude from expression (4.18) that, in order to determine K_{01}, p_{11} and f_{11} must be known in advance. However, it will be shown in Appendix 4A that only knowledge of p_{10} and f_{10} is necessary. In other words, the determination of the eigenvalue for a problem of a given order, here K_{01}, requires knowledge of the eigenfunctions of one, or more, order *less*, here p_{10}.

For (l,m)=(1,2) we get the second order correction to the acoustic wave by the mean flow

$$iK_{00}p_{12} + \gamma\,\nabla\cdot u_{12} = -ik_{02}\,p_{10} - i\,K_{01}\,p_{11} \qquad (4.19)$$

$$-\gamma p_{11}\nabla\cdot\bar{u} - \bar{u}.\nabla\,p_{11} - \gamma p_{02}\,\nabla\cdot u_{10} - u_{10}.\nabla\,p_{02}$$

$$iK_{00}u_{12} + \frac{\nabla\,p_{12}}{\gamma} = -iK_{02}\,u_{10} - i\,K_{01}\,u_{11} \qquad (4.20)$$

$$- p_{11}.\nabla \bar{u} - \bar{u}.\nabla u_{11} - iK_{00}\rho_{02}u_{10}$$

From these equations and following the same procedure used above to determine K_{01}, we deduce the following expression for K_{02}

$$2K_{02}K_{00}\,E_{10}^2 = -\int_s p_{10}f_{12}\,ds + \int_s p_{12}f_{10}\,ds + F \qquad (4.21)$$

where,

$$F = -iK_{00}\,K_{01}\int_v p_{11}p_{10}dv + i\,K_{00}\int_v (\bar{u}\,.\,\nabla\ p_{11}\,)\,p_{10}\,dv$$

$$+\gamma\,i\,K_{00}\int_v (p_{11}\,\nabla\,.\bar{u}\,)\,p_{10}\,dv + i\,K_{00}\int_v (\,u_{10}\,.\,\nabla\ p_{02}\,)\,p_{10}\,dv$$

$$+\gamma\,i\,K_{00}\int_v (\,p_{02}\,\nabla\,.u_{10}\,)\,p_{10}\,dv - \gamma\,i\,K_{01}\int_v p_{10}\,\nabla\,.u_{11}\,dv$$

$$+\int_v (\,\nabla\,.\,(\bar{u}\,.\,\nabla\,u_{11} + u_{11}\,.\,\nabla\,\bar{u})\,)\,p_{10}\,dv - iK_{00}\int_v p_{10}\nabla\,.(\,\rho_{02}\,u_{10})\,dv$$

4.3.3. *Application.*

Now the above results for the linear coefficients K_{01} and K_{02}, in the expansion of the complex frequency K in the average Mach number, will be applied to practical problems. First, we apply Eq. (4.16) to the longitudinal modes of the model of the combustion chamber shown on Figure 4.1. In this sketch, A_p and A_N represent the admittance functions at the boundaries. For $B_{00} = 0$, the frequencies of the longitudinal acoustic modes of the chamber are integer multiples of

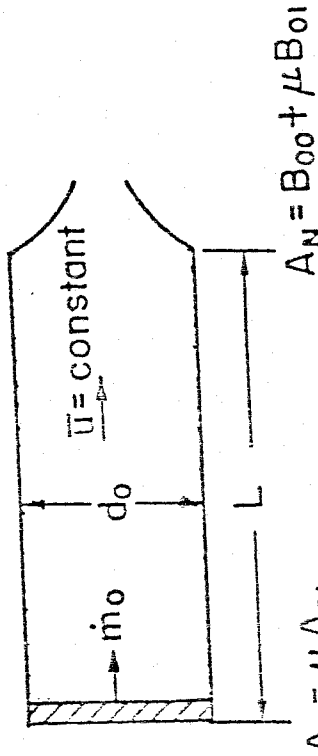

Figure 3.1 Schematic of a longitudinal rocket.

the fundamental. Application of Eq. (4.18) gives

$$K_{01} = -i\gamma\,(A_{01} - B_{01})$$

where A_{01} and B_{01} represent the first coefficient in the expansion of the admittance function at each boundary. The growth rate of the wave is

$$\alpha_{01} = \gamma(A_{01}^{(r)} - B_{01}^{(r)})$$

where the superscript (r) refers to the real part of the quantity.

The case where B_{00} is pure imaginary and $A_p = 0$ yields the following expression for K_{01} :

$$K_{01} = \frac{i\gamma B_{01}(1 + e^{-2iK_{00}})}{2(1 + \gamma B_{00})}$$

where the unperturbed frequencies are given by

$$K_{00} = \tan^{-1}(i\gamma B_{00})$$

Since B_{00} is different from zero, the solutions for this equation are not integer multiples of the fundamental. From the expression for K_{01}, the linear growth rate is

$$\alpha_{01} = -\gamma B_{01}^{(r)} \cos^2 K_{00}$$

This case will also be the basis for the application carried out later in the analysis, Section 4.4.2.2.

As a second example, the expression of the linear growth rate of the wave will be derived for the problem of a cylindrical rocket shown on Figure 4.2. Assuming the steady burning rate to be constant, we get from a mass balance for a control volume limited between 0 and x the following expression for the axial velocity, averaged over the cross-section,

$$\bar{u} = 4\frac{r_0}{d_0}x$$

where r_0 is the constant burning rate and d_0 is the diameter of the chamber. For simplicity, we neglect the response of the propellant to unsteady flow in the chamber. By applying Eq. (4.18) we get

$$K_{01} = i\gamma B_{01} + i\frac{c}{2}(1 + \gamma)$$

where $c = 4\frac{r_0}{d_0}$. The linear growth rate is then

$$\alpha_{01} = -\gamma B_{01}^{(r)} - \frac{c}{2}(1 + \gamma)$$

This expression for α_{01} shows clearly the effect of the gradient of the steady state velocity on the growth rate of the wave. This arises from the loss of acoustic energy through the nozzle by convection.

A similar expression for K_{02} can be found by using Eq. (4.21). For example, for the case of Figure 4.1, with B_{00} pure imaginary and $A_p = 0$, the expression for K_{02} is

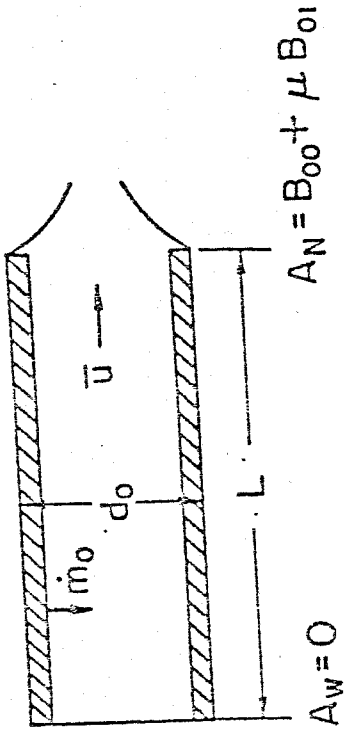

Figure 3.2 Schematic of a cylindrical rocket.

$$K_{02} = -i\frac{\gamma^2 B_{01}^2(1 - e^{-4iK_{00}})}{4(1 + \gamma B_{00})^2}$$

Now that we have determined the linear growth rate for any mode, the nonlinear problem will be treated. Expansions (4.8)-(4.10) must be changed in order to accommodate the nonlinearity.

4.4. The nonlinear problem

4.4.1. *Introduction* . Finite amplitude *standing* waves are the most encountered finite amplitude waves in combustion chambers. They have been the object of investigation for a long time. Stoker[4] investigated the periodic motions of nonlinear systems having infinitely many degrees of freedom. Penney and Price[5] examined finite periodic gravity waves in a perfect fluid. Three-dimensional standing surface waves of finite amplitude have been analyzed, using the perturbation method, by Verma and Keller[6]. Concus[7] discussed standing capillary-gravity waves. Tadjbakhsh and Keller[8] examined the standing surface waves of finite amplitude. McQuery[9] studied periodic solutions to a class of autonomous and nonautonomous partial differential equations, using the perturbation technique.

For the particular case of pressure ocillations in combustion chambers, Maslen and Moore[10] examined the periodic solutions of transverse waves in a cylindrical rocket, using a perturbation technique. They determined *numerically* the shift of frequency due to the nonlinearity of the wave motion. Zinn[11] applied the perturbation technique to three-dimensional conservation equations in combustion chambers. However, the structure of his expansion differs from in the sense that the behavior of the wave in space was predetermined except in one coordinate. The special effects of the boundary conditions on the structure of the expansion was not mentioned. Moreover, in reference 11 the author did not either point out the particularity of the longitudinal modes, or link the results of the analysis to those of the expansion in the normal modes of the acoustic field.

In this section we examine the finite amplitude periodic standing waves in combustion chambers. The extension of the analysis to traveling waves is straightforward. The basic procedure consists in expanding the unknown

frequency and the waveform in two small parameters: the average Mach number of the flow and, as we have done in Chapter 2, a measure of the wave amplitude, for example the amplitude of the fundamental. These expansions are then substituted in the conservation equations and terms of like powers are equated. Once this is done, the method leads to a sequence of linear problems. The first of these is homogeneous (the linearized problem) while the rest are inhomogeneous. The solvability (here the satisfaction of the boundary conditions) criteria for the inhomogeneous equations yield the coefficients in the expansions of the frequency and the waveform in the small parameters. Since we are interested in the influence of the nonlinearity of the conservation equations on the linear frequency and waveform, the boundary conditions are assumed to be linear, i.e., independent of the wave amplitude, but they may depend on the average Mach number.

It is convenient to distinguish two cases: first, the general case where the frequencies of the modes taken into consideration are not all integer multiples of the fundamental; and second, the case of pure longitudinal modes whose frequencies are integer multiples of the fundamental. The first case is treated in the next section while the second will the subject of the next chapter.

4.4.2. *General Case* .

In this section, the frequencies of the modes taken into consideration are not integer multiples of the fundamental. The expansion is generated as follows. We start with one mode in the linear regime and then, taking into account the structure of the nonlinearities of the conservation equations, we add additional modes to the expansion. For example, if we start with a linear wave of the form ε cost, then the second order nonlinarity ($u.\nabla u$, etc.) generates a second harmonic of the form $\frac{1}{2}\varepsilon^2 \cos 2t$ and a shift of the mean values of the form $\frac{1}{2}\varepsilon^2$. Both terms are of second order in the amplitude ε. The same nonlinearity again

will couple the second order terms with the first order term ε cost, to generate third order terms and so forth. The following expansion is generated following these guidelines.

4.4.2.1 *Expansion in amplitude and average Mach number.*

Expand p, ρ and $\underline{u}$ as follows

$$p = 1 + \mu^2 p_{02} + ... + \varepsilon (p_{10,1} + \mu p_{11,1} + \cdots) e^{iKt} + \varepsilon^2(p_{20,0} + \mu p_{21,0} + \cdots)$$

$$+ \varepsilon^2 (p_{20,2} + \mu p_{21,2} + \cdots) e^{2iKt}$$

$$+ \varepsilon^3(p_{30,1} + \mu p_{31,1} + \cdots) e^{iKt} + \varepsilon^3(p_{30,3} + \mu p_{31,3} + \cdots) e^{3iKt} + \cdots + c.c.$$

where c.c. stands for complex conjugate. The density ρ and velocity $u = \mu\bar{u} + u'$ have similar expansions.

The pressure p is a real quantity. Therefore, using the complex notation, each term in the expansion has, in general, to be accompanied by its conjugate. Since the conservation equations are nonlinear, the expansion using complex notation *must* include the complex conjugate of each term in the expansion because the nonlinearity will couple the quantity with its complex conjugate. This coupling does not occur in linear problems and, therefore, the inclusion of the complex conjugate has no effect on the analysis of linear problems.

The above expansion is similar to the one given by Eq. (2.13) in Chapter 2 . The only difference is that here we have a *double* expansion in both the wave amplitude (the same as in (2.30)) and in the average Mach number. The inclusion of a second parameter, the average Mach number, is required to treat the interactions between the mean flow and the acoustic field. Equations (4.15)-

(4.17) in Section 4.3 showed how the inclusion of this parameter allows determination of such interactions.

The dimensionless complex frequency K is expanded as follows

$$K = K_{00} + \mu K_{01} + \mu^2 K_{02} + \cdots + \varepsilon(K_{10} + \mu K_{11} + \ldots) + \varepsilon^2(K_{20} + \mu K_{21} + \cdots) + \text{etc.}$$

In this expansion, K_{00} is the eigenvalue to the linear acoustics problem. The eigenfunction $p_{10,1}$ of this problem is a first order in ε. Similarly, K_{10} and K_{20} correspond respectively to the second and third order acoustics problems.

4.4.2.2 *Detailed expansion* . We now substitute the expansions of p, u, ρ, and K in the conservation equations (4.5)-(4.7) and we match the coefficients of $\varepsilon^l \mu^m e^{niKt}$.

For (l,m,n) = (2,0,0), we get

$$-2\alpha_{00}p_{20,0} + \gamma\nabla .u_{20,0} = -\gamma p_{10,1}\nabla .u^*_{10,1} - \gamma p^*_{10,1}\nabla .u_{10,1} - u^*_{10,1}.\nabla\, p_{10,1} \qquad (4.22)$$

$$- u_{10,1}.\nabla\, p^*_{10,1}$$

$$-2\alpha_{00}u_{20,0} + \frac{\nabla\, p_{20,0}}{\gamma} = -u_{10,1}.\nabla\, u^*_{10,1} - u^*_{10,1}.\nabla\, u_{10,1} + i\rho_{10,1}K^*_{00}u^*_{10,1} \qquad (4.23)$$

$$- i\rho^*_{10,1}K_{00}u_{10,1}$$

where $(\,)^*$ denotes complex conjugate of the quantity and α_{00} is defined by

$$K_{00} = \omega_{00} - i\alpha_{00}$$

In general, α_{00} is not equal to zero and corresponds to the linear growth rate of the acoustic wave with no mean flow. $u_{20,0}$ and $p_{20,0}$ can be determined by solving (4.22) and (4.23). This yields a d.c shift in the mean flow due to the nonlinearity of the wave. This phenomenon is called acoustic streaming and it corresponds to the time-independent flow of fluid induced by the nonlinear acoustic field. It was first introduced by Rayleigh[12]. A thorough discussion on this phenomenon is reported in reference 13.

The following calculation is aimed at demonstrating that the coefficient K_{10}, in the expansion of the complex frequency K, vanishes. We will prove also that there cannot be such terms as $\varepsilon^2 e^{iKt}$ in the expansion. Assume that there are such terms and equate the coefficients of $\varepsilon^2 e^{iKt}$ in the conservation equations, to find

$$iK_{00}p_{20,1} + \gamma\nabla .u_{20,1} = -iK_{10}p_{10,1} \tag{4.24}$$

$$iK_{00}u_{20,1} + \frac{\nabla p_{20,1}}{\gamma} = -iK_{10}u_{10,1} \tag{4.25}$$

From these two equations and from the linear acoustic equations (4.12)-(4.13) (in those equations p_{10} and u_{10} are the same as $p_{10,1}$ and $u_{10,1}$ here), one gets

$$\nabla^2 p_{20,1} + K_{00}^2 p_{20,1} = -2K_{10}K_{00}p_{10,1}. \tag{4.26}$$

The solution of this equation is the sum of a trivial solution to the homogeneous

problem

$$\nabla^2 p_{20,1} + K_{00}^2 p_{20,1} = 0.$$

and a non-trivial solution proportional to K_{10}. The trivial solution has the same form as the solution of the linear problem (4.15) and, since this trivial solution is a second order term, it can be neglected in comparison with the linear term. We are left with the non-trivial solution, a solution which is proportional to K_{10}.

Now we apply to Eq. (4.26) the same technique used in Section 4.3 to obtain K_{01}. After some manipulations, we obtain the following expression for K_{10}

$$2K_{10}K_{00}\, E_{10,1}^2 = -\int_S p_{10,1} f_{20,1}\, ds + \int_S p_{20,1} f_{10,1}\, ds \qquad (4.27)$$

with $f_{lm,n} = \underline{n}.\nabla\, p_{lm,n}$ and $E_{10,1}^2 = \int_V p_{10,1}^2 dv$. Since the boundary conditions are assumed to be linear, $p_{20,1}$ and $f_{20,1}$ satisfy a linear relationship identical to the one between $p_{10,1}$ and $f_{10,1}$; see Appendix 4A for details. The direct conclusion is that the right-hand side of (4.27) is zero. This means that

$$K_{10} = 0.$$

Moreover, $p_{20,1}$, being proportional to K_{10}, is equal to zero. Using Eq. (4.25), one deduces that $u_{20,1}$ is proportional to K_{10} and, therefore also vanishes.

Now we turn to the determination of the second order acoustics equations. By equating the coefficients of $\varepsilon^2\, e^{2iKt}$ we get

$$2iK_{00}p_{20,2} + \gamma\nabla\cdot u_{20,2} = -\gamma p_{10,1}\nabla\cdot u_{10,1} - u_{10,1}\cdot\nabla p_{10,1} \tag{4.28}$$

$$2iK_{00}u_{20,2} + \frac{\nabla p_{20,2}}{\gamma} = -u_{10,1}\cdot\nabla u_{10,1} \tag{4.29}$$

with $f_{20,2} = \underline{n}\cdot\nabla p_{20,2}$ on the boundary. These equations can be solved for $p_{20,2}$ and $u_{20,2}$. The expressions for $p_{20,2}$ and $u_{20,2}$ are needed in the following calculation to determine K_{20}.

The coefficient K_{20} will be determined from equating the coefficients of $\varepsilon^3 e^{iKt}$. In doing so, we obtain the following system for $p_{30,1}$ and $u_{30,1}$

$$iK_{00}p_{30,1} + \gamma\nabla\cdot u_{30,1} = -iK_{20}p_{10,1} - \gamma p_{20,2}\nabla\cdot u^{*}_{10,1} - \gamma p^{*}_{10,1}\nabla\cdot u_{20,2} \tag{4.30}$$

$$- u^{*}_{10,1}\nabla p_{20,2} - \gamma p_{20,0}\nabla\cdot u_{10,1} - \gamma p_{10,1}\nabla\cdot u_{20,0}$$

$$- u_{10,1}\nabla p_{20,0} - u_{20,0}\nabla p_{10,1} - u_{20,2}\cdot\nabla p^{*}_{10,1}$$

$$iK_{00}u_{30,1} + \frac{\nabla p_{30,1}}{\gamma} = -iK_{20}u_{10,1} - u_{20,2}\cdot\nabla u^{*}_{10,1} - u^{*}_{10,1}\cdot\nabla u_{20,2} \tag{4.31}$$

$$- u_{10,1}\cdot\nabla u_{20,0} - u_{20,0}\cdot\nabla u_{10,1} - iK_{00}\rho^{*}_{10,1}u_{20,0} + iK^{*}_{00}\rho_{20,2}u^{*}_{10,1}$$

$$- \rho_{10,1}(u_{10,1}\cdot\nabla u^{*}_{10,1} + u^{*}_{10,1}\cdot\nabla u_{10,1}) - \rho^{*}_{10,1}\, u_{10,1}\cdot\nabla u_{10,1} - iK_{00}\rho_{20,0}u_{10,1}$$

with $f_{30,1} = \underline{n}\cdot\nabla p_{30,1}$ on the boundaries. Elimination of $u_{30,1}$ between these two

equations yields the following Helmholtz equation

$$\nabla^2 p_{30,1} + K_{00}^2 p_{30,1} = -iK_{00}(-iK_{20}p_{10,1} - \gamma p_{20,2}\nabla . u^*_{10,1} - \gamma p^*_{10,1}\nabla . u_{20,2} \quad (4.32)$$

$$- u^*_{10,1}\nabla p_{20,2} - \gamma p_{20,0}\nabla . u_{10,1} - \gamma p_{10,1}\nabla . u_{20,0} - u_{10,1}\nabla p_{20,0} - u_{20,0}\nabla p_{10,1}$$

$$-u_{20,2}.\nabla p^*_{10,1} - u^*_{20,0}.\nabla p_{10,1})$$

$$+ \gamma\nabla .(-iK_{20}u_{10,1} - u_{20,2}.\nabla u^*_{10,1} - u^*_{10,1}.\nabla u_{20,2}$$

$$- u_{10,1}.\nabla u_{20,0} - u_{20,0}.\nabla u_{10,1} - iK_{00}\rho^*_{10,1}u_{20,0} + iK^*_{00}\rho_{20,2}u^*_{10,1}$$

$$- \rho_{10,1}(u_{10,1}.\nabla u^*_{10,1} + u^*_{10,1}.\nabla u_{10,1}) - \rho^*_{10,1} u_{10,1}.\nabla u_{10,1} - iK_{00}\rho_{20,0}u_{10,1})$$

Each term on the right hand side of this equation is determined from the results of lower order calculations. Now we write (2.32) as follows

$$\nabla^2 p_{30,1} + K_{00}^2 p_{30,1} = -2\, K_{20}\, K_{00} + h_{30,1}$$

and we apply to this equation the same technique developed in Section 4.3 to find K_{01}. The final result is the following expression for K_{20}

$$2\, K_{20}\, K_{00} E^2_{10,1} = \gamma \int_S p_{10,1} f_{30,1} ds - \gamma \int_S p_{30,1} f_{10,1} ds + \int_V h_{30,1}\, p_{10,1} dv \qquad (4.33)$$

where $f_{30,1} = \underline{n}.\nabla p_{30,1}$. K_{20} represents the effects, on the linear frequency and

growth rate, of the nonlinearity of the conservation equations.

As we have seen above, K_{20} corresponds to the third order acoustic problem. In the determination of this coefficient from expression (4.33), one needs to know only the second, or lower, order terms, i.e. $p_{30,1}$ needs not be known. In appendix 3B we show the point.

4.5. Application of the results

Now the results elaborated above, mainly expression (4.33), will be applied to the one-dimensional model of the combustion chamber shown on Figure 4.1. The linear unperturbed frequencies are given by

$$K_{00} = \tan^{-1}(- i\gamma B_{00})) \tag{4.34}$$

where

$$B_{00} = \frac{u_{10,1}}{p_{10,1}} \qquad \text{at } x = 1. \tag{4.35}$$

In order to have longitudinal modes whose frequencies are not integer multiples of the fundamental, we choose B_{00} to be pure imaginary. The overtones of a solution to (4.34) are not solutions. Therefore, the general formulation for the determination of the effects of the nonlinearity of the conservation equations can be applied. For simplicity, the boundary conditions for different harmonics are taken as follows

$$\frac{u_{10,1}}{p_{10,1}} = \frac{u_{m0,1}}{p_{m0,1}} = B_{00} \tag{4.36}$$

where m = 1,2,3, etc. The values of the dimensionless frequency shift K_{20} for

different values of the dimensionless admittance function B_{00} are determined from (4.33) and given in table 4.1.

Table 4.1. Dimensionless Frequency Correction

Admittance	Frequency Correction K_{20}
i 0.5	- 0.70766 + i 0.000
i 1.0	-1.7037 + i 0.000
i 1.5	-2.2664 + i 0.000
i 2.0	- 2.6533 + i 0.000
i 2.5	-2.93372 + i 0.000

For clarity, we plot these values on Figure 4.3, where ω_{00} is the real part of K_{00}. To obtain the dimensional frequency shift $K_{20}^{(d)}$ we use the definition of the dimensionless time in Section 4.2, to get

$$K_{20}^{(d)} = K_{20} \frac{a_0}{L.}$$

As we see from this table, the expansion presented in Section 4.4.2 is capable of handling the third order acoustics in a straightforward, but lengthy, manner. In reference 14, we see a difficulty in using the expansion in the normal modes to handle the third order acoustics. Also, we notice that the correction K_{20} is pure real and, therefore, we cannot deduce anything about the effects of the nonlinearity on the growth of the wave. This can be handled, although not done here, within framework of the above analysis by including real parts in the boundary conditions (4.36). These effects were first shown by Betchov[15], using a

method of characteristics, in the treatment of pressure oscillations in a column of gas. Chester[16] generalized the results of Betchov by using a regular perturbation scheme. Collins[17] , in treating the vibrations of a string, used the resulting, or asymptotic, amplitude as a small parameter. Jiminez[18] extended the approach of Collins to the pressure oscillations in a column of gas. However, the objective of this section was simply to demonstrate the capability of the expansion to handle higher-than-second order acoustic problems. The determination of the amplitude and the conditions for existence of the limit cycle will be dealt with in the next chapter for the particular case of pure longitudinal modes.

In Chapter 3, we discussed two methods of solutions to nonlinear partial differential equations: the asymptotic-perturbation method and the perturbation-averaging method. Having applied the asymptotic-perturbation technique to the conservation equations, we apply now the perturbation-averaging technique.

4.6. Expansion using the perturbation-averaging technique

4.6.1. *Introduction* .

In this section we will show how to apply Green's theorem to reduce the system of conservation equations (4.5)-(4.7) to a system of nonlinear second order ordinary differential equations. Then, this system will be reduced further, using the Method of time averaging, to a system of first order nonlinear ordinary differential equations. The approach presented here is a simplification of the general approach presented by Culick[19] and a direct application of the perturbation-averaging technique to second order in the amplitude.

In Section 4.6.2, we reduce the conservation equations of the flow field in combustion chambers to a nonlinear hyperbolic equation (4.42). Application of Green's theorem is shown in detail, leading ultimately to a system of nonlinear

oscillators (4.46).

Section 4.6.3 starts from this system and shows in detail the application of the Method of time averaging, yielding a system of first order nonlinear ordinary differential equations (4.53).

4.6.2. *Presentation of the method .*

This method has been applied by Culick[19] to the general problem of conservation equations in combustion chamber. The following two sections are a simplification of the general formulation given in reference 19 to the case where there is one phase and no mass addition. Therefore, the problem reduces to that of nonlinear acoustics with mean flow. We start from the conservation equations in dimentionless form

$$\frac{\partial p}{\partial t} + \gamma\, p \nabla \underline{u} + \underline{u} \nabla\ p = 0 \tag{4.37}$$

$$\rho\left(\frac{\partial \underline{u}}{\partial t} + \underline{u} \nabla\, \underline{u}\right) + \frac{\nabla p}{\gamma} = 0 \tag{4.38}$$

$$p\, \rho^{-\gamma} = 1 \tag{4.39}$$

Write now the pressure,density and velocity in the following form

$$p = \bar{p} + p'$$

$$\rho = \bar{\rho} + \rho'$$

$$u = \bar{u} + u'$$

Expand p' and u' in the normal modes of the chamber as follows

$$p' = \sum_{i=0}^{\infty} \eta_i(t)\psi_i(x) \tag{4.40}$$

$$u' = \sum_{i=1}^{\infty} \frac{\dot{\eta}_i(t)}{\gamma k_i^2} \nabla \psi_i(x)$$

where the ψ_i satisfy

$$\nabla^2 \psi_i + k_i^2 \psi_i = 0 \tag{4.41}$$

and

$$\nabla \psi_i = 0 \tag{4.42}$$

on the boundary. It is easy to verify that the expansion (4.40)-(4.41) satisfies the linearized version of the equations (4.37)-(4.39). By replacing p and u by their expansions (4.40) in equations (4.37)-(4.39) and retaining terms of order ε, $\varepsilon\mu$ and ε^2, one gets

$$\frac{\partial^2 p'}{\partial t^2} - \nabla^2 p' = +\gamma \nabla .(\bar{u}.\nabla u' + u'.\nabla \bar{u} + u'.\nabla u'))$$

$$-\gamma\frac{\partial}{\partial t}(p'\nabla\cdot\bar{u}+p'\nabla\cdot u')-\frac{\partial p'}{\partial t}(u'.\nabla p'+\bar{u}.\nabla p')+\gamma\nabla\cdot(\rho'\frac{\partial u'}{\partial t})$$

For simplicity, we will focus on the one dimensional problem with constant cross sectional area. The equation above becomes

$$\frac{\partial^2 p'}{\partial t^2}-\frac{\partial^2 p'}{\partial x^2}=+\gamma(\bar{u}\frac{\partial^2 u'}{\partial x^2}+2\frac{d\bar{u}}{dx}\frac{\partial u'}{\partial x}+u'\frac{d^2\bar{u}}{dx^2}+\frac{1}{2}\frac{\partial^2 u'^2}{\partial x^2})$$

$$-\gamma(\frac{\partial p'}{\partial t}\frac{\partial\bar{u}}{\partial x}+p'\frac{\partial^2\bar{u}}{\partial x\partial t}+p'\frac{\partial^2 u'}{\partial x\partial t}+\frac{\partial p'}{\partial t}\frac{\partial u'}{\partial x}) \qquad (4.43)$$

$$-(\frac{\partial u'}{\partial t}\frac{\partial p'}{\partial x}+u'\frac{\partial^2 p'}{\partial x\partial t}+\bar{u}\frac{\partial^2 p'}{\partial x\partial t}+\frac{\partial\bar{u}}{\partial t}\frac{\partial p'}{\partial x})+\gamma(\frac{\partial u'}{\partial t}\frac{\partial\rho'}{\partial x}+\rho'\frac{\partial^2 u'}{\partial x\partial t}).$$

Equation (4.43) is a nonlinear hyperbolic equation. We now apply Green's Theorem to this equation. First, Green's theorem can be written in the following form

$$\int_v f\nabla^2 g\,dv=\int_s f\,\nabla g.ds-\int_v\nabla f.\nabla g\,dv \qquad (4.44)$$

where v and s are respectively the volume and surface; for one-dimensional problems, with constant cross-section, the volume becomes a line and the surface becomes a point boundary. Second, multiply both sides of (4.43) by ψ_i and of (4.41) by p', subtract the results, integrate over the volume and use Green's Theorem and equation (4.42) to find

$$[\psi_i \frac{\partial p'}{\partial x}]_0^1 - k_i^2 \int_0^1 p'\psi_i dx - \frac{d^2}{dt^2}\int_0^1 p'\psi_i dx =$$

$$-\gamma\int_0^1 (\bar{u}\frac{\partial^2 u'}{\partial x^2} + 2\frac{d\bar{u}}{dx}\frac{\partial u'}{\partial x} + u'\frac{d^2\bar{u}}{dx^2} + \frac{1}{2}\frac{\partial^2 u'^2}{\partial x^2})\psi_i dx$$

$$+\gamma\int_0^1 (\frac{\partial p'}{\partial t}\frac{\partial \bar{u}}{\partial x} + p'\frac{\partial^2\bar{u}}{\partial x\partial t} + p'\frac{\partial^2 u'}{\partial x\partial t} + \frac{\partial p'}{\partial t}\frac{\partial u'}{\partial x})\psi_i dx$$

$$+\int_0^1 (\frac{\partial u'}{\partial t}\frac{\partial p'}{\partial x} + u'\frac{\partial^2 p'}{\partial x\partial t} + \bar{u}\frac{\partial^2 p'}{\partial x\partial t} + \frac{\partial \bar{u}}{\partial t}\frac{\partial p'}{\partial x})\psi_i dx - \gamma\int_0^1 (\frac{\partial u'}{\partial t}\frac{\partial \rho'}{\partial x} + \rho'\frac{\partial^2 u'}{\partial x\partial t})\psi_i dx \quad (4.45)$$

Here, following (4.41) and (4.42), $\psi_i = \cos i\pi x$. The boundary conditions are contained in the first term of (4.45). We approximate $\frac{\partial p'}{\partial x}$ by $-\rho_0\frac{\partial u'}{\partial t}$ and u' by[19],

$$u' = -\gamma\rho_0\sum_{n=1}^{\infty}(R_n^{(r)} + i\frac{R_n^{(i)}}{\omega_n}\frac{\partial}{\partial t})\dot{\eta}_n(t)\psi_n\psi_j$$

$$= -\gamma\sum_{n=1}^{\infty}[R_n^{(r)}\dot{\eta}(t)\psi_n\psi_j - i R_n^{(i)}\omega_n\eta_n(t)\psi_n\psi_j],$$

where the approximation $\ddot{\eta}_n + \omega_n^2\eta_n = 0$ has been made in the last term. The terms $R_n^{(r)}$ and $R_n^{(i)}$ correspond respectively to the real and imaginary parts of the admittance functions at the boundary for the mode n. By replacing p' and u' by their expansions (4.40) in (4.45), one is led to evaluate the following integrals

$$\frac{d^2}{dt^2}\int_0^1 p'\psi_i dx = -\frac{1}{2}\frac{\omega_i^2}{a^2}\eta_i$$

$$\int_0^1 \frac{d\bar{u}}{dx}u'\psi_i dx = \sum_{n=1}^{\infty}\eta_n\int_0^1 \frac{d\bar{u}}{dx}\psi_n\psi_i dx$$

$$\int_0^1 \frac{d\bar{u}}{dx}\frac{\partial p'}{\partial t}\psi_i dx = \sum_{n=1}^{\infty}\dot{\eta}_n\int_0^1 \frac{d\bar{u}}{dx}\psi_n\psi_i dx$$

$$\int_0^1 \frac{d\bar{u}}{dx}\frac{\partial p'}{\partial t}\psi_i dx = \sum_{n=1}^{\infty}\dot{\eta}_n\int_0^1 \frac{d\bar{u}}{dx}\psi_n\psi_i dx$$

$$\int_0^1 \bar{u}\frac{\partial^2 u'}{\partial^2 x}\psi_i dx = -\sum_{n=1}^{\infty}\frac{\dot{\eta}_n}{\gamma}\int_0^1 \bar{u}\psi_n\psi_i dx$$

$$\int_0^1 u'\frac{d^2\bar{u}}{d^2 x}\psi_i dx = \sum_{n=1}^{\infty}\frac{1}{\gamma k_n^2}\dot{\eta}_n\int_0^1 \bar{u}\psi_n\psi_i dx$$

$$\int_0^1 \bar{u}\frac{\partial^2 p'}{\partial x\partial t}\psi_i dx = \sum_{n=1}^{\infty}\dot{\eta}_n\int_0^1 \bar{u}\frac{d\psi_n}{dx}\psi_i dx.$$

We see that the linear terms can be written in the following form

$$\ddot{\eta}_i + \omega_i^2\eta_i = \sum_{n=1}^{\infty}\left(E_{ni}\eta_n + D_{ni}\dot{\eta}_n\right)$$

where the constants E_{ni} and D_{ni} are integrals depending on the steady state conditions and the normal modes ψ_n and ψ_i.

The same technique as above will now be applied to the nonlinear terms in (4.42). We are led to evaluate the following expressions :

$$\frac{1}{2}\int_0^1 \frac{\partial^2 u'^2}{\partial^2 x}\psi_i dx = \sum_{n=1}^{\infty}\sum_{m=1}^{\infty} \frac{\dot\eta_n\dot\eta_m}{\gamma^2 k_n^2 k_m^2}\int_0^1 \frac{d}{dx}(\psi_n \frac{d\psi_m}{dx})\psi_i dx$$

$$\int_0^1 \frac{\partial p'}{\partial t}\frac{\partial u'}{\partial x}\psi_i dx = \sum_{n=1}^{\infty}\sum_{m=1}^{\infty} \frac{\dot\eta_n\dot\eta_m}{\gamma k_m^2}\int_0^1 \psi_n\psi_m\psi_i dx$$

$$\int_0^1 p'\frac{\partial^2 u'}{\partial t\partial x}\psi_i dx = -\frac{1}{\gamma a^2}\sum_{n=1}^{\infty}\sum_{m=1}^{\infty} \eta_n\eta_m\int_0^1 \psi_n\psi_m\psi_i dx$$

$$\int_0^1 \frac{\partial u'}{\partial t}\frac{\partial p'}{\partial x}\psi_i dx = -\frac{1}{\gamma a^2}\sum_{n=1}^{\infty}\sum_{m=1}^{\infty} \eta_n\eta_m\int_0^1 \frac{d\psi_n}{dx}\frac{d\psi_m}{dx}\psi_i dx$$

$$\int_0^1 u'\frac{\partial^2 p'}{\partial x\partial t}\psi_i dx = \sum_{n=1}^{\infty}\sum_{m=1}^{\infty} \frac{\dot\eta_n\dot\eta_m}{k_m^2}\int_0^1 \frac{d\psi_n}{dx}\frac{d\psi_m}{dx}\psi_i dx.$$

We see that the nonlinear terms can be put in the form

$$\sum_{n=1}^{\infty}\sum_{m=1}^{\infty} (A_{mni}\,\eta_n\eta_m + B_{mni}\dot\eta_n\dot\eta_m)$$

where the constants A_{mni} and B_{mni} are function only of the normal modes ψ_m, ψ_n and ψ_i .

In conclusion, we finally have the following system of equations for non-linear oscillators; one oscillator for each mode :

$$\ddot{\eta}_i + \omega_i^2 \eta_i = \sum_{n=1}^{\infty} (E_{ni}\eta_n + D_{ni}\dot{\eta}_n) + \sum_{n=1}^{\infty}\sum_{m=1}^{\infty} (A_{mni}\eta_m\eta_n + B_{mni}\dot{\eta}_m\dot{\eta}_n) \equiv F_n \quad (4.46)$$

E_{nn} is found to be proportional to the imaginary part $R_n^{(i)}$ of the linear response of the n^{th} mode. This remark will be used in the next section to show that the linear frequency shift is proportional to $R_n^{(i)}$

4.6.3. *Application of the Method of Averaging* .

The purpose of this section is to show how to apply the Method of Averaging to a system of ordinary differential equations representing a system of oscillators. The analysis to follow is only for longitudinal modes. Without loss of generality, we will show the method by applying it to system (4.46). Write now

$$\eta_i(t) = A_i(t)\ \sin\omega_i t + B_i(t)\cos\omega_i t$$

and assume Minorsky's[20] condition

$$\dot{A}_i(t)\sin\omega_i t + \dot{B}_i(t)\cos\omega_i t = 0. \quad (4.47)$$

The velocity and acceleration are then

$$\dot{\eta}_i = \omega_i\, A_i(t)\ \cos\omega_i t - \omega_i\, B_i(t)\ \cos\omega_i t$$

$$\ddot{\eta}_i = \omega_i(\dot{A}_i\cos\omega_i t - \omega_i A_i\sin\omega_i t) - \omega_i(\dot{B}_i\sin\omega_i t + \omega_i B_i\cos\omega_i t) \quad (4.48)$$

Equations (4.46) and (4.48) give

$$\omega_i \dot{A}_i \cos\omega_i t - \omega_i \dot{B}_i \sin\omega_i t = F_n \tag{4.49}$$

Equations (4.47) and (4.49) may be solved for $\dot{A}_i(t)$ and $\dot{B}_i(t)$, giving

$$\dot{A}_i(t) = \frac{1}{\omega_i} F_n \cos\omega_i t \tag{4.50}$$

$$\dot{B}_i(t) = -\frac{1}{\omega_i} F_n \sin\omega_i t \tag{4.51}$$

Now, we average (4.50)-(4.51) over the highest period $\frac{2\pi}{\omega_1}$, and assume that all $\dot{A}_i$ and $\dot{B}_i$ are approximately constant over that period of averaging, producing the formulas

$$\frac{dA_n}{dt} = \frac{1}{2n\pi} \int_0^{\frac{2\pi}{\omega_1}} F_n \cos\omega_n t dt$$

$$\frac{dB_n}{dt} = -\frac{1}{2n\pi} \int_0^{\frac{2\pi}{\omega_1}} F_n \sin\omega_n t dt.$$

Replace F_n by its expression in (4.46) and calculate the integrals, to find[19] the following set of equations :

$$\frac{dA_n}{dt} = \alpha_n A_n + \Theta_n B_n + n\frac{\beta}{2} \sum_{i=1}^{\infty} [A_i(A_{n-i} - A_{i-n} - A_{n+i}) - B_i(B_{n-i} + B_{i-n} + B_{n+i})] \tag{4.53a}$$

$$\frac{dB_n}{dt} = \alpha_n B_n - \Theta_n A_n + n\frac{\beta}{2}\sum_{i=1}^{\infty}[A_i(B_{n-i} + B_{i-n} + B_{n+i}) + B_i(A_{n-i} - A_{i-n} + A_{n+i})] \quad (4.53b)$$

where $\beta = \frac{\gamma+1}{8\gamma}\omega_1$. The coefficient Θ_n is found to be proportional to E_{nn} in Eq. (4.46). However, we found in the last section that E_{nn} was proportional to the imaginary part $R_n^{(i)}$ of the linear response. Therefore, Θ_n is proportional to $R_n^{(i)}$. This result will be used in Chapters 6 and 7 to discuss the influence of the imaginary parts $R_n^{(i)}$ on the stability of limit cycles.

Equations (4.53) constitute the basis of calculations in Chapter 6 regarding the determination of the amplitude and the conditions for existence and stability of limit cycles.

4.7. Concluding remarks

In this chapter, we used the two techniques, asymptotic-perturbation in Section 4.4 and perturbation-averaging in Section 4.6, to expand the conservation equations in combustion chambers. The asymptotic-perturbation technique was carried to third order in the amplitude of the fundamental while the perturbation-averaging technique was carried only to second order in the amplitude. In the following chapters, we limit the discussion to longitudinal modes only. In Chapter 4, we determine, using the asymptotic-perturbation technique, the amplitude and the conditions for existence of limit cycles. Chapter 5 deals with the stability of the limit cycle. In Chapter 6, we apply, using the the perturbation-averaging technique, to the results obtained in Section 4.6. We will also determine there the amplitude and the conditions for existence and stability of limit cycles. Chapters 7 and 8 deal with triggering of pressure oscillations in combustion chambers.

Appendix 4A

ON THE STRUCTURE OF THE BOUNDARY CONDITIONS

For illustration, we start with the following system of partial differential equations

$$\frac{\partial p}{\partial t} + \frac{\partial u}{\partial x} = \mu L_p[p, u] \tag{A.1}$$

$$\frac{\partial u}{\partial t} + \frac{\partial p}{\partial x} = \mu L_u[p, u] \tag{A.2}$$

with

$$L_B[p, u, \mu] = 0. \text{ on the boundaries} \tag{A.3}$$

where μ is a small parameter; L_p, L_u, and L_B are linear operators. For example

$$L_p[p, u] = c_1(x)p + c_2(x)\frac{\partial p}{\partial x} + d_1(x)u + d_2(x)\frac{\partial u}{\partial x}$$

We will show in the following calculations that the boundary conditions (A.3) can be written in the form

$$L_B^{(p)}(p) + \mu L_B^{(\mu)}(p, u) = 0. \tag{A.4}$$

where $L_B^{(p)}$ and $L_B^{(\mu)}$ are linear operators. Note that there is only one argument, here p, in $L_B^{(p)}$. The direct conclusion of (A.4) is that, in the determination of the

eigenvalues of order n, one needs only the eigenfunctions of order (n-1) or less. The following analysis will show the point.

Write Eqs. (A.1) and (A.2) as follows

$$L_1 p + L_2 u = \mu L_p(p, u) \tag{A.5}$$

$$L_3 u + L_4 p = \mu L_u(p, u) \tag{A.6}$$

where $L_1 = L_3 = \frac{\partial}{\partial t}$ and $L_2 = L_4 = \frac{\partial}{\partial x}$ are linear operators with inverses L_1^{-1}, etc. Equations (A.5) and (A.6) reduce to

$$u = -L_2^{-1} L_1 p + \mu L_2^{-1} L_p(p, u) = L_5(p) + \mu L_6(p, u) \tag{A.7}$$

$$u = -L_3^{-1} L_4 p + \mu L_3^{-1} L_u(p, u) = L_7(p) + \mu L_8(p, u) \tag{A.8}$$

These two equations can, in general, be solved to give a simple equation in p alone. Moreover, substitution of (A.7) in (A.3) gives

$$L_B(p, L_5(p) + \mu L_6(p, u), \mu) = 0.$$

This equation can be expanded in powers of μ

$$L_B(p, L_5(p)) + \mu \frac{\partial L_B}{\partial \mu}(p, L_5(p) + \mu L_6(p, u)) + \cdots = 0.$$

which can be written in the following form

$$L_B^{(p)} + \mu L_B(\mu)(p, u) + \cdots = 0.$$

which is Eq. (A.4). For example, the boundary conditions can be of the following form

$$\frac{\partial p}{\partial x} + c_1(x)p + \mu L_p(p, u) = 0.$$

For this form of boundary conditions, it is very useful to define the linear unperturbed problem with the following boundary conditions

$$\frac{\partial p_{10}}{\partial x} + c_1(x)p_{10} = 0$$

In the application of Green's theorem, the surface integrals (here point values, since one-dimensional problem) in expressions (4.18) and (4.21), Chapter 4, contain only terms of lower order than the eigenvalue. For example, in expression (4.18), in order to determine K_{01}, we need only to know the unperturbed acoustics modes p_{10} and u_{10}. In fact, the term under the surface integral sign is

$$p_{10}f_{11} - f_{10}p_{11} = [(-c_1(x)p_{11} + L_p(p_{10}, u_{10})]p_{10} - [(-c_1(x)p_{10})]p_{11} + 0(\mu)$$

$$= L(p_{10}, u_{10})p_{10} + 0(\mu)$$

Therefore, one needs only the expression of $L(p_{10}, u_{10})$ in $L(p, u)$ to determine K_{01}. In general, if the boundary conditions are defined as follows

$$L_B^{(p)}(p) + \mu L_B^{(u)}(p, u) = 0.$$

then the linear problem should be defined with the following boundary conditions

$$L_B^{(p)}(p) = 0.$$

The analysis can be extended easily to nonlinear and three-dimensional problems. The only modification is to substitute the small parameter μ by the amplitude parameter ε and the linear operators L_p, L_u and L_B by the nonlinear operators N_p, N_u and N_B. One direct conclusion is that, in order to determine K_{10} from expression (4.27), one needs only to know p_{10} and u_{10}. Similarly, in order to determine K_{20} from expression (4.33), one needs to know only $p_{20,2}$, $u_{20,2}$ and lower order terms.

REFERENCES 4

1. Morse, P. M. and Ingard, K. U. " *Theoretical Acoustics*," McGraw Hill Book Company, 1953.

2. Culick, F. E. C. " Acoustic Oscillations in Solid Propellant Rockets Chambers," *Acta Astronautica*, Vol. 12, NO. 2, 1966.

3. Flandro, G. A. "Stability Prediction for Solid Propellant Rocket Motors With High Speed Mean Flow," AFRPL-TR 79-98, 1980.

4. Stoker, G. G. " Periodic Motions in Non-Linear Systems Having Infinitely Many Degrees of Freedom, " *Actes du Colloque Internationale des Vibrations Non Lineaires*. Publication Ministere de L'air, No. 281, Paris, pp. 61, 1953

5. Penney, W. G. and Price, A. T. " Finite Amplitude Periodic Stationary Gravity Waves in a Perfect Fluid," *Phil. Trans. Roy. Soc. London* , A 244, pp. 254, 1952.

6. Verma, G. R. and Keller, J. B. " Three-Dimensional Standing Surface Waves of Finite Amplitude," *Physics of Fluids* 5, pp. 52, 1962.

7. Concus, P. J. " Standing Capillary-Gravity Waves of Finite Amplitude," *Jour. Fluid Mech.*, Vol. 14, pp. 568, 1962.

8. Tadjbakhsh, I and Keller, J. B. " Surface Standing Waves," *Jour. Fluid Mech.*, Vol. 2, pp. 442, 1960.

9. McQuery, C. E. " On Periodic Solutions of Autonomous and Nonautonomous Partial Differential Equations of Motion of Certain Elastic Media," Ph. D. Dissertation, The University of Texas, 1966.

10. Maslen, S. H. and Moore, F. K. " On Strong Transverse Wave Without Shock in a Circular Cylinder," Jour. Aeronautical Sciences, Vol. 23, No. 6, pp. 583, 1956.

11. Zinn, B. T. " A Theoritical Study of Nonlinear Combustion Instability in Liquid-Propellant Rocket Engines," *AIAA Journal*, Vol. 6, No. 10, 1966.

12. Rayleigh, Lord " *Theory of Sound*," Dover Publication, N.Y. 1945.

13. Nyborg, W. L. " Acoustic Streaming," in *Physical Acoustics*, Vol. 2B, Academic Press, N.Y. 1965. See also for the same author " Acoustic Streaming Due to Attenuated Plane Wave," *Jour. Acoust. Soc. of America*, Vol. 25, No. 1, pp. 68, 1953.

14. Culick, F. E. C. "Some Recent Results for Nonlinear Waves Motion in Solid Propellant Rockets," *AIAA* paper 79-1208, 1979.

15. Betchov, R. " Nonlinear Oscilations of a Column of Gas," *Physics of Fluids* 3, pp. 205, 1956.

16. Chester, W. "Resonant Oscillations in Closed Tubes," *J. Fluid Mech.* , Vol. 18, pp. 44, 1964.

17. Collins, W. D. " Forced Oscillations of Systems Governed by One-Dimensional Nonlinear Wave Equations." *Quarterly Journal of Mech. and Appl. Math.* , Vol. 24, pp. 129, 1971.

18. Jiminez, J. " Nonlinear Gas Oscillations in Pipes. Part I. Theory," *J. Fluid Mech.*, Vol. 59, pp. 23, 1973.

19. Culick, F. E. C. " Nonlinear Behavior of Acoustic Waves in Combustion Chambers," *Acta Astronautica*, Vol. 3 , No. 9, Sept. 1976.

20. Minorsky, N. " *Nonlinear Oscillations*," D. Van Nostrand Co., Princeton N.J., 1962.

Chapter 5

LONGITUDINAL MODES: AMPLITUDE AND CONDITIONS FOR EXISTENCE AND STABILITY OF THE LIMIT CYCLES

5.1. Introduction

The stability of longitudinal modes for pressure oscillations in combustion chambers has been the object of investigation for a long time. Chu and Ying[1] examined the nonlinear thermally driven ocillations in a pipe with a traveling shock wave, using a characteristic perturbation method. They predicted that the fluctuation could attain a limiting value but they did not determine the expression for the limit cycle amplitude. Sirignano[2] also used a shock wave model to examine the nonlinear stability of pressure ocillations in combustion chambers. The expression for the amplitude of the limit cycle was found using a *numerical* routine. Marxman and Wooldrige[3] examined the interaction between a traveling shock wave and a burning surface. Zinn and Lores[4] and Lores and Zinn[5] treated a similar problem by expanding the acoustic quantities in the normal modes of the acoustic field in the chamber. The limit cycle was found by solving *numerically* a set of second order coupled nonlinear ordinary differential equations. The technique developed here treats only the asymptotic solution. Direct *analytical* results for the amplitude of the limit cycle will be presented. Its advantage is its capabitility to handle high orders in a straightforward manner.

The case of pure longitudinal modes must be treated differently from the general case presented in the last chapter, Section 4.4.2. In Section 4.2 we show the point. A new double expansion in the wave amplitude and in the average Mach number is introduced. For simplicity, the analysis in this section is carried out to second order in the wave amplitude. Appendix 5B deals with higher orders. The dependence of the complex frequency of the wave on the wave

amplitude is determined. The analysis is applied to a one-dimensional problem. The amplitude and the conditions for existence of limit cycles for pressure oscillations are determined. The effects of the dispersion, or frequency-dependence, of the responses of the different processes in the chamber to pressure ocillations are shown to be essential in establishing the limit cycle.

5.2. A simple proof for need to change the expansion

In the expansion presented in Chapter 4, Section 4.4.2, we treated the general case of acoustical modes whose frequencies are not integer multiples of the fundamental. The reason for restricting the discussion there to that kind of mode will be shown in the following calculations. For illustration, we use the one-dimensional model shown in Figure 4.1 with $B_{00} = 0$. From the last chapter, Eq. (4.34), the linear, unperturbed frequencies of the longitudinal modes are integer multiples of the fundamental. The linear acoustic problem becomes, from Eqs. (4.12) and (4.13) in Chapter 4,

$$iK_{00}p_{10,1} + \gamma \frac{du_{10,1}}{dx} = 0 \tag{5.1}$$

$$iK_{00}u_{10,1} + \frac{dp_{10,1}}{\gamma dx} = 0 \tag{5.2}$$

with $\frac{dp}{dx} = 0$ at $x = 0,1$. This system yields, with ε in (4.8) being taken as half the amplitude of the fundamental, expressions for $p_{10,1}$ and $u_{10,1}$

$$p_{10,1} = (e^{iK_{00}x} + e^{-iK_{00}x}) \tag{5.3}$$

$$u_{10,1} = -\frac{1}{\gamma}(e^{iK_{00}x} - e^{-iK_{00}x}) \tag{5.4}$$

with $K_{00} = n\,\pi$ where n is an arbitrary integer. Keeping these results in mind, we write down the system of second order acoustics equations, Eqs. (4.28)-(4.29) in the last chapter give

$$2iK_{00}p_{20,2} + \gamma\frac{du_{20,2}}{dx} = -\gamma p_{10,1}\frac{du_{10,1}}{dx} - u_{10,1}\frac{dp_{10,1}}{dx} \tag{5.5}$$

$$2iK_{00}u_{20,2} + \frac{dp_{20,2}}{\gamma dx} = -u_{10,1}\frac{du_{10,1}}{dx} - i\,K_{00}\,\rho_{10,1}u_{10,1} \tag{5.6}$$

with $\rho_{10,1} = \frac{p_{10,1}}{\gamma}$ from the energy equation (4.7) in the last chapter. The above system yields, after substituting for $p_{10,1}$ and $u_{10,1}$ their expressions (5.3)-(5.4),

$$\frac{d^2u_{20,2}}{dx^2} + 4\,K_{00}^2\,u_{20,2} = -2\,\gamma\,K_{00}^2\,(1 + \frac{1}{\gamma})\,(e^{2iK_{00}x} - e^{-2iK_{00}x})$$

The solution to this equation is

$$u_{20,2} = A\,e^{2iK_{00}x} + B\,e^{-2iK_{00}x} + \frac{1}{2}\gamma\,i\,K_{00}\,x\,(1 + \frac{1}{\gamma})\,(e^{2iK_{00}x} - e^{-2iK_{00}x}) \tag{5.7}$$

where A and B are constants. Assume further that

$$\frac{dp_{20,2}}{dx}(0) = \frac{dp_{20,2}}{dx}(1) = 0.$$

Using (5.6), Eq. (5.7) then gives

$$K_{00}\,(1 + \frac{1}{\gamma}) = 0.$$

which is impossible. Therefore, the expansion presented in Section 4.4.2 is not valid for pure longitudinal modes whose frequencies are integer multiples of the fundamental.

5.3. Presentation of the expansion

5.3.1. *Introduction to the expansion* . As we have seen in the preceding section, the expansion breaks down when the mode considered is purely longitudinal with $K_{00} = n\pi$. In this section we will show how to handle this case. For clarity of presentation, the expansion here is carried out only to second order in the wave amplitude. Appendix 5A deals with the general formulation to any order. Expand p, ρ and $\underline{u}$ as follows

$$p = 1 + \mu^2 p_{02} + \cdots + \varepsilon\,(\,p_{10,1} + \mu p_{11,1} + \ldots)\,e^{iKt} \tag{5.8}$$

$$+ \varepsilon\,(\,\delta_2^{(1)} p_{10,2}\,e^{2\alpha g_2^{(1)}(\mu)\,t} + \mu p_{11,2} + \cdots\,)\,e^{2iKt}$$

$$+ \varepsilon\,(\,\delta_3^{(1)} p_{10,3}\,e^{3\alpha g_3^{(1)}(\mu)\,t} + \mu p_{11,3} + \ldots)\,e^{3iKt} + \cdots +$$

$$+ \varepsilon^2(\,p_{20,0} + \mu p_{21,0} + \cdots\,)$$

$$+ \varepsilon^2(\,p_{20,1} + \mu p_{21,1} + \cdots\,)e^{iKt}$$

$$+ \varepsilon^2 \left(\delta_2^{(2)} p_{20,2}\, e^{2\alpha g_2^{(2)}(\mu)t} + \mu p_{21,2} + \cdots \right) e^{2iKt}$$

$$+ \varepsilon^2 \left(\delta_3^{(2)} p_{30,2}\, e^{3\alpha g_3^{(2)}(\mu)t} + \mu p_{31,2} + \cdots \right) e^{3iKt} + \ldots.$$

The density ρ and velocity $u = \mu\bar{u} + u'$ have similar expansions. The complex frequency K is expanded as follows

$$K = K_{00} + \mu K_{01} + \mu K_{02} + \cdots + \varepsilon(K_{10} + \mu K_{11} + \ldots) + \varepsilon^2(K_{20} + \mu K_{21} + \cdots) + \text{etc.}$$

The terms $p_{10,2}$, $p_{11,2}$, etc., are introduced in order to avoid the indeterminacy of $p_{20,2}$, $p_{21,2}$, etc. noted above. The terms $e^{2\alpha g_2^{(1)}(\mu)t}$, $e^{3\alpha g_3^{(1)}(\mu)t}$, etc., are introduced in order to avoid the double determinacy of K_{01} (see Eq. (5.11)). The term $e^{2\alpha g_2^{(2)}(\mu)t}$ is introduced to avoid the double determination of K_{11}. The terms $\delta_2^{(1)}$, $\delta_3^{(1)}$, etc., will yield the amplitudes of the higher modes.

5.3.2. *Detailed expansion and results* . In this section, we will match the coefficients of $\varepsilon^l \mu^m e^{inKt}$ and we will show how expansion (5.4) will allow us to determine the limit cycle. First, we note that $p_{10,1}$, $p_{10,2}$, etc., correspond to the linear acoustics modes. The components $p_{11,1}$, $p_{11,2}$, etc., correspond to the first order distortion of the linear acoustics modes by the mean flow. The treatment of these components is similar to the one presented in Section 4.3, Chapter 4. We will treat here only the nonlinear components of the waveform. The analysis here is essentially for one-dimensional oscillations, but for the sake of maintaining a parallel with Section 4.4.2, Chapter 4, we use the notation for three-dimensional motions. We start with (l,m,n)=(2,0,0) to get from the conservation equations

$$-2\,\alpha_{00}p_{20,0} + \gamma\nabla\cdot u_{20,0} = -\gamma\, p_{10,1}\nabla\cdot u^{*}_{10,1} - \gamma\, p^{*}_{10,1}\nabla\cdot u_{10,1} \tag{5.9}$$

$$- u^{*}_{10,1}\cdot\nabla\, p_{10,1} - u_{10,1}\cdot\nabla\, p^{*}_{10,1}$$

$$-2\,\alpha_{00}u_{20,0} + \frac{\nabla\, u_{20,0}}{\gamma} = -u_{10,1}\cdot\nabla\, u^{*}_{10,1} - u^{*}_{10,1}\cdot\nabla\, u_{10,1} \tag{5.10}$$

$$+ i\,K_{00}\rho_{10,1}u^{*}_{10,1} - i\,K_{00}\rho^{*}_{10,1}u_{10,1}$$

The terms $p_{20,0}$ and $u_{20,0}$ represent, as mentioned in Section 4.4.2, Chapter 4, the time-independent flow of fluid induced by the nonlinear acoustic field, or acoustic streaming.

A problem arises in the treatment of the equations of acoustics streaming when $\alpha_{00} = 0$: since the analysis is one-dimensional, each equation is a first order ordinary differential equation in $p_{20,0}$ or $u_{20,0}$ *alone*. If the *two* boundary conditions are given in terms of $p_{20,0}$ or $u_{20,0}$ alone then the problem can not be solved. However, we can circumvent the problem as follows. Assume first that α_{00} is different from zero, eliminate $u_{20,0}$ or $p_{20,0}$ between Eqs. (5.9) and (5.10), and *then* set $\alpha_{00} = 0$, to find a *second* order ordinary differential equation in $u_{20,0}$ or $p_{20,0}$ and the difficulty is removed. For the remaining analysis in this section, the acoustics streaming effects have no further influence since we limit the analysis here to second order in the wave amplitude. However, their influence will become apparent when we deal with higher order expansions; see Chapter 8, Section 8.2.

Now we determine the coefficients $g_2^{(1)}$, etc., because they will be needed later to calculate K_{10}, K_{11}, etc. For simplicity, we limit the analysis to the first

term $g_{20}^{(1)}$ in the expansion of $g_2^{(1)}(\mu)$ in μ

$$g_2^{(1)} = g_{20}^{(1)} + \mu\, g_{21}^{(1)} + \text{etc.}$$

and only K_{10} will be determined. By equating the coefficients of $\varepsilon\mu e^{2iKt}$ in the conservation equations and *then* by taking the limit $\alpha = 0$, we get

$$2\, iK_{00}p_{11,2} + \gamma\, \nabla \cdot u_{11,2} = (-2iK_{01} + 2\alpha_{01}^{(1)}g_{20}^{(1)})\, p_{10,2} - \gamma\, p_{10,2}\, \nabla \cdot u_{10,2} - \bar{u} \cdot \nabla\ p_{10,2}.$$

$$2\, iK_{00}u_{11,2} + \frac{\nabla\ p_{11,2}}{\gamma} = (-2iK_{01} + 2\alpha_{01}^{(1)}g_{20}^{(1)})\, u_{10,2} - \bar{u} \cdot \nabla\, u_{10,2} - u_{10,2} \cdot \nabla\ \bar{u}$$

To these equations we apply the same technique used in Section 3.3 to determine K_{01}. The result is

$$4(k_{01} - i\alpha_{01}^{(1)}g_{20}^{(1)})\, k_{00}\, E_{10,2}^2 = -\int_S p_{10,1}f_{11,2}\, ds + \int_S p_{11,2}f_{10,1}\, ds \qquad (5.11)$$

$$-\frac{i}{K_{00}} \int_V (\nabla \cdot (\bar{u} \cdot \nabla\ u_{10,2} + u_{10,2} \cdot \nabla\, \bar{u}))\, p_{10,1}\, dv$$

$$+ i\, K_{00} \int_V (\bar{u} \cdot \nabla\ p_{10,2})\, p_{10,1}\, dv + \gamma\, i\, K_{00} \int_V (p_{10,2}\, \nabla \cdot \bar{u})\, p_{10,1}\, dv$$

where

$$f_{1m,n} = \underline{n} \cdot \nabla\ p_{1m,n}$$

$$E_{10,2}^2 = \int_v p_{10,2}^2 dv.$$

However, K_{01} is determined by equating the coefficients of $\varepsilon\mu e^{iKt}$ as shown in Section 4.3, Eq. (4.18), in the last chapter. We see that if $g_2^{(1)}$ were not present in the expansion, Eq. (5.11) would give another value for K_{01} and the expansion would break down. This is the reason for introducing $g_2^{(1)}$.

We now direct our attention to the determination of K_{10}. There are two ways to do so. First, we equate the coefficients of $\varepsilon^2\mu^0 e^{iKt}$ and *then* we take the limit $\alpha = 0$, to get

$$iK_{00}p_{20,1} + \gamma\nabla \cdot u_{20,1} = -iK_{10}p_{10,1} - \gamma\delta_2^{(1)}p_{10,2}\nabla \cdot u_{10,1}^* - \gamma\delta_2^{(1)}p_{10,1}^*\nabla \cdot u_{10,2}$$

$$- \delta_2^{(1)}u_{10,1}^*.\nabla\, p_{10,2} - \delta_2^{(1)}u_{10,2}.\nabla\, p_{10,1}^*$$

$$iK_{00}u_{20,1} + \frac{\nabla\, p_{20,1}}{\gamma} = -iK_{10}u_{10,1} - \delta_2^{(1)}u_{10,1}^*.\nabla\, u_{10,2}$$

$$- 2iK_{000}\delta_2^{(1)}\rho_{10,1}^*u_{10,2} + iK_{00}\delta_2^{(1)}\rho_{10,2}u_{10,1}^*$$

The expression for the coefficient K_{10} is obtained following the same technique used in Section 4.3, Chapter 4, to determine K_{01}. The result is

$$2\,K_{10}K_{00}E_{10,1}^2 = -\int_s p_{10,1}f_{20,1}ds + \int_s f_{10,1}p_{20,1}ds + \int_v h_{10,1}p_{10,1}dv \qquad (5.12)$$

where

$$h_{10,1} = -\gamma\delta_2^{(1)}p_{10,2}\nabla .u_{10,1}^{*} - \gamma\delta_2^{(1)}p_{10,1}^{*}\nabla .u_{10,2}$$

$$- \delta_2^{(1)}u_{10,1}^{*}\nabla\, p_{10,2} - \delta_2^{(1)}u_{10,2}\nabla\, p_{10,1}^{*}$$

$$+ \nabla .\,(- \delta_2^{(1)}u_{10,1}^{*}.\nabla\, u_{10,2} - \delta_2^{(1)}u_{10,2}.\nabla\, u_{10,1}^{*} - 2iK_{00}\delta_2^{(1)}\rho_{10,1}^{*}u_{10,2} + iK_{00}\delta_2^{(1)}\rho_{10,2}u_{10,1}^{*}).$$

This equation corresponds to a relationship between K_{10} and $\delta_2^{(1)}$. Another way to determine determine K_{10} is by equating the coefficients of $\varepsilon^2\mu^0 e^{2iKt}$ and *then* by taking $\alpha = 0$, to obtain

$$2iK_{00}p_{20,2} + \gamma\nabla .u_{20,2} = -2(iK_{10} + \alpha_{10}g_{20}^{(1)})\delta_2^{(1)}\, p_{10,2} - \gamma p_{10,1}\nabla .u_{10,1} - u_{10,1}\,\nabla\, p_{10,1}$$

$$2iK_{00}u_{20,2} + \frac{\nabla\, p_{20,2}}{\gamma} = -2(iK_{10} + \alpha_{10}g_{20}^{(1)})\delta_2^{(1)}u_{10,2} - u_{10,1}.\nabla\, u_{10,1} - iK_{00}\rho_{10,1}u_{10,1}.$$

These two equations yield

$$8\delta_2^{(1)}(K_{10} - i\alpha_{10}g_{20}^{(1)})\, K_{00}E_{10,2}^2 = -\int_s p_{10,1}\nabla\, p_{20,2}ds \qquad (5.13)$$

$$+ 2iK_{00}\int_v p_{10,1}(\, u_{10,1}.\nabla\, p_{10,1}\,)dv + 2i\gamma K_{00}\int_v p_{10,1}(\, p_{10,1}\nabla .u_{10,1}\,)dv$$

$$+ 2i\gamma K_{00}\int_v p_{10,1}(u_{10,1}.\nabla\, u_{10,1} + iK_{00}\rho_{10,1}u_{10,1})dv.$$

This is another relationship between K_{10} and $\delta_2^{(1)}$. Eqs. (5.12) and (5.13)

determine uniquely K_{10} and $\delta_2^{(1)}$.

The limiting amplitudes correspond to the values of ε which make the imaginary part of the complex frequency K vanish. The values of ε determine the amplitude of the first mode and the coefficient $\delta_2^{(1)}$ determines the amplitude of the second mode when the limit cycle is reached.

5.4. Existence of limit cycles

In the preceding section, we have shown how to determine the terms in the expansion of the complex frequency K

$$K = K_{00} + \mu K_{01} + \cdots + \varepsilon(K_{10} + \ldots) + \varepsilon^2(K_{20} + \cdots) + \text{etc.}$$

The imaginary part of this quantity is

$$\alpha = \alpha_{00} + \mu\alpha_{01}^{(1)} + \cdots + \varepsilon(\alpha_{10} + \ldots) + \varepsilon^2(\alpha_{20} + \cdots) + \text{etc.} \qquad (5.14)$$

When we limit the expansion of K to first order in μ and to first order in ε, then the growth rate α becomes

$$\alpha = \alpha_{00} + \mu\alpha_{01}^{(1)} + \varepsilon\alpha_{10}$$

The limit cycle is then reached when α vanishes, i.e.

$$\alpha_{00} + \mu\alpha_{01}^{(1)} + \varepsilon\alpha_{10} = 0$$

The coefficients α_{00} and $\alpha_{01}^{(1)}$ correspond to the linear problem and, in general, exist. The existence of a limit cycle reduces to the existence of a non-zero value for α_{10}. This result will be applied in the next section to a one-dimensional

problem.

When we limit the expension of K to second order in ε, then we have, from (5.14),

$$\alpha = \alpha_{00} + \mu\alpha_{01}^{(1)} + \varepsilon\,\alpha_{10} + \varepsilon^2\,\alpha_{20}$$

The existence criteria become

1) α_{10} should exist and be non–zero.

2) α_{20} should exist and be non–zero.

3) $\alpha_{10}^2 - 4\,(\alpha_{00} + \mu\alpha_{01}^{(1)})\,\alpha_{20} > 0$.

The discussion can, of course, be extended to any order in μ and ε. It should be emphasized that this discussion is valid also for the general case treated in Chapter 4, Section 4.4.

5.5. Application of the results

Now the above results will be applied to the longitudinal model of the combustion chamber shown in Figure 4.1. The conditions for existence and the amplitude of the limit cycle will determined.

First, Eq. (5.11) yields the following relationship between K_{10} and $\delta_2^{(1)}$

$$\delta_2^{(1)} = \frac{2K_{10}}{K_{00}(\frac{1}{\gamma} + 1)}. \qquad (5.15)$$

Second, Eq. (5.13) gives

$$\delta_2^{(1)} = \frac{K_{00}(1 + \frac{1}{\gamma})}{(4K_{10} - 4i\alpha_{10}g_{20}^{(1)})}$$

Using (5.12), this reduces to

$$K_{10} = \frac{K_{00}^2 (1 + \frac{1}{\gamma})^2}{8K_{10} - 8i\alpha_{10}g_{20}^{(1)}}. \qquad (5.16)$$

On the other hand, Eq. (5.9) yields the following expression for $g_{20}^{(1)}$

$$2(K_{01} - i\alpha_{01}^{(1)}g_{20}^{(1)}) = i\gamma(B_{01}^{(2)} - A_{01}^{(2)}) \equiv - i\, \alpha_{01}^{(2)} \qquad (5.17)$$

where $\mu\alpha_{01}^{(1)}$ is the growth rate of the first mode and $\mu\alpha_{01}^{(2)}$ is the growth rate of the second mode. In particular, when K_{01} is a pure imaginary, i.e., $K_{01} = - i\, \alpha_{01}^{(1)}$, then

$$g_{20}^{(1)} = \frac{\alpha_{01}^{(2)} - 2\alpha_{01}^{(1)}}{2\alpha_{01}^{(1)}}$$

Thus, from (5.16),

$$\alpha_{10} = \frac{K_{00}}{2}(1 + \frac{1}{\gamma})(- \frac{\alpha_{01}^{(1)}}{\alpha_{01}^{(2)}})^{\frac{1}{2}} \qquad (5.18)$$

The frequency, when the limit cycle is approached, should be real, giving

$$\mu\alpha_{01}^{(1)} + \varepsilon\,\alpha_{10} = 0$$

which reduces, using (5.18), to

$$\varepsilon = \frac{\mu}{4\beta}\left(-\alpha_{01}^{(1)}\alpha_{01}^{(2)}\right)^{\frac{1}{2}} \tag{5.19}$$

where $\beta = \frac{K_{00}}{8}\left(1 + \frac{1}{\gamma}\right)$. Define

$$\alpha_1 = \mu\,\alpha_{01}^{(1)}\,,\ \alpha_2 = \mu\,\alpha_{01}^{(2)}$$

to get

$$\varepsilon = \frac{1}{4\beta}\sqrt{-\alpha_1\alpha_2} \tag{5.20}$$

We now define

$$\overline{p_1} = \varepsilon p_{10,1}e^{iKt} + \text{c.c.},\ \overline{p_2} = \varepsilon\delta_2^{(1)}p_{10,2}e^{iKt} + \text{c.c.} \tag{21}$$

From expansion (5.8), we see that, when we neglect the distortion by the mean flow and nonlinear terms, $\overline{p_1}$ and $\overline{p_2}$ correspond respectively to the first and second modes. Using Eq. (5.3), $\overline{p_1}$ becomes

$$\overline{p_1} = 4\,\varepsilon\cos\omega x\cos\omega t \tag{5.22}$$

where $\omega = K_{00}$. Using (5.20), we get the amplitude of the first mode

$$a_{10} = 4\,\varepsilon \equiv \frac{1}{\beta}\sqrt{-\alpha_1\alpha_2} \tag{5.23}$$

The second mode disturbance will be determined as follows. Eq. (5.15) gives

$$\delta_2^{(1)} = \frac{-2\,i\,\alpha_{10}}{K_{00}(\frac{1}{\gamma}+1)}$$

Using Eq. (5.18), we get

$$\delta_2^{(1)} = -i(-\frac{\alpha_{01}^{(1)}}{\alpha_{01}^{(2)}})^{\frac{1}{2}} \tag{5.24}$$

The second mode disturbance becomes, using (5.3) and (5.24),

$$\overline{p_2} = -2i\,\varepsilon\cos 2\omega x\,(-\frac{\alpha_{01}^{(1)}}{\alpha_{01}^{(2)}})^{\frac{1}{2}}(e^{iKt} - e^{-iKt}) \equiv -4\,\varepsilon\cos 2\omega x\,\sin 2\omega t(-\frac{\alpha_{01}^{(1)}}{\alpha_{01}^{(2)}})^{\frac{1}{2}}$$

Hence, we get, using (5.20), the following expression for the amplitude of the second mode

$$a_{20} = \frac{\alpha_1}{\beta} \tag{5.25}$$

5.6. Discussion of the results

Equations (5.23) and (5.25) yield the amplitudes of the first and the second harmonics of the limit cycle. These results will be found again in Chapter 5 when the expansion in the normal modes of the chamber is treated. That constitutes a strong support of our expansion.

It is essential to notice here that, in order to reach a limit cycle, α_{10} must exist be non-zero, giving, from (5.18),

$$\alpha_1 \alpha_2 < 0 \tag{5.26}$$

This means that both a source of energy and a sink of energy should be present. This is a direct proof of the effect of the dispersion, in the sense of dependence on the frequency, of the boundary conditions on the establishment of the limit cycle.

A physical interpretation of the condition (5.26) is that , in order for a limit cycle to exist, at least one mode should extract energy from the wave while another mode is supplying energy to it. The transfer of energy from one mode to another is done by the nonlinear motion of the wave. For example, the non-linear convection term $u.\nabla u$ in the conservation equations can be perceived as a vehicle transfering energy between the first and the second modes. The limit cycle is reached when the processes supplying energy to the wave balance the processes extracting energy from the wave.

5.7. Stability of the limit cycle

5.7.1. *Introduction* . In the last section, we used the asymptotic-perturbation method to determine the amplitude and the conditions for existence of limit cycles for pressure oscillations in combustion chambers. The crucial point of whether such limit cycles physically exist, i.e. are stable, is treated in this section.

The technique we follow here consists in linearizing the conservation equations near the limit cycle solution. The result is a system of of *linear* partial differential equations with periodic coefficients. This system is similar to the

system of Bloch waves[6] encountered in the theory of electrons in crystals. The solution to this system is found by expanding the solution in the normal modes of the reduced system obtained by neglecting the time-dependent parts. Application of Green's theorem (Chapter 4, Section 4.6) then yields a system of second order linear ordinary differential equations with periodic coefficients, one equation for each mode. This system can be treated used the Floquet theory[7]. However, the structure of the periodic coefficients makes the treatment by the method of time-averaging particularly easy, especially for longitudinal modes where the final result reduces to a system of first order linear ordinary differential equations with *constant* coefficients. The study of the stability of such a system is straightforward and very abundant in the literature.

For simplicity, the following analysis will be directed to the treatment of longitudinal modes partly because, in the last chapter, the limit cycles were found only for the longitudinal modes, partly because of the relative simplicity of the calculations. Only two modes are taken into account. However, the analysis covered in this chapter can easily be applied to many modes and to three-dimensional problems once the limit cycles are found.

5.7.2. *Analysis* . The objective is first, to linearize the conservation equations near the limit cycles; and second, to study the stability of the limit cycle by applying Green's theorem, or spacial averaging, and the method of time-averaging. We start from the conservation equations

$$\frac{\partial p}{\partial t} + \gamma\, p \nabla \cdot \underline{u} + \underline{u} \cdot \nabla\, p = 0 \tag{5.27}$$

$$\rho\left(\frac{\partial \underline{u}}{\partial t} + \underline{u} \cdot \nabla\, \underline{u} \right) + \frac{\nabla\, p}{\gamma} = 0 \tag{5.28}$$

$$p\,\rho^{-\gamma} = 1 \tag{5.29}$$

For illustration, only one-dimensional problems will be treated. Moreover, we limit the expansion of the pressure, density, and velocity to two modes

$$p = 1 + \overline{p_1} + \overline{p_2} + p'$$

$$\rho = 1 + \overline{\rho_1} + \overline{\rho_2} + \rho'$$

$$u = \overline{u} + \overline{u_1} + \overline{u_2} + u'$$

where($\overline{p_1}$, $\overline{p_2}$).($\overline{\rho_1}$, $\overline{\rho_2}$)., and ($\overline{u_1}$, $\overline{u_2}$) are the first and the second mode components of the limit cycle. To make matters simple, we will focus on the case treated in Chapter 4, Section 4.5, where we found

$$\overline{p_1} = a_{10} \cos \omega x \cos \omega t \tag{5.30}$$

$$\overline{p_2} = a_{20} \cos 2\omega x \sin 2\omega t \tag{5.31}$$

where

$$a_{10} = \frac{1}{\beta}\sqrt{-\alpha_1\alpha_2}\,,\; a_{20} = \frac{\alpha_1}{\beta}$$

The expressions for $\overline{u_1}$, etc. can be found from the linear acoustics equations using (5.27) and (5.28). For example

$$\overline{u_1} = -\frac{a_{10}}{\gamma} \sin\omega x \sin\omega t \tag{5.32}$$

On the other hand, p', ρ' and u' are small perturbations near the limit cycle. The linearization yields the following system of partial differential equations

$$\frac{\partial p'}{\partial t} + \gamma \frac{\partial u'}{\partial x} = h_1 \tag{5.33}$$

$$\frac{\partial u'}{\partial t} + \frac{\partial p'}{\gamma \partial x} = h_2 \tag{5.34}$$

where

$$h_1 = -\gamma p' \frac{\partial(\overline{u} + \overline{u_1} + \overline{u_2})}{\partial x} - \gamma (1 + \overline{p_1} + \overline{p_2}) \frac{\partial u'}{\partial x} - u' \frac{\partial(\overline{p_1} + \overline{p_2})}{\partial x} \tag{5.35}$$

$$-(\overline{u} + \overline{u_1} + \overline{u_2}) \frac{\partial p'}{\partial x}$$

$$h_2 = -(1 + \overline{\rho_1} + \overline{\rho_2}) \frac{\partial u'}{\partial x} \tag{5.36}$$

$$-u'(1 + \overline{\rho_1} + \overline{\rho_2}) \frac{\partial(\overline{u} + \overline{u_1} + \overline{u_2})}{\partial x} \quad (1 + \overline{\rho_1} + \overline{\rho_2})(\overline{u} + \overline{u_1} + \overline{u_1}) \frac{\partial u'}{\partial x}$$

$$-p' \frac{\partial(\overline{u} + \overline{u_1} + \overline{u_2})}{\gamma \partial t} \quad -p'(\overline{u} + \overline{u_1} + \overline{u_2}) \frac{\partial(\overline{u} + \overline{u_1} + \overline{u_2})}{\gamma \partial x}$$

Equations (5.33) and (5.34) yield

$$\frac{\partial^2 p'}{\partial t^2} - \frac{\partial^2 p'}{\partial x^2} = \frac{\partial h_1}{\partial t} - \frac{\partial h_2}{\partial x} = H_1 \tag{5.37}$$

Since $\overline{p_1}$, etc., represent, from the previous chapter, the components of the limit cycle and, therefore, are harmonic functions of time, Eq. (5.37) is a linear, *parametric*, inhomogeneous hyperbolic equation.

In Section 5.7.1, we apply Green's theorem to equation (5.37), using the technique described in Chapter 4, Section 4.6, to obtain a system of two ordinary, linear differential equations with time-dependent coefficients. This system will be reduced in Section 5.7.2, using the method of time-averaging, to a system of ordinary differential equations with constant coefficients. The standard stability analysis is then applied to obtain conditions for stability of the limit cycle.

5.7.2.1 *Application of Green's Theorem* . Expand the pressure and velocity as follows

$$p' = \eta_1(t)\cos\omega x + \eta_2(t)\cos 2\omega x$$

$$u' = -\frac{\dot{\eta}_1(t)}{\gamma\omega}\sin\omega x - \frac{\dot{\eta}_2(t)}{2\gamma\omega}\sin 2\omega x ,$$

and apply Green's theorem (see Chapter 4, Section 4.6) to Eq. (5.37). This technique consists here of multiplying Eq. (5.37) by $\cos \omega_i x$, i = 1,2, integrating the results over the total length of the chamber, and using Green's theorem, to find the following system of ordinary differential equations

$$\ddot{\eta}_1 + \omega_1^2\eta_1 = D_{11}\dot{\eta}_1 + C_1\cos\omega t\eta_2(t) + C_2\sin\omega t\dot{\eta}_2(t)$$

$$+ C_3\cos 2\omega t\eta_1(t) + C_4\sin 2\omega t\dot{\eta}_1(t) \qquad (5.38)$$

$$\ddot{\eta}_2 + \omega_2^2\eta_1 = D_{22}\dot{\eta}_2 + F_1\cos\omega t\eta_1(t)B + F_2\sin\omega t\dot{\eta}_1(t) \qquad (5.39)$$

where

$$\omega_2 = 2\omega_1 = 2\omega$$

$$D_{11} = -2\,\alpha_1\,,\ D_{22} = -2\,\alpha_2$$

$$C_1 = \frac{5}{4}\,a_{10}\,\omega^2\left(-1 + \frac{1}{\gamma}\right)$$

$$C_2 = \frac{1}{4}\,a_{10}\,\omega\left(-1 + \frac{3}{2\gamma}\right)$$

$$C_3 = a_{20}\,\omega\left(1 - \frac{3}{2\gamma}\right)$$

$$C_4 = \frac{5}{4}\,a_{20}\omega^2\left(-1 + \frac{1}{\gamma}\right)$$

$$F_1 = \frac{1}{2} a_{10}\omega^2\left(-1 + \frac{1}{\gamma}\right)$$

$$F_2 = -\frac{1}{2} a_{10}\omega\left(1 + \frac{3}{\gamma}\right)$$

System (5.38)-(5.39) will be reduced further using the method of time-averaging. The point is to reduce this system of *second* order linear *parametric*, differential equations to a system of first order linear differential equations with *constant* coefficients. Thus, the stability of the limit cycle can be studied in a much easier way.

5.7.2.2 *Application of the Method of Averaging* . The description of the method was described in Chapter 4, Section 4.6. Expand η_1 and η_2 as follows

$$\eta_1(t) = A_1(t)\sin \omega t + B_1(t)\cos \omega t$$

$$\eta_2(t) = A_2(t)\sin 2\omega t + B_2(t)\cos 2\omega t$$

Substitution of these expressions in (5.38) and (5.39) yields, after application of the method, the following system of ordinary differential equations for the A_i and B_i

$$\frac{dA_1}{dt} = \alpha_1 A_1 + c_1 B_1 + c_2 B_2 \qquad (5.40)$$

$$\frac{dB_1}{dt} = \alpha_1 B_1 + c_3 A_1 + c_4 A_2 \qquad (5.41)$$

$$\frac{dA_2}{dt} = \alpha_2 A_2 + d_1 B_1 \tag{5.42}$$

$$\frac{dB_2}{dt} = \alpha_2 B_2 + d_3 A_1 \tag{5.43}$$

where

$$c_1 = -c_4 = -\beta\, a_{20}$$

$$c_2 = -c_3 = -\beta\, a_{10}$$

$$d_1 = -d_3 = -2\,\beta a_{10}$$

and $\beta = \frac{\omega}{8}(1 + \frac{1}{\gamma})$. The stability of the limit cycle is now reduced to the stability of the trivial equilibrium point of the system (5.40)-(5.43). By writing $A_1 = U_1 e^{\lambda t}$, etc., where U_1, etc., are constant, and replacing these expressions in the above linear system we get a linear system of equations for U_1, etc., of the form

$$M\vec{X} = 0$$

where M is the matrix of the linear system and $\vec{X}$ represent U_1, etc. This system has non-zero solutions only when its determinant vanishes. This gives a polynomial equation in λ, the characteristic polynomial. The conditions under which the limit cycle is stable are reduced to those under which all the roots of this polynomial have negative real parts. Many textbooks treat this problem; see

reference 8, for example. These conditions are commonly known as Routh-Hurwitz or Lienard criteria. For a polynomial of the form

$$P(\lambda) = \lambda^4 + a_3\lambda^3 + a_2\lambda^2 + a_1\lambda$$

these criteria are

$$a_1 > 0,\ a_3 > 0,\ a_2a_3 - a_1 > 0.$$

For the system in question the characteristic polynomial is

$$P(\lambda) = \lambda^4 - 2\lambda^3(\alpha_1 + \alpha_2) + \lambda^2(\alpha_2^2) + \lambda(2\alpha_1\alpha_2^2 + 4\alpha_1^2\alpha_2).$$

The stability conditions are then given, by applying Lienard criteria,

$$\alpha_1+\alpha_2 > 0$$

$$4\alpha_1^2\alpha_2 + 2\alpha_1\alpha_2^2 > 0$$

$$4\alpha_1\alpha_1^2 + 4\alpha_1^2\alpha_2 - 2\alpha_2^3 > 0.$$

These conditions reduce to

$$2\alpha_1 + \alpha_2 < 0 \qquad (5.44)$$

$$\alpha_1 + \alpha_2 > 0 \tag{5.45}$$

$$\alpha_1 > 0. \tag{5.46}$$

To these one must add, Eq. (5.23), the existence condition $\alpha_1\alpha_2 < 0$.

5.8. Discussion of the results

The results are shown on Figure 5.1. As we see from the graph, in order to get a stable limit cycle, *the first mode should be unstable. The second mode should be stable and should decay at least twice as fast as the growth of the first mode.* The major conclusions from the above analysis are first, that *the stability of the limit cycle depends only on the linear coefficients, and second, that the nonlinear coefficient β affects only the amplitude of the limit cycle.* The existence of both a source of energy ($\alpha_1 > 0$) and a sink of energy ($\alpha_2 < 0$) is necessary to obtain a limit cycle. The same results will be found in Chapter 6 using a completely different technique[9]. The purpose of the next chapter is to support the expansion presented in Chapters 3 and 4. We shall show, by using the perturbation-averaging method, that we obtain the same results, reported in this chapter, regarding the amplitude and the conditions for existence and stability of the limit cycle. More results will be elaborated regarding the influence of the imaginary parts of the linear responses of the different processes in combustion chambers.

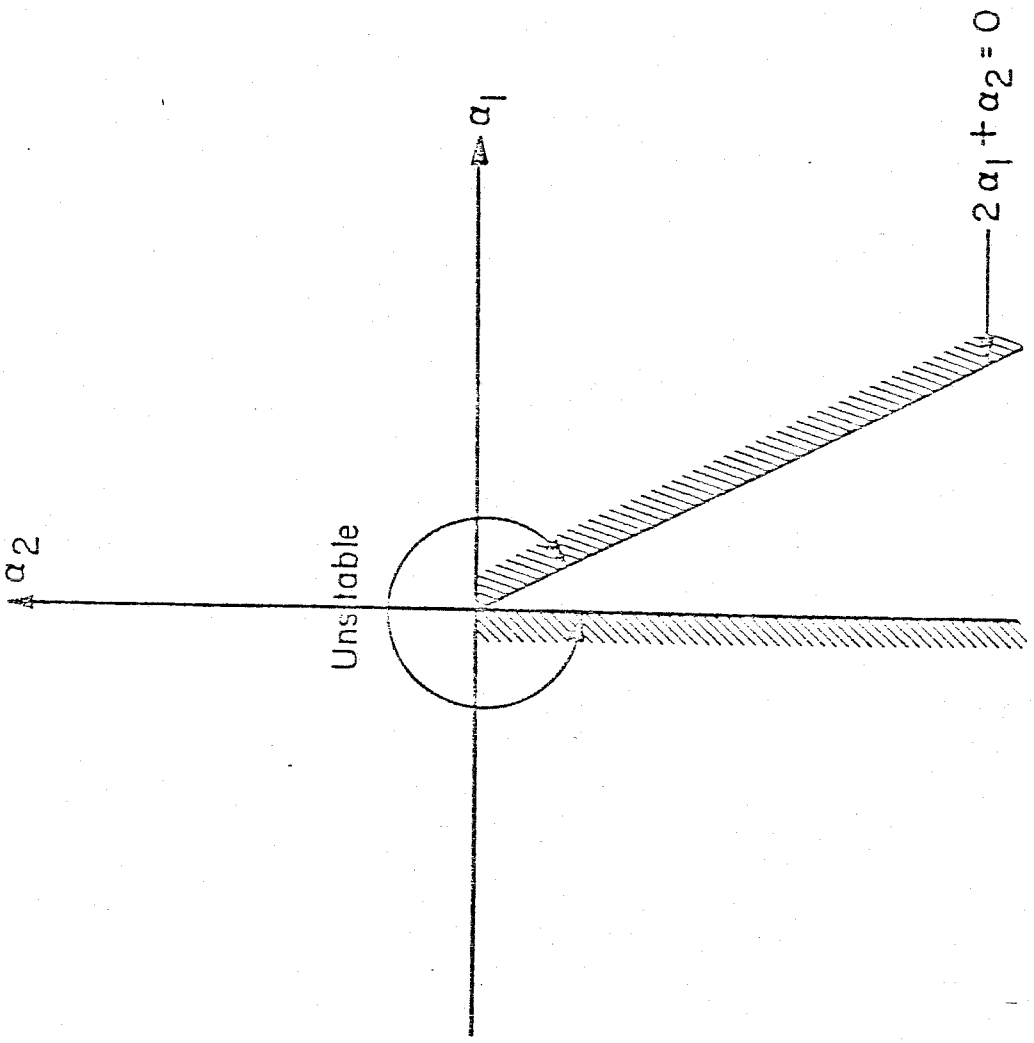

Figure 5.1 Domaine of stability for two nonlinear oscillators.

Appendix 5A

GENERAL REASON FOR CHANGING EXPANSION

In Section 5.2, Chapter 5, we presented a simple example showing the need to change the expansion presented in Chapter 4 when we treat longitudinal modes whose frequencies are integer multiples of the fundamental. In this appendix we present the general reason for changing the expansion presented in Chapter 4.

The conservation equations (4.5)-(4.7) in Chapter 4 can be reduced, by eliminating ρ and u, to a nonlinear partial differential equation which, for one-dimensional problems, has the following form

$$\frac{\partial^2 p}{\partial t^2} - \frac{\partial^2 p}{\partial x^2} = N_p(p) \tag{A.1}$$

with

$$\frac{dp}{dx} = N_B(p) \quad \text{on the boundary.}$$

where N_p and N_B are two nonlinear operators. We further expanded p as follows

$$p = 1 + \mu^2 p_{02} + ... + \varepsilon (p_{10,1} + \mu p_{11,1} + \cdots) e^{iKt} \tag{A.2}$$

$$+ \varepsilon^2 (p_{20,0} + \mu p_{21,0} + \cdots) + \varepsilon^2 (p_{20,2} + \mu p_{21,2} + \cdots) e^{2iKt}$$

For the case of longitudinal modes whose frequencies are integer multiples of the fundamental, we have

$$\frac{d^2 p_{10,1}}{dx^2} + K^2 p_{10,1} = 0 \tag{A.3}$$

with

$$\frac{dp_{10,1}}{dx} = 0 \text{ at } x = 0,1. \tag{A.4}$$

The solutions to (A.3) satisfying (A.4) are

$$p_{10,1}^{(n)} = \cos K_{00}^{(n)} x \tag{A.5}$$

with

$$K_{00}^{(n)} = n\pi,\ n = 0, 1, 2, \cdots \tag{A.6}$$

These solutions constitute a complete set of orthogonal functions.

As we see from expansion (A.2), we include one mode only in the linear part of the expansion, say $p_{10,1}^{(1)}$. The nonlinear term $p_{20,2}(x)$ then satisfies

$$\frac{d^2 p_{20,2}}{dx^2} + 4K_{00}^{(1)2} p_{20,2} = N_p^{(2)}(p_{10,1}^{(1)}) \tag{A.7}$$

where $N_p^{(2)}$ is the quadratic part of N_p. Since the set of functions $p_{10,1}^{(n)}$ are a complete set of functions, $p_{20,2}$ and $N_p^{(2)}(p_{10,1}^{(1)})$ can be expanded in terms of these functions

$$p_{20,2} = c_0 + c_1 p^{(1)}_{10,1} + c_2 p^{(2)}_{10,1} + \text{etc.} \tag{A.8}$$

$$N_p^{(2)}(p^{(1)}_{10,1}) = d_0 + d_1 p^{(1)}_{10,1} + d_2 p^{(2)}_{10,1} + \text{etc.} \tag{A.9}$$

with d_2, in general, is different from zero. For example, if $N_p^{(2)}(p^{(1)}_{10,1}) = p^{(1)}_{10,1}{}^2$ then $d_0 = d_2 = \frac{1}{2}$ and $d_1 = 0$. Substitute expansions (A.8) and (A.9) in (A.7) and equate the coefficients of $p^{(2)}_{10,1}$, to get

$$c_2 \left[4K_{00}^{(1)2} - K_{00}^{(2)2} \right] = d_2 \tag{A.10}$$

where use has been made of

$$\frac{d^2 p^{(2)}_{10,1}}{dx^2} + K_{00}^{(2)2}\, p^{(2)}_{10} = 0$$

However, for longitudinal modes whose frequencies are integer multiples of the fundamental, we have, from (A.6),

$$K_{00}^{(2)2} = 4K_{00}^{(1)2}$$

Eq. (A.10) then reduces to

$$0 = d_2$$

In general d_2 is different from zero. Therefore, expansion (A.2) breaks down. One way to overcome this difficulty is by introducing in (A.2) a second harmonic of the *same* order as the first harmonic, i.e.

$$p = 1 + \mu^2 p_{02} + ... + \varepsilon (p_{10,1} + \mu p_{11,1} + \cdots) e^{iKt} \qquad (A.11)$$

$$+ \varepsilon (p_{10,2} + \mu p_{11,2} + \cdots) e^{2iKt}$$

$$+ \varepsilon^2 (p_{20,0} + \mu p_{21,0} + \cdots) + \varepsilon^2 (p_{20,2} + \mu p_{21,2} + \cdots) e^{2iKt} + ...$$

This is the basis of the expansion used in Chapter 5.

The analysis is general and can, of course, be extended to any number of modes and any reasonable type of nonlinearities.

Appendix 5B

GENERAL FORMULATION FOR LONGITUDINAL MODES

In this appendix we extend the analysis presented in Chapter 5, Section 5.2, to any number of modes. The extension to higher orders in the wave amplitude is the subject of Chapter 8, Section 8.2. To save space, we show in detail the expansion of the pressure alone

$$p = 1 + \mu^2 p_{02} + \cdots + \varepsilon (p_{10,1} + \mu p_{11,1} + ...) e^{iKt}$$

$$+ \varepsilon (\delta_2^{(1)} p_{10,2} e^{2\alpha g_2^{(1)}(\mu) t} + \mu p_{11,2} + \cdots) e^{2iKt}$$

$$+ \varepsilon (\delta_3^{(1)} p_{10,3} e^{3\alpha g_3^{(1)}(\mu) t} + \mu p_{11,3} + ...) e^{3iKt} + \cdots +$$

$$+ \varepsilon^2 (p_{20,0} + \mu p_{21,0} + \cdots)$$

$$+ \varepsilon^2 (p_{20,1} + \mu p_{21,1} + \cdots) e^{iKt}$$

$$+ \varepsilon^2 (\delta_2^{(2)} p_{20,2} e^{2\alpha g_2^{(2)}(\mu) t} + \mu p_{21,2} + \cdots) e^{2iKt}$$

$$+ \varepsilon^2 (\delta_3^{(2)} p_{30,2} e^{3\alpha g_3^{(2)}(\mu) t} + \mu p_{31,2} + \cdots) e^{3iKt} + \cdots + c.c. \qquad (B.1)$$

The coefficients $g_2^{(2)}$, $g_3^{(2)}$, etc., are introduced to resolve the multiple determination of K_{11}, K_{12}, etc. In fact, gathering terms in $\varepsilon^2\mu e^{iKt}$ in the conservation equations leads, after application of Green's theorem, to an expression for K_{11}. Another expression is obtained from equating the coefficients of $\varepsilon^2\mu e^{2iKt}$. In the absence of $g_2^{(2)}$, we are faced with generally two different values for the same coefficient, and the expansion breaks down. A similar situation exists for K_{12}. In general, the introduction of $g_j^{(m)}(\mu)$ allows the single determination of $K_{m-1,n}$, j = 2,3,4 ..., and m, n = 1,2,3,... .

In a concise form, the expansion (B.1) can be written in the following form

$$p = 1 + \sum_{m=1}^{\infty} \mu^{2m} p_{0,2m} + \sum_{l=1}^{\infty} \sum_{n=0}^{\infty} \varepsilon^l \left[\delta_l^{(n)} p_{l0,n} e^{n g_l^{(n)}(\mu) t} + \sum_{m=1}^{\infty} \mu^m p_{lm,n} \right] e^{inKt} + c.c.$$

where $\delta_l^{(n)} = 1$ and $g_l^{(n)} = 0$ for n = 0,1. Similarly, the expansions of the density and velocity are respectively

$$\rho = 1 + \sum_{m=1}^{\infty} \mu^{2m} \rho_{0,2m} + \sum_{l=1}^{\infty} \sum_{n=0}^{\infty} \varepsilon^l \left[\delta_l^{(n)} \rho_{l0,n} e^{n g_l^{(n)}(\mu) t} + \sum_{m=1}^{\infty} \mu^m \rho_{lm,n} \right] e^{inKt} + c.c.$$

$$u = \mu \bar{u} + \sum_{l=1}^{\infty} \sum_{n=0}^{\infty} \varepsilon^l \left[\delta_l^{(n)} u_{l0,n} e^{n g_l^{(n)}(\mu) t} + \sum_{m=1}^{\infty} \mu^m u_{lm,n} \right] e^{inKt} + c.c.$$

As an illustration of how to apply the expansion (B.1) to many modes, we extend the results shown, for two modes, in Section 5.3.2. to three modes. We will show how to determine the coeficient K_{10} in the expansion of the complex frequency in the wave amplitude. There are three ways to determine K_{10}. First, we equate the coefficients of $\varepsilon^2\mu^0 e^{iKt}$ in the conservation equations to get

$$ik_{00}p_{20,1} + \gamma\nabla\cdot u_{20,1} = -ik_{10}p_{10,1} - \gamma\delta_2^{(1)}p_{10,2}\nabla\cdot u_{10,1}^{*} - \gamma\delta_2^{(1)}p_{10,1}^{*}\nabla\cdot u_{10,2} \quad \text{(B.2)}$$

$$- \delta_2^{(1)}u_{10,1}^{*}\cdot\nabla\, p_{10,2} - \delta_2^{(1)}u_{10,2}\cdot\nabla\, p_{10,1}^{*}$$

$$- \gamma\delta_2^{(1)}\delta_3^{(1)}p_{10,3}\nabla\cdot u_{10,2}^{*} - \gamma\delta_2^{(1)}\delta_3^{(1)}p_{10,2}^{*}\nabla\cdot u_{10,3}$$

$$- \delta_2^{(1)}u_{10,1}^{*}\cdot\nabla\, p_{10,2} - \delta_2^{(1)}u_{10,2}\cdot\nabla\, p_{10,1}^{*}$$

$$- \delta_2^{(1)}\delta_3^{(1)}u_{10,2}^{*}\cdot\nabla\, p_{10,3} - \delta_2^{(1)}\delta_3^{(1)}u_{10,3}\cdot\nabla\, p_{10,2}^{*}$$

$$ik_{00}u_{20,1} + \frac{\nabla\, p_{20,1}}{\gamma} = -ik_{10}u_{10,1} - \delta_2^{(1)}u_{10,1}^{*}\cdot\nabla\, u_{10,2} \quad \text{(B.3)}$$

$$- \delta_2^{(1)}u_{10,2}\cdot\nabla\, u_{10,1}^{*} - \delta_2^{(1)}2iK_{00}\rho_{10,1}^{*}u_{10,2} + \delta_2^{(1)}iK_{00}\rho_{10,2}u_{10,1}^{*}$$

$$- \delta_2^{(1)}\delta_3^{(1)}u_{10,2}^{*}\cdot\nabla\, u_{10,3} - \delta_2^{(1)}\delta_3^{(1)}u_{10,3}\cdot\nabla\, u_{10,2}^{*}$$

$$- \delta_2^{(1)}\delta_3^{(1)}3iK_{00}\rho_{10,2}^{*}u_{10,3} + \delta_2^{(1)}\delta_3^{(1)}2K_{00}\rho_{10,3}u_{10,2}^{*}$$

Following the same technique leading to Eq. (5.11) in Chapter 5, we get from Eqs. (B.2) and (B.3) a relationship among K_{10}, $\delta_2^{(1)}$, and $\delta_3^{(1)}$.

Another relationship among K_{10}, $\delta_2^{(1)}$, and $\delta_3^{(1)}$ can be found by equating the coefficients of $\varepsilon^2\mu^0 e^{2iKt}$. By doing so, we get

$$2ik_{00}p_{20,2} + \gamma\nabla \cdot u_{20,2} = -2(ik_{10}p_{10,1} + \alpha_{10}g_{20}^{(1)})\delta_2^{(1)}p_{10,2} \qquad (B.4)$$

$$-\gamma p_{10,1}\nabla \cdot u_{10,1} - u_{10,1}\cdot\nabla\, p_{10,1} - \delta_3^{(1)}\gamma p_{10,3}\nabla \cdot u_{10,1}^{*} - \delta_3^{(1)}u_{10,1}^{*}\cdot\nabla\, p_{10,3}$$

$$2ik_{00}u_{20,2} + \nabla\,\frac{p_{20,2}}{\gamma} = -2(ik_{10}p_{10,1} + \alpha_{10}g_{20}^{(1)})\delta_2^{(1)}u_{10,2} \qquad (B.5)$$

$$-u_{10,1}\cdot\nabla\, u_{10,1} - \delta_3^{(1)}u_{10,3}\cdot\nabla\, u_{10,1}^{*} - \delta_3^{(1)}u_{10,1}^{*}\cdot\nabla\, u_{10,3}$$

$$-iK_{00}\rho_{10,1}u_{10,1} + \delta_3^{(1)}iK_{00}\rho_{10,3}u_{10,1}^{*} - \delta_3^{(1)}iK_{00}\rho_{10,1}^{*}u_{10,3}$$

Following the same analysis leading to Eq. (5.13), Eqs. (B.4) and (B.5) give a second relationship between K_{10}, $\delta_2^{(1)}$, and $\delta_3^{(1)}$.

Finally, a third relationship connecting K_{10}, $\delta_2^{(1)}$, and $\delta_3^{(1)}$ is obtained by first equating the coefficients of $\varepsilon^2\mu^0 e^{3iKt}$ in the conservation equations, to get

$$3ik_{00}p_{20,3} + \gamma\nabla \cdot u_{20,3} = -3(ik_{10}p_{10,1} + \alpha_{10}g_{30}^{(1)})\delta_3^{(1)}p_{10,3} \qquad (B.6)$$

$$-\delta_2^{(1)}\gamma p_{10,1}\nabla \cdot u_{10,2} - \delta_2^{(1)}u_{10,2}\cdot\nabla\, p_{10,1}$$

$$-\delta_2^{(1)}\gamma p_{10,2}\nabla \cdot u_{10,1} - \delta_2^{(1)}u_{10,1}\cdot\nabla\, p_{10,2}$$

$$3ik_{00}u_{20,3} + \nabla\,\frac{p_{20,3}}{\gamma} = -3(ik_{10}p_{10,1} + \alpha_{10}g_{30}^{(1)})\delta_3^{(1)}u_{10,3} \qquad (B.7)$$

$$- \delta_2^{(1)} u_{10,2} \cdot \nabla u_{10,1} - \delta_2^{(1)} u_{10,1} \cdot \nabla u_{10,2}$$

$$- \delta_2^{(1)} 2iK_{00} \rho_{10,1} u_{10,2} - \delta_2^{(1)} iK_{00} \rho_{10,2} u_{10,1}$$

The same analysis leading to Eq. (5.13) allows the determination of the desired relationship. Consequently, K_{10}, $\delta_2^{(1)}$, and $\delta_3^{(1)}$ are uniquely determined. The limiting amplitude corresponds to the values of ε for which the imaginary part of the complex frequency K vanish. The values of ε determine the amplitude of the first mode. The coeficients $\delta_2^{(1)}$, and $\delta_3^{(1)}$ determine respectively the amplitudes of the second and the third mode.

REFERENCES 5

1. Chu, B. T. and Ying, S. J. " Thermally Driven Nonlinear Oscillations in a Pipe With a Traveling Shock Wave ," *Phys. Fluids*, Vol. 6, pp. 1636, 1963.

2. Sirignano, W.A " Theoretical Study of Nonlinear Combustion Instabilities : Longitudinal Mode," Technical Report No. 677, Department of Aerospace and Mechanical Sciences, Princeton University, March 1964.

3. Marxman, G. A. and Wooldrige, C. E. 'Finite amplitude axial instability in solid rocket combustion," in *Eleventh Symposium on Combustion*, Combustion Institute, pp. 115-127, 1968.

4. Zinn, B. T. and Lores, M. E. " Application of the Galerkin Method in the Solution of Nonlinear Axial Combustion Instabilities Problems in Liquid Rockets ," *Combustion Science and Technology*, Vol. 4, pp. 269, 1972.

5. Lores, M. E. and Zinn, B. T. " Nonlinear Longitudinal Combustion Instabilities in Rockets Motors ," *Combustion Science and Technology* , Vol. 7, pp. 245, 1973.

6. Bloch, F. "Uber die quatenmechanic der electronen in Kristalligittern," *Z. Phys.*, 52 , pp. 555-600, 1928.

7. Floquet, G. " Sur Les Equations Differentielles Lineaires a Coefficients Periodics," *Ann. Ecole Norm.* , 12, pp. 47-89, 1883.

8. Gantmacher, F. R. "*The Theory of Matrices*," Chelsea Publishing Company, New York, 1960.

9. Culick, F. E. C. 'Nonlinear Behavior of Acoustic Waves in Combustion Chambers," *Acta Astronautica*, Vol. 3, pp. 735-757, 1976.

Chapter 6

EXPANSION IN THE NORMAL MODES OF THE ACOUSTIC FIELD : AMPLITUDE AND CONDITIONS FOR EXISTENCE AND STABILITY OF LIMIT CYCLES

6.1. Introduction

In Chapters 4 and 5 we obtained some results regarding the amplitude and the conditions for existence and stability of limit cycles for pressure oscillations in combustion chambers, by using the asymptotic-perturbation method. In this chapter, we will support these results by using the second technique, the perturbation-averaging method. This technique was presented in Chapter 3, Section 3.3. In Chapter 4, Section 4.6, we applied this technique to the conservation equations in combustion chambers and, for pure longitudinal modes, we obtained the system of equations (4.52)-(4.53) of ordinary differential equations for the behavior in time of the different modes. The same equations were reported in reference 1.

In this chapter, we start from those equations to determine the amplitude and the conditions for existence and stability of limit cycles. Consequently, the following analysis is limited to longitudinal modes only. More results than those found in Chapters 4 and 5 will be elaborated, mainly the influence of the imaginary parts of the linear responses of the different processes in the combustion chamber. Broadly, the analysis breaks into two parts. First, for a chosen type of limit cycle (there are two types), the conditions for existence and the amplitudes of the limit cycles are found. Then a perturbation procedure is used to examine the stability of the limit cycle.

We begin with the case when the fundamental frequency of the limit cycle is equal to the fundamental frequency of the acoustic modes of the chamber. First, two modes are treated. The amplitude and the conditions for existence and stability of limit cycles are determined. The results agree with those of Chapters 4 and 5. Moreover, the influence of the initial conditions is shown. The crucial importance of the imaginary parts of the linear responses of the different processes in the chamber is demontrated. Second, we treat three modes in order to confirm the results found in the treatment of two modes and to generalize the method of solution to many modes.

The second case, when the fundamental frequency of the limit cycle is slightly different from the fundamental frequency of the acoustic modes of the chamber, is examined. The amplitude and frequency of the limit cycle are determined. Under certain conditions (shown in Appendix 6A), these two cases correspond to the only possible types of limit cycles.

Because of the availabilty of data on solid propellant rocket motors, the analytical results will be applied solely to that kind of system. We will compare our results with the numerical solutions reported in reference 2 and with the experimental results reported in reference 3. But the validity and the scope of application are much wider and the results can be applied to any sort of chamber.

6.2. Preliminary

We start the analysis from the results reported in reference 1 and shown in some detail in Chapter 4, Section 4.6. In that section, we showed, following reference 1, that the pressure oscillation, written in the form

$$p' = \sum_{i=1}^{\infty} \eta_i(t) \cos \omega_i x$$

is governed by the following system of equations for nonlinear oscillators, one oscillator for each mode:

$$\ddot{\eta}_i + \omega_i^2 \eta_i = f_i(\eta_j , \dot{\eta}_j) \tag{6.1}$$

i=1,2, ... , j=1,2, ..., and f_i is a second order nonlinear polynomial. By applying the method of averaging[1], the following system of ordinary differential equations is obtained

$$\frac{dA_n}{dt} = \alpha_n A_n + \vartheta_n B_n$$

$$+ n\frac{\beta}{2} \sum_{i=1}^{\infty} \left[A_i(A_{n-i} - A_{i-n} - A_{n+i}) - B_i(B_{n-i} + B_{i-n} + B_{n+i}) \right] \tag{6.2}$$

$$\frac{dB_n}{dt} = \alpha_n B_n - \vartheta_n A_n$$

$$+ n\frac{\beta}{2} \sum_{i=1}^{\infty} \left[A_i(B_{n-i} + A_{i-n} - B_{n+i}) + B_i(A_{n-i} - A_{i-n} + A_{n+i}) \right] \tag{6.3}$$

where $n = 1, 2, ..., \beta = \frac{\gamma + 1}{8\gamma} \omega_1$ and $\eta_i(t) = A_i(t) \sin \omega_i t + B_i(t) \cos \omega_i t$. The coefficients α_n and ϑ_n are the linear coefficients and correspond respectively to the linear growth rate and to the linear frequency shift of the n^{th} mode. We refer the reader to Chapter 4, Section 4.6 for more details leading to Eqs. (6.2)-(6.3).

In particular, in Chapter 4, Section 4.6, we show that the Θ_n are proportional to the imaginary parts of the linear responses of the n^{th} mode. This result will be used in the discussion in Section 6.3.1.3.

Equations (6.2) and (6.3) were obtained by applying the method of time averaging to Eqs. (6.1). It is interesting to mention that expansion of the solutions to (6.1) in two-time scales gives results identical[4] to those obtained by the method of time averaging.

In what follows, we will treat two cases. First, the case when the coefficients A_i and B_i reach constant values for large time; and second, the case where A_i and B_i reach harmonic oscillations for large time. These cases yield periodic solutions of the form $\eta_i(t) = A_i(t) \sin \omega_i t + B_i(t) \cos \omega_i t$, and, therefore, they correspond to limit solutions. In Appendix 6A, we show that, under certain conditions, these are the only possible cases. The first case corresponds to the case when the fundamental frequency of the limit cycle is equal to the fundamental frequency of the acoustic modes of the chamber and it will be referred to as " Zero frequency shift case ". The second case corresponds to a slight difference of the fundamental frequency of the limit cycle from the fundamental acoustic frequency of the chamber and it will be referred to as " Non-zero shift of frequency case".

6.3. Case of zero frequency shift

In this section, we will consider the case when the coefficients A_i and B_i in $\eta_i(t) = A_i(t) \sin \omega_i t + B_i(t) \cos \omega_i t$ will reach constant values for $t \to \infty$. The system to be solved is the following

$$\alpha_n A_n + \vartheta_n B_n + n\frac{\beta}{2}\sum_{i=1}^{\infty}\left[A_i(A_{n-i} - A_{i-n} - A_{n+i}) - B_i(B_{n-i} + B_{i-n} + B_{n+i})\right] = 0. \qquad (6.4)$$

$$\alpha_n B_n - \vartheta_n A_n + n\frac{\beta}{2}\sum_{i=1}^{\infty}\Big[A_i(B_{n-i} + A_{i-n} + B_{n+i}) + B_i(A_{n-i} - A_{i-n} + A_{n+i})\Big] = 0. \qquad (6.5)$$

6.3.1. *Two modes* .

In this section, the particular case of two nonlinear oscillators is fully treated. The amplitude and the conditions for existence and stability will be determined. For two modes, Eqs. (6.4) and (6.5) become

$$\alpha_1 A_1 + \vartheta_1 B_1 - \beta\,(\,A_1A_2 + B_1B_2\,) = 0. \qquad (6.6)$$

$$-\vartheta_1 A_1 + \alpha_1 B_1 + \beta\,(\,B_1A_2 - A_1B_2\,) = 0. \qquad (6.7)$$

$$\alpha_2 A_2 + \vartheta_2 B_2 + \beta\,(\,A_1^2 - B_1^2\,) = 0. \qquad (6.8)$$

$$-\vartheta_2 A_2 + \alpha_2 B_2 + 2\,\beta\,B_1A_1 = 0. \qquad (6.9)$$

To solve (6.6)-(6.9) it is convenient to write A_i and B_i as follows

$$A_i = r_i\cos\nu_i, \qquad B_i = r_i\sin\nu_i, \qquad i=1,2.$$

Equations (6.6)-(6.9) then reduce to

$$\frac{\alpha_1}{\cos\psi_1} r_1\cos(\nu_1-\psi_1) - \beta r_1 r_2\cos(\nu_1-\nu_2) = 0 \qquad (6.10)$$

$$\frac{\alpha_1}{\cos\psi_1} r_1 \sin(\nu_1-\psi_1) + \beta r_1 r_2 \sin(\nu_1-\nu_2) = 0 \qquad (6.11)$$

$$\frac{\alpha_2}{\cos\psi_2} r_2 \cos(\nu_2-\psi_2) + \beta r_1^2 \cos 2\nu_1 = 0 \qquad (6.12)$$

$$\frac{\alpha_2}{\cos\psi_2} r_2 \sin(\nu_2-\psi_2) + \beta r_1^2 \sin 2\nu_1 = 0 \qquad (6.13)$$

where

$$\psi_i = \text{Arctan}\ \frac{\vartheta_i}{\alpha_i}, \qquad i = 1,2$$

We now multiply (6.10) by $\sin(\nu_1-\psi_1)$, (6.10) by $\cos(\nu_1-\psi_1)$, and we subtract the results to get

$$\tan(\nu_1-\psi_1) = -\tan(\nu_1-\nu_2)$$

On the other hand, multiplication of (6.12) by $\sin(\nu_2-\psi_2)$, (6.13) by $\cos(\nu_2-\psi_2)$, and subtraction of the results yield

$$\tan(\nu_2-\psi_2) = \tan 2\nu_1$$

The last two equations have the solutions

$$\nu_2 = 2\nu_1 - \psi_1 + m\pi, \quad \nu_2 = 2\nu_1 + \psi_2 + n\pi \qquad (6.14a,b)$$

In order for the solutions to Eqs. (6.14a) and (6.14b) to exist, (6.14a) and (6.14b) should be satisfied simultaneously, giving

$$\psi_1 + \psi_2 = (m - n)\pi$$

However, by definition of the arctan, $-\frac{\pi}{2} < \psi_i < \frac{\pi}{2}$. Consequently

$$\psi_1 = -\psi_2$$

which, from the definition of ψ_i, gives

$$\frac{\vartheta_1}{\alpha_1} = -\frac{\vartheta_2}{\alpha_2} \tag{6.15}$$

If this condition were not satisfied, then (6.14a) and (6.14b) would have no solution. Consequently, Eqs. (6.7)-(6.9) would also have no solutions. Therefore, condition (6.15) is the condition for existence of a limit cycle with zero frequency shift. The same condition will be found again in Section 6.4, Eq. (6.56).

By taking into account (6.14a,b) and (6.15), we find from Eqs. (6.10)-(6.13)

$$r_2 = \frac{\alpha_1}{\beta\cos\psi_1}, \qquad r_1^2 = -\frac{\alpha_1\alpha_2}{\beta^2\cos\psi_1\cos\psi_2}$$

However, since $-\frac{\pi}{2} < \psi_i < \frac{\pi}{2}$, we should have

$$\alpha_1\alpha_2 < 0. \tag{6.16}$$

This is identical to condition (4.23) for existence of limit cycle determined in Chapter 4 using the asymptotic-perturbation technique. Condition (6.16) assures the existence of the limit cycle and shows clearly the necessity of having both a source and a sink of energy. The amplitude of the limit cycle can be expressed via the values of A_i and B_i

$$A_i = r_i\cos\nu_i, \qquad B_i = r_i\sin\nu_i, \qquad i=1,2.$$

The system (6.1) of nonlinear oscillators is autonomous: i.e., if $\eta(t)$ is a solution then $\eta(t - t_1)$ is also a solution for any t_1. Therefore, because we are also dealing with the asymptotic solution (limit cycle), assumed to be periodic, one phase in the expansion of the limit cycle in its Fourier components is arbitrary. This is equivalent to saying that one of the ν_i is arbitrary, say $\nu_1 = 0$. This gives

$$A_{10} = \frac{1}{\beta\cos\psi_1}\left(-\alpha_1\alpha_2\right)^{\frac{1}{2}}$$

$$= \frac{1}{\beta}\left(-\alpha_1\alpha_2\left(1 + \frac{\vartheta_1^2}{\alpha_1^2}\right)\right)^{\frac{1}{2}}$$

$$B_{10} = 0.$$

$$A_{20} = \frac{\alpha_1}{\beta}$$

$$B_{20} = \frac{\vartheta_1}{\beta}$$

For the particular case of $\theta_1 = \theta_2 = 0$, we have

$$A_{10} = \frac{1}{\beta}(-\alpha_1\alpha_2)^{\frac{1}{2}}, \quad B_{10} = 0$$

$$A_{20} = \frac{\alpha_1}{\beta}, \quad B_{20} = 0.$$

These expressions are identical to expressions (5.21) and (5.22) determined in Chapter 5, using the asymptotic-perturbation method, for the amplitude of the first and the second harmonics.

Once the equilibrium points A_{i0} and B_{i0} , i = 1,2, are found, their stability can be examined by linearizing the system (6.6)-(6.9) near these points. The eigenvalues of the linear system should all have negative real parts. Linearization of (6.2)-(6.2) produces the following equations:

$$\frac{dA_1}{dt} = (\alpha_1 - \beta A_{20}) A_1 + (\vartheta_1 - \beta B_{20}) B_1 - (\beta A_{10})A_2 - (\beta B_{10})B_2$$

$$\frac{dB_1}{dt} = (-\vartheta_1 - \beta B_{20}) A_1 + (\alpha_1 + \beta A_{20}) B_1 + (\beta B_{10})A_2 - (\beta A_{10})B_2$$

$$\frac{dA_2}{dt} = (2\beta A_{10}) A_1 - (2\beta B_{10}) B_1 + \alpha_2 A_2 + \vartheta_2 B_2$$

$$\frac{dB_2}{dt} = (2\beta B_{10}) A_1 + (2\beta A_{10}) B_1 - \vartheta_2 A_2 + \alpha_2 B_2$$

By writing $A_1 = U_1 e^{\lambda t}$, etc., where U_1, etc., are constant, and replacing these expressions in the above linear system we get a linear system of equations for U_1, etc., of the form

$$M\vec{X} = 0$$

where M is the matrix of the linear system and $\vec{X}$ represent U_1, etc. This system has non-zero solutions only when its determinant vanishes. This gives a polynomial equation in λ, the characteristic polynomial. For the system in question, the characteristic polynomial is

$$P(\lambda) = \lambda^4 - 2\lambda^3(\alpha_1 + \alpha_2) + \lambda^2(\alpha_2^2 + \vartheta_2^2 + 4\vartheta_1\vartheta_2)$$

$$+ \lambda\, 2\alpha_1\alpha_2(2\alpha_1 + \alpha_2)\left(1 + \frac{\vartheta_2^2}{\alpha_1^2}\right) \qquad (6.17)$$

The conditions under which the limit cycle is stable are reduced to those under which all the roots of this polynomial have negative real parts. Many textbooks treat this problem (see reference 5 for example). In Chapter 5, we have seen that these conditions are known as the Routh-Hurwitz or Lienard criteria. As we have noted there, for a polynomial of the form

$$P(\lambda) = \lambda^4 + a_3\lambda^3 + a_2\lambda^2 + a_1\lambda$$

these criteria are

$$a_1 > 0,\ a_3 > 0,\ a_2a_3 - a_1 > 0.$$

In the following calculations, we will determine explicit results for two cases: $\vartheta_1 = \vartheta_2 = 0$ and $\vartheta_1, \vartheta_2 \neq 0$.

6.3.1.1 $\vartheta_1 = \vartheta_2 = 0$: *Imaginary parts of linear responses vanish .*

The case when $\vartheta_1 = \vartheta_2 = 0$ is carried out to completion. Equation (6.17) reduces to

$$P(\lambda) = \lambda^4 - 2\lambda^3(\alpha_1 + \alpha_2) + \lambda^2(\alpha_2^2) + \lambda(2\alpha_1\alpha_2^2 + 4\alpha_1^2\alpha_2).$$

The stability conditions are then given, by applying Lienard criteria,

$$\alpha_1+\alpha_2 > 0$$

$$4\alpha_1^2\alpha_2 + 2\alpha_1\alpha_2^2 > 0$$

$$4\alpha_1\alpha_1^2 + 4\alpha_1^2\alpha_2 - 2\alpha_2^3 > 0.$$

These conditions can be simplified to

$$2\alpha_1 + \alpha_2 < 0 \qquad (6.18)$$

$$\alpha_1 + \alpha_2 > 0 \qquad (6.19)$$

$$\alpha_1 > 0. \tag{6.20}$$

To these one must add the existence condition (6.16). These results are the same as those found in Chapter 5, Eqs. (5.18)-(5.20), and are shown on Figure 5.1. This constitutes a strong support of the expansion in the asymptotic amplitude discussed in Chapters 3, 4, and 5. As we see from the graph, in order to get a stable limit cycle, *the first mode should be unstable. The second mode should be stable and should decay at least twice as fast as the growth of the first mode.*

Without the nonlinear coupling, the first mode is unstable, so there is a source of energy for the system; the second mode is stable, and energy is extracted from the system. The nonlinear coupling channels energy from the first mode to the second mode. We say that the energy flows from the first to the second mode. When the limit cycle is reached, the effects of the sink and source of energy compensate and the energy in the wave system remains constant in time.

To demonstrate the independence of the limit cycle from general initial conditions, the system of equations (6.1) and (6.2) has been integrated numerically. Figures 6.1a and 6.1b show the behavior in time of the amplitude of different harmonics for different initial conditions. Figures 6.2a and 6.2b show the influence of the linear damping coefficient α_2 on the rate at which the limit cycle is reached and on the limiting amplitude. We conclude that the higher the damping is, the faster the limit cycle is reached and the higher the amplitude of the first mode is. Figure 6.3b shows the behavior in time of the pressure amplitude when the conditions (6.18)-(6.20) are not satisfied; it is clearly seen that, while the existence condition (6.16) is satisfied, the limit cycle is unstable, i.e., it cannot exist numerically. That was predicted by the analytical results (6.18)-

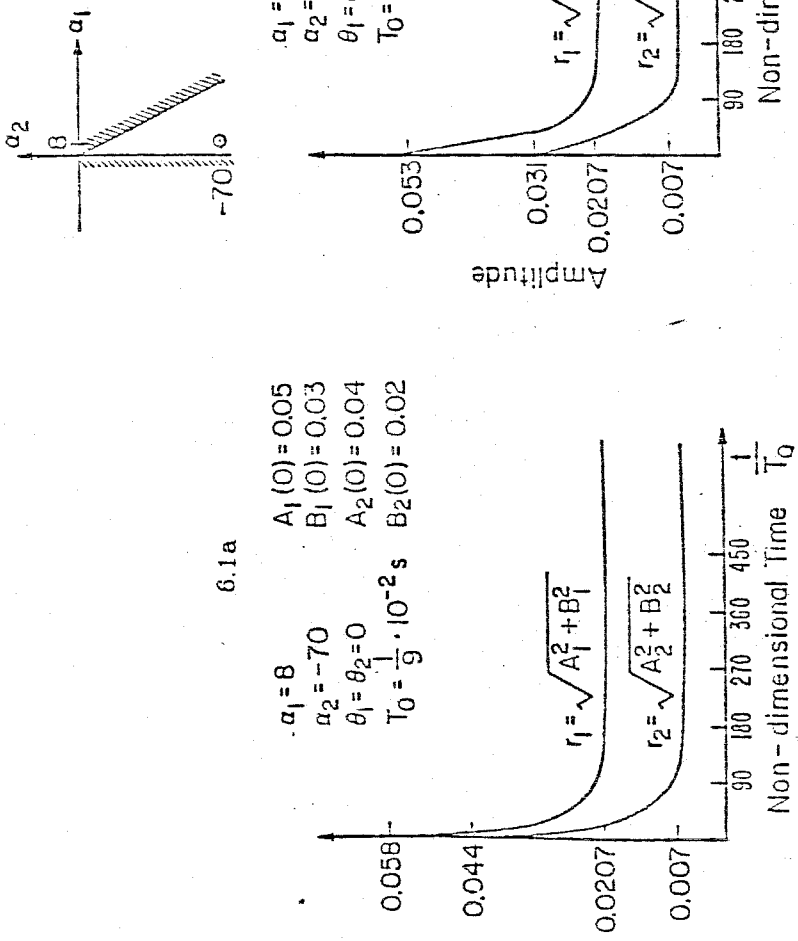

Figure 6.1 The non-influence of the initial conditions on the limit cycle amplitude.

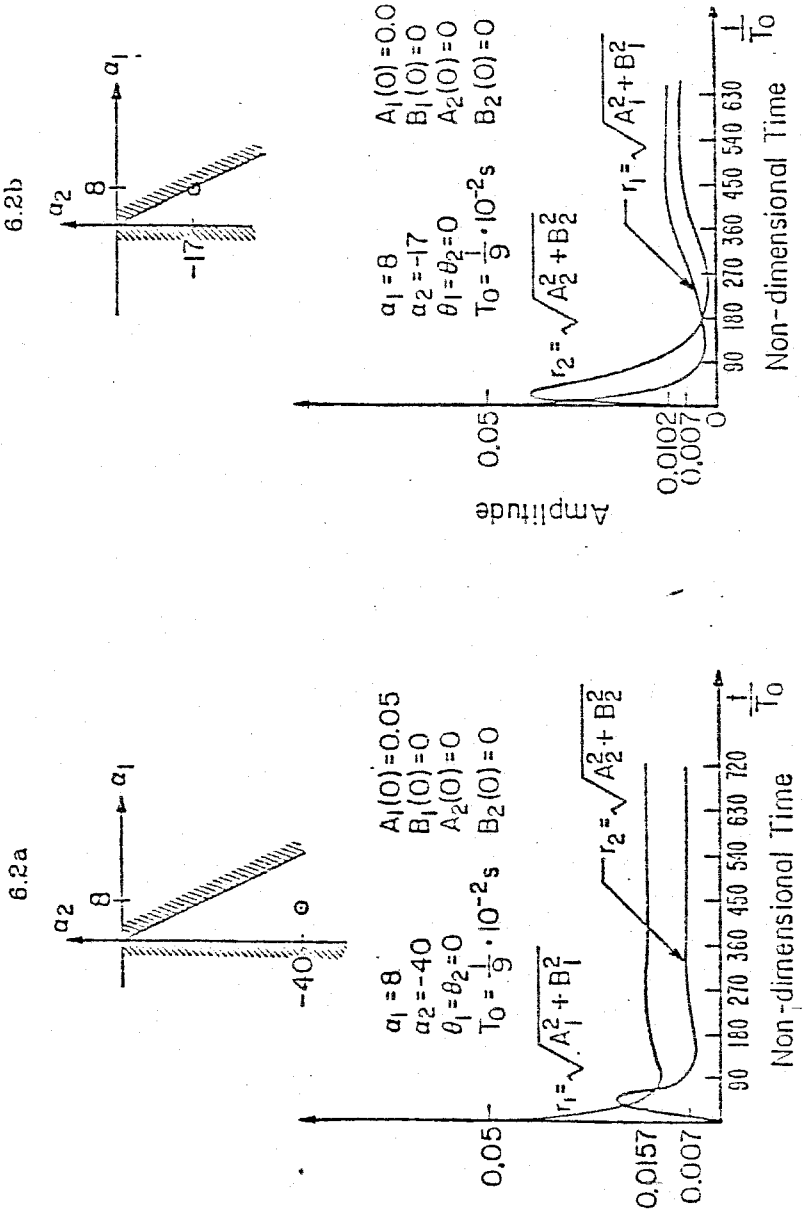

Figure 6.2 Influence of the damping rate a_2 on the speed of reaching the limit cycle.

(6.20).

In all these examples, the numerical results agree completely with the analytical predictions in the sense that the numerical solution of the system of equations (6.2) and (6.3) yields the same behavior predicted by the analysis regarding the conditions for existence and stability, and amplitude of limit cycles.

6.3.1.2 *Stability criteria for special initial conditions* .

The following remarks demonstrate that the initial conditions, under very special circumstances, can change the stability criteria (6.18)-(6.20). Let us assume that the initial conditions are of the following form

$$B_1(0) = B_2(0) = 0.$$

and that ϑ_1, ϑ_2 both vanish. The direct conclusion is that the two modes are in phase. This will be shown to be the reason for relaxing the stability criteria given above. Equations (6.6)-(6.9), in this case, become

$$\alpha_1 A_1 - \beta A_1 A_2 = 0. \tag{6.21}$$

$$\alpha_2 A_2 + \beta A_1^2 = 0. \tag{6.22}$$

B_1 and B_2 vanish for all times. System (6.19)-(6.20) has the following solution

$$A_{10} = \frac{\sqrt{(-\alpha_1 \alpha_2)}}{\beta}, \quad A_{20} = \frac{\alpha_1}{\beta}$$

By linearizing the system (6.21)-(6.22) near the above solution, it is easily shown that the stability criterion is simply

$$\alpha_1 > 0, \quad \alpha_2 < 0. \tag{6.23}$$

The criterion (6.23) is much less restrictive than the criteria (6.18)-(6.20). However, the initial conditions here are very restrictrive. The criteria (6.18)-(6.20) are the general ones under general initial conditions. Figure 6.3b, in comparison with Figure 6.3a, illustrates clearly the influence of the initial conditions on the stability criteria (6.18)-(6.20). The only differences between these two figures are the initial conditions; in Figure 6.3b, where the initial conditions are not in phase, the limit cycle is unstable as predicted by the stability criteria (6.18)-(6.20); in Figure 6.3a, where the initial conditions are in phase, the limit cycle is stable as predicted by the criterion (6.23).

6.3.1.3 $\vartheta_1, \vartheta_2 \neq 0$: *Imaginary parts of linear responses non-zero .*

We now treat the case in which ϑ_1 and ϑ_2 different from zero, while always satisfying the condition (6.15) for zero frequency shift in the limit cycle. The point is to show that the stability criteria (6.18)-(6.20) are still valid but are not necessary. It will be shown that the imaginary parts greatly affect the stability and amplitude of the limit cycle. Ultimately, the direction of energy flow among modes will depend on these imaginary parts.

In order for the characteristic polynomial (6.17) to have all roots with negative real parts, the following conditions should simultaneously be satisfied according to the Lienard criteria

$$\alpha_1 + \alpha_2 < 0.$$

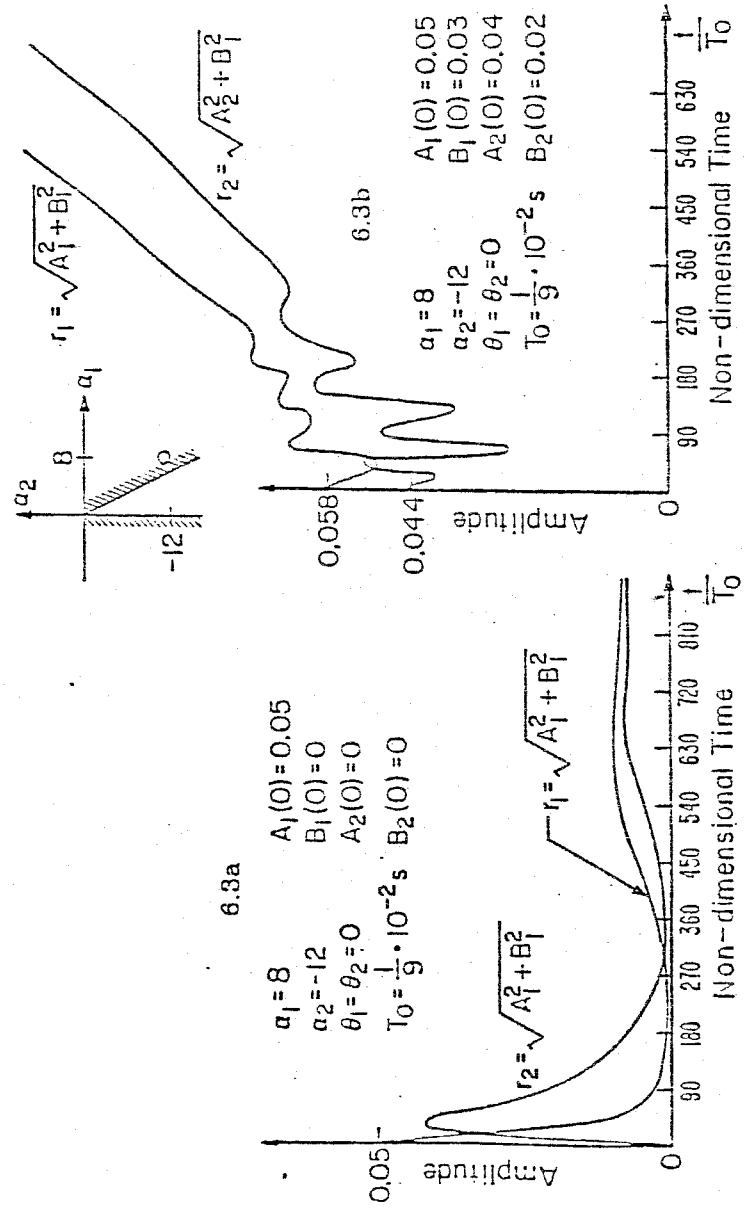

Figure 6.3 Influence of the initial conditions on the stability criteria.

$$2\alpha_1 + \alpha_2 < 0.$$

$$2\alpha_2\vartheta_2^2\left(-\frac{\alpha_1^2}{\vartheta_1^2} - 3 + 2\frac{\alpha_1}{\alpha_2^2}(2\alpha_1 + \alpha_2)\right) > 0.$$

The first two conditions amount to the same conditions (6.18)-(6.19) found for the case $\vartheta_1 = \vartheta_2 = 0$. But the third condition implies two possibilities. First $\alpha_2 < 0$; this case yields the same result (6.20) found for $\vartheta_1 = \vartheta_2 = 0$. Second, $\alpha_2 > 0$; this case yields the following stability condition

$$\alpha_2 < 2\frac{\alpha_1(2\alpha_1 + \alpha_2)}{\alpha_2(3 + \frac{\alpha_1^2}{\vartheta_1^2})} \tag{6.24}$$

This condition shows clearly that it is possible to get a stable limit cycle when the first mode is stable and the second mode is unstable. In conclusion, the conditions (6.18)-(6.20) are *sufficient* here but *not necessary*.

To illustrate the results, Figure 6.4 shows an example of numerical integration of the system of ordinary differential equations when the first mode is stable, the second mode is unstable, and when the criterion (6.24) is satisfied but the criteria (6.18)-(6.20) are not. The limit cycle in this case is stable, in contradiction to the stabiltity criteria (6.18)-(6.20) but consistent with the criterion (6.24).

In the case when the first mode is stable (a sink of energy) and the second mode is unstable (a source of energy), the nonlinear coupling channels the energy from the second to the first mode. The direct conclusion here is that the energy can flow "backward" from the higher to the lower modes. Whether this

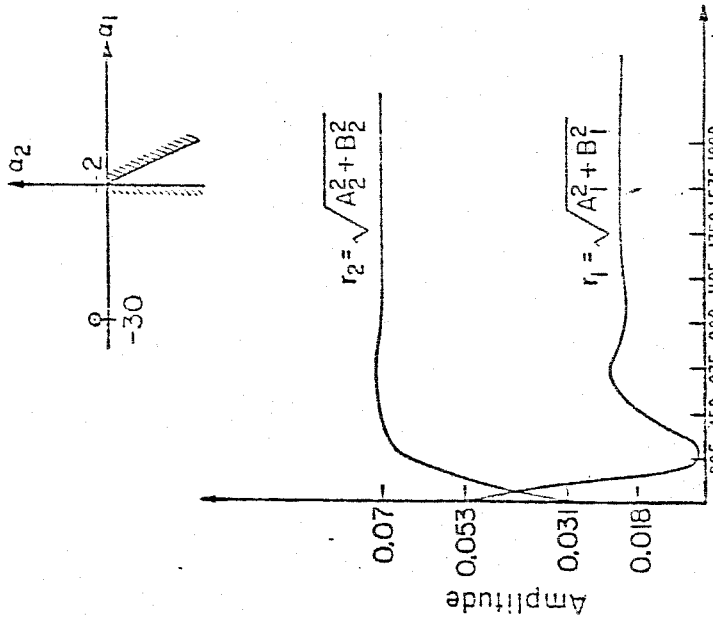

Figure 6.4 Influence of the imaginary parts on the stability conditions.

occurs depends on the values of $(\vartheta_1,\vartheta_2)$ which correspond to the imaginary parts of the combustion responses.

This is, up to our knowledge, the first time such an effect has been shown. The imaginary parts do indeed play a major role in the process of limiting the pressure oscillations in combustion chambers. Relying only on the real parts of the responses of the different processes in the chamber yields insufficient, sometimes misleading, information about the processes causing a limit cycle.

6.3.2. *Three modes .*

Now, the system of 3 nonlinear oscillators will be treated. A general approach for solving a system of many nonlinear oscillators can be constructed. The purpose of this section is to show that a stable limit cycle is unique and that the analysis can be carried out to any number of oscillators.

The uniqueness of a stable limit cycle is an important feature to investigate, since it is a specific characteristic of multi-degree of freedom systems. In fact, for the multi-degree of freedom system (6.2)-(6.3), the limit cycle corresponds to the equilibrium points of this system, i.e. the values of A_n and B_n which make $\frac{dA_n}{dt}$ and $\frac{dB_n}{dt}$ vanish. These values are roots of the system (6.4)-(6.5) of second order multivariable polynomials. For a single degree of freedom system, the limit cycle changes stability when we move from one limit cycle to the adjacent one. For example, Figure 7.2, in Chapter 7, shows the phase diagram for the single degree of freedom system

$$\frac{dA}{dt} = \alpha A + bA^2 + cA^3$$

We see from the graph that the limit cycle changes stability when we move from one limit cycle to the adjacent one.

For a multi-degree of freedom system the situation is quite different. There are no general rules as to the alternation of the stability of limit cycles. In section 6.3.1 we examined the case of two oscillators. We obtained two different limit cycles: the origin and a non-trivial limit cycle. If now conditions (6.18) and (6.19) are not satisfied while (6.20) is satisfied, then both limit cycles are unstable. Therefore, we have two adjacent limit cycles which have the same behavior regarding stability, i.e. both are unstable. This is a clear contradiction to the rule for a single degree of freedom systems.

By extending the analysis to three modes, we would like to enhance this conclusion and to support another conclusion about the stability of limit cycles for system (6.1), i.e. the stable limit cycle is unique, in the sense that if the system is linearly unstable then there is *at most one stable* asymptotic oscillatory behavior no matter what the initial conditions.

First, we will show how to extend the analysis to many modes. The discussion of stability for three modes will follow. Write

$$Z_j = A_j + i\,B_j \quad j=1,2,3.$$

where $i = \sqrt{-1}$. Thus, for a system of 3 nonlinear oscillators, system of equations (6.2) and (6.3) gives, when the limit cycle is reached,

$$\frac{\alpha_1}{\cos\psi_1} e^{i\psi_1} Z_1^* - \beta\,(\,Z_1\,Z_2^* + Z_2\,Z_3^{*)} = 0 \qquad (6.25)$$

$$\frac{\alpha_2}{\cos\psi_2} e^{i\psi_2} Z_2^* + \beta\,(\,Z_1^{*2} - 2\,Z_1\,Z_3^{*)} = 0 \qquad (6.26)$$

$$\frac{\alpha_3}{\cos\psi_3} e^{-i\psi_3} Z_3 + 3\beta Z_1 Z_2 = 0 . \qquad (6.27)$$

where * stands for complex conjugate. Elimination of Z_3 between (6.26) and (6.27) yields

$$\frac{\alpha_2}{\cos\psi_2} e^{i\psi_2} Z_2^* + \beta (Z_1^{*2} + 6\beta \frac{Z_1 Z_1^* Z_2^* \cos\psi_3 e^{i\psi_3}}{\alpha_3}) = 0. \qquad (6.28)$$

We now eliminate Z_2 between (6.28) and (6.25) to get, for $y = Z_1 Z_1^*$,

$$c_0 y^2 + c_1 y + c_2 = 0 \qquad (6.29)$$

where

$$c_0 = 3 \frac{\beta^4}{\alpha_3} \cos\psi_3 e^{-i\psi_3} + 36 \beta^4 \frac{\alpha_1}{\alpha_3^2} \frac{\cos^2\psi_3}{\cos\psi_1} e^{i\psi_1} + 6 \frac{\beta^4}{\alpha_3} \cos\psi_3 e^{-i\psi_3}$$

$$c_1 = 12 \beta^2 \alpha_1 \frac{\alpha_2}{\alpha_3} \frac{\cos\psi_3}{\cos\psi_1 \cos\psi_2} \cos(\psi_2 + \psi_3) e^{i\psi_1} + \beta^2 \frac{\alpha_2}{\cos\psi_2} e^{-i\psi_2}$$

$$c_2 = \frac{\alpha_1 \alpha_2^2}{\cos\psi_1 \cos^2\psi_2} e^{i\psi_1}.$$

The conditions under which Eq. (6.29) has real and positive roots are the conditions for existence of a limit cycle, since $y = Z_1 Z_1^*$ is a positive quantity.

Following the same procedure, the analysis can be extended to larger number of modes. However, the algebraic manipulations become cumbersome.

In the following calculation we treat the special case of three modes with $\vartheta_1 = \vartheta_2 = \vartheta_3 = 0$ The coefficients c_0, c_1, and c_2 become

$$c_0 = 9\frac{\beta^4}{\alpha_3} + 36\,\beta^4\,\frac{\alpha_1}{\alpha_3^2},\quad c_1 = 12\,\beta^2\,\alpha_1\frac{\alpha_2}{\alpha_3} + \beta^2\alpha_2\,,\quad c_2 = \alpha_1\alpha_2^2 \tag{6.30}$$

Since, in the limit cycle, one phase is arbitrary, we can choose Z_1 to be real, i.e. $y = A_1^2$. Equation (6.28) then shows that Z_2 is real. Consequently, from (6.27), Z_3 is also real. This means that when $\theta_i = 0$ there are, in the limit cycle, no phase shifts among modes.

The condition for existence of real roots for Eq (6.29) is that the discriminant $c_1 - 4c_0c_2$ be positive, i.e.

$$1 - 12\frac{\alpha_1}{\alpha_3} > 0. \tag{6.31}$$

In addition, the acceptable roots should be positive, since here $y = A_1^2$. In the case of one limit cycle only, the product of roots of Eq. (6.29) should be < 0, since one root is then positive and the second root is negative, i.e. an unacceptable root. The product of roots of Eq. (6.29) is $\frac{c_2}{c_0}$. Therefore, we should have, using (6.30),

$$\frac{\alpha_1\alpha_3}{36\frac{\alpha_1}{\alpha_3} + 9} < 0. \tag{6.32}$$

Inequalities (6.31) and (6.32) are the conditions to obtain a unique limit cycle. These two inequalities can be simplified to

$$-\frac{1}{4} < \frac{\alpha_1}{\alpha_3} < 0 \tag{6.33}$$

On the other hand, in order to obtain two limit cycles, the product $\frac{c_2}{c_0}$ of roots of (6.29) and their sum $-\frac{c_1}{c_0}$ must be positive. These conditions give, using (6.30) and (6.31),

$$\frac{\alpha_1}{4\alpha_1 + \alpha_3} > 0 \tag{6.34}$$

$$\alpha_3(\alpha_3 - 12\alpha_1) > 0 \tag{6.35}$$

$$\alpha_1\alpha_3(12\alpha_1\alpha_2 + \alpha_2\alpha_3) < 0 \tag{6.36}$$

Therefore, under these conditions, we have in general two limit cycles. Their stability can be examined in a straightforward manner, as in the case of two nonlinear oscillators. However, the algebra is too complicated to be reduced to a simple analytical form in terms of α_1, α_2, and α_3. In fact, the roots of Eq. (6.29), which are the values of the limit cycles, are not simple functions of α_1, α_2, and α_3. The linearization of system (6.2)-(6.3) near these values yields a linear system with complicated coefficients in terms of α_1, α_2, and α_3. Finally, the stability conditions according to Lienard criteria give a complicated set of conditions in terms of α_1, α_2, and α_3. However, a parametric study is easy to examine.

The parametric study is carried out as follows. For a set of values for α_1, α_2, and α_3, Eq. (6.29) is solved, to get the values of the limit cycles. The system (6.2)-(6.3) is then linearized near these values and the stability conditions are

determined using a numerical routine. The calculation has been repeated for some thousand sets of values for α_1, α_2, and α_3, all satisfying conditions (6.34)-(6.36) for existence of two limit cycles. From this parametric study, we find that always when two limit cycles exist they are both unstable.

The parametric study is now extended to the sets of values of α_1, α_2, and α_3 satisfying condition (6.33) for existence of a unique limit cycle. We find that it is possible to obtain a stable limit cycle. As an illustration, Figure 6.5a and 6.5b show the results of the numerical integration of Eqs. (6.2) and (6.3) for three oscillators and with α_1, α_2, and α_3 satisfying condition (6.33). The limit cycle is stable and its amplitude is exactly the one acceptable root of (6.29).

It appears that the values of the amplitudes of the limit cycles have simple expressions for the particular case of $|\alpha_1| << |\alpha_2| << |\alpha_3|$ and that the stability discussion is easy to carry out analytically. With the following calculation we examine this particular case.

The special case of $|\alpha_1| << |\alpha_2| << |\alpha_3|$ is treated to completion for the initial conditions $B_1(0) = B_2(0) = B_3(0) = 0$. Consequently, from (6.2)-(6.3), $B_n(t)$ vanish, since $\theta_n = 0$. System (6.4)-(6.5) then yields the following approximate relations for the limit cycle amplitudes

$$\alpha_1 A_1 - \beta A_1 A_2 = 0. \tag{6.37}$$

$$\alpha_2 A_2 + \beta A_1^2 = 0. \tag{6.38}$$

$$\alpha_3 A_3 + 3\beta A_1 A_2 = 0. \tag{6.39}$$

where we have assumed

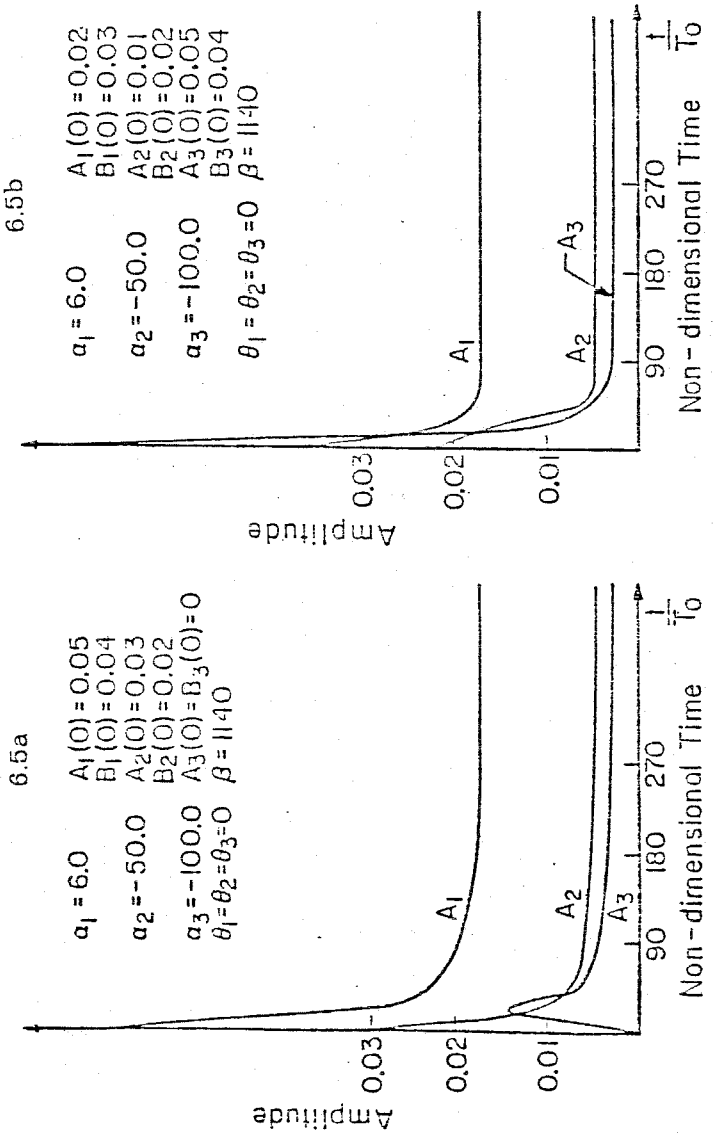

Figure 6.5 Case of three oscillators with $\alpha_4 = 0$.

$$| A_1 | << | A_2 | << | A_3 | \tag{6.40}$$

This approximation will be justified by the following results. In fact, Eqs. (6.37)-(6.39) have the solutions

$$A_{10} = \pm \frac{1}{\beta}\sqrt{-\alpha_1\alpha_2},\ A_{20} = \frac{\alpha_1}{\beta},\ A_{30} = \pm \frac{3}{\beta}\frac{\alpha_1}{\alpha_3}\sqrt{-\alpha_1\alpha_2} \tag{6.41}$$

Since $| \alpha_1 | << | \alpha_2 | << | \alpha_3 |$, it is seen that approximation (6.40) is compatible with solutions (6.41). It is interesting to notice from (6.41) that the existence condition is now simply

$$\alpha_1\alpha_2 < 0$$

We now linearize system (6.2)-(6.3) near the above solutions and we calculate the characterisic polynomial, as for two nonlinear oscillators, to get

$$p(\lambda) = \lambda^3 - \lambda^2(\alpha_2 + \alpha_3) + \lambda(\alpha_2\alpha_3) + 2\alpha_1\alpha_2\alpha_3$$

According to the Lienard criteria, the stability conditions are then,

$$\alpha_1\alpha_2\alpha_3 > 0.$$

$$\alpha_2 + \alpha_3 < 0.$$

$$\alpha_2\alpha_3 (-\alpha_1 + \alpha_2 - \alpha_3) > 0.$$

These inequalities, in addition to the existence condition $\alpha_1\alpha_2 < 0$, can be simplified to

$$\alpha_1 > 0, \ \alpha_2 < 0 , \ \alpha_3 < 0.$$

The direct conclusion here is that all the modes higher than first have to be stable. Moreover, from (6.41) we have two different roots. This seems to contradict our earlier conclusion that when two different limit cycles exist they are both unstable. However, these roots have only a sign difference and actually they correspond to the same limit cycle. In fact, when we replace these roots in $\eta_i(t)= A_i(t) \sin \omega_i t + B_i(t) \cos \omega_i t$, we see that these roots correspond to two limit cycles with a phase difference of π. However, as we have seen in Section 6.3.1 (discussion after Eq. (6.16)), a limit cycle is determined to a phase shift in time. Therefore, these two roots correpond to the same limit cycle. The point of this remark is to notice that having different roots for Eqs. (6.4)-(6.5) does not always mean having different limit cycles.

Now that we have completed the discussion of the case for zero frequency shift in the limit cycle, we extend the analysis in the next section to the case of non-zero frequency shift. Some results for the amplitudes and the frequency shift of the limit cycle will be presented.

6.4. Case of non-zero frequency shift

In this section, we will consider the case where the coefficients A_i reach the oscillatory behavior $A_i = \delta_i\cos(\nu_i t + \psi_i)$ and B_i reach $B_i = \delta_i\sin(\nu_i t + \psi_i)$ for $t \to \infty$. Substitution into $\eta_i(t) = A_i(t) \sin\omega_i t + B_i(t)\cos\omega_i t$ gives

$$\eta_i(t) = \delta_i \sin((\omega_i + \nu_i)t + \psi_i)$$

Thus, in the limit cycle, the amplitude $\eta_i(t)$ will oscillate with a fundamental frequency of $\omega_i + \nu_i$. The ν_i are yet unknown. The amplitude of the limit cycle as well as its frequency will be determined. The difference from the last section is that here the limit cycle is oscillating with a fundamental frequency different from the fundamental acoustic frequency of the chamber. The frequency shift is ν_1.

We treat fully the case of two nonlinear oscillators. The case of three oscillators is integrated only numerically in order to confirm the results found for two oscillators. The coefficients A_i and B_i , i=1,2, then satisfy the following system of equations

$$\frac{dA_1}{dt} = \alpha_1 A_1 + \vartheta_1 B_1 - \beta \left(A_1 A_2 + B_1 B_2 \right) \tag{6.42}$$

$$\frac{dB_1}{dt} = -\vartheta_1 A_1 + \alpha_1 B_1 + \beta \left(B_1 A_2 - A_1 B_2 \right) \tag{6.43}$$

$$\frac{dA_2}{dt} = \alpha_2 A_2 + \vartheta_2 B_2 + \beta \left(A_1^2 - B_1^2 \right) \tag{6.44}$$

$$\frac{dB_2}{dt} = -\vartheta_2 A_2 + \alpha_2 B_2 + 2\,\beta\, B_1 A_1. \tag{6.45}$$

The ψ_i represent the phase of each oscillator and should be taken into account. However, because the above system is autonomous, one phase is arbitrary, say, $\psi_1 = 0$. Thus, by using the limit expressions of A_i and B_i, Eqs. (6.42)-(6.45)

reduce to the following system :

$$-\nu_1\,\delta_1\sin\nu_1 t = \alpha_1\,\delta_1\cos\nu_1 t + \vartheta_1\,\delta_1\sin\nu_1 t$$

$$-\beta\,\delta_1\delta_2\cos\left(\left(\nu_1-\nu_2\right)t-\psi_2\right) \qquad (6.46)$$

$$\nu_1\,\delta_1\cos\nu_1 t = -\vartheta_1\,\delta_1\cos\nu_1 t + \alpha_1\,\delta_1\sin\nu_1 t$$

$$+\beta\,\delta_1\delta_2\sin\left(\left(\nu_1-\nu_2\right)t-\psi_2\right) \qquad (6.47)$$

$$-\nu_2\,\delta_2\sin\left(\nu_2 t+\psi_2\right) = \alpha_2\,\delta_2\cos\left(\nu_2 t+\psi_2\right)$$

$$+\vartheta_2\,\delta_2\sin\left(\nu_2 t+\psi_2\right)+\beta\,\delta_1^2\cos 2\nu_1 t \qquad (6.48)$$

$$\nu_2\,\delta_2\cos\left(\nu_2 t+\psi_2\right) = -\vartheta_2\,\delta_2\cos\left(\nu_2 t+\psi_2\right)$$

$$+\alpha_2\,\delta_2\sin\left(\nu_2 t+\psi_2\right)+\beta\,\delta_1^2\sin 2\nu_1 t. \qquad (6.49)$$

Multiply Eq. (6.46) by $\cos\nu_1 t$, Eq. (6.47) by $\sin\nu_1 t$ and add the results, to find

$$\alpha_1\delta_1-\beta\,\delta_1\,\delta_2\cos\left(\left(2\nu_1-\nu_2\right)t-\psi_2\right)=0.$$

This equation should be satisfied at any (large) time, therefore

$$\nu_2 = 2\,\nu_1,\ \alpha_1 - \beta\delta_2\cos\psi_2 = 0. \tag{6.50}$$

The values of ψ_2 and δ_2 have yet to be determined. Multiply now Eq. (6.46) by $\sin\nu_1 t$, Eq. (6.47) by $\cos\nu_1 t$ and subtract the results to find

$$-\nu_1 = \vartheta_1 - \beta\delta_2\sin(\,(\,2\nu_1 - \nu_2\,)\,t - \psi_2\,)$$

Then, with $2\nu_1 = \nu_2$ from (6.50),

$$-\nu_1 = \vartheta_1 + \beta\delta_2\sin(\,\psi_2\,) \tag{6.51}$$

Eqs. (6.50) and (6.51) then yield

$$\tan\psi_2 = -\left(\frac{\vartheta_1 + \nu_1}{\alpha_1}\right) \tag{6.52}$$

A second relation is obtained by multiplying Eq. (6.48) by $\cos(\nu_2 t + \psi_2)$, Eq. (6.49) by $\sin(\nu_2 t + \psi_2)$ and adding the results to find

$$\alpha_2\delta_2 + \beta\,\delta_1^2\cos(\,(\,2\,\nu_1 - \nu_2\,)t - \psi_2\,) = 0.$$

This equation should be satisfied at any (large) time, giving $\nu_2 = 2\,\nu_1$ again and

$$\alpha_2\delta_2 + \beta\delta_1^2\cos\psi_2 = 0. \tag{6.53}$$

Finally, multiply Eq. (6.48) by $\sin(\nu_1 t + \psi_2)$, Eq. (6.49) by $\cos(\nu_2 t + \psi_2)$, and subtract the results to find

$$-\nu_2\delta_2 = \vartheta_2\delta_2 - \beta\delta_1^2\sin(\,(\,2\nu_1 - \nu_2)\,t - \psi_2\,)$$

This becomes, with $2\nu_1 = \nu_2$,

$$\delta_2(\nu_2 + \vartheta_2) + \beta\delta_1^2\sin\psi_2 = 0. \tag{6.54}$$

Equations (6.53) and (6.54) then imply

$$\tan\psi_2 = (\frac{\vartheta_2 + \nu_2}{\alpha_2}) \tag{6.55}$$

Equations (6.52) and (6.55) yield the following expression for the frequency shift

$$\nu_1 = -\frac{\alpha_2\vartheta_1 + \vartheta_2\alpha_1}{2\,\alpha_1 - \alpha_2} \tag{6.56}$$

Therefore, the frequency shift is zero when $\alpha_2\vartheta_1 + \vartheta_2\alpha_1 = 0$. This is exactly the condition (6.15) for zero frequency shift. Using the result (6.56), Eq. (6.51) then gives

$$\delta_2 = \frac{\alpha_1}{\beta}(1 + (\frac{2\vartheta_1 - \vartheta_2}{2\alpha_1 + \alpha_2})^2\,)^{\frac{1}{2}} \tag{6.57}$$

Substituting this result in (6.53) then yields

$$\delta_1^2 = -\frac{\alpha_1\alpha_2}{\beta^2}(1 + (\frac{2\vartheta_1 - \vartheta_2}{2\alpha_1 + \alpha_2})^2\,) \tag{6.58}$$

The last two equations show that the amplitudes of the two modes have increased when $\vartheta_i \neq 0.$, in comparison with the amplitudes of the two modes in the past section when $\vartheta_i = 0$. For existence of solutions, we should have, from (6.58) and as before,

$$\alpha_1 \alpha_2 < 0.$$

To verify the analytical results, Figures 6.6a and 6.6b show the numerical solutions of the system (6.42)-(6.45) of ordinary differential equations for different initial conditions. The limiting amplitudes have exactly the same values given by the formulas (6.57) and (6.58).

By studying the stability of the limit cycle, the direction of energy flow can be handled in the same manner as for the case of zero frequency shift. The treatment is more complicated since the linearization of the system of non-linear oscillators leads to a *parametric* linear system. The approach presented in Chapter 5 can easily be used to solve this linear system. This is not done here.

In order to enhance our conclusion that the stability conditions of the limit cycle for the case $\vartheta_i = 0$ are *sufficient* for the stability of the limit cycle for the case $\vartheta_i \neq 0$, the system of equations (6.2)-(6.3) has been integrated numerically for three modes with two arbitrary sets of ϑ_i but for the same set of α_i used in Figures 6.5. Figures 6.7a and 6.7b show that the limit cycle is indeed stable, independently of the ϑ_i. This extends the conclusion reached above for two non-linear oscillators.

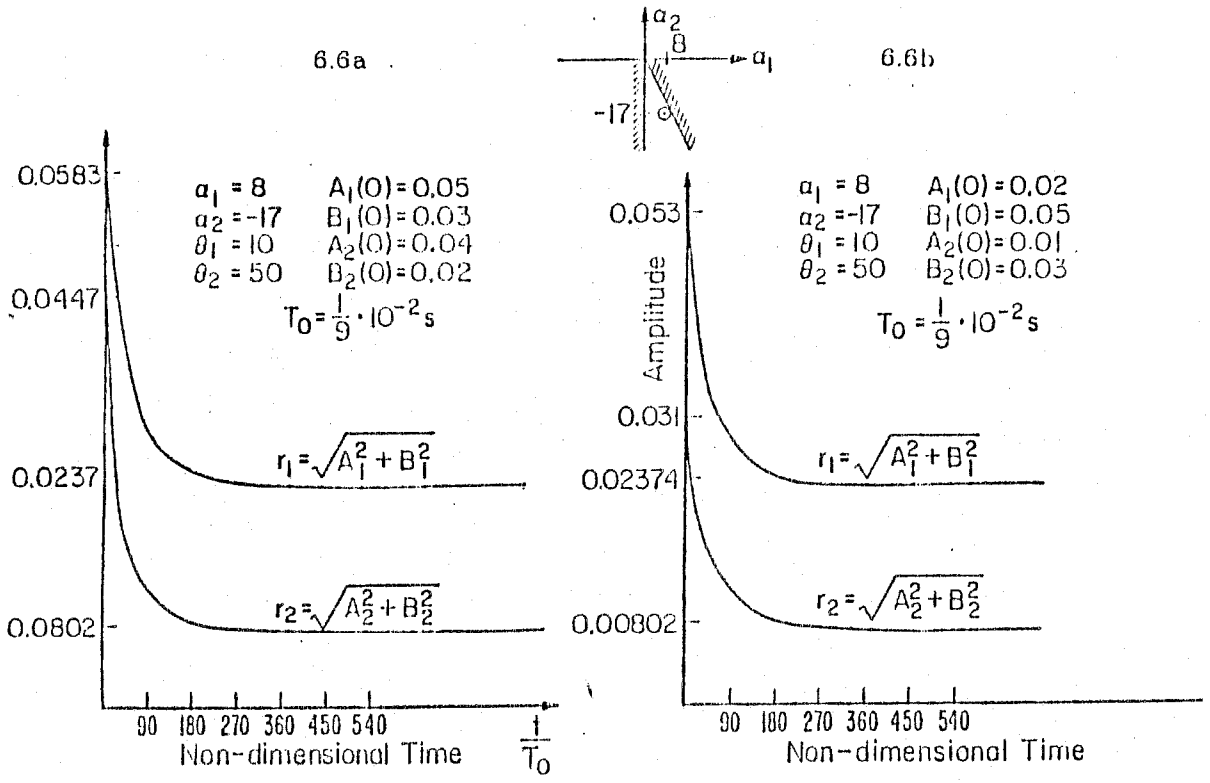

Figure 6.6 Influence of the imaginary parts on the increase of the amplitude of the limit cycle

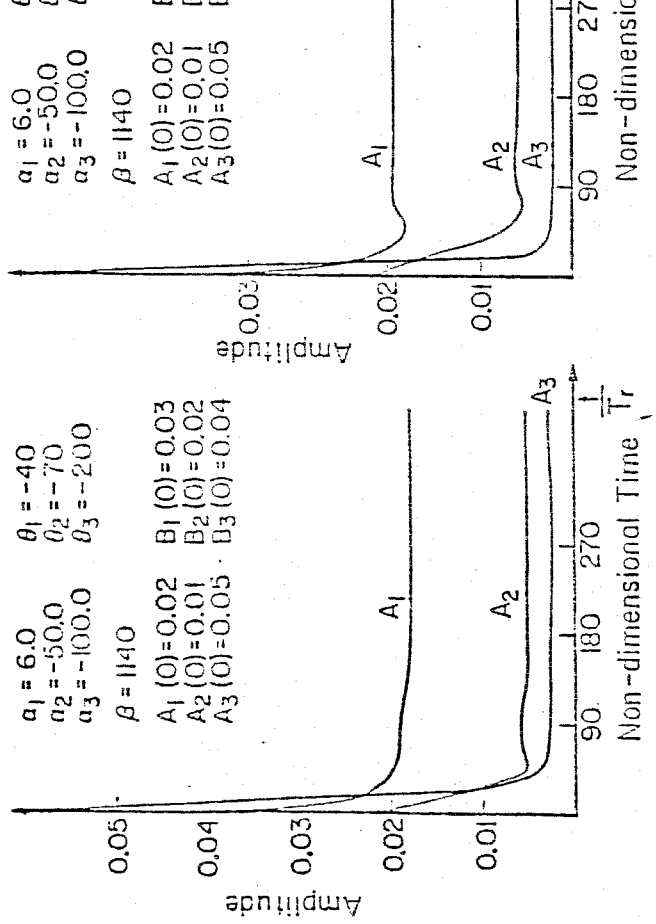

Figure 6.7 Case of three oscillators with $\theta_i \neq 0$.

6.5. Comparison with numerical solutions and experimental results

First, we will compare the results of this analysis with the numerical solutions reported in reference 2. Second, comparison will be made with some experimental results reported in reference 3.

6.5.1. *Comparison with some numerical results .*

In 2, Levine and Baum used a numerical technique based on a finite difference scheme to solve the longitudinal waves in the combustion chamber of a solid propellant rocket motor. Figures 6.8 show two of their results. Figure 6.8a shows the waveform of the pressure oscillations for a flow without particles, while Figure 6.8b is for flow with 2 μ particles. The initial disturbance contains only the fundamental mode but the final waveform (large time) contains higher harmonics. The fundamental mode grows initially in time, indicating that the first mode is unstable and with a growth rate α_1 given approximately by the initial exponential growth rate of the pressure. The amplitude of the second harmonic will be used as a basis for comparing our theoretical results and the numerical results in these figures. This amplitude can be determined from the numerical data by a Fourier analysis of the waveform. The growth rate of the first mode can be determined from the variation of the amplitude at the initial growth of the wave. In the numerical results[2], the relative energy density of the first three modes were respectively 0.813, 0.103, and 0.033 for the case in Figure 6.8a, and 0.811, 0.102, and 0.038 for the case in Figure 6.8b. These numbers show that the approximation $|\alpha_1| << |\alpha_2| << |\alpha_3|$ is likely, following (6.40)-(6.41), to be valid here. On the other hand, the frequency shift is zero in Figure 6.8a and very small in Figure 6.8b, indicating that it is safe to assume that $\vartheta_1 = 0$. Therefore, the amplitude of the second harmonic, given approximately, Eq. (6.41), by

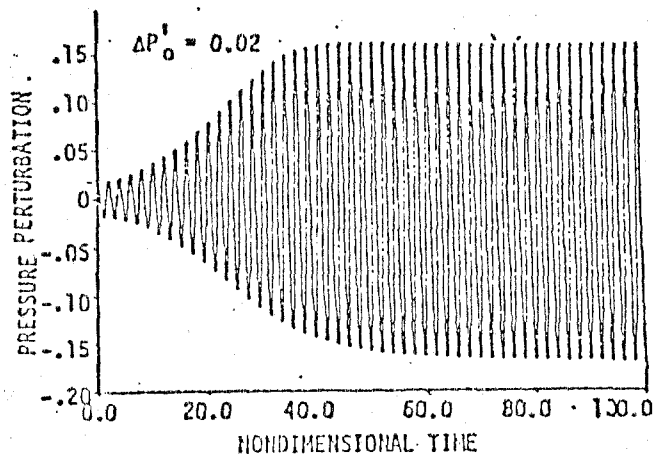

Figure 6.8a Time evolution of pressure oscillations at the head end of a motor (no particles). *Reference 6.2.*

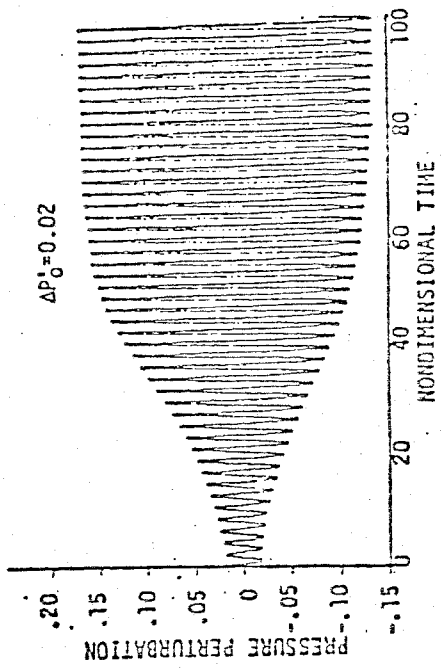

Figure 6.8b Time evolution of pressure oscillations at the head end of a motor (15%, 2 micron particles). Reference 6.2.

$$A_{20} = \frac{\alpha_1}{\beta}$$

can indeed be a criterion for comparison. Table 6.1 shows a comparison of the value of the spectral density of the second mode (proportional to the square of the amplitude) between our analysis and the results reported in 2. Good agreement is found for the case of Figure 6.8a. The error increases in the case of Figure 6.8b because we neglected the imaginary parts. The trend of error is in agreement with Eqs. (6.57)-(6.58).

Since here the first mode is unstable and the second and third modes are stable, the energy of the wave is flowing from the first mode to the second and the third modes.

Table 6.1. Comparison between Analysis and Numerical Results of Ref. 2

		Spectral density of second mode		
	α_1 s^{-1}	Analysis	Numerical Ref. 2	Error %
Figure 6.8a	81.31	0.1215	0.103	17.9%
Figure 6.8b	48.26	0.077	0.102	24.3%

6.5.2. *Comparison with some experimental results* .

In the experiments reported by Beckstead et al[3], they carried out a series of experiments on the performance of laboratory devices for testing solid propellants. In particular, they changed the combustion area of the solid propellant and they determined, at the same time, the growth α_1 of the first mode and the final amplitude of the limit cycle. But, from our analysis, the final amplitude is given by

$$A = \sqrt{(A_1^2 + A_2^2)} = \frac{1}{\beta}\sqrt{\alpha_1(\alpha_1 - \alpha_2)} \tag{6.59}$$

by limiting the number of modes to two. Considering the fact that for practical problems the damping is approximately independent of the combustion area and the growth rate of the first mode is small compared to the damping rate of the second mode, it is safe to assume from our analytical results (6.59) that the amplitude varies as the square root of the growth rate of the first mode when the combustion area changes. This criterion is used to compare with the experiments in 3. Figure 6.9 shows the result of the comparison. A fairly good agreement is found.

6.6. Concluding remarks

In this chapter, we have shown, following a second order expansion in the pressure amplitude and using the perturbation-averaging technique, analytical results for the amplitude and the conditions for existence and stability of limit cycles for pressure oscillations in combustion chambers. The results agree completely with those presented of Chapters 4 and 5 using the asymptotic-perturbation technique. This constitutes a strong support to the asymptotic-perturbation technique and to the results regarding the amplitudes and the conditions for existence and stability of limit cycles.

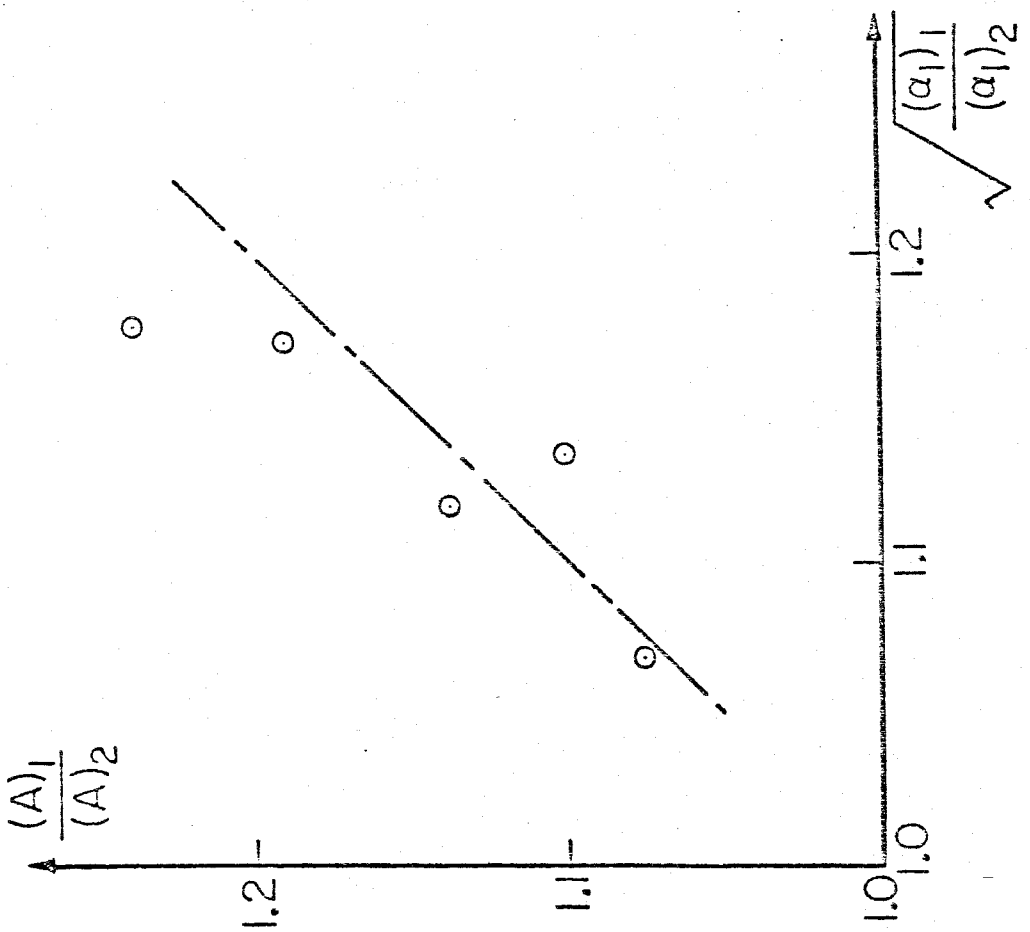

Figure 6.9 Comparison of the analytical results with the experimental ones given in reference 6.3. The straight line represents the approximate analytical results. The circles represent experimental data points.

Moreover, further results were obtained regarding the influence of the linear responses of the different processes in the chamber on the stability of the limit cycle and on the energy exchange among modes.

In the next chapter we show that the system of equations (6.2) and (6.3) apparently does not explain triggering, or nonlinear instability, for pressure oscillations in combustion chambers. A formal analysis for triggering is discussed and application of the results to the analysis of some experimental data is carried out.

Appendix 6A

Possible Limit Cycles

In this appendix we will show that the limit cycle can have, under certain conditions, only two forms. To fix ideas, we treat two modes only and we deal with the pressure at a given location, say, x=0. The pressure has then the following expression

$$p' = \eta_1(t) + \eta_2(t)$$

Since we are looking for periodic solutions, the pressure should be periodic and with fundamental frequency, say, $\omega + \nu$. Now, expand the pressure into its Fourier components

$$p' = a_1 \sin((\omega + \nu)t + \psi_1)$$

$$+ a_2 \sin(2(\omega + \nu)t + \psi_2) + \text{etc.} \qquad (A.1)$$

On the other hand

$$p' = A_1(t)\sin\omega t + B_1(t)\cos\omega t$$

$$+ A_2(t)\sin 2\omega t + B_2(t)\cos 2\omega t \qquad (A.2)$$

Equating equations (A.1) and (A.2) yields

$$\sin\omega t(A_1(t) - a_1\cos(\nu t + \psi_1))$$

$$+ \cos\omega t(B_1(t) - a_1\sin(\nu t + \psi_1))$$

$$+ \sin 2\omega t(A_2(t) - a_2\cos(2\nu t + \psi_2))$$

$$+ \cos 2\omega t(B_2(t) - a_2\sin(2\nu t + \psi_2)) = 0. \qquad (A.3)$$

Two direct solutions of (A.3) are

$$A_1(t) = \text{constant}, \quad \nu = 0.$$

and

$$A_1(t) = a_1\sin(\nu t + \psi_1) \qquad (A.4)$$

This is the origin of the two cases treated in the main text.

Now assume that $A_1(t)$, etc., oscillate with a frequency much smaller than ω, and the shift of frequency ν is small compared to ω. Multiply (A.3) by $\sin\omega t$ and integrate over one period, keeping in mind that the coefficient of $\sin\omega t$ remains approximately constant. The direct result is that this coefficient should vanish in order for (A.3) to be satisfied:

$$A_1(t) - a_1\sin(\nu t + \psi_1) = 0$$

That is exactly equation (A.4). Therefore, under the assumption of a very small

shift of frequency, we have only the cases treated in the main text. It is worth noticing here that this assumption was essential in applying the method of averaging in reference 1.

If this assumption is not satisfied, then a number of cases are possible. For example

$$A_1(t) = a_1\cos(\nu t + \psi_1) + \cos\omega t$$

$$B_1(t) = a_1\sin(\nu t + \psi_1) - \sin\omega t, \text{ etc.}$$

are solutions of equation (A.3).

REFERENCES 8

1. Culick, F. E. C. " Nonlinear Behavior of Acoustic Waves in Combustion Chambers," *Acta Astronautica*, Vol. 3 , No. 9, Sept. 1976.

2. Levine, J. N. and Baum, J. D." A Numerical Study of Nonlinear Instabilities in Solid Rockets Motors," *AIAA* paper 81-1524, July 1981.

3. Beckstead, M. W., Bennion, D. U., Butcher, A. G., and Peterson, N. L. " *Variable Area T-Burner Investgation*," AFRPL-TR-72-85.

4. Culick, F. E. C., private communication

5. Gantmacher, F. R. "*The Theory of Matrices*," Chelsea Publishing Company, New York, 1960.

Chapter 7

TRIGGERING OF PRESSURE OSCILLATIONS

7.1. Introduction

In this chapter we treat the problem of triggering of pressure oscillations in combustion chambers using the perturbation-averaging technique. The analysis is based on a third order expansion in the pressure amplitude; only two modes will be accounted for. We will show major mechanisms responsible for triggering and how they affect this phenomenon. The reason for studying this problem is the realization that triggering, or nonlinear instability, is a general phenomenon and is not related to a particular chamber geometry or to a specific propellant. This is, to our knowledge, the first global analytical representation of triggering.

The analysis in Chapter 6 was limited to determination of the limit cycle when the system is linearly unstable, i.e. when one or more modes is linearly unstable. It cannot predict nonlinear instability, or triggering. In fact, the system (6.2)-(6.3) in Chapter 6 yields

$$\frac{1}{2}\frac{d}{dt}\sum_{i=1}^{\infty}(A_i^2 + B_i^2) = \sum_{i=1}^{\infty}\alpha_i(A_i^2 + B_i^2)$$

Therefore, the nonlinearity disappears when we calculate the rate of change of energy of the wave. For a linearly stable system, all the α_i are negative and the energy of the wave decays in time, whatever the initial conditions. It is therefore impossible to produce a non-trivial limit cycle if all modes are stable.

The analysis must evidently be extended in order to explain how a linearly stable system can be pulsed into instability. By this we mean that for small initial disturbances the system is stable, but for large initial disturbances the wave amplitude will grow in time, leveling off toward a non-trivial limit cycle.

The idea of pursuing a general analytical investigation of triggering phenomenon is motivated partly by earlier works on the subject. Powell[1] used an approximate-numerical analysis to examine, among other things, triggering of pressure oscillations in liquid propellant rockets. He expanded the acoustic quantities in the normal modes of the acoustic field; the resulting set of equations for nonlinear oscillators was solved numerically. Kooker and Zinn[2] studied triggering in solid propellant rockets by solving numerically the conservation equations. Powell et al[3] used an approximate-numerical analysis with a nonlinear combustion response to investigate triggering in solid propellant rocket motors. Finally, Levine and Baum[4] examined triggering by solving numerically the conservation equations using different forms for the combustion response.

The point in the following calculations is to interpret *analytically* some results reported in references 1-4. The aim is to deduce a general *formalism* for triggering. Having deduced a formalism, application of the results to some experimental data will be carried out. In this chapter, only the perturbation-averaging technique will be used to carry the analysis, because of the simplicity to handle the discussions. In Chapter 8, we compare the uses of the perturbation- averaging technique and the asymptotic-perturbation technique in the treatment of triggering in combustion chambers.

7.2. Discussion and interpretation of some previous works

In this section, we discuss some results reported in references 1 and 2. Some interpretations of the results will be given and a general formalism of triggering phenomenon in *any* type of systems will be presented.

In reference 1, Powell examined two types of modes for pressure oscillations in liquid propllant rockets. When only one radial mode is taken into account, he finds (p. 232) numerically, to second order in the pressure amplitude, that triggering in the sense of an *unstable* limit cycle is possible. At the same time, from the conservation equations, he also finds a coupling of the radial mode with itself. Keeping these results in mind, we consider the following nonlinear differential equation

$$\frac{dA}{dt} = \alpha A + b A^2 \tag{7.1}$$

where α is the linear growth rate and b is the coefficient of the self-coupling term. Figure 7.1 shows the phase diagram (A, $\dot{A}$). From this diagram, we see that for a linearly stable system, i.e. $\alpha < 0$, the system becomes unstable if the initial disturbance is greater than A_1. The equilibrium point A_1 is called an unstable limit cycle. Consequently the numerical result is recovered through the simple interpretation given by Eq. (7.1)

Also in reference 1, the author considers the case of the interaction, to second order in the amplitude, between the first and the second tangential modes. From his approximate analysis he finds no self-coupling. However, there is a cross-coupling nonlinearity of one mode with the other. From his numerical computations, he finds (p.200) that it is impossible to predict triggering in the sense of a stable limit cycle. This phenomenon can be interpreted as follows. Consider the system of two nonlinear differential equations

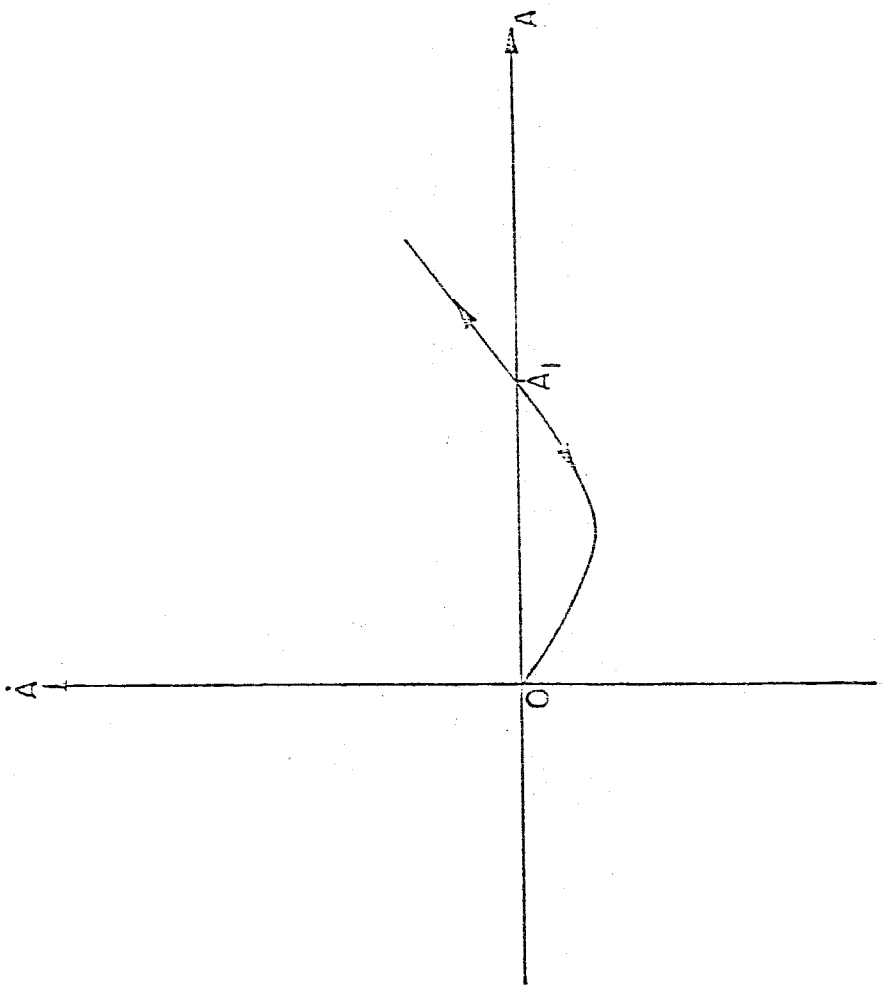

Figure 7.1 Phase Diagram for Eq_j (7.1)

$$\frac{dA_1}{dt} = \alpha_1 A_1 + b_1 A_1 A_2 \tag{7.2}$$

$$\frac{dA_2}{dt} = \alpha_2 A_2 + b_2 A_1^2 \tag{7.3}$$

In the limit cycle, we have

$$\frac{dA_1}{dt}, \frac{dA_2}{dt} = 0.$$

giving the limit cycle amplitude

$$A_{10} = \left(\frac{\alpha_1 \alpha_2}{b_1 b_2}\right)^{\frac{1}{2}} \tag{7.4}$$

$$A_{20} = -\frac{\alpha_1}{b_1} \tag{7.5}$$

We see that for triggering to occur we should have

$$\frac{\alpha_1 \alpha_2}{b_1 b_2} > 0.$$

However, for a linearly stable system α_1 and α_2 are < 0. Consequently, we must have

$$b_1 b_2 > 0.$$

To study the stability of the limit cycle, we linearize Eqs. (7.2) and (7.3) near the limit cycle. Write

$$A_1 = A_{10} + A'_1,\ A_2 = A_{20} + A'_2$$

and substitute these expressions in (7.2)-(7.3), to get a system of linear equations in A'_1 and A'_2

$$\frac{dA'_1}{dt} = (\alpha_1 + b_1 A_{20})A'_1 + b_1 A_{10} A'_2 \tag{7.6}$$

$$\frac{dA'_2}{dt} = \alpha_2 A_2 + 2b_2 A_{10} A'_1 \tag{7.7}$$

By writing $A'_1 = U_1 e^{\lambda t}$, etc., where U_1, etc., are constant, and replacing these expressions in the above linear system we get a linear system of equations for U_1, etc., of the form

$$M\vec{X} = 0$$

where M is the matrix of the linear system and $\vec{X}$ represent U_1, etc. This system has non-zero solutions only when its determinant vanishes. This gives a polynomial equation in λ, the characteristic polynomial. For the system in question, the characteristic polynomial is

$$P(\lambda) = \lambda^2 - \lambda\,\alpha_2 - \alpha_1\alpha_2 \tag{7.8}$$

where use has been made of (7.4)-(7.5). The product of roots of (7.8) is $-\alpha_1\alpha_2$. However, for a linearly stable system α_1 and α_2 are < 0. Therefore the product

of roots is negative. Consequently, the only possibility is that one root has a positive real part while the second root has a negative real part. The direct conclusion is that the limit cycle is unstable whatever b_1 and b_2. This means it is impossible to get triggering in the sense of a stable limit cycle. This is a direct interpretation of the result cited above.

We now turn to another result reported in reference 1. Powell extends his analysis to third order in the wave amplitude. First, he considers the first tangential mode, for which there is no self-coupling in the second order approximation but a third order self-coupling. From his numerical results he concludes that triggering is possible only in the sense of an unstable limit cycle. This conclusion can be interpreted as follows. Consider the following nonlinear differential equation

$$\frac{dA}{dt} = \alpha A + c A^3 \tag{7.9}$$

The limit cycle amplitude is simply

$$A_1 = \left(- \frac{\alpha}{c} \right)^{\frac{1}{2}}$$

The second order term is missing because there is no self-coupling to second order. For a linearly stable system α_1 is < 0. Consequently, triggering is possible only if $c > 0$. The phase diagram is similar to the diagram shown on Figure 3.1 in Chapter 2 but with reversed arrows. It is clear that a non-trivial stable limit cycle cannot exist. Therefore, a model represented by Eq. (7.9) cannot represent triggering in the sense of a non-trivial limit cycle. This explains the numerical result cited above.

Powell further extended his computation to the treatment of the first radial mode, for which there are a second order and a third order self-couplings. From his numerical computations, he concludes that triggering in the sense of a stable non-trivial limit cycle for a linearly stable system is possible. This can be interpreted as follows. Consider the following nonlinear differential equation

$$\frac{dA}{dt} = \alpha A + b A^2 + c A^3 \tag{7.10}$$

The phase diagram of this equation is shown on Figure 7.2 for the case where

$$b \neq 0,\ b^2 - 4\alpha c > 0,\ c < 0. \tag{7.11}$$

In the following we will show that conditions (7.11) are necessary and sufficient for Eq. (7.10) to have a stable non-trivial limit cycle while the system being linearly stable. In fact, the non-trivial limit cycles are the roots of

$$\alpha + b A + c A^2 = 0. \tag{7.12}$$

If conditions (7.11) are satisfied then Eq. (7.12) has two distinct roots, say A_1 and A_2. Eq. (7.10) can then be written as follows

$$\frac{dA}{dt} = \alpha A(A - A_1)(A - A_2) \tag{7.13}$$

If the product $\frac{c}{\alpha}$ of roots of (7.12) is < 0 then A_1 and A_2 are of opposite sign, say $A_1 > 0$ and $A_2 < 0$. The phase diagram is similar to the diagram shown on Figure 3.1 in Chapter 2 but with reversed arrows. For an initial disturbance greater than A_1, $\frac{dA}{dt}$ becomes positive and A grows indefinitely. If the initial disturbance

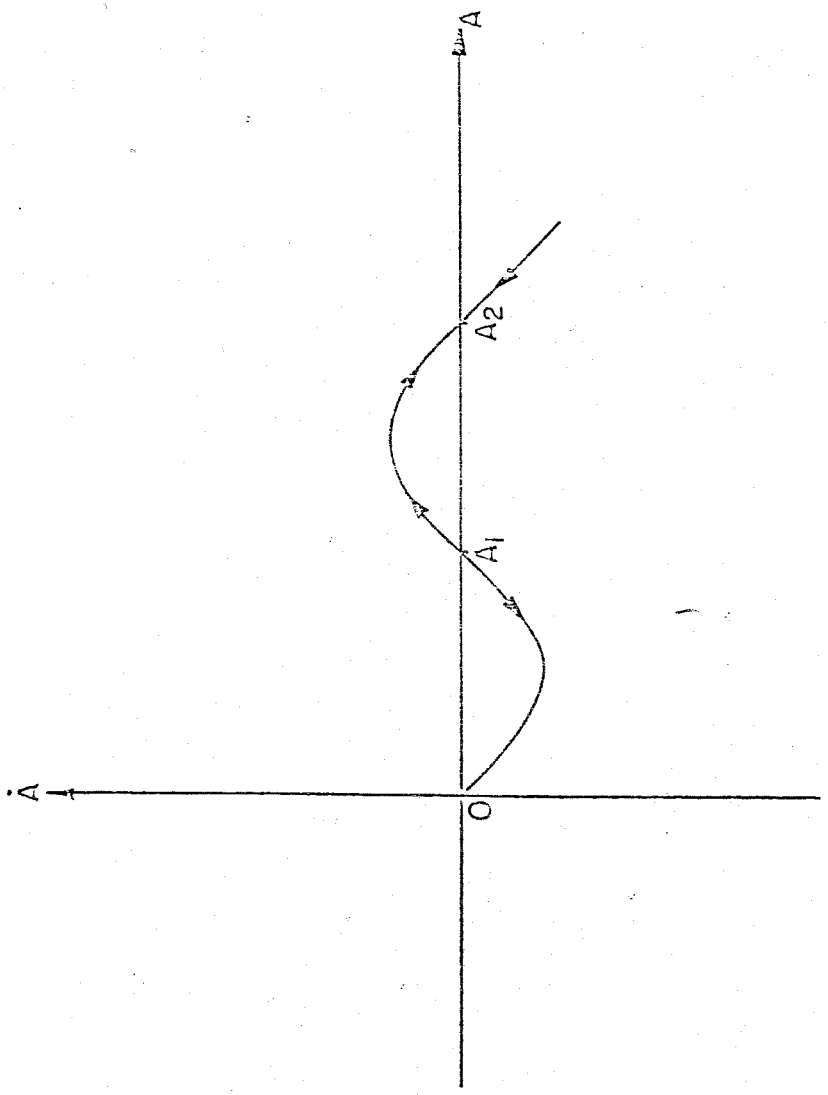

Figure 7.2 Phase Diagram for Eq. (7.10)

is smaller than A_1, then $\frac{dA}{dt}$ becomes negative and A decays to zero. The same holds true for A_2. A_1 and A_2 are said to correspond to unstable limit cycles.

On the other hand, if $\frac{c}{\alpha}$ is positive then A_1 and A_2 are of the same sign, say positive with $A_1 < A_2$. The phase diagram for this case is shown on Figure 7.2. For an initial disturbance smaller than A_1, $\frac{dA}{dt}$ is negative for $\alpha < 0$ and A decays in time toward the trivial limit cycle $A = 0$. However, for an initial condition greater than A_1 but smaller than A_2, $\frac{dA}{dt}$ becomes positive for $\alpha < 0$ and A grows in time toward A_2. Finally, for an initial condition greater than A_2, $\frac{dA}{dt}$ becomes negative for $\alpha < 0$ and A decays in time toward A_2. A_1 is said to be an unstable non-trivial limit cycle while A_2 is said to be a stable non-trivial limit cycle. Consequently, Eq. (7.10) explains why the third order analysis in reference 1 of the first radial mode is capable of predicting triggering in the sense of a stable non-trivial limit cycle.

We will now discuss some results on triggering reported by Kooker and Zinn[2]. In reference 2, Kooker and Zinn integrated numerically the conservation equations in solid propellant rockets, using a characteristic method. First, they use a steady state burning rate as a representation of the combustion processes. No triggering is found. Second, they include, along with the steady state burning rate, nonlinear particle damping in the conservation equations. Triggering occurs. In the following calculations we give an interpretation of the second conclusion regarding the role of the nonlinear particle damping. The first conclusion regarding the insensitivity of triggering to the steady burning rate will be discussed in the next section.

In reference 5, a model representing a second order nonlinear particle damping is presented and a modal analysis leads to the following system of equations

$$\frac{dA_1}{dt} = \alpha_1 A_1 + b_1 A_1 A_2 + c_1 A_1^2 \tag{7.14}$$

$$\frac{dA_2}{dt} = \alpha_2 A_2 + b_2 A_1^2 \tag{7.15}$$

where A_1 and A_2 are respectively the amplitude of the first and the second modes; $b_1 A_1 A_2$ corresponds to the nonlinear gasdynamics; $c_1 A_1^2$ to the nonlinear particle damping; and $b_2 A_1^2$ to the nonlinear gasdynamics. For $c_1 = 0$, Eqs. (7.14) and (7.15) reduce to Eqs. (7.2) and (7.3). However, in contradiction to Eqs. (7.2) and (7.3), Eqs. (7.14) and (7.15) do predict triggering in the sense of a stable non-trivial limit cycle. Figure 7.3 shows the existence of triggering for a particular set of coefficients α_1, α_2, b_1, b_2, and c_1. From this figure, it is seen that for a small (0.05) initial disturbance the wave decays in time but for a large (0.18) initial disturbance the wave grows to a non-trivial limit cycle. Therefore, Eqs. (7.14) and (7.15) may indeed interpret the numerical results of reference 2 noted above.

This result is important because of the structure of Eqs. (7.14) and (7.15). These equations contain only a *second* order nonlinearity. If only one mode, say A_1, were taken into account then these equations would reduce to Eq. (7.1), which, we know from Figure 7.1, cannot predict triggering in the sense of a stable non-trivial limit cycle. The mode coupling to second order, along with the self-coupling, assure the establishment of triggering. This is a simple example showing that new phenomena can occur when we deal with many modes. For one

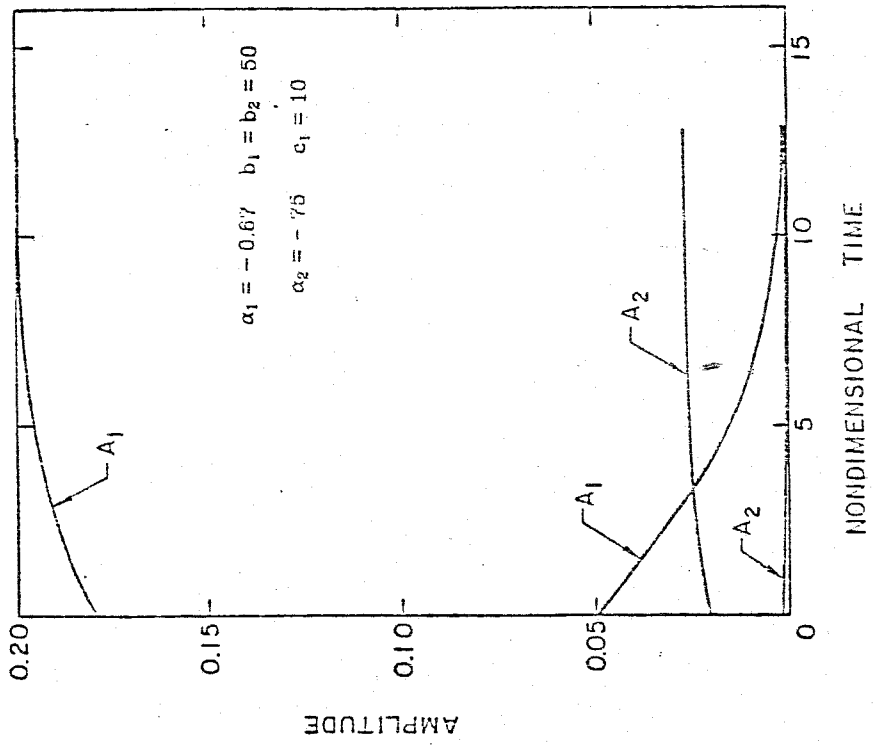

Figure 7.3 Proof of the ability of Eqs. (7.14) and (7.15) to predict triggering.

mode, triggering is absent. For two modes, triggering can occur.

Another important feature of Eqs. (7.14) and (7.15) is the role of the self-coupling term $c_1 A_1^2$. In the absence of such a term, Eqs. (7.14) and (7.15) reduce to Eqs. (7.2) and (7.3), and triggering disappears, as we have seen there.

The conclusion from these remarks is that a *second* order model can indeed predict triggering providing two criteria are met

a) The model includes a process representing a *self-coupling* mechanism

b) The analysis includes at least two modes.

The necessity of these criteria is only likely to be true, since we have not discussed the effects of the "out-of-phase" components. This is the object of the next section.

7.3. Justification for neglecting out-of-phase components

It is essential to notice that in all the formalism given in Section 7.2 and in the remainder of this chapter we neglect the "out-of-phase" components B_i, defined throughout Chapter 6. In the following discussion, we will give some justifications.

In Chapter 6, Section 6.3.1.3, we found the inclusion of the Θ_i, which corresponds to the imaginary parts of the linear responses, was not necessary for stability. In fact, we found in that section that if the limit cycle is stable when the imaginary parts are absent, it is also stable when the imaginary parts are present. These imaginary parts are largely responsible for the presence of the "out-of-phase" components. In fact, from Eqs. (6.2) and (6.3) in Chapter 6, we see that if the Θ_i are zero and if $B_i(0)$ are also zero, then $B_i(t)$ vanish at all time. We may therefore expect that the results elaborated in this chapter give sufficient criteria but probably not necessary criteria for triggering.

However, in the following discussion we will show that the stability criteria found in this chapter are not even sufficient. In chapter 6, Section 6.3.1.2, we found that the stability criterion (6.23) for the case when we neglected the "out-of-phase" components is less restrictive than the stability criteria (6.18)-(6-20) found in Section 6.3.1 for the case when the "out-of-phase" components are present. In both sections, we have $\theta_i = 0$. This means that without the presence of the "out-of-phase" components, the stability criteria may not valid. Strictly speaking, the results on stability of the limit cycle elaborated in this chapter are neither necessary nor sufficient for stability analysis. The treatment of "out-of-phase" components is a requirement in order to draw unambiguous conclusions as to whether triggering occurs. This will be the subject of future work.

Fortunately, some experimental data[7] favor the hypothesis that triggering is largely amplitude-dependent. In fact, in reference 7 some experiments are reported on pulsing a linearly stable solid propellant rocket into instability (more details will be given in Section 7.7). In particular, they change the waveform of the initial pulse (series MSA 12 to 18). Consequently, the phase relationships among different modes in the structure of the waveform vary, changing the values of the "out-of-phase" components $B_n(0)$, n =1,2, etc. The authors conclude that the amplitude of the pulse is the principal factor involved in triggering. Nevertheless, they pointed out that there may be some secondary effects of the pulse waveform that need to be better understood and that differences in waveform initially generated may be significant; generally, the amplitude appears to be the dominant factor.

One direct consequence of neglecting the " out-of-phase" components is that, for two modes, the number of nonlinear differential equations is reduced to 2 instead of 4, thus making the discussion of the conditions for existence and stability of the triggering limit easy to examine.

7.4. Relationship between the form of the combustion response and triggering

The oscillatory motions found in solid propellant rocket motors have a common feature; the motion depends mainly on some sort of coupling between the motion and the propellant. The interaction mainly occurs in a very thin layer near the propellant surface. Therefore, it is appropriate to represent the interaction by an admittance function relating the combustion rate of the propellant to the pressure and velocity fluctuations.

One basic assumption in the analysis in Chapter 6 is that the boundary conditions are linear. The nonlinearity represents only second order nonlinear gasdynamics. Here, we will assume that the boundary conditions are nonlinear; numerical results for this type of system are available for comparison. However, the formalism is general and can represent many nonlinear processes in the chamber, no matter what their origin. Only the nonlinearity of the combustion response, along with the gasdynamics nonlinearity, will be accounted for. The nonlinearity of the nozzle response can be incorporated without additional difficulties.

In the following calculations, we will consider for comparison only cylindrical solid propellant rockets with constant cross-section; the numerical results in references 3 and 4 have been obtained only for this type of system.

We consider first a second order nonlinear pressure combustion response of the form

$$\frac{m'}{p'} = \mu_p + b\,\frac{\partial p'}{\partial t} \tag{7.16}$$

where μ_p is the linear combustion response and b is an arbitrary coefficient. The dimensionless equations for a simplified model of a one-dimensional cylindrical

rocket motor (Figure 7.4), in dimensionless form, is

$$\frac{\partial p}{\partial t} + \gamma\, p \nabla .u + u.\nabla\, p = T\dot{m} \tag{7.17}$$

$$\rho\left(\frac{\partial u}{\partial t} + u .\nabla\, u \right) + \frac{\nabla\, p}{\gamma} = - u\dot{m} \tag{7.18}$$

$$T\, p^{-\frac{\gamma - 1}{\gamma}} = 1 \tag{7.19}$$

where $\dot{m}$ is the mass burning rate, $\dot{m} = \rho_s\, r$ with ρ_s the propellant density, T is the temperature, and u is the velocity. One notices that equation (7.19) does not include the entropy change due to mass injection. The inclusion of the entropy change in the energy equation (7.19) will change the right-hand side of (7.17) from $T\dot{m}$ to $\dot{m}$. For a real evolution we have $T\, p^{-\frac{n_p - 1}{n_p}} = 1$, where n_p is the polytropic exponent $1 < n_p < \gamma$. For practical problems $\gamma = 1.2$; therefore replacing n_p by γ is not a serious error. The assumption of an isentropic evolution of the flow will facilitate the expansion.

In the expansion of the pressure, temperature, and velocity in the normal modes of the chamber and the use of Green's theorem (see Chapter 4, Section 4.6), the right-hand side of (7.17) will enter as $\frac{\partial}{\partial t}(T\, \dot{m})$ and the right-hand side of (7.18) will enter as $\frac{\partial}{\partial x}(- u\, \dot{m})$.

Expand now the pressure, temperature, and velocity,

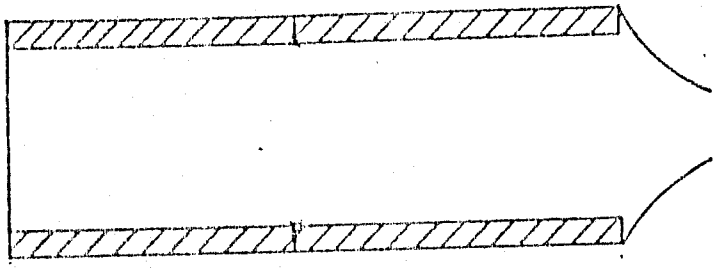

Figure 7.4 Model for one-dimensional cylindrical solid propellant rocket.

$$T = \bar{T} + T', \quad p = \bar{p} + p', \quad u = \bar{u} + u'$$

where $\bar{T}$, $\bar{p}$, $\bar{u}$ correspond to the steady state conditions. Writing the unsteady pressure and velocity expansions[6] in two modes only :

$$p' = \eta_1(t)\cos\omega x + \eta_2(t)\cos 2\omega x$$

$$u' = -\frac{\dot{\eta}_1(t)}{\gamma\omega}\sin\omega x - \frac{\dot{\eta}_2(t)}{2\gamma\omega}\sin 2\omega x ,$$

as in Section 4.6, we now apply Green's theorem to Eqs. (7.17) and (7.18) to find the system of equations for two nonlinear oscillators:

$$\ddot{\eta}_1 + \omega^2\eta_1 = [1]_{NG} + b(\dot{\eta}_1\dot{\eta}_2 - \frac{5}{2}\omega^2\eta_1\eta_2)$$

$$+ bc_0[\frac{5}{3}\eta_1\dot{\eta}_1 - \frac{1}{2}\eta_1\dot{\eta}_2 - \frac{1}{2}\eta_2\dot{\eta}_1 + \frac{14}{15}\eta_2\dot{\eta}_2] \qquad (7.20)$$

$$\ddot{\eta}_2 + 4\omega^2\eta_2 = [2]_{NG} + b(\dot{\eta}_1^2 - \frac{1}{2}\omega^2\eta_1^2)$$

$$+ bc_0[-\frac{5}{4}\eta_1\dot{\eta}_1 + \frac{8}{15}\eta_1\dot{\eta}_2 + \frac{8}{15}\eta_2\dot{\eta}_1 + \frac{3}{4}\eta_2\dot{\eta}_2] \qquad (7.21)$$

where $c_0 = 4\frac{r_0}{d_0}$, with r_0 the steady state burning rate and d_0 the diameter of the chamber; ω is the dimensionless frequency; and $[1]_{NG}$ and $[2]_{NG}$ are the same as those arising from the nonlinear gasdynamics given in Section 6.3. The

influence of μ_p is included in the linear parts of $[1]_{NG}$ and $[2]_{NG}$. The term c_0 shows the presence of the mean flow velocity

$$\bar{u} = c_0 x$$

However, we will find, by applying the method of time-averaging, that the influence of $\bar{u}$ disappears. Assume that η_1 and η_2 to have the forms

$$\eta_1 = A_1(t)\sin\omega t, \quad \eta_2 = A_2(t)\sin 2\omega t$$

and apply the method of time-averaging to find the following system of non-linear ordinary differential equations

$$\frac{dA_1}{dt} = \alpha_1 A_1 - \beta_1 A_1 A_2 \tag{7.22}$$

$$\frac{dA_2}{dt} = \alpha_2 A_2 + \beta_2 A_1^2 \tag{7.23}$$

where

$$\beta_1 = b\frac{\omega}{16}, \text{ and } \beta_2 = b\frac{\omega}{8}$$

We see clearly that the influence of the steady state velocity has disappeared, since there is no c_0 in (7.22) and (7.23).

The system (7.22)-(7.23) is a particular case of the system (7.2)-(7.3) However, for α_1 and α_2 both negative, we showed in the treatment of Eqs. (7.2) and (7.3) in the last section that, for any β_1 and β_2, system (7.2)-(7.3) could not yield

a stable non-trivial limit cycle. Therefore, the *form* (7.16) of the combustion response cannot predict triggering.

We consider now a second order nonlinear pressure combustion response of the form

$$\frac{m'}{p'} = \mu_p + b\, p'$$

where μ_p is the linear combustion response and b is an arbitrary coefficient. Following the same procedure leading to Eqs. (7.22) and (7.23), we find that no nonlinear contribution is obtained. Therefore, this form of combustion response may have little effect on the nonlinear behavior of the wave.

We now treat a second order nonlinear pressure combustion response of the form

$$\frac{m'}{p'} = \mu_p + c \left| \frac{\partial p'}{\partial t} \right| \tag{7.24}$$

where c is an arbitrary coefficient. This form may well represent a second order nonlinear velocity coupling. The velocity coupling corresponds to the effects of the component of flow velocity parallel to the propellant surface. In fact, from the linear analysis in Chapter 3, Eq. (3.12), we have

$$\frac{\partial u'}{\partial x} = -\frac{1}{\gamma}\frac{\partial p'}{\partial x}$$

The absolute value corresponds to the basic characteristic of velocity coupling : the burning response to velocity fluctuations is sensitive to the amplitude of the velocity but unsensitive to its direction.

We now reduce the system of equations (7.17)-(7.19), following the same procedure leading to Eqs. (7.22) and (7.23). The result is the following system of equations for the amplitudes A_1 and A_2.

$$\frac{dA_1}{dt} = \alpha_1 A_1 - \beta A_1 A_2 + c_1 A_1^2 \tag{7.25}$$

$$\frac{dA_2}{dt} = \alpha_2 A_2 + \beta A_1^2 + c_2 A_2^2 \tag{7.26}$$

where

$$c_1 = \frac{40}{9\pi^2}\omega c(\omega), \quad c_2 = \frac{20}{9\pi^2}\omega c(2\omega) \tag{7.27}$$

where c, defined in (7.24), is assumed, for generality, to be frequency-dependent. We see clearly that the absolute value is responsible for the presence of the self-coupling terms $c_1 A_1^2$ and $c_2 A_2^2$. Triggering, in the sense of a stable non-trivial limit cycle is found. Unlike the result established in Chapter 6, Section 6.2, it can be shown that the stability of the limit cycle depends also on the nonlinear coefficients. In fact, Figure 7.5 shows the existence of triggering for a particular set of coefficients α_1, α_2, β, and c_1, with $c_2 = 0$. From this graph it is clearly seen that for a small (0.05) initial disturbance the wave decays in time but for a large (0.18) initial disturbance the wave grows toward a non-trivial limit cycle. If the stability of the limit cycle were independent of c_1, then the conclusion should hold for $c_1 = 0$. However, for $c_1 = 0$, Eqs. (7.25) and (7.26) reduce to Eqs. (7.2) and (7.3), for which no triggering, in the sense of a stable non-trivial limit cycle, is possible. Therefore, for $c_1 = 0$, the stable non-trivial limit cycle becomes unstable. Consequently, stability of the limit cycle depends on the nonlinear

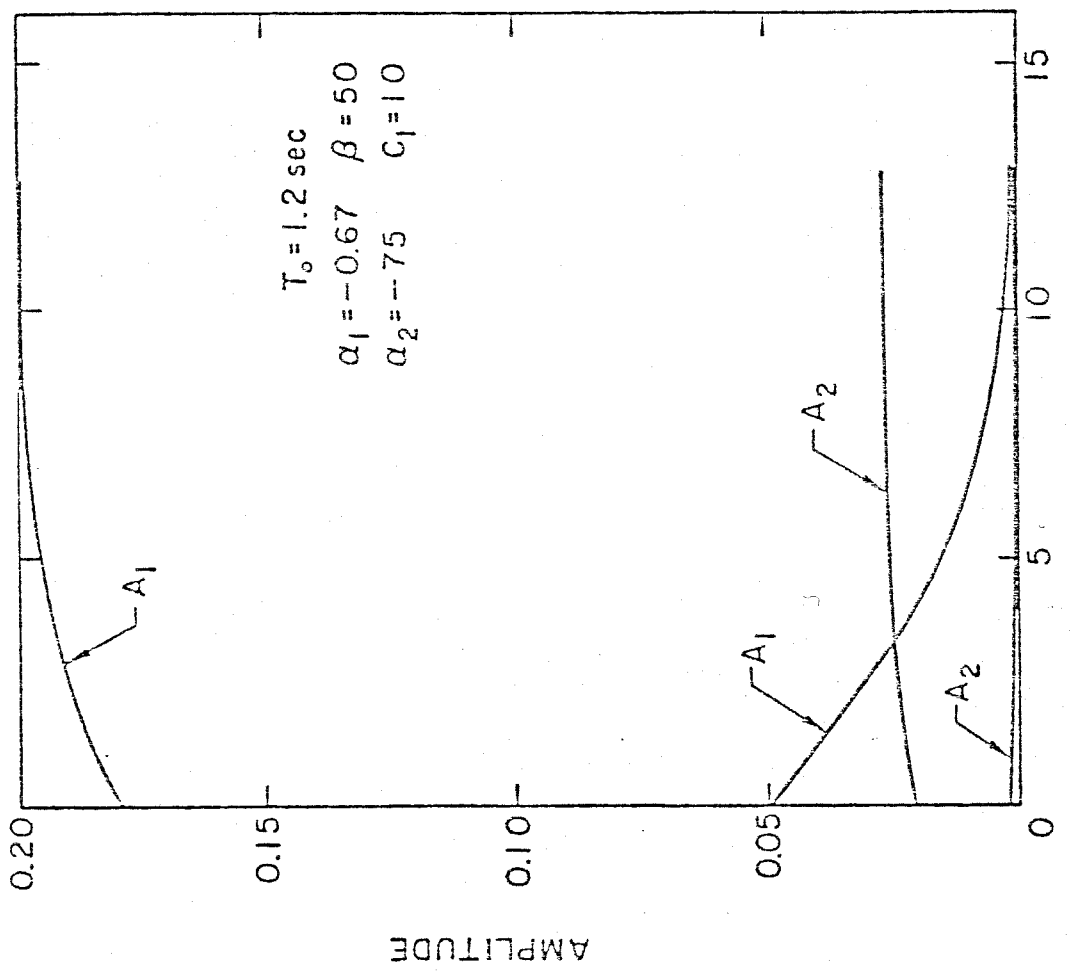

Figure 7.5 Proof of the ability of second order nonlinear velocity coupling to predict triggering.

coefficients.

The above discussion may explain some numerical results reported in references 3 and 4. In fact, in reference 3 (p. 93), an approximate form is used for the combustion response similar to the response given by (7.24). Triggering in the sense of a non-trivial stable limit cycle seems to occur, although the conclusion is not shown in a clear way. In reference 4, the conservation equations are integrated numerically and a combustion response similar to (7.24) is used in the numerical scheme. Triggering is clearly shown to exist.

We treat now a third order analysis. Our purpose is to discuss the influence of a third order combustion response on triggering. Assume that the response has the form

$$\frac{m'}{p'} = \mu_p + b_1 p' + f_1 \frac{\partial p'}{\partial t} + b_2 p'^2 + f_2 p' \frac{\partial p'}{\partial t} + h_2 \left(\frac{\partial p'}{\partial t}\right)^2 \tag{7.28}$$

where b_1, f_1, b_2, f_2, and h_2 are arbitrary coefficients. Following the same procedure leading to Eqs. (7.22) and (7.23), we get

$$\frac{dA_1}{dt} = \alpha_1 A_1 - \beta_1 A_1 A_2 + d_1 A_1^3 \tag{7.29}$$

$$\frac{dA_2}{dt} = \alpha_2 A_2 + \beta_2 A_1^2 + d_2 A_1^2 A_2 \tag{7.30}$$

The coefficients β_1 and β_2 are dependent on both the nonlinear gasdynamics and the nonlinear combustion response. The coefficients d_1 and d_2 depend only on the nonlinear combustion response. Triggering does occur. The stability of the limit cycle depends on the nonlinear as well as on the linear coefficients. Figure

7.6 shows the existence of triggering for a particular set of coefficients. The triggering phenomenon here is quite similar to the one shown on Figure 7.5.

Also it is assumed that the phases, i.e. the B_i, are not important. In Chapter 8, Section 8.1, it is shown that in the expansion to third order in the pressure amplitude, the third order terms in the expansion of the nonlinear gasdynamics term $\rho u \frac{\partial u}{\partial x}$ contain only coupling terms between the A_i and B_i. Therefore, neglecting the B_i implies neglecting third order contributions of the nonlinear gasdynamics. The effect of this assumption has not yet been assessed. One direct result is that, for two modes, the number of nonlinear differential equations is reduced to 2, thus making the discussion of stability and existence of triggering limit easy to handle.

From the above results, one concludes that triggering may also be due mainly to the energy exchange among modes and to a *third* order nonlinear pressure coupling. This result is important in the sense that an adequate representation of the pressure coupling *alone* may well predict triggering. However, in this case, the analysis should be extended to third order.

In the process of demonstrating that the form (7.28) leads to Eqs. (7.29) and (7.30), we have noticed in the calculations that h_2 is the only important coefficient among the coefficients of third order terms, since it leads to the third order term cA^3. Later in the analysis, Section 7.4, h_2 will be found to be associated, for a specific form of burning rate, to the time-lag in the combustion response.

It should emphasized that an expansion of the steady state burning rate $r = ap^n$ in the pressure amplitude can never yield a term of the form $h_2(\frac{\partial p'}{\partial t})^2$. This is an explanation why in reference 2 triggering is not predicted with a

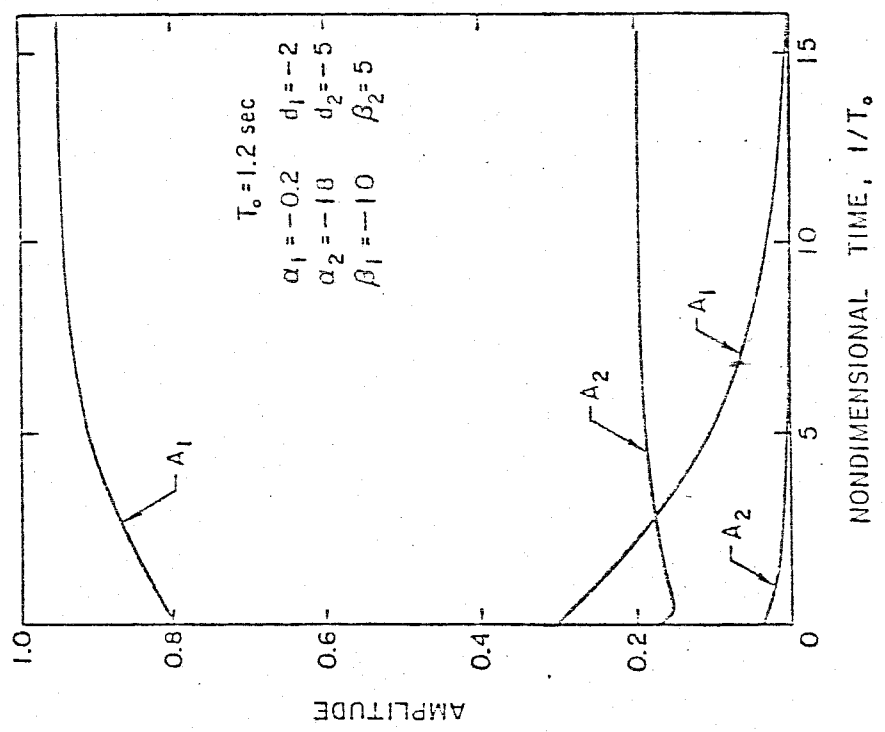

Figure 7.6 Proof of the ability of third order nonlinear pressure coupling to predict triggering.

simple quasi-steady combustion response.

We now turn to the general formulation for a burning rate which can predict triggering. In order to obtain a model which can represent some physical phenomenon, both velocity and pressure couplings should be present. We expand the combustion response as follows

$$\frac{m'}{p'} = \mu_p + b_1 \left| \frac{\partial p'}{\partial t} \right| + b_2 p'^2 + f_2 p' \frac{\partial p'}{\partial t} + h_2 \left(\frac{\partial p'}{\partial t} \right)^2 \qquad (7.31)$$

This form includes both pseudo second order nonlinear velocity coupling and third order nonlinear pressure coupling. The nonlinear velocity coupling $p' \left| \frac{\partial p'}{\partial t} \right|$ is not truly a second order because of the absolute value. Triggering does occur. For one mode, conditions (7.11) should be satisfied. Therefore, whether one mode is sufficient to predict triggering depends on the various parameters in (7.30), i.e. on the model for the combustion response. The coefficient h_2 is found to be the only important coefficient among third order term coefficients. Later in the analysis, h_2 will be found to be associated, for a specific form of burning rate, with the time-lag in the combustion response.

To make the analysis directly applicable, we treat only triggering of pressure oscillations in solid propellant rockets. However, the analysis yields results which can be generalized to other systems.

A detailed formulation for triggering is presented below. From the conservation equations of one-dimensional flow in solid propellant rocket motors, the existence of triggering for pressure oscillations in combustion chambers is proved. For a given set of parameters, one stable limit cycle is shown to exist. The main reason for existence and stability is the equilibrium among velocity coupling, nonlinear driving of the combustion (mostly due to the time lag

between the pressure and the combustion response), and the energy exchange among the acoustic modes of the chamber.

An application to some experimental results, reported in reference 7, will be carried out in Section 7.6. Good prediction of the results is achieved. Then we apply the analysis to some numerical solutions reported in reference 2.

Some forms of the burning rate proposed in earlier works lead to forms of the combustion response postulated here as prerequisite for triggering. In the theory of deflagration of solid propellant, a simple model[8] relating the propellant burning rate to the pressure is given by

$$r(t) = r_0(t)\left(1 + \frac{\psi \kappa}{r_0^3(t)} \frac{dr_0(t)}{dt}\right) \tag{7.32}$$

where r_0 is the steady state burning rate: $r_0 = ap^n$ with n the burning rate exponent; ψ is a constant having a value close to unity, dependent on the propellant and the combustion model; and κ is the thermal diffusivity of the solid propellant.

The choice of this expression for the burning rate is taken mainly because of the simplicity in carrying out the expansion in the amplitude and still predict triggering. Moreover, every term in expression (7.31) has some physical meaning. Consequently, the coefficients of the expansion correspond to some physical parameters.

It is true that the linear (A,B) model[9] represents more faithfully the combustion processes in the propellant. In reference 9, a critical review of different *linear* combustion responses is presented. In the following, we present a short summary of the (A,B) model since we will need later in the analysis the

time-lag deduced from the (A,B) model for comparison (Section 7.6 .) This model produces the following relation between fluctuations of the burning rate and pressure:

$$\frac{m'}{p'} = \frac{nAB}{\lambda + \frac{A}{\lambda} - (1 + A) + AB} \tag{7.33}$$

where A and B are related to the propellant combustion parameters. Usually A is in the range of 10 and B in the range of 1 for practical propellants; see reference 9 for more details. The coefficient λ here is a complex quantity and is the root of the following equation

$$\lambda(\lambda - 1) = i\Omega$$

where here $\Omega = \frac{\kappa\omega}{r_0^2}$ is the dimensionless frequency. With $\lambda = \lambda^{(r)} + i\lambda^{(i)}$, the roots of this equation become

$$\lambda^{(r)} = \frac{1}{2}\left[1 + \frac{1}{2^{\frac{1}{2}}}\left[(1 + 16\Omega^2)^{\frac{1}{2}} + 1\right]^{\frac{1}{2}}\right]^{\frac{1}{2}} \tag{7.34}$$

$$\lambda^{(i)} = \frac{1}{22^{\frac{1}{2}}}\left[(1 + 16\Omega^2)^{\frac{1}{2}} - 1\right]^{\frac{1}{2}} \tag{7.35}$$

These results will be used in Section 7.6 to deduce an expression for the time-lag. In fact, expression (7.33) can be written, for harmonic motion, as

$$m_0 e^{i\omega t} = |\mu_p| p_0 e^{i\omega t} e^{-\varphi} \equiv p_0 e^{i\omega(t - \frac{\varphi}{\omega})}$$

where $|\mu_p| e^{i\omega t} e^{-\varphi}$ is a simple expression for the right-hand side of (7.33), with μ_p the amplitude and φ the phase of the complex response. Therefore, one may define a time-lag by

$$\tau = \frac{\varphi}{\omega} \tag{7.36}$$

However, when it comes to nonlinear burning rates, there is, so far as we know, no simple *nonlinear* model other than (7.32). Model (7.32) gives, despite its limitations[10], a simple means for predicting triggering, as we will see in the next section. In the following discussion, we will consider only the form (7.32) for combustion response.

An imaginary part in the combustion response to pressure oscillations represents a time-lag. Following a similar reasoning, a nonlinear combustion model should reflect a similar behavior, i.e., the nonlinear combustion response should reflect a time-lag. The time-lag concept in a combustion chamber was first introduced by Crocco and Cheng[11] for concentrated combustion and by Cheng[12] for the specific problem of solid propellant rockets. Their attention was focused on the abnormal pressure peaks in rockets and their analysis was solely linear. To interpret triggering of pressure oscillations in liquid propellant rockets, Sirignano[13] used a shock wave model with a time-lag in the propellant combustion. His analysis predicted triggering but did not give either the threshold value or the final amplitude. Recognizing these shortcomings, Mitchell[14] calculated numerically the final amplitude, after tedious algebraic manipulations. It is difficult to interpret the relative importance of the different physical

processes. The point here is to present a model which can be used to predict, in a simple way, both the threshold and the final amplitudes.

It is true that including a time-lag introduces an imaginary part in the combustion response and, therefore, neglecting the "out-of-phase" components, as we have done in the last section, becomes inconsistent. In the following calculations, we will show the point. Assume, for simplicity, that $\dot{m} = ap^n(t - \tau)$, write $\dot{m} = m_0 + m'$ and $p = 1 + p'$, to find, by linearization,

$$m' = an[p' - \tau \frac{\partial p'}{\partial t}]$$

Using this expression on the right-hand sides of the conservation equations (7.17) and (7.18) and applying successively Green's theorem and the method of time-averaging (see Section 4.6) give the following contribution of the time-lag τ to the behavior in time of the "out-of-phase" component B_1 of the fundamental acoustic mode :

$$\frac{dB_1}{dt} = -\frac{1}{2} an\tau\omega^2 A_1$$

where A_1 is the "in-phase " component of the first mode. Since in the frame of our analysis in this chapter A_1 is taken into account and B_1 is not, we see clearly some inconsistency in introducing a time-lag. However, we still keep our hypothesis that the the "out-of-phase" components are not important for stability, mainly because of the justifications given in Section 7.3.

We are looking for a combustion response of the form (7.31), since this form can predict triggering. The following representation of the burning rate

$$r(t) = r_0(t-\tau)\left(1 + \frac{\psi\kappa}{r_0^3(t-\tau)}\frac{dr_0(t-\tau)}{dt} + g\,|u'|\,\right) \tag{7.37}$$

yields, after expansion in the pressure amplitude, the desired form (7.31). The term $g\,|u'|$ may represent velocity coupling with g an arbitrary coefficient. This is similar to $c\left|\frac{\partial p'}{\partial t}\right|$ in form (7.24).

Following the same analysis leading to Eqs. (7.22) and (7.23) and taking into account the results (7.25)-(7.26) and (7.29)-(7.30), we get

$$\frac{dA_1}{dt} = \alpha_1 A_1 - \beta A_1 A_2 + G_1 A_1^2 + c_1\omega^2 A_1^3 + d_1\omega^2 A_1 A_2^2 \tag{7.38a}$$

$$\frac{dA_2}{dt} = \alpha_2 A_2 + \beta A_1^2 + G_2 A_2^2 + c_2\omega^2 A_2^3 + d_2\omega^2 A_1^2 A_2 \tag{7.38b}$$

The details are presented in Appendix 7A. Here, only the coefficient β represents the nonlinear gasdynamics. The coefficients c_i, d_i, $i = 1,2$, are functions of ratio γ of the specific heats, the burning rate exponent n, and the area ratio and they are proportional to the coefficient h_2 in (7.30). Moreover, the coefficient c_1 is found in Appendix 7A, Eq. (A.9) to be positive. Since α_1 is negative for a linearly stable system, $\frac{c_1}{\alpha_1}$ is negative. Therefore, conditions (7.11) are not satisfied for the first mode. However, as we will see in the applications, the coupling between A_1 and A_2 will allow triggering to occur. The conclusion here is that, for solid propellant rockets and with the model (7.32) for the combustion response, we need at least two modes to predict triggering.

The coefficient h_2 is found in Appendix 7A, by expanding the burning rate expression in the pressure amplitude, to be proportional to the time-lag τ. The coefficients G_1 and G_2 represent either nonlinear particle losses, as we have seen in the analysis leading to Eqs. (7.14)-(7.15) in Section 7.2, or velocity coupling, as we have seen in the analysis leading to Eqs. (7.25)-(7.26). In the case of velocity coupling, the coefficients G_1 and G_2 are similar to c_1 and c_2 in (7.27). In the case of particle damping, Jensen and Beckstead[5] give the following expressions :

$$G_1 = -\frac{2}{3\pi^2} c_m \frac{d}{\mu} \left(\frac{\bar{\rho}}{\gamma' \bar{p}}\right)^{\frac{1}{2}} \cdot \frac{\omega^3 \tau_0^2}{(1 + 3c_m)^{\frac{1}{2}}} \tag{7.39}$$

and $G_2 = 8G_1$. The parameters in (7.39) are defined as follows. $\bar{\rho}$ is the mean flow density; $\bar{p}$ is the mean flow pressure; μ is the gas viscosity; d is the particle diameter; $c_m = \frac{\bar{\rho}_p}{\bar{\rho}}$, with $\bar{\rho}_p$ is the particle density per unit volume of the mixture; γ' is the effective heat ratio for the mixture and defined by $\gamma' = \frac{C_p + C\frac{\rho_p}{\bar{\rho}}}{C_v + C\frac{\rho_p}{\bar{\rho}}}$, with C_p, C_v, and C respectively the heat capacity of the gas at constant pressure, the heat capacity of the gas at constant volume, and the heat capacity of the particle; τ_0 is the relaxation time due to particle attenuation and is defined by $\tau_0 = \frac{\rho_{pm} d^2}{18\mu}$, with ρ_{pm} the density of the particulate material per unit volume of particles. Appendix 7A contains the details of the calculation leading to Eqs. (7.38), along with the details for the expressions of c_i and d_i, i = 1,2.

7.5. Determination of the limit cycle

In the following calculations we determine the limit cycle for pressure oscillations with a combustion response of the general form (7.31). In the limit cycle, Eqs. (7.38) become

$$\alpha_1 A_1 - \beta A_1 A_2 + G_1 A_1^2 + c_1 \omega^2 A_1^3 + d_1 \omega_2 A_1 A_2^2 = 0. \tag{7.40a}$$

$$\alpha_2 A_2 + \beta A_1^2 + G_2 A_2^2 + c_2 \omega^2 A_2^3 + d_2 \omega^2 A_1^2 A_2 = 0 \tag{7.40b}$$

The last equation gives

$$A_1^2 = \frac{-\alpha_2 A_2 - G_2 A_2^2 - c_2 \omega^2 A_2^3}{\beta + d_2 \omega^2 A_2} \tag{7.41}$$

Equations (7.40a) and (7.41) then yield

$$y^6 + e_5 y^5 + e_4 y^4 + e_3 y^3 + e_2 y^2 + e_1 y + e_0 = 0 \tag{7.42}$$

where $y = A_2$ and e_i are functions of the different parameters in Eqs. (7.38), given by the following expressions :

$$e_0 = \delta_0^2, \quad e_1 = 2\delta_0\delta_1 + \alpha_2\beta G_1^2$$

$$e_2 = \delta_1^2 + 2\delta_0\delta_2 + \ + G_1^2(\beta G_2 + \alpha_2 d_2 \omega^2)$$

$$e_3 = 2\delta_0\delta_3 + 2\delta_1\delta_2 + G_1^2(c_2\beta\omega^2 + d_2G_2\omega^2)$$

$$e_4 = \delta_2^2 + 2\delta_1\delta_3 + \ + G_1^2(c_2d_2\omega^4)$$

$$e_5 = 2\delta_2\delta_3, \ \ e_6 = \delta_3^2$$

where

$$\delta_0 = \alpha_1\beta$$

$$\delta_1 = \alpha_1 d_2\omega^2 - \beta^2 - c_1\alpha_2\omega^2$$

$$\delta_2 = -\beta d_2\omega^2 - c_1G_2\omega^2 + \beta d_1\omega^2$$

$$\delta_3 = (d_1d_2 - c_1c_2)\omega^4$$

The different limit cycles are found by solving Eq. (7.42). The acceptable solutions are the real roots of (7.42) which give a positive value to the right-hand side of Eq. (7.41).

The stability of a given solution (A_{10},A_{20}) is handled by linearizing the system (7.38) near this solution and by calculating the eigenvalues of the obtained linear system, as we have done before in Chapter 6, Section 6.3, for two and three oscillators.

7.6. Comparison with some experimental results

In order to show that the above theory can indeed predict triggering, Equations (7.38) are first applied to the series MSA-19 to 26 of the experiments reported in reference 7 on triggering phenomenon in subscale solid propellant motors, shown on Figure 7.7a. In these experiments, a smokeless cylindrical solid propellant rocket motor was pulsed into instability and both the threshold value and the final amplitude were recorded. No solid particles were present in the flow; thus the coefficients G_1 and G_2 may represent only velocity coupling.

Figure 7.7b shows the numerical integration of Eqs. (7.38) for a particular set of experiments in reference 7. It is clearly seen from this figure that triggering can indeed be predicted. A stable non-trivial limit cycle is reached for the pressure oscillations in a linearly stable (α_1 and α_2 are negative) system. The values of the parameters shown on Figure 7.7a are chosen such that the limit cycle amplitude is close to the experimental one. G_1 is taken to be positive (driving term) and G_2 to be negative (damping term). It is worth noticing here that the value 2.10^{-4}s of the time-lag used in the comparison lies well in the range of values of time-lag reported in reference 12. For comparison, the value of the time-lag given by expression (7.36) from the (A,B) model, where the values of A and B are respectively 11.5 and 0.86 (given in reference 7), is approximately 7.10^{-5}s. This is in the same range as 2.10^{-4}s. The values -1.0 and -50.0 for α_1 and α_2 lie in the practical range of linear decay rates. No physical explanation has been found for the coefficients G_1 and G_2 apart from the association with velocity coupling.

It is essential to notice that Eq. (7.42) has in general six roots. Consequently, we have, in general, six different limit cycles. From the numerical solution of (7.42) for the set of values shown on Figure 7.7a, we get four different limit cycles, two roots being complex quantities. However, we see from Figure

7.7 b that for quite different initial disturbances, 0.07 and 0.13, the wave ultimately reaches the *same* limit cycle. This suggests that a stable non-trivial limit cycle may be unique.

The parametric study of thec triggering phenomenon is carried out by varying the values of the parameters α_1, α_2, τ, G_1, and G_2. Over one thousand sets of values for these parameters are taken. For each set the roots of Eq. (7.42) are calculated using a numerical routine. The stability is then examined by linearizing Eqs. (7.38) near the limit cycle. It is found that triggering is very sensitive to the decay rate α_1 of the first mode. The lower is the value $|\alpha_1|$, the higher is the limit cycle amplitude. If both G_1 and G_2 vanish, then the triggering phenomenon disappears. Also from the parametric study, we have found that always the stable limit cycle is unique. This is found for a wide range of the parameters. For a given set of parameters, many limit cycles can exist but at most one is stable.

Figure 7.7c shows the triggering threshold. When the initial pulse amplitude is below a certain value the wave decays. The low value of 0.004 represents the initial rate of change of the pressure and not the pulse amplitude. The amplitude of the pulse is deduced from the geometry, the location of the pulser, and the duration of the pulse. For practical pulsers, this rate corresponds, as it is the case in this application, to approximately 8% of the mean pressure.

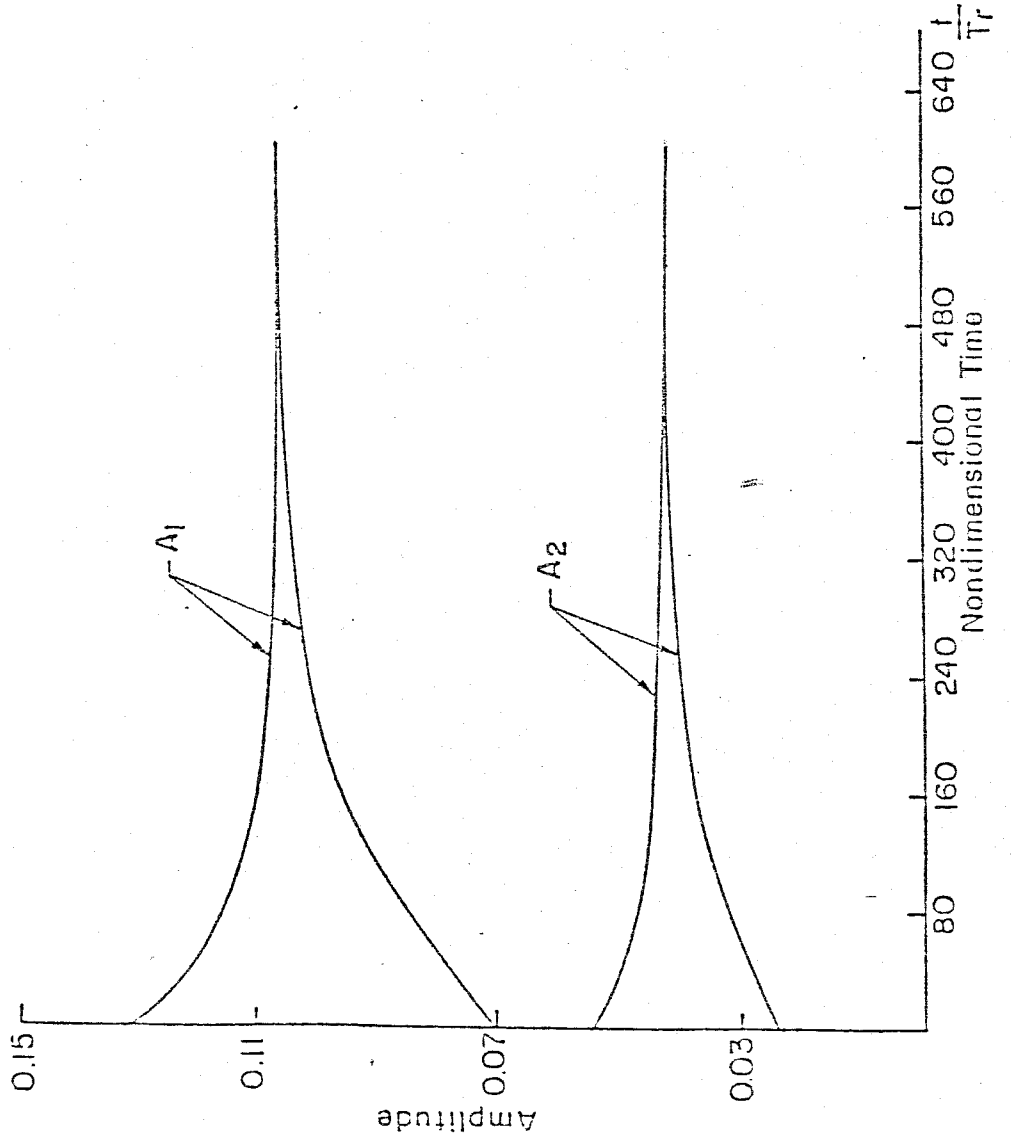

Figure 7.7b. Existence of a non-trivial stable limit cycle.

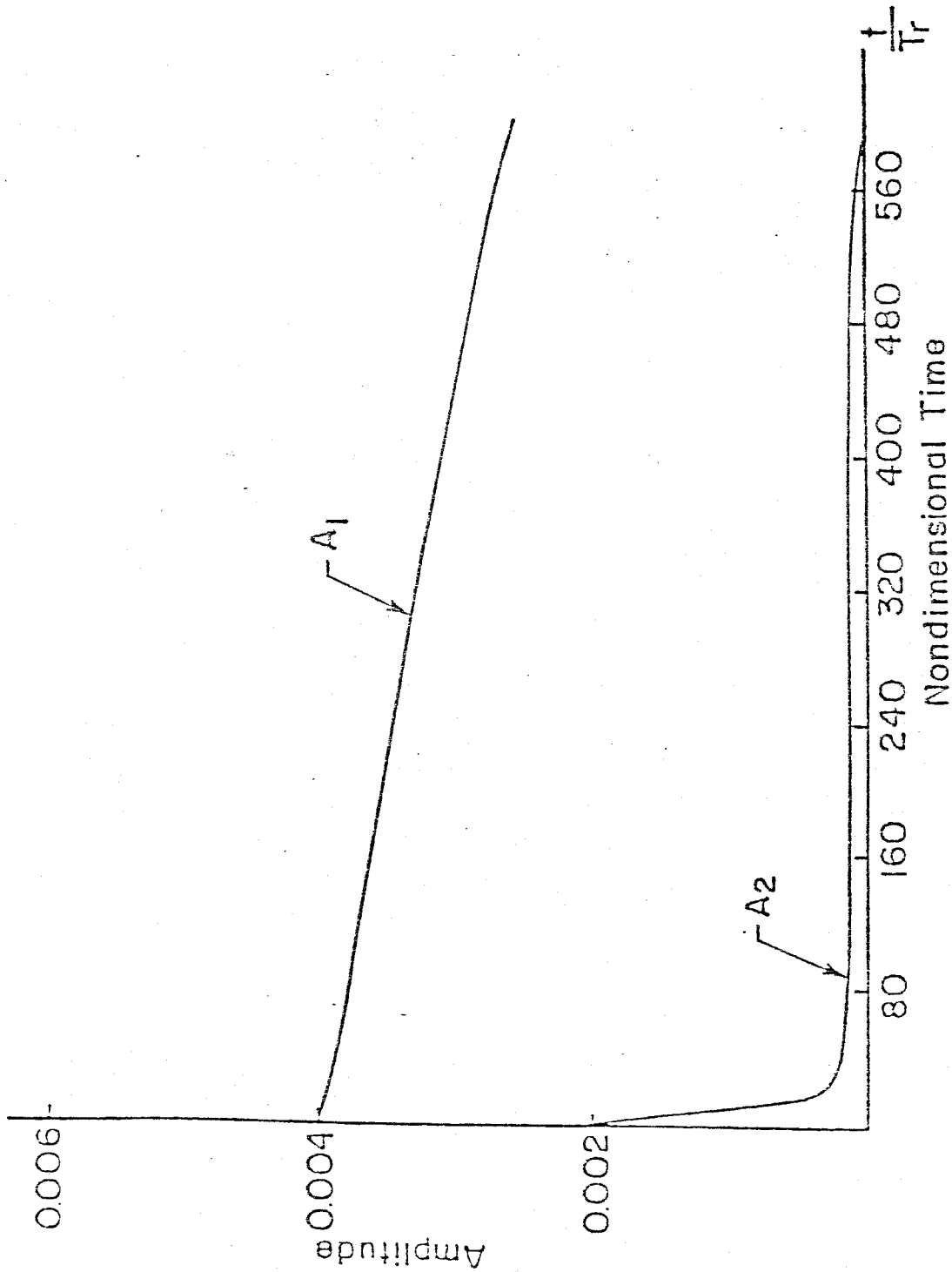

Figure 7.7c Threshold of triggering.

Table 7.1. Comparison between Our Analysis and Experimental Results of Ref. 7

	Analysis	Experiment Ref. 7	Error%
Limiting Amplitude	0.106	0.122	14%
Pulse Amplitude (psi)	86.8	108.	19.6%

Table 7.1 shows a comparison between the theoretical and the experimental results. The theory seems to predict well both the limit cycle amplitude and triggering threshold. of velocity coupling if we include the nonlinear particle losses.

7.7. Comparison with some numerical solutions

In reference 2, a numerical integration of the conservation equations in a one-dimensional solid propellant rocket is reported. In that work, the combustion model used did not include velocity coupling. However, particle attenuation was accounted for. The point here is not to apply exactly our analysis to the particular problem treated in 2 but rather to show that our model can predict triggering in the absence of velocity coupling if we include the nonlinear particle losses.

Equations (7.38) are applied to the case of the cylindrical rocket shown in Figure 7.8. In this case, both G_1 and G_2 are negative. They correspond, as we have seen in (7.39), to nonlinear particle losses, with $G_2 = 8G_1$.

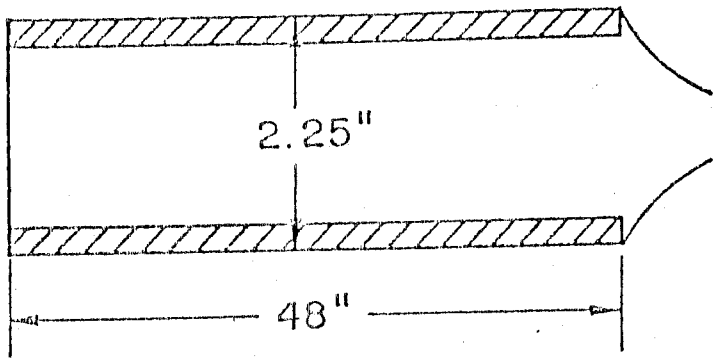

$r_o = a\left(\frac{P}{P_o}\right)^n$ $\quad n = 0.5, a = 0.01\ m s^{-1}$ $\quad \tau = 2.10^{-4} s$

$P_o = 1500\ psi$ $\quad \gamma = 1.23$ $\quad \alpha_1 = -1.0\ s^{-1}$

$T_o = 3000°\ k$ $\quad K = 2.7.10^{-7} m^2 s^{-1}$ $\quad \alpha_2 = -50.0\ s^{-1}$

$N = 400\ Hz$ $\quad \rho_s = 1.7.10^3\ Kg\ m^{-3}$ $\quad G_1 = -250\ s^{-1}$

$T_r = \frac{1}{N}$ $\quad \omega = 2\pi N$ $\quad G_2 = -2000\ s^{-1}$

Figure 7.8 The numerical example used in reference 7.2.

In Figure 7.9, it is clearly seen that triggering can indeed be predicted without the inclusion of velocity coupling. A stable limit cycle, as before, is unique. Figure 7.10 shows the time history for an initial pulse just below the triggering threshold for pressure oscillations. Figure 7.11 shows the sensitivity of triggering to the decay rate α_1 of the first mode. In this figure, all the parameters in Figure 7.8 remain the same except that α_1 has now the value of -3 instead of -1. Even for a very large initial disturbance of 0.25, the wave decays in time. This suggests that triggering may not occur if α_1 is above a certain value. Since α_1 is highly sensitive to the ratio of the cross-section area of the chamber to the propellant area, there may be a limit of this ratio above which no triggering can occur.

7.8. Concluding remarks

In this chapter we presented a general formalism for triggering of pressure oscillations in combustion chambers. A second order model for the nonlinear processes in the chamber may indeed predict triggering if two conditions are met

a) The model incorporates a process representing a coupling of a mode with itself

b) The analysis includes at least two modes.

A third order analysis can predict triggering without a second order self-coupling of the mode with itself. To predict triggering, two conditions must be satisfied

a) There is a third order self-coupling

b) The analysis includes at least two modes.

Both features disagree completely with the classical results of one-degree of freedom analysis. The multi-degree of freedom systems do indeed show some peculiar effects not known for the one-degree of freedom systems.

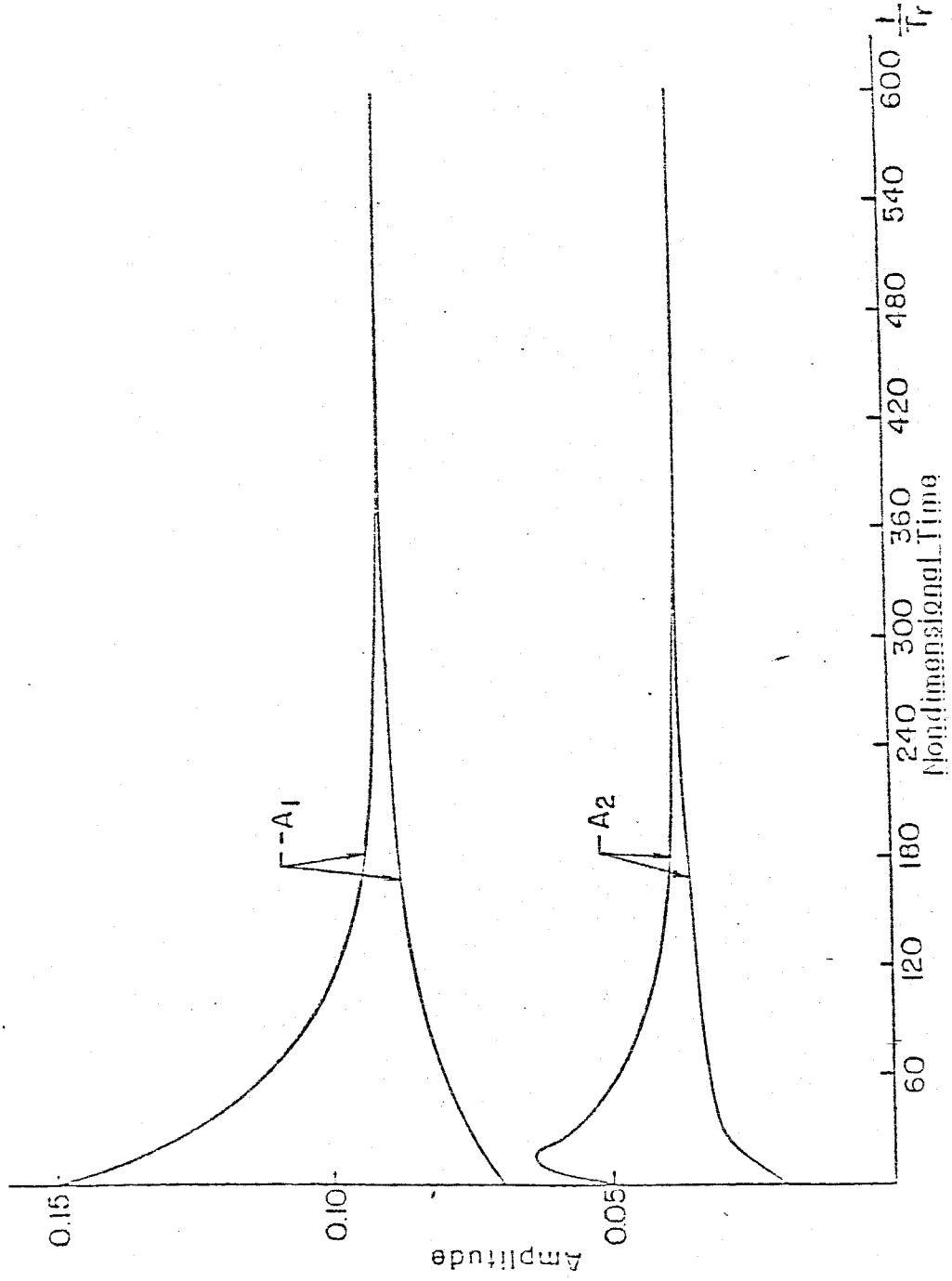

Figure 7.9 Triggering and limit cycle existences.

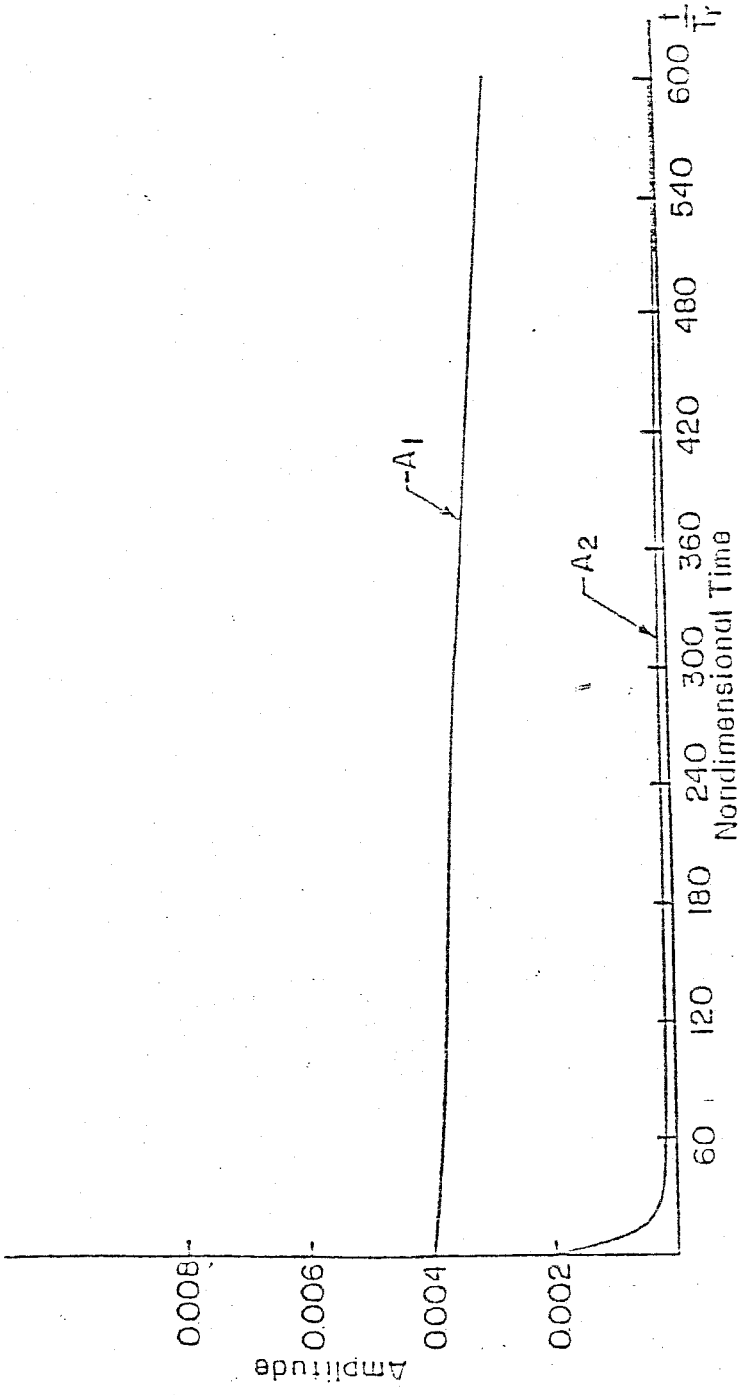

Figure 7.10 Threshold of triggering.

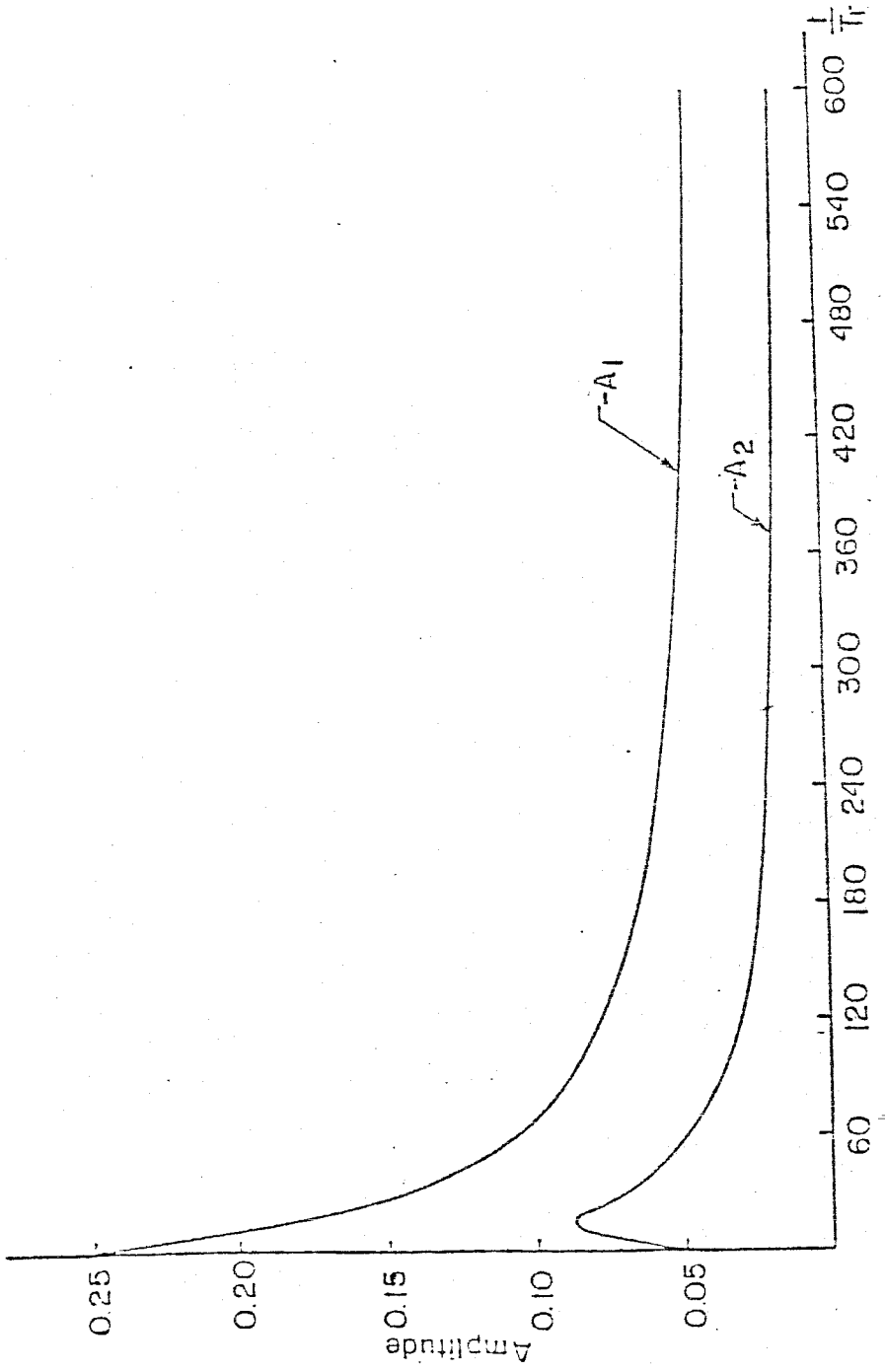

Figure 7.11 Sensitivity of the triggering to the decay rate of the first mode.

Significantly for applications, we identified some global mechanisms involved in triggering. For example, the mechanism producing a term having the form $p'|\frac{\partial p'}{\partial t}|$ in the vicinity of the propellant surface may indeed be a major source for triggering. The same can be said about the mechanism producing a $p'(\frac{\partial p'}{\partial t})^2$ term. On the other hand, a mechanism producing terms proportional to p'^2 is very likely to have no effects on triggering. A mechanism producing $p'\frac{\partial p'}{\partial t}$ probably has very little effect on triggering. These results will help, for example, refine modeling the boundary layer near the surface of the propellant to identify new mechanisms responsible for triggering. This approach should be investigated. If these mechanisms can be associated with some physical phenomena, then the results will largely enhance our physical understanding of the triggering phenomenon.

We have also proposed a practical formulation for prediction of triggering in combustion chambers. The analysis was based on a nonlinear model of the combustion response to pressure oscillations. The effects of the energy exchange among modes, velocity coupling, pressure coupling, and nonlinear particle attenuation were shown in detail. The model was applied to the particular case of solid propellant rocket motors. Good prediction of experimental results and good agreement with numerical solutions were achieved.

We have shown also that it is of fundamental importance to include the " out-of-phase " components for an accurate stability analysis. In fact, the major weakness of the analysis presented in this chapter is the omission of the " out-of-phase " components. The inclusion of these components should yield unambiguous results for the occurence of triggering. This will be the subject of future work.

Appendix 7A

EQUATIONS FOR THE LIMIT CYCLES

In this appendix, we will show in detail how to get Eqs. (7.38) for the limit cycles, following model (7.32) for the combustion response. We start with the formulation of the transient burning rate of solid propellant

$$r(t) = r_0(t-\tau)\left(1 + \frac{\psi\,\kappa}{r_0^3(t-\tau)}\frac{dr_0(t-\tau)}{dt}\right) \tag{A.1}$$

where $r_0 = ap^n$ is the steady state burning rate. With dimensionless variables, a simplified set of conservation equations in a rocket motor is

$$\frac{\partial p}{\partial t} + \gamma\, p\nabla .u + u.\nabla\, p = T\dot{m} \tag{A.2}$$

$$\rho\left(\frac{\partial u}{\partial t} + u\,.\nabla\, u\right) + \frac{\nabla\, p}{\gamma} = -\,u\dot{m} \tag{A.3}$$

$$T\, p^{-\frac{\gamma-1}{\gamma}} = 1 \tag{A.4}$$

where $\dot{m}$ is the mass burning rate, $\dot{m} = \rho_s\, r$ with ρ_s the propellant density, T is the temperature, and u is the velocity. Notice that equation (A.4) does not include the entropy change due to mass injection. The inclusion of the entropy change in the energy equation (A.4) will change the right-hand side of (A.2) from $T\dot{m}$ to $\dot{m}$. For a real evolution we have $T\, p^{-\frac{n_p-1}{n_p}} = 1$, where n_p is the polytropic

exponent $1 < n_p < \gamma$. For practical problems $\gamma = 1.2$, therefore replacing n_p by γ is believed not to be a serious error. The assumption of an isentropic evolution of the flow will facilitate the expansion.

In the expansion of the pressure, temperature, and velocity in the normal modes of the chamber and the use of Green's theorem (see Chapter 4, Section 4.6), the right-hand side of (A.2) will enter as $\frac{\partial}{\partial t}(T \dot{m})$ and the right-hand side of (A.3) will enter as $\frac{\partial}{\partial x}(- u \dot{m})$.

First, we will deal with the unsteady term $\frac{\psi \kappa}{r_0^2(t-\tau)} \frac{dr_0(t-\tau)}{dt}$. Write

$$\frac{\partial}{\partial t}(T \dot{m}) = \frac{\partial}{\partial t}[T\rho_s r_0(t-\tau)(1 + \frac{\psi \kappa}{r_0^3(t-\tau)} \frac{dr_0(t-\tau)}{dt})] \qquad (A.5)$$

$$\frac{\partial}{\partial x}(- u \dot{m}) = \frac{\partial}{\partial x}[- u\rho_s r_0(t-\tau)(1 + \frac{\psi \kappa}{r_0^3(t-\tau)} \frac{dr_0(t-\tau)}{dt})] \qquad (A.6)$$

expand the pressure, temperature, and velocity,

$$T = \bar{T} + T', \quad p = \bar{p} + p', \quad u = \bar{u} + u'$$

where $\bar{T}$, $\bar{p}$, $\bar{u}$ correspond to the steady state conditions

Expansion of the unsteady term $\frac{\psi \kappa}{r_0^2(t-\tau)} \frac{dr_0(t-\tau)}{dt}$ in the pressure amplitude, with $r_0 = ap^n$, shows easily that the coefficient of $p'(\frac{\partial p'}{\partial t})^2$ is always proportional to τ. This means that the coefficient h_2 in Eq. (7.31) is proportional to τ. This remark is used at the end of Section 7.5.

We now write the unsteady pressure and velocity expansions[6] in two modes only :

$$p' = \eta_1(t)\cos\omega x + \eta_2(t)\cos 2\omega x$$

$$u' = -\frac{\dot{\eta}_1(t)}{\gamma\omega}\sin\omega x - \frac{\dot{\eta}_2(t)}{2\gamma\omega}\sin 2\omega x\,,$$

We now apply Green's theorem to Eqs. (A.2) and (A.3), as we have done in the analysis leading to Eqs. (7.22) and (7.23) in Section 7.4, to obtain two equations for two nonlinear oscillators, one oscillator for each mode. The details of the resuits at this step are very lengthy. Only the final results, following application of the method of time-averaging will be shown in detail. To this system of equations for nonlinear oscillators we apply the method of time-averaging after expanding η_1 and η_2 as follows

$$\eta_1 = A_1(t)\sin\omega t, \quad \eta_2 = A_2(t)\sin 2\omega t$$

This leads to the following system of nonlinear ordinary differential equations

$$\frac{dA_1}{dt} = \alpha_1 A_1 - \beta A_1 A_2 + c_1\omega^2 A_1^3 + d_1\omega^2 A_1 A_2^2 \qquad (A.7)$$

$$\frac{dA_2}{dt} = \alpha_2 A_2 + \beta A_1^2 + c_2\omega^2 A_2^3 + d_2\omega^2 A_1^2 A_2 \qquad (A.8)$$

where

$$c_1 = [V_1 + W_1],\ c_2 = [V_2 + W_2]$$

with

$$V_1 = -\frac{\omega^2}{32\gamma}\tau(n+1).8[\frac{1}{4}\xi - \frac{1}{16kL}\sin(4k\xi)]$$

$$W_1 = \frac{3}{64}\{\tau(\frac{\gamma-1}{\gamma}(n+1) - (n+1)(n+2))$$

$$-3\tau(\frac{1}{\gamma}\frac{\gamma-1}{\gamma^2} - \frac{(n+1)(n+2)}{2} + \frac{\gamma-1}{\gamma}(n+1))\}$$

$$\cdot\frac{8}{3}[\frac{3}{4}\xi + \frac{1}{2kL}\sin(2k\xi) + \frac{1}{12kL}\sin(4k\xi)]$$

$$V_2 = -\frac{\omega^2}{8\gamma}\tau(n+1).8[\frac{1}{4}\xi - \frac{1}{32kL}\sin(8k\xi)]$$

$$W_2 = \frac{3}{16}\{\tau(\frac{\gamma-1}{\gamma}(n+1) - (n+1)(n+2))$$

$$-2\tau(\frac{1}{\gamma}\frac{\gamma-1}{\gamma^2} - \frac{(n+1)(n+2)}{2} + \frac{\gamma-1}{\gamma}(n+1))\}$$

$$\cdot\frac{8}{3}[\frac{3}{4}\xi + \frac{1}{4kL}\sin(4k\xi) + \frac{1}{32kL}\sin(8k\xi)]$$

On the other hand d_1 and d_2 are given by

$$d_1 = \frac{1}{4}\{\tau(\frac{\gamma-1}{\gamma}(n+1) - (n+1)(n+2))$$

$$- \frac{9}{2}\tau(\frac{1}{\gamma}\frac{\gamma-1}{\gamma^2} - \frac{(n+1)(n+2)}{2} + \frac{\gamma-1}{\gamma}(n+1)\}$$

$$.4[\frac{1}{2}\xi + \frac{3}{8kL}\sin(2k\xi) + \frac{1}{8kL}\sin(4k\xi) + \frac{1}{24kL}\sin(6k\xi)]$$

$$d_2 = \frac{1}{16}\{\tau(\frac{\gamma-1}{\gamma}(n+1) - (n+1)(n+2))$$

$$- 9\tau(\frac{1}{\gamma}\frac{\gamma-1}{\gamma^2} - \frac{(n+1)(n+2)}{2} + \frac{\gamma-1}{\gamma}(n+1)\}$$

$$.4[\frac{1}{2}\xi + \frac{3}{8kL}\sin(2k\xi) + \frac{1}{8kL}\sin(4k\xi) + \frac{1}{24kL}\sin(6k\xi)]$$

where ξ is the length of the propellant. For the case presented on Figure 7.7a we have

$$c_1 = 0.0306708\psi\tau,\ c_2 = -0.1004227\psi\tau,\ d_1 = 0.8049125\psi\tau,\ d_2 = 0.605345\psi\tau$$

Since ψ and τ are positive, c_1 is positive and condition (7.11) in Chapter 7 cannot be satisfied for one mode. The treatment of two modes is therefore necessary.

Remark: The expansion of the steady state term $r_0(t-\tau)$ should, in general, be taken into account. However, for practical values of the burning rate exponent n, the heat ratio γ, and heat diffisuvity κ, it can be shown that this

contribution is negligible compared to the contribution of the unsteady term.

REFERENCES 7

1. Powell, E. A. " Application of the Galerkin Method in the Solution of Combustion-Instability Problems," Ph. D. Thesis, Goeogia Inst. of Tech., Sept. 1970.

2. Kooker, D. E. and Zinn, B. T. " Triggering Axial Instabilities in Solid Rockets: Numerical Predictions," *AIAA* paper 73-1298.

3. Powell, E. A.; Padmanabhan, M. S. ; and Zinn, B. T. " Approximate Nonlinear Analysis of Solid Rocket Motors and T-Burners ", AFRPL-TR-77, Vol. 2.

4. Levine, J. N. and Baum, J. D." A numerical Study of Nonlinear Instabilities in Solid Rockets Motors," *AIAA* paper 81-1524, July 1981.

5. Jensen, R. C. and Beckstead, M. W. "Nonlinear Mechanisms of Solid Propellant Instabilities," *AIAA* paper 73-1297, November 1973.

6. Culick, F. E. C. " Nonlinear Behavior of Acoustic Waves in Combustion Chambers," *Acta Astronautica*, Vol. 3 , No. 9, Sept. 1976.

7. Micheli, P. L. et al " Experiments on Subscale Tactical Solid Propellant Rockets," Aerojet Corporation, Sacramento, CA, 1982. (To be published).

8. von Elbe, G. " Solid Propellant Ignition and Response of Combustion to Pressure Transients," *AIAA* paper 66-668.

9. Culick, F. E. C. " A Review of Calculations for the Unsteady Burning of a Solid Propellant," *AIAA* Journal, Vol. 6, pp. 2241, Dec. 1968.

10. Kuo, K. K. and Coates, G. R. "Review of Dynamics Responses of Solid Propellants in Guns and Rocket Propulsion Systems," *Sixteenth Int. Symp. on Combustion*, The Combustion Institute, 1976.

11. Crocco, L. and Cheng, S. I. " High Frequency Combustion Instability in Rockets Motors with Concentrated Combustion," *Journal of The American Rocket Society*, Vol. 23, 1953, pp. 301-303.

12. Cheng, S. I. " High Frequency Combustion Instability in Solid Propellant Rockets," *Journal of The American Rocket Society*, Vol. 24, 1954, pp. 27-32.

13. Sirignano, W.A " Theoretical Study of Nonlinear Combustion Instabilities : Longitudinal Mode," Technical Report No. 677, Department of Aerospace and Mechanical Sciences, Princeton University, March 1964.

14. Mitchell, C. E." Axial Mode Shock Wave Combustion Instability in Liquid Propellant Rocket Engines," Ph. D. Thesis, Princeton University, July 1967.

Chapter 8

THIRD ORDER ACOUSTICS

Third order acoustics has long been the object of investigation. For application to liquid propellant rocket motors, Zinn[1] predicted triggering *qualitatively* by extending the expansion of the conservation equations to third order in the amplitude. Using an expansion in the normal modes of the acoustic field, Powell[2] treated the problem of third order acoustics for the case of radial and tangential acoustic modes in liquid propellant rockets. Culick[3] encountered difficulties when he attempted to extend the perturbation-averaging method to third order.

In this chapter, we deal with only pure longitudinal modes. Our purpose is first, to justify some simplifications taken in the last chapter, mainly the omission of the third order nonlinear gasdynamics; second, to extend the asymptotic-perturbation method presented in chapter 4 to higher orders in the amplitude; and third, to discuss the applicability of the perturbation-averaging and asymptotic-perturbation methods to the problem of triggering.

We compare in this chapter the application of the perturbation-averaging and asymptotic-perturbation methods to the problem of triggering. The expansion of the conservation equations is carried to third order in the amplitude of the wave. We concentrate here mainly on the nonlinearity arising from the gasdynamics within the volume of the chamber.

In Chapter 3, Section 3.3, we compared the two methods in the solution, to third order in the amplitude, of a single nonlinear hyperbolic equation. We found that for that equation it was advantageous to use the asymptotic-

perturbation method. Especially, we pointed out that the influence of the second order d.c. shift on the first and the second mode was difficult to incorporate using the perturbation-averaging technique. A similar situation will be found in this chapter regarding the conservations equations in combustion chambers.

In Chapters 4 to 6, we expanded the conservation equations to second order in the amplitude, using the two methods of expansion. We found that the two methods yielded the same results regarding amplitude and conditions for existence and stability of limit cycles. However, in Chapter 7 we showed that the second order analysis, with nonlinearity arising only from the gasdynamics, was incapable of predicting triggering. We extended the analysis there to third order in the amplitude using the perturbation-averaging method. However, as we pointed out there, we neglected the contribution of third order nonlinear gasdynamics. Only the third order nonlinear boundary conditions were taken into account. In this chapter, Section 8.1, we will treat this contribution and justify the approximation made in Chapter 7, Section 7.3, regarding the omission of the third order acoustics when the "out-of-phase" components are neglected. We will also compare the contributions of the third order acoustics arising respectively from the gasdynamics and the nonlinear boundary conditions.

In Chapters 4 and 5, we applied the asymptotic-perturbation method to the conservation equations for the case of pure longitudinal modes. However, we limited the expansion there to second order in the amplitude. The nonlinearity arose only from the nonlinear gasdynamics. We found from Eq. (4.26) that a non-trivial limit cycle could not exist if the system is linearly stable. Therefore, the triggering phenomenon could not be explained within that analysis. In this chapter, Section 8.2, we extend the formal expansion to any order in the wave amplitude and in the average Mach number of the mean flow. However, we carry out the calculations in detail only for the third order acoustics arising from the

gasdynamics. We will show that this method, unlike the perturbation-averaging method, is capable of incorporating the full contribution of the third order nonlinear gasdynamics. In particular, the effects of the second order d.c. shift on the acoustic modes are taken into account. This is an extension of the conclusion reached in Chapter 3, Section 3.3.

The triggering phenomenon is discussed in Section 8.2.3, using the asymptotic-perturbation method. We will show in that section how to determine the limit cycles and how to study the stability of a given limit cycle.

Finally, a comparison between the perturbation-averaging and asymptotic-perturbation methods regarding the prediction of triggering is carried out in Section 8.3. Some conclusions as to when to use each method are drawn.

8.1. Third order acoustics: Perturbation-averaging technique

In this section, we apply the perturbation-averaging technique to study the third order acoustics. We concentrate on the nonlinearity arising from gasdynamics. We limit the discussion to pure nonlinear acoustics with no mean flow, since our main objective in this section is to determine the influences of the third order acoustics. The conservation equations are

$$\frac{\partial p}{\partial} + \gamma p \nabla \cdot \underline{u} + \underline{u} \cdot \nabla p = 0$$

$$\rho\left(\frac{\partial \underline{u}}{\partial t} + \underline{u} \cdot \nabla \underline{u} \right) + \frac{\nabla p}{\gamma} = 0$$

$$p \rho^{-\gamma} = 1$$

Expand the pressure, velocity, and density as follows

$$p = 1 + \varepsilon p' \, , \, u = \bar{u} + \varepsilon u' \, , \, \rho = 1 + \varepsilon \rho'$$

In the conservation equations, the only obvious third order term is

$$\rho' u' . \nabla u' \tag{8.1}$$

All the other terms are of second order or less. However, there are other third order terms. In fact, the expansion of the isentropic relation $\frac{p}{\rho^\gamma} = 1$ in the pressure amplitude yields

$$\rho' = \frac{p'}{\gamma} + \frac{1}{\gamma}\left(\frac{1}{\gamma} - 1\right)p'^2 + \text{etc.}$$

Therefore, second order terms like $\rho' \frac{\partial u'}{\partial t}$ include third order terms which should be included in the analysis. However, the contribution of $\frac{1}{\gamma}\left(\frac{1}{\gamma} - 1\right)p'^2$ is shown[4] to be very small compared to $\rho' u' . \nabla u'$ for $\gamma < 1.2$, and that the smaller γ is, the smaller the contribution is. The exact relationship between p and ρ is generally of the form

$$\frac{p}{\rho^n} = 1$$

where $1 < n < \gamma$, n being the polytropic exponent. Consequently, the actual correction is even smaller than expected. Therefore, the third order contribution from $\rho' \frac{\partial u'}{\partial t}$ will not be included in the analysis in this section.

Moreover, a full treatment of the third order nonlinear gasdynamics should include the effects of the steady state shift (d.c shift). In fact, a coupling between the first order terms and the second order steady state shift terms produces third order terms. However, it is very difficult to include such effects using the expansion in the normal modes. This is the main reason why it is more accurate to use the asymptotic-perturbation technique when the order of perturbation exceeds 2. This is the subject of the next section.

8.1.1. *Expansion of the third order acoustics* . In this section, only the term (8.1) will be considered. By applying Green's theorem (Chapter 4, Section 4.6) to the conservation equations, the term (8.1) is represented by a term of the form

$$\gamma \int \nabla \psi_n \, (\rho' u' . \nabla u') dv \tag{8.2}$$

where ψ_n is a normal mode of the chamber. We limit the expansion in the normal modes of the chamber to three,

$$p' = \eta_1(t)\cos\omega x + \eta_2(t)\cos 2\omega x + \eta_3(t)\cos 3\omega x$$

$$u' = -\frac{\dot{\eta}_1(t)}{\gamma\omega}\sin\omega x - \frac{\dot{\eta}_2(t)}{2\gamma\omega}\sin 2\omega x - \frac{\dot{\eta}_3(t)}{3\gamma\omega}\sin 3\omega x$$

$$\rho' = \frac{1}{\gamma}p' \tag{8.3}$$

Now the application of Green's theorem yields the following contribution of the term (8.1) to the system of nonlinear oscillators for the $\eta_i(t)$, i = 1,2,3. For

the first oscillator, we have

$$\ddot{\eta}_1 + \omega^2\eta_1 = \text{First and Second order terms} + F_1^{(3)} \tag{8.4}$$

where

$$F_1^{(3)} = -\frac{1}{8\gamma^2}\eta_1\dot{\eta}_1\dot{\eta}_1 + \frac{1}{8\gamma^2}\eta_1\dot{\eta}_1\dot{\eta}_3 - \frac{1}{24\gamma^2}\eta_1\dot{\eta}_3\dot{\eta}_1 - \frac{1}{4\gamma^2}\eta_2\dot{\eta}_1\dot{\eta}_2 - \frac{1}{16\gamma^2}\eta_2\dot{\eta}_2\dot{\eta}_3$$

$$+ \frac{1}{24\gamma^2}\eta_2\dot{\eta}_3\dot{\eta}_2 + \frac{1}{8\gamma^2}\eta_3\dot{\eta}_1\dot{\eta}_1 - \frac{1}{8\gamma^2}\eta_3\dot{\eta}_1\dot{\eta}_3 - \frac{1}{16\gamma^2}\eta_3\dot{\eta}_2\dot{\eta}_2$$

For the second oscillator, we get

$$\ddot{\eta}_2 + \omega_2^2\eta_2 = \text{First and Second order terms} + F_2^{(3)} \tag{8.5}$$

where

$$F_2^{(3)} = -\frac{1}{4\gamma^2}\eta_1\dot{\eta}_2\dot{\eta}_1 + \frac{1}{8\gamma^2}\eta_1\dot{\eta}_2\dot{\eta}_3 - \frac{1}{12\gamma^2}\eta_1\dot{\eta}_3\dot{\eta}_2 - \frac{1}{4\gamma^2}\eta_2\dot{\eta}_1\dot{\eta}_3$$

$$- \frac{1}{8\gamma^2}\eta_2\dot{\eta}_2\dot{\eta}_2 - \frac{1}{12\gamma^2}\eta_2\dot{\eta}_3\dot{\eta}_1 - \frac{1}{4\gamma^2}\eta_3\dot{\eta}_1\dot{\eta}_2 + \frac{1}{8\gamma^2}\eta_3\dot{\eta}_2\dot{\eta}_1 - \frac{1}{4\gamma^2}\eta_3\dot{\eta}_2\dot{\eta}_3$$

and finally, for the third oscillator, we obtain

$$\ddot{\eta}_3 + \omega_3^2\eta_3 = \text{First and Second order terms} + F_3^{(3)} \tag{8.6}$$

where

$$\frac{F_3^{(3)}}{3\gamma} = -\frac{1}{8\gamma^2}\eta_1\dot{\eta}_1\dot{\eta}_1 - \frac{1}{16\gamma^2}\eta_1\dot{\eta}_2\dot{\eta}_2$$

$$-\frac{1}{12\gamma^2}\eta_1\dot{\eta}_3\dot{\eta}_1 + \frac{1}{8\gamma^2}\eta_2\dot{\eta}_1\dot{\eta}_2$$

$$-\frac{1}{16\gamma^2}\eta_2\dot{\eta}_2\dot{\eta}_1 - \frac{1}{12\gamma^2}\eta_2\dot{\eta}_3\dot{\eta}_2 - \frac{1}{24\gamma^2}\eta_3\dot{\eta}_3\dot{\eta}_3$$

We will now apply the Method of Averaging (see Chapter 4, Section 4.6 for details) to equations (8.4)-(8.6). Expand $\eta_i(t)$ in the usual form

$$\eta_i(t) = A_i(t)\sin\omega_i(t) + B_i(t)\cos\omega_i(t)$$

After lengthy calculations, with the use of the method of averaging described in Section 4.6, the following system of ordinary differential equations is obtained :

$$\frac{dA_1}{dt} = \text{First and Second order terms} \qquad (8.7)$$

$$+\delta[-B_1(A_1^2 + B_1^2) - B_3(A_1^2 - B_1^2) - B_3(A_2^2 - B_1^2) + 2A_1B_1A_3 + 2A_2B_2A_3]$$

$$\frac{dB_1}{dt} = \text{First and Second order terms} \qquad (8.8)$$

$$+\delta[+A_1(A_1^2 + B_1^2) + A_3(A_1^2 - B_1^2) - B_3(A_2^2 - B_1^2) + 2A_1B_1B_3 - 2A_2B_2B_3]$$

$$\frac{dA_2}{dt} = \text{First and Second order terms} \tag{8.9}$$

$$+ \delta[\, 4\, B_3(A_1A_2 + B_1B_2) + 4\, A_3(A_2B_1 - B_2A_1) - 2\, B_2(A_2^2 + B_1^2)]$$

$$\frac{dB_2}{dt} = \text{First and Second order terms} \tag{8.10}$$

$$+ \delta[\, -4A_3(A_1A_2 + B_1B_2) + 4\, B_3(A_2B_1 - B_2A_1) + 2\, A_2(A_2^2 + B_1^2)]$$

$$\frac{dA_3}{dt} = \text{First and Second order terms} \tag{8.11}$$

$$+ \delta[\, B_1(\, -3\, A_1^2 + B_1^2) - 3\, B_1(A_2^2 - B_2^2) + 6\, A_1A_2B_2 - 3\, B_3(A_3^2 + B_3^2)]$$

$$\frac{dB_3}{dt} = \text{First and Second order terms} \tag{8.12}$$

$$+ \delta[\, A_1(\, -3\, B_1^2 + A_1^2) + 3\, A_1(A_2^2 - B_2^2) + 6\, B_1A_2B_2 - 3\, A_3(A_3^2 + B_3^2)].$$

The new parameter arising with the third order term is $\delta = \frac{\omega}{32\gamma^2}$. The first and second order terms are the same as those given by Eqs. (6.2) and (6.3) in Chapter 6.

8.1.2. *Application to triggering* . It is clearly seen from this system that the third order nonlinearity presented here consists in coupling among the A_i

and the B_i. Neglecting the phases, i.e. neglecting the B_i, implies neglecting the third order nonlinear gasdynamics term $\rho' u' \cdot \nabla u'$. This is the reason why we did not include the contribution of the third order acoustics arising from the gasdynamics in the analysis presented in Chapter 7.

It is interesting to notice, from Eqs. (8.7)-(8.12), that there are no self-coupling terms, either to second order or to third order, due to the nonlinear gasdynamics. However, from the discussion following Eqs. (7.14)-(7.15) and (7.29)-(7.30), we found that such features were very likely to be essential in causing triggering. Consequently, the third order acoustics arising from the gasdynamics may not produce triggering. We found from Section 7.3 that the nonlinear boundary conditions might yield self-coupling terms, and, therefore, may cause triggering. For a volumetric process to cause triggering, the only requirement seems to be that the structure of the process possess some terms similar to those given by expressions (7.24) and (7.28). The nonlinear gasdynamics does not satisfy these requirements and, therefore, may not contribute, by itself, to triggering.

However, as we mentioned in Chapter 7, Section 7.3, the "out-of-phase" components may influence the stability of the limit cycle. The third order contribution of the gasdynamics may influence the stability of the limit cycle by changing the phase relationships among modes. This will be the subject of future work.

In the following calculations, we will establish how the energy of the wave may change due to the influence of the gasdynamics. Multiply $\frac{dA_i}{dt}$ by A_i and $\frac{dB_i}{dt}$ by B_i in Eqs. (8.7)-(8.12), and add the results to find

$$\frac{1}{2}\frac{d}{dt}[r_1^2 + r_2^2 + r_3^2] = \alpha_1 r_1^2 + \alpha_2 r_2^2 + \alpha_3 r_3^2 + \delta r_1^3 r_3 \sin(\nu_3 - 3\nu_1) \qquad (8.13)$$

where $A_i = r_i \cos\nu_i$ and $B_i = r_i \sin\nu_i$.

Eq. (8.13) implies that initially the energy of the wave may increase if the right-hand side of (8.13) becomes positive. However, this does not necessarily mean that triggering occurs. To check the possibility of triggering, Eqs. (8.7)-(8.12) have been integrated numerically for over a thousand sets of values of α_1, α_2, α_3, and δ. For a given set, the initial conditions have been varied in such a way that the right-hand side of (8.13) becomes positive. Despite an initial growth, the wave always decays in time to zero. From a physical point of view, this can be interpreted as follows. The nonlinear gasdynamics treated here serves only as a means of transfer of energy among modes. It does not contribute to the growth or decay of the wave. The initial growth of the wave, suggested by Eq. (8.13), may be due to incomplete representation of the third order acoustics arising from the nonlinear conservation equations, mainly the absence of the effects of second order d.c. shift on the acoustic modes. This is a reason for using the asymptotic-perturbation method in the next section.

8.2. Third order acoustics: Asymptotic-perturbation technique

In this section, we extend the analysis presented in Chapter 5, Section 5.3, to higher order in the wave amplitude and to any number of modes. To show the generality of the approach, we include the effects of the average Mach number of the mean flow. The direct application is the determination of the third order acoustics arising from the gasdynamics.

8.2.1. *General formulation of the expansion* .

In this section we extend the expansion presented in Section 5.3 to higher order in the pressure amplitude using the asymptotic-perturbation technique. To save

space, we show in detail the expansion of the pressure alone

$$p = 1 + \mu^2 p_{02} + \cdots + \varepsilon (p_{10,1} + \mu p_{11,1} + ...) e^{iKt}$$

$$+ \varepsilon (\delta_2^{(1)} p_{10,2} e^{2\alpha g_2^{(1)}(\mu) t} + \mu p_{11,2} + \cdots) e^{2iKt}$$

$$+ \varepsilon (\delta_3^{(1)} p_{10,3} e^{2\alpha g_3^{(1)}(\mu) t} + \mu p_{11,3} + ...) e^{3iKt} + \cdots +$$

$$+ \varepsilon^2 (p_{20,0} + \mu p_{21,0} + \cdots)$$

$$+ \varepsilon^2 (p_{20,1} + \mu p_{21,1} + \cdots) e^{iKt}$$

$$+ \varepsilon^2 (\delta_2^{(2)} p_{20,2} e^{2\alpha g_2^{(2)}(\mu) t} + \mu p_{21,2} + \cdots) e^{2iKt}$$

$$+ \varepsilon^2 (\delta_3^{(2)} p_{30,2} e^{3\alpha g_3^{(2)}(\mu) t} + \mu p_{31,2} + \cdots) e^{3iKt} \qquad (8.14)$$

$$+ \varepsilon^3 (p_{30,1} + \mu p_{31,1} + \cdots) e^{iKt}$$

$$+ \varepsilon^3 (\delta_2^{(3)} p_{30,2} e^{2\alpha g_2^{(3)}(\mu) t} + \mu p_{31,2} + \cdots) e^{2iKt}$$

$$+ \varepsilon^3 (\delta_3^{(3)} p_{30,3} e^{3\alpha g_3^{(3)}(\mu) t} + \mu p_{31,3} + \cdots) e^{3iKt} + \cdots + c.c.$$

The coefficients $g_2^{(2)}$, $g_3^{(2)}$, etc., are introduced to resolve the multiple determination of K_{11}, K_{12}, etc., as we have discussed earlier in Chapter 5, Section 5.3. Gathering terms in $\varepsilon^2\mu e^{iKt}$ in the conservation equations and application of Green's theorem, leads to an expression for K_{11}. Another expression is obtained by equating the coefficients of $\varepsilon^2\mu e^{2iKt}$. In the absence of $g_2^{(2)}$, we are faced with generally two different values for the same coefficient, and the expansion breaks down. A similar situation exists for K_{12}. In general, the introduction of $g_j^{(n)}(\mu)$ allows the single determination of $K_{n-1,m}$, j = 2,3,4 ..., and m, n = 1,2,3,... .

The introduction of $\delta_2^{(2)}$, $\delta_3^{(2)}$, etc., allows unique determination of K_{20}. In fact, collecting terms in $\varepsilon^3\mu^0 e^{iKt}$ yields a relationship betwee K_{20} and $\delta_2^{(2)}$. Another relationship is obtained by equating the terms in $\varepsilon^3\mu^0 e^{2iKt}$. The coefficients K_{20} and $\delta_2^{(2)}$ are therefore uniquely determined. A similar situation exists for $\delta_2^{(3)}$ in the determination of K_{30}. In general, the introduction of $\delta_1^{(n)}$ allows the single determination of K_{n0}.

The effects of the d.c shift terms $p_{20,0}$ and $u_{20,0}$ on the acoustic modes will be included when we deal with the third order acousticas, mainly Eqs. (8.21) and (8.22). Moreover, the effects of the mean flow are easily incorporated to any order.

More concisely, the expansion (8.14) can be written in the following form

$$p = 1 + \sum_{m=1}^{\infty} \mu^{2m} p_{0,2m} + \sum_{l=1}^{\infty}\sum_{n=0}^{\infty} \varepsilon^l \left[\delta_l^{(n)} p_{l0,n} e^{n g_l^{(n)}(\mu) t} + \sum_{m=1}^{\infty} \mu^m p_{lm,n} \right] e^{inKt} + c.c.$$

where $\delta_1^{(n)} = 1$ and $g_1^{(n)} = 0$ for n = 0,1. Similarly, the expansions of the density and velocity are respectively

$$\rho = 1 + \sum_{m=1}^{\infty} \mu^{2m}\rho_{0,2m} + \sum_{l=1}^{\infty}\sum_{n=0}^{\infty} \varepsilon^{l}\left[\delta_l^{(n)}\rho_{l0,n}e^{ng_l^{(n)}(\mu)t} + \sum_{m=1}^{\infty}\mu^{m}\rho_{lm,n}\right] e^{inKt} + c.c.$$

$$u = \mu\bar{u} + \sum_{l=1}^{\infty}\sum_{n=0}^{\infty} \varepsilon^{l}\left[\delta_l^{(n)}u_{l0,n}e^{ng_l^{(n)}(\mu)t} + \sum_{m=1}^{\infty}\mu^{m}u_{lm,n}\right] e^{inKt} + c.c.$$

For $\mu = 0$, this expansion reduces simply to that of the pure acoustics problem with no mean flow.

This expansion will be applied in the next section to the determination of the contribution of the nonlinear gasdynamics. A discussion of the use of the results to examine triggering of pressure oscillations in combustion chambers will follow.

8.2.2. *Determination of the third order acoustics .*

In Chapter 5, Section 5.3, we carried the calculations to second order in the wave amplitude and determined an expression for the coefficient K_{10} in the expansion of the complex frequency K in the asymptotic amplitude. In this section, we will carry the calculations to third order in the wave amplitude and we will show in detail the steps necessary to determine K_{20}. The results will be applied to study triggering of pressure oscillations in combustion chambers.

For simplicity, we limit the expansion (8.14) to two modes only. First, we determine the coefficient $g_{21}^{(1)}$ because it will be needed later in the analysis (Eqs. (8.19)-(8.20)) leading to the determination of K_{20}. To determine $g_{21}^{(1)}$, we equate the coefficients of $\varepsilon\mu e^{2iKt}$ in the conservation equations. By doing so, we get

$$2\,iK_{00}p_{12,2} + \gamma\,\nabla\cdot u_{12,2} = (\,-2(\,iK_{01} + \alpha_{01}^{(1)}g_{20}^{(1)}\,)\,p_{11,2}$$

$$+\,(\,-2(\,iK_{02} + \alpha_{01}^{(1)}g_{21}^{(1)} + \alpha_{02}^{(1)}g_{20}^{(1)})\,p_{10,2}\,\delta_2^{(1)} \qquad (8.15)$$

$$+\,(\,-\gamma\,p_{11,2}\,\nabla\cdot\bar{u} - \bar{u}\cdot\nabla\;p_{10,2}) + (\,-\gamma\,p_{02}\,\nabla\cdot u_{10,2} - u_{10,2}\cdot\nabla\;p_{02})\delta_2^{(1)}$$

$$2\,iK_{00}u_{12,2} + \frac{\nabla\;p_{12,2}}{\gamma} = (\,2(\,-iK_{01} + \;+\alpha_{01}^{(1)}g_{20}^{(1)})p_{11,2}$$

$$+\,2(\,-iK_{02} + \;+\alpha_{01}^{(1)}g_{21}^{(1)} + \alpha_{02}^{(1)}g_{20}^{(1)})p_{10,2}\delta_2^{(1)} \qquad (8.16)$$

$$-\gamma u_{11,2}\cdot\nabla\,\bar{u} - \bar{u}\cdot\nabla\,u_{11,2} - 2iK_{00}\rho_{02}u_{10,2}\delta_2^{(1)}.$$

Following the same technique leading to Eq. (5.11) in Chapter 5, we find a relationship between K_{02} and $g_{21}^{(1)}$, the coefficients $g_{20}^{(1)}$ and $\delta_2^{(1)}$ being already determined in Chapter 4, Section 4.4. However, K_{02} is determined by equating the coefficients of $\varepsilon\mu e^{iKt}$ as we have done in Chapter 4, Section 4.3. Consequently, $g_{21}^{(1)}$ is set uniquely.

Second, we determine $g_{20}^{(2)}$, since it will be needed later in the analysis (Eqs. (8.21)-(8.24)) to calculate K_{20}. The determination of $g_{20}^{(2)}$ is based on the uniqueness of K_{11}. In fact, collecting coefficients proportional to $\varepsilon^2\mu e^{iKt}$ yields

$$iK_{00}p_{21,1} + \gamma\,\nabla\cdot u_{21,1} = -iK_{11}p_{10,1} - iK_{10}p_{11,1} - iK_{01}p_{20,1}$$

$$- \gamma p_{20,1}\nabla .\bar{u} - \bar{u}.\nabla\, p_{20,1} - \gamma\delta_2^{(1)} p_{10,2}\nabla .u_{11,1}^{*}$$

$$- \delta_2^{(1)} u_{11,1}^{*}.\nabla\, p_{10,2} - \gamma\delta_2^{(1)} p_{11,1}^{*}\nabla .u_{10,2} - \delta_2^{(1)} u_{10,2}.\nabla\, p_{11,1}^{*}$$

$$= - iK_{11} p_{10,1} + W_p \qquad (8.17)$$

$$iK_{00} u_{21,1} + \nabla\, \frac{p_{21,1}}{\gamma} = - iK_{11} u_{10,1} - iK_{10} u_{11,1} - iK_{01} u_{20,1}$$

$$- u_{20,1}.\nabla\, \bar{u} - \bar{u}.\nabla\, u_{20,1} - \delta_2^{(1)} u_{10,2}.\nabla\, u_{11,1}^{*}$$

$$- \delta_2^{(1)} u_{11,1}^{*}.\nabla\, u_{10,2} - 2iK_{00}\rho_{10,1}^{*} u_{11,2} - 2iK_{00}\delta_2^{(1)}\rho_{11,1}^{*} u_{10,2}$$

$$- \delta_2^{(1)}\rho_{10,1}^{*} u_{10,2}.\nabla\, \bar{u} - \delta_2^{(1)}\rho_{10,1}^{*}\bar{u}.\nabla\, u_{10,2} - 2iK_{01}\delta_2^{(1)}\rho_{10,1}^{*} u_{10,2}$$

$$+ iK_{00}\rho_{11,2} u_{10,1}^{*} + iK_{01}\delta_2^{(1)}\rho_{10,2} u_{10,1}^{*}$$

$$= -iK_{11} + W_u \qquad (8.18)$$

Following the same analysis leading to Eq. (5.12) in Chapter 5, Eqs. (8.17) and (8.18) produce an expression for K_{11}. However, another expression for K_{11} can be deduced by equating the coefficients of $\varepsilon^2\mu e^{2iKt}$. By doing so, we get the following two equations

$$2\,iK_{00}p_{21,2} + \gamma\,\nabla\,.\,u_{21,2} = -2(\,iK_{11} + \alpha_{01}^{(1)}g_{20}^{(2)} + \alpha_{11}g_{20}^{(1)}\alpha_{10}g_{21}^{(1)})\delta_2^{(1)}p_{10,2}$$

$$-2(\,iK_{01} + \alpha_{01}^{(1)}g_{20}^{(2)})\delta_2^{(2)})p_{20,2} - 2\,(\,iK_{10} + \alpha_{10}g_{20}^{(1)})p_{11,2}$$

$$+ (\,-\gamma\,p_{10,1}^{*}\nabla\,.u_{11,2} - u_{11,2}.\nabla\,p_{10,1}^{*}) + (\,-\gamma\,p_{10,2}\,\nabla\,.u_{11,1}^{*} - u_{11,1}^{*}.\nabla\;\;p_{10,2})\delta_2^{(1)}$$

$$+ (\,-u_{10,2}.\nabla\,p_{11,1}^{*} - \gamma p_{11,1}^{*}\nabla\,.u_{10,2})\delta_2^{(1)} + (\,-\gamma\,p_{11,2}\,\nabla\,.u_{10,1}^{*} - u_{10,1}^{*}.\nabla\;\;p_{11,2})$$

$$+ (\,-\gamma\,p_{11,1}\,\nabla\,.u_{10,1} - u_{10,1}.\nabla\;\;p_{11,1}) + (\,-\gamma\,p_{10,1}\,\nabla\,.u_{11,1} - u_{11,1}.\nabla\;\;p_{10,1})$$

$$+ (\,-\gamma\,p_{20,2}\,\nabla\,.\bar{u} - \bar{u}.\nabla\;\;p_{20,2})\delta_2^{(1)}$$

$$= c_1K_{11} + g_{20}^{(2)}(c_2 + c_3\delta_2^{(2)}) + c_4\delta_2^{(2)} + c_5 \qquad (8.19)$$

$$2\,iK_{00}u_{21,2} + \nabla\;\frac{p_{21,2}}{\gamma} = -2(\,iK_{11} + \alpha_{01}^{(1)}g_{20}^{(2)} + \alpha_{11}g_{20}^{(1)} + \alpha_{10}g_{21}^{(1)})\delta_2^{(1)}u_{10,2}$$

$$-2(\,iK_{01} + \alpha_{01}^{(1)}g_{20}^{(2)})\delta_2^{(2)})u_{20,2} - 2(\,iK_{10} + \alpha_{10}g_{20}^{(1)})u_{11,2}$$

$$+ (\,-u_{10,1}^{*}\nabla\,u_{11,2} - u_{11,2}.\nabla\,u_{10,1}^{*}) + (\,-u_{10,2}\,.\nabla\,u_{11,1}^{*} - u_{11,1}^{*}.\nabla\;\;u_{10,2})\delta_2^{(1)}$$

$$+ (\,-u_{11,2}\,.\nabla\,u_{10,1}^{*} - u_{10,1}^{*}.\nabla\,u_{11,2}) + (\,-u_{10,1}\,.\nabla\,u_{11,1} - u_{11,1}.\nabla\,u_{10,1})$$

$$+ (- u_{20,2} .\nabla \bar{u} - \bar{u}.\nabla \ u_{20,2})\delta_2^{(2)} - \rho_{10,1}u_{10,1}.\nabla \bar{u} - \rho_{10,1}\bar{u}.\nabla \ u_{10,1}$$

$$- \rho_{20,1}u^*_{10,1}.\nabla \bar{u} - \rho_{20,1}\bar{u}.\nabla \ u^*_{10,1} - iK_{00}\rho_{10,1}u_{11,1}$$

$$- iK_{01}\rho_{10,1}u_{10,1} - iK_{00}\rho_{11,1}u_{10,1} - 2iK_{00}\rho^*_{10,1}u_{11,2} - 2iK_{00}\delta_2^{(1)}\rho^*_{11,1}u_{10,2}$$

$$- 2(\ iK_{01} + \alpha_{01}^{(1)}g_{20}^{(1)}) \ \delta_2^{(1)}\rho^*_{10,1}u_{10,2}$$

$$= d_1K_{11} + g_{20}^{(2)}(d_2 + d_3\delta_2^{(2)}) + d_4\delta_2^{(2)} + d_5 \qquad (8.20)$$

where c_i and d_i are here functions of lower order terms. These lower order terms were determined in Chapter 5, Section 5.3; consequently they are known quantities, and hence so are the c_i and d_i. It is worth noticing that the coefficient $g_{21}^{(1)}$ is present on the right-hand sides of (8.19) and (8.20). This is the reason why we first determined $g_{21}^{(1)}$ by Eqs. (8.15) and (8.16). Following the same analysis leading to Eq. (5.13) in Chapter 5, Eqs. (8.19) and (8.20) yield a relationship among K_{11}, $\delta_2^{(2)}$, and $g_{20}^{(2)}$. However, K_{11} is already determined from Eqs. (8.17) and (8.18). Consequently, we are left with a relationship between $\delta_2^{(2)}$ and $g_{20}^{(2)}$. This relationship will be used later in the analysis (Eqs. (8.21)-(8.24)) to determine K_{20}.

We now return to determination of K_{20}. The results elaborated above concerning the expression of $g_{20}^{(2)}$ will be needed in the analysis. There are two ways to determine K_{20}. First, we equate the coefficients of $\varepsilon^3\mu^0e1iKt$ in the conservation equations to get

$$iK_{00}p_{30,1} + \gamma \nabla . u_{30,1} = -iK_{20}\, p_{10,1} - iK_{10}\, p_{20,1}$$

$$+ (-\gamma\, p_{20,2}\nabla .u^{*}_{10,1} - u^{*}_{10,1}.\nabla\, p_{20,2})\delta_2^{(2)} + (-\gamma\, p^{*}_{10,1}\nabla .u_{20,2} - u_{20,2}.\nabla\, p^{*}_{10,1})\delta_2^{(2)}$$

$$+ (-\gamma\, p_{10,2}\nabla .u^{*}_{20,1} - u^{*}_{20,1}.\nabla\, p_{10,2})\delta_2^{(1)} + (-\gamma\, p^{*}_{20,1}\nabla .u_{10,2} - u_{10,2}.\nabla\, p^{*}_{20,1})\delta_2^{(1)}$$

$$+ (-\gamma\, p_{10,1}{}^{*}\nabla .u_{20,0} - u_{20,2}.\nabla\, p_{10,1}) + (-\gamma\, p_{20,0}\nabla .u_{10,1} - u_{10,1}.\nabla\, p_{20,0})$$

$$= e_1 K_{20} + e_2\delta_2^{(2)} + e_3 \qquad (8.21)$$

$$iK_{00}u_{30,1} + \nabla \frac{p_{30,1}}{\gamma} = -iK_{20}\, u_{10,1} - iK_{10}\, u_{20,1}$$

$$+ (-u_{20,2}.\nabla\, u^{*}_{10,1} - u^{*}_{10,1}.\nabla\, u_{20,2})\delta_2^{(2)} + (-u_{10,2}.\nabla\, u^{*}_{20,1} - u^{*}_{20,1}.\nabla\, u_{10,2})\delta_2^{(1)}$$

$$+ (-u_{10,1}.\nabla\, u_{20,0} - u_{20,0}.\nabla\, u_{10,1}) - 2iK_{00}\delta_2^{(2)}\rho^{*}_{10,1}u_{20,2}$$

$$+ iK_{00}\delta_2^{(1)}\rho_{10,2}u^{*}_{20,1} + iK_{00}\delta_2^{(2)}\rho_{20,2}u^{*}_{10,1} - 2iK_{00}\delta_2^{(1)}\rho^{*}_{20,1}u_{10,2}$$

$$-\rho_{10,1}u^{*}_{10,1}.\nabla\, u_{10,1} - \rho_{10,1}u_{10,1}.\nabla\, u^{*}_{10,1} - \rho^{*}_{10,1}u_{10,1}.\nabla\, u_{10,1}$$

$$-\rho_{10,1}u^{*}_{10,2}.\nabla\, u_{10,2}\,|\delta_2^{(1)}|^2 - \rho_{10,1}u_{10,2}.\nabla\, u^{*}_{10,2}\,|\delta_2^{(1)}|^2$$

$$= e_4 K_{20} + e_5 \delta_2^{(2)} + e_6 \tag{8.22}$$

where e_i are here functions of lower order terms. These lower order terms were determined in Chapter 5, Section 5.3; consequently they are known quantities, and hence so are the e_i .

Following the same analysis leading to Eq. (5.13) in Chapter 5, Eqs. (8.21) and (8.22) yield a relationship between K_{20} and $\delta_2^{(2)}$. It is worth noticing here that the d.c shift terms $p_{20,0}$ and $u_{20,0}$ are present in Eqs (8.21) and (8.22), consequently they influence the expression of K_{20}. We found some difficulties in including these effects in Section 8.1, using the perturbation-averaging technique.

A second relationship between K_{20} and $\delta_2^{(2)}$ is obtained by equating the coefficients of $\varepsilon^3\mu^2 e^{2iKt}$. By doing so, we get

$$2iK_{00}p_{30,2} + \gamma \nabla \cdot u_{30,2} = -2(iK_{20} + \alpha_{20}g_{10}^{(2)})\delta_2^{(1)}p_{10,2}$$

$$-2(iK_{10} + \alpha_{10}g_{20}^{(2)})\delta_2^{(2)}p_{20,2} + (-\gamma\, p_{10,1}\nabla \cdot u_{20,1} - u_{20,1}\cdot\nabla\, p_{10,1})$$

$$+ (-\gamma\, p_{20,0}\nabla \cdot u_{10,2} - u_{10,2}\cdot\nabla\, p_{20,0})\delta_2^{(1)} + (-\gamma\, p_{10,2}\nabla \cdot u_{20,0} - u_{20,0}\cdot\nabla\, p_{10,2})\delta_2^{(1)}$$

$$= w_1 K_{20} + w_2 \delta_2^{(2)} + w_3 \tag{8.23}$$

$$2iK_{00}u_{30,2} + \nabla \frac{p_{30,2}}{\gamma} = -2(iK_{20} + \alpha_{20}g_{10}^{(2)})\delta_2^{(1)}u_{10,2}$$

$$- 2(iK_{10} + \alpha_{10}g_{20}^{(2)})\delta_2^{(2)}u_{20,2} + (- u_{10,1}.\nabla\, u_{20,1} - u_{20,1}.\nabla\, u_{10,1})$$

$$+ (- u_{20,0}.\nabla\, u_{10,2} - u_{10,2}.\nabla\, u_{20,0})\delta_2^{(1)} - iK_{00}\rho_{10,1}u_{20,1}$$

$$- iK_{00}\rho_{20,1}u_{10,1} - iK_{10}\rho_{10,1}u_{10,1}$$

$$= w_4K_{20} + w_5\delta_2^{(2)} + w_6 \qquad (8.24)$$

where w_i are functions of lower order terms. These lower order terms were determined in Chapter 5, Section 5.3, consequently they are known quantities, and hence so are the w_i . Following the same analysis leading to Eq. (5.13) in Chapter 5, Eqs. (8.23) and (8.24) yield a second relationship between K_{20} and $\delta_2^{(2)}$. Consequently, K_{20} and $\delta_2^{(2)}$ are uniquely determined.

It is essential to notice that K_{10} and K_{20} are not necessarily unique for a given configuration of the chamber. In fact, the algebraic equations relating $\delta_2^{(2)}$ and K_{20} are in general quadratic because of the nonlinear relationships between $g_{20}^{(2)}$ and $\delta_2^{(2)}$ given by Eqs. (8.19) and (8.20). This means that the coefficient w_5 is in general function of $\delta_2^{(2)}$. Therefore, (8.24) is a nonlinear relationship between K_{20} and $\delta_2^{(2)}$.

It is worth noticing here that $g_{20}^{(2)}$ is present in the relationships between K_{20} and $\delta_2^{(2)}$. This is the reason for determining $g_{20}^{(2)}$ by Eqs. (8.17)-(8.20). Moreover, in the determination of $g_{20}^{(2)}$ by Eqs. (8.19) and (8.20), the coefficient $g_{21}^{(1)}$ is present. This is the reason for determining $g_{21}^{(1)}$ by Eqs. (8.15) and (8.16).

It is evident that the procedure is lengthy, even for only two modes. However, the analysis is straightforward and systematic and, therefore, amenable to

computer progamming. All the nonlinear terms are included. This was difficult to achieve by the use of the perturbation-averaging technique presented in Section 8.1. No formal explicit results, similar to expression (5.16) for K_{10} in Chapter 5, are obtained here for the expression of K_{20}. This will be the subject of future work. The purpose here is mainly to establish that the technique can be extended to higher orders.

8.2.3. *Application to triggering* .

In Chapter 5, Section 5.4, we discussed, using the asymptotic-perturbation method, the existence of limit cycles. In particular, we treated the case when we limit the expansion of the complex frequency K to second order in the amplitude. As we have seen in Chapter 4, Section 4.4, this corresponds to the third order acoustics. In that case, we have from Section 5.4 the following expansion of the growth rate α:

$$\alpha = \alpha_{00} + \mu\alpha_{01}^{(1)} + \varepsilon\,\alpha_{10} + \varepsilon^2\,\alpha_{20}$$

The existence criteria become

1) α_{10} should exist and be non–trivial.

2) α_{20} should exist and be non–trivial.

3) $\alpha_{10}^2 - 4\,(\alpha_{00} + \mu\alpha_{01}^{(1)})\,\alpha_{20} > 0$.

For a given α_{10} and α_{20}, we have in general two different roots, say ε_1 and ε_2. Consequently, there are in general two different limit cycles for given values of α_{10} and α_{20}. For each root, the waveform of the limit cycle is given, as we have

seen in Section 5.5, by

$$\overline{p_1} = \varepsilon p_{10,1} e^{iKt} + \text{c.c.}, \quad \overline{p_2} = \varepsilon \delta_2^{(1)} p_{10,2} e^{iKt} + \text{c.c.}$$

where $\overline{p_1}$ and $\overline{p_2}$ are respectively the first and second Fourier components of the limit cycle. It is essential to notice that α_{10} and α_{20} are not necessarily unique for a given configuration of the chamber, as we have seen at the end of the last section.

The stability of each limit cycle is examined following exactly the same technique presented in Chapter 5. The results of this examination yield some conditions, similar to those found in Section 5.2, on the stability of the limit cycle. If for a linearly stable engine, these conditions are not satisfied, then this limit cycle is unstable and may correspond to a triggering threshold. This is similar to the stability of the equilibrium point A_1 in Figure 7.1 for one-degree of freedom systems.

However, if the stability conditions are satisfied, then the limit cycle corresponds to the asymptotic oscillatory behavior, or triggering limit. This is similar to the stability of the equilibrium point A_2 in Figure 7.2 in the last chapter for one-degree of freedom systems.

It is essential to notice that we are dealing here with many modes. Consequently, both limit cycles may well be unstable or, a priori, stable. However, the later possibility is unlikely to occur, since we have seen in the last chapter, Section 7.7, that a non-trivial stable limit cycle seems to be unique. The point of this remark is to notice that having two different limit cycles does not necessarily mean that one limit cycle is stable while the other one is unstable. This is a clear contradiction to the rule for one-degree of freedom systems where for two adjacent limit cycles one has to be stable while the other is unstable.

8.3. Concluding remarks

Now that we have discussed triggering, using both the perturbation-averaging and the asymptotic-perturbation methods, we compare the two methods regarding the prediction of triggering. Some conclusions as to when to use each method are drawn.

We start with the advantages and disadvantages of the method of perturbation-averaging in describing triggering. We notice first from Eqs. (8.7)-(8.12) that the inclusion of many modes is simple to carry out. This is an advantage in the treatment of steep-fronted waves where many modes should be taken into account. Moreover, as we have seen in Chapter 7, the behavior of the wave in time up to the limit cycle can be described. Therefore, the initial disturbances can easily be incorporated, giving the influence of the initial conditions on triggering. In addition to that, we can determine how fast a triggering limit is reached by examining by examining the behavior of the wave in time. This is important information. For example, in the case of solid propellant rockets, it is very useful to know, from the approximate analysis, that triggering is reached before or after the burnout of the propellant. In the latter case, the analysis should be changed, since after the burnout there is no more combustion in the chamber.

However, as we have seen in Section 8.1, it is very difficult to fully represent the third order nonlinear gasdynamics, mainly the effects of the second order d.c. shift terms on the acoustic modes. Moreover, the extension of the perturbation-averaging method to higher order in the amplitude is not straightforward. This is a disadvantage in the sense that the method may fail to represent some physical phenomena which do not show up to second order in the amplitude. Also, we notice in Section 8.1 that it is not straightforward to include the effects of the average Mach number of the mean flow. This is clearly

a disadvantage in the application of this method to high speed flow engines.

We now discuss the advantages and disadvantages of the asymptotic-perturbation method in predicting triggering. First, we notice from Section 8.2 that we can fully represent the third order nonlinear gasdynamics, especially the effects of the second order d.c shift terms on the acoustic modes. Second, as we have also seen in Section 8.2, the analysis can be extended in a systematic way to any order in the wave amplitude This is a clear advantage, since we can, in general, fully represent any physical phenomenon, no matter what the order at which it occurs. We notice further from Section 8.2, that it is straighforward to include the effects of the average Mach number of the mean flow. This is a clear advantage when we deal with high speed flow engines.

However, it is very cumbersome to include many modes in the application of the asymptotic-perturbation method. Even for two modes, in order to represent the third order acoustics of the nonlinear gasdynamics, the procedure was very lengthy in Section 8.2. This is a clear disadvantage in treating steep-fronted waves where many modes should be present. Moreover, the method is incapable, by construction, of predicting the behavior in time of the wave. Therefore, it is impossible to assess directly the influence of the initial disturbances. However, the stability discussion offers adequate information about the influence of the initial conditions. In fact, an unstable limit cycle may correspond to the threshold amplitude, therefore giving a limit for the values of the initial conditions for which there is no triggering. Another disadvantage is the inability of the method to assess how fast a triggering limit is reached, since the explicit behavior in time is unknown.

In final count, when we are interested mostly in the existence of triggering and when the number of modes is not of crucial importance, i.e. no steep-fronted waves, or the flow speed is high then the asymptotic-perturbation

method has a clear edge over the perturbation-averaging method in the sense that all the phenomena involved can be fully represented. However, when we are interested in steep-fronted waves, i.e. many modes, with low speed flow or when the evolution in time of the wave is of crucial importance, then the perturbation-averaging method offers a simple and efficient, but presently incomplete, technique of treating triggering.

One may even use both techniques conjointly. We may start with the perturbation-averaging method to get some information about the wave behavior in time. The method of asymptotic-perturbation is used afterward to include all the mechanisms in the system.

REFERENCES 6

1. Zinn, B. T. " A Theoritical Study of Nonlinear Combustion Instability in Liquid-Propellant Rocket Engines," *AIAA Journal*, Vol. 6, No. 10, 1966.

2. Powell, E. A. " Application of the Galerkin Method in the Solution of Combustion-Instability Problems," Ph. D. Thesis, Goeogia Inst. of Tech., Sept. 1970.

3. Culick, F. E. C. 'Some Recent Results for Nonlinear Waves Motion in Solid Propellant Rockets," *AIAA* paper 79-1208, 1979.

4. Culick, F. E. C., private communication.

Chapter 9

CONCLUSION

In this report, we have studied the conditions for existence and stability, and amplitudes of limit cycles for pressure oscilations in combustion chambers. The analysis has been based on expansion of the general conservation equations in the pressure amplitude. Two techniques were used. The first is an asymptotic-perturbation in which the asymptotic oscillatory behavior is sought by expanding the asymptotic solution in a measure of the amplitude of the wave, usually the amplitude of the fundamental. The second is a perturbation-averaging technique where an approximate solution is sought by applying a perturbation method followed by an expansion of the solution in the normal modes of the acoustic field in the chamber. It was shown that, to third order in the amplitude of the wave, both techniques yielded the same results for the amplitude and the conditions for existence and stability of the limit cycle. However, while the first technique can be extended to higher orders in the pressure amplitude, the second technique suffers serious difficulties. The advantage of the second technique is in its ability to handle easily a large number of modes.

In the approximation to second order, we found the following results. A stable limit cycle seems to be unique. Under very special conditions, the initial conditions affect the stability of the limit cycle. The imaginary parts of the linear responses of the different processes strongly influence the stability criteria and the amplitude of the limit cycle. They affect the exchange of energy among modes.

We also presented a general formalism for triggering of pressure oscillations in combustion chambers. A second order model for the nonlinear

processes in the chamber can indeed predict triggering if two conditions are met

a) the model incorporates a process representing a coupling of a mode with itself; and

b) the analysis includes at least two modes.

A third order analysis can predict triggering without a second order self-coupling of the mode with itself. To predict triggering, two conditions must be satisfied

a) there is a self-coupling to third order; and

b) the analysis includes at least two modes.

Both features disagree completely with the classical results of one-degree of freedom analysis. The multi-degree of freedom systems do indeed show some peculiar effects not known for the one-degree of freedom systems.

More importantly, we identified some global mechanisms involved in triggering. In the special case of solid propellant rockets, we examined the consequences of special forms of the response of combustion to oscillations. For example, a mechanism producing a $p'\left|\frac{\partial p'}{\partial t}\right|$ term may indeed be a major source for triggering. The same can be said for a mechanism producing a $p'\left(\frac{\partial p'}{\partial t}\right)^2$. On the other hand, a mechanism producing terms proportional to p'^2 is very likely to have no effects on triggering. Likewise, a mechanism producing $p'\frac{\partial p'}{\partial t}$ has, probably, very little effect on triggering. These results will help guide modeling the boundary layer near the surface of a burning solid propellant to identify new mechanisms responsible for triggering. This approach should be investigated. If these mechanisms can be associated with some physical phenomena, then the results will greatly enhance our physical understanding of the

triggering phenomenon.

We also proposed a practical formulation for prediction of triggering in combustion chambers. The analysis was based on a nonlinear model of the combustion response to pressure oscillations. The effects of the energy exchange among modes, velocity coupling, pressure coupling, and nonlinear particle attenuation were shown in detail. The model was applied to the particular case of solid propellant rocket motors. Good prediction of experimental results and good agreement with numerical solutions were achieved.

In the framework of the third order theory, a model of the combustion response including both a pseudo *second* order nonlinear velocity coupling *and* energy exchange among modes predicts triggering. A model including a *third* order nonlinear pressure response *and* energy exchange among modes can predict triggering. A stable limit cycle seems to be unique. The triggering phenomenon in solid propellant rockets seems to be due mainly to three factors : pseudo second order nonlinear velocity coupling , third order nonlinear pressure coupling in the combustion response, and energy exchange among modes. However, in principle, second order nonlinear particle damping may replace the velocity coupling as a factor for triggering. In this work, nonlinear pressure coupling has been related mainly to a time-lag between a pressure fluctuation and the burning rate.

We showed also that it is of fundamental importance to include the " out-of-phase " components for an accurate stability analysis. In fact, the major weakness of the analysis presented in the treatment of triggering in this work is the omission of the " out-of-phase " components. The inclusion of these components should yield unambiguous results as to whether triggering occurs. This will be the subject of future work.

For the prediction of triggering by the perturbation-averaging technique, we notice first that the inclusion of many modes is simple to carry out. This is an advantage in the treatment of steep-fronted waves where many modes should be taken into account. Moreover, the behavior of the wave in time up to the limit cycle can be described. Therefore, the initial disturbances can easily be incorporated, giving the influence of the initial conditions on triggering. In addition to that, we can determine from the behavior in time of the wave, the rate at which the triggering limit is reached.

However, it is very difficult to represent fully the third order nonlinear gasdynamics, mainly the effects of the second order d.c. shift terms on the acoustic modes. Moreover, the extension of the perturbation-averaging method to higher order in the amplitude is not straightforward. This is a disadvantage in the sense that the method may fail to represent some physical phenomena which do not show up to second order in the amplitude. Also, it is not straightforward to include the effects of the average Mach number of the mean flow. This is clearly a disadvantage in the application of this method to engines in which the flow may reach high speed.

By using the asymptotic-perturbation method to predict triggering, we can fully represent the third order nonlinear gasdynamics, especially the effects of the second order d.c shift terms on the acoustic modes. Also, the analysis can be extended in a systematic way to any order in the wave amplitude This is a clear advantage, since we can, in general, fully represent any physical phenomenon, irrespective of the order in the wave amplitude at which it occurs. Moreover, it is straighforward to include the effects of the average Mach number of the mean flow. This is obviously important when we deal with high speed flow engines.

However, it is very cumbersome to include many modes in the application of the asymptotic-perturbation method. Even for two modes, in order to

represent the third order acoustics of the nonlinear gasdynamics, the procedure is very lengthy. This is a disadvantage in treating steep-fronted waves where many modes should be present. Moreover, the method is incapable, by definition, of predicting the behavior in time of the wave. Therefore, it is impossible to assess directly the influence of initial disturbances. However, the stability discussion offers adequate information about the influence of the initial conditions. In fact, an unstable limit cycle may correspond to the threshold amplitude, therefore giving a limit for the values of the initial conditions for which there is no triggering. Another disadvantage is the incapability of the method to assess how fast a triggering limit is reached, since the explicit behavior in time is unknown.

In final count, when we are interested mostly in the existence of triggering and when the number of modes is not of crucial importance, i.e. no steep-fronted waves, or the flow speed is high then the asymptotic-perturbation method has a clear edge over the perturbation-averaging method in the sense that all the phenomena involved can be fully represented. However, when we are interested in steep-fronted waves, i.e. many modes, with low speed flow or when the evolution in time of the wave is of crucial importance, then the perturbation-averaging method offers a simple and efficient, although incomplete, technique of treating triggering.

One may even use both techniques conjointly. We may start with the perturbation-averaging method to get some information about the wave behavior in time. The method of asymptotic-perturbation may then be used subsequently to include all the mechanisms in the system.

Future research in the area of nonlinear instabilities of pressure oscillations in combustion chambers may have three directions. The first direction is the extension of the perturbation-averaging technique to many modes and to

higher orders. The second one is the study of the influence of the phase relationships among modes on triggering. The third direction is the elaboration of explicit results regarding the third order acoustics using the asymptotic-perturbation technique Being able to handle these problems may greatly enhance our understanding of the nonlinear processes in combustion chambers, mainly the combustion response to pressure oscillations and to velocity fluctuations.

The application of the results of this work to real engineering problems will be much expanded if we can extend the results for axial modes to three dimensional problems in which axial, radial, and tangential modes coexist.